HIERARCHICAL CONTROL AND MULTILEVEL OPTIMIZATION OF A REHEAT FURNACE AND STEEL REVERSING MILL

by

WILTON NORRIS BAILEY

A thesis submitted for the
Degree of
Doctor of Philosophy

The City University (London)
Department of Systems Science

October, 1981

Dedicated to my

Mother and Father

CONTENTS

LIST OF ILLUSTRATIONS AND TABLES

Figures

Figures

Figures

Tables

Tables

ACKNOWLEDGEMENTS

I would like to thank Professor Peter Roberts for introducing the project to me and for his continued support throughout the research period. My thanks also to [redacted] for his patience in the teaching of the programming of the Ferranti Argus 500. My colleagues, [redacted] and [redacted], I would like to thank for their warm friendly discussions (and chess matches) and, also, special thanks to [redacted] for valuable discussions in relation to topics in chapter 4.

Many thanks to [redacted] who typed this thesis with patience and care.

Finally, many thanks to the Science Research Council (U.K.) who provided the financial means for doing the research.

DECLARATION

The author grants discretionary powers to the University Librarian to allow the thesis to be copied in whole or part without further reference to the author.

PUBLICATIONS

Parts of this work were used as the basis of two papers, viz:

(i) "Optimal slab reduction in a reversing mill with an odd number of passes"
Seventh Triennial World Congress of the International Federation of Automatic Control, Helsinki, Finland, 12-16 June, 1978 (Pergamon Press)

(ii) "Hierarchical optimization for a reheat furnace and rolling mill system"
2nd Symposium on Large-Scale Systems: Theory and Applications (IFAC), Toulouse, France, 25-27 June, 1980.

ABSTRACT

This thesis examines the integrated control of a steel hot plate system consisting of a reheat furnace and a controlled reversing plate mill. Alternative multilevel techniques are proposed for the optimal control of the system where the objective is to minimise fuel consumption in the reheat furnace and minimise power consumption in the rolling mill. The alternative schemes are analysed, paying particular attention to their practical utility, resulting in a recommended feasible scheme based on the interaction prediction principle in which intermediate results from the iterative optimisation can be applied directly to the plant. In this scheme the temperature of the slab leaving the furnace is considered as an interaction variable and is under the direct control of the supremal coordinator. Infimal unit problems, which comprise the optimisation of the reheat furnace and rolling mill, respectively, are investigated in detail and simulation results are presented to illustrate the proposed control schemes.

The task of the reheat furnace subsystem is, with minimum fuel consumption, to heat the moving slabs to a defined exit temperature which is specified by the supremal coordinator. Control is performed in pre-heat, heat and soaking zones, taking account of interaction effects between the latter two zones. At a given push rate, steady state optimisation is performed using orthogonal search taking account of soaking zone entry gradient constraints.

The reversing plate mill subproblem of providing final plates of steel of given thickness, within a desired temperature range, at maximum throughput and minimum utilisation of energy is solved by dynamic programming with the constraint that there must be an odd number of passes during slab reduction.

In this thesis, emphasis is given to the practical on-line considerations of applying the multilevel optimisation scheme, including the effects of quantization. As well as presenting simulated results, the thesis describes a semi-pilot-scale plant investigation where the reheat furnace is represented by an electrically-heated travelling load oven and the rolling mill is simulated within a process control computer.

PRINCIPAL NOMENCLATURE

c	specific heat
e	furnace emissivity
e_f	flame emissivity
e_s	slab emissivity
e_i	roll energy required for the i^{th} pass
f_i	roll force during the i^{th} pass
F_{max}	maximum allowable roll force
h_{i+1}	slab thickness after the i^{th} pass
Δh_i	slab reduction on the $(i+1)^{th}$ pass
h_{max}	maximum allowable value of slab thickness for rolling
h_{min}	minimum " " " " " " "
H	the set of quantized values of slab thickness
k	thermal conductivity
ℓ_i	total time required on the i^{th} pass
ℓ_d	slab reversal time
M	number of quantization intervals in admissible temperature range
N	number of passes of slab through rollers
p_n'	empirically determined constants of rolling mill simulation
P	number of quantization intervals in admissible thickness range
Q	reciprocal of the smallest allowable fractional decrement in roll setting
r_i	roll setting during the i^{th} pass
R	the set of allowable roll settings for any given pass
s	slab thickness in furnace
t	time
T	the set of quantized values of slab temperature
T_f	absolute value of flame temperature in furnace
T_p	furnace temperature in the preheat zone

T_H furnace temperature in the heat zone

T_S " " " " soak "

T_{PP} temperature in preheat zone with preheat zone on only

T_{PH} " " heat " " " " " "

T_{HP} " " preheat " " heat " " "

T_{HH} " " heat " " " " " "

T_{HS} " " soak " " " " " "

T_{SH} " " heat " " soak " " "

T_{SS} " " soak " " " " " "

u_1 preheat zone power input set point

u_2 heat " " " " "

u_3 soak " " " " "

v slab push rate

θ slab temperature

θ_o initial slab temperature on input to furnace

θ_f final slab temperature at furnace exit

θ_i slab temperature before the i^{th} roll pass

θ_{max} maximum allowable slab temperature

θ_{min} minimum allowable slab temperature

θ_s slab surface temperature

$\theta_{s\ max}$ maximum allowable slab surface temperature

θ_{soak} slab entry temperature on input to soak zone

θ_d desired slab output temperature

ρ slab density

Ω set of all admissible quantized states for rolling

Ω_N set of all admissible states which can be taken into Ω_o in N passes

Ω_o set of all admissible final states

σ Stefan-Boltzmann constant

1.0 INTRODUCTION

Modern technology and economic reasons, in a world increasingly aware of its limited resources, have led to more and more integrated complex industrial systems, e.g. steelworks, petrochemical complexes, etc. These large-scale systems become very difficult and sometimes even impossible to control in a satisfactory way. This situation has led to ideas concerning the concept of "work-sharing" in management and control systems. The management and control problems can be solved in this way, and small improvements in productivity can lead to significant economic and social effects in the environment of large industrial complexes (Mesarovic et al, 1970).

The traditional concept of control, in application to industrial process sytems, concerns the problem of how to vary certain inputs to the system so that (a) designated output variables are held at fixed values or made to follow predetermined time trajectories, or (b) the state vector of the system is transferred (optimally) from some initial value to a specified final value. However, there has been an increasing tendency to consider control from a broader and more general perspective. Strong contributing factors to this trend are

(i) the increasing application of computers in process control, providing the hardware and software means for implementing more sophisticated control concepts, and

(ii) the growing awareness and acceptance of a "systems approach" in the design and control of industrial process systems.

The objective of integrated systems control, in a very general sense, is to achieve the most efficient utilization of resources (e.g. materials, energy, the environment, labour, capital, etc.) in the production of goods. These goods must satisfy quality specifications and be consistent with goals and constraints that may be imposed by society. Thus, integrated systems control is concerned with the broad spectrum of decision-making and control functions (e.g. process control, operations control, scheduling, planning, etc.) that play a role in the effective operation of the system with respect to its production goals.

The performance of the processing system depends upon a variety of factors including (Lefkowitz et al, 1976):

(a) production specification and process design

(b) the nature of resources available and environmental constraints

(c) the choice of processing conditions, allocation of resources, scheduling of operating sequences, etc.

Thus, two phases of system evolution with respect to information processing and decision-making functions can be distinguished, i.e. the design phase and the operating phase.

The Design Phase

This phase concerns implementation of overall system objectives through the design of the production means. There is a variety of disturbances that affect the design process and hence can stimulate consideration of a design modification or even re-initiation of the design process. Some of these disturbances include major changes in product specifications or quality requirements, technological developments with respect to a new product or a new method of production, etc.

Decisions at the design phase tend to be strongly conditioned by subjective and, sometimes, non-quantifiable factors. Traditionally, the human designer plays a dominant role. However, methods and techniques of computer-aided design are becoming increasingly important in coupling the capabilities of the computer (i.e. rapid communication, handling of large data bases, fast-time simulation of the consequences of alternative policies, etc.) with the judgement, experience and intuitive aspects of the human designer.

The Operating Phase

Here, the decisions and control actions are chosen to determine operating conditions, throughput rates, sequencing of operations, etc., so that product specifications are satisfied along with the constraints imposed by environmental interactions, technological factors, etc. Further considerations may then include the optimization of performance with respect to utilization of resources, production efficiency, etc.

The decision-making and control actions are carried out in a system that is evolving in real time and, hence, must respond to the effects of:

(a) variations in input conditions (e.g. changes in product demand, order sequence, raw material composition)

(b) time-varying characteristics of processing units

(c) changes in objective function owing to economic factors, environmental constraints, etc.

(d) errors and inadequacies in the models used in determining the decisions and control actions.

Furthermore, the decision-making processes cover time-scales ranging from very short span control operations to long-range planning processes.

In general, the boundary separating the design and operating phases, in the evolution of a system, may not be sharp and it is quite feasible that aspects of the long-range planning associated with the operation of the system may well include aspects of the design phase, i.e. replacement of a production unit or modification of a process design.

The Hierarchical Control Approach

Due to the fact that industrial systems are characteristically large, complex and, in most cases, time-varying, the solution of the overall problem, considered above, is extremely difficult, if not unfeasible, with existing analytical and computational capabilities. Consequently, current practice tends towards empirical and suboptimal solutions to locally defined problems. Due to rising energy costs, labour costs, etc., attempts are being made, albeit in an ad hoc procedure, for the integration and coordination of the locally defined subproblems.

The multilevel and multilayer hierarchical structuring of the decision-making and control system (Mesarovic et al, 1970) is considered as the basic approach to handling the overall problem. The approach embodies the following features, viz:

(1) Based on local criteria and on local information sets, the complex system is decomposed into a number of coupled subsystems. Each of the subsystems has its own set of decision-making and control functions. Due to subsystem interactions and because of overall system objectives and constraints, it is necessary to coordinate the objectives (i.e. goals) of the local controllers.

(2) The overall system decision-making and control problem is decomposed into various subproblems, each of which has its own objective function, model, constraint set, etc. Integration of the subproblems is necessary to ensure satisfaction of the objectives and constraints associated with the overall system, since the subproblems essentially interact, e.g. the solution of a planning problem can affect the scheduling problem.

(3) In consideration of the costs associated with model development, on-line computations, etc., the complex system relationships are approximated by simplified and aggregated models which correspond to each stage and level of decision-making. The incorporation of means for on-line updating of the models through feedback of relevant data is an essential feature of the information system. This is necessary since industrial systems are characteristically time-varying (i.e. ageing of components, etc.), subject to a wide range of continually varying inputs, and are also subject to equipment breakdowns, etc.

Most of the above underlying concepts and terminology have their origins in the pioneering work of Mesarovic and his group (Mesarovic et al, 1970; Mesarovic, 1970) who developed a conceptual and analytical foundation for hierarchical structures and multilevel coordination theory. Some workers (Lefkowitz et al, 1976; Singh and Titli, 1978b; Findeisen et al, 1978) have made modifications to the basic theory. For example, more explicit concern for on-line implementation and the effects of disturbance inputs, and the focussing on achieving feasible, suboptimal performance objectives as opposed to a "mathematical" optimum, etc.

The bulk of literature in the field, with the possible exception of Findeisen et al, 1980, is oriented to decomposition and multilevel coordination theory and its application to optimization and mathematical programming problems of various kinds. Lefkowitz (1966) first described the essential features of the functional multilayer hierarchy. Recent technological advances in microprocessors and the increased involvement of control engineers have given rise to issues concerning decentralized decision-making, distributed data bases and computing power and hierarchical control. There is a powerful trend towards on-line

optimization, non-linear dynamic optimization, periodic optimization and decentralized-coordinated control, and many workers have been involved in these fields, viz: Mesarovic et al (1970); Chong et al (1975); Findeisen (1978), (1979); Singh et al (1978a), (1978b). Aside from these theoretical issues, there is a trend, from the computer scientist's side, to study and build large hierarchical computer structures (Oshima et al, 1972; Guran et al, 1978).

In spite of these "remarkable" issues, there is still a lack of a general theory and there are few integrated methodological approaches in the basic problem "how to build hierarchical control systems using the available technology?". Also, there is a relative shortage in reporting hierarchical control philosophy (not hierarchical computer systems) implemented in actual industrial complexes, although a few papers can be noted on this subject, viz: Findeisen et al (1970); Tazaki et al (1972).

Lefkowitz et al (1976) have carried out an excellent review of Integrated Industrial Systems Control, as applied to the steel industry. The steel-making industry was selected as the first system for a case study of the integrated systems approach. There were several reasons for this choice, viz:

(i) steel is a basic industry

(ii) it is a very complex industry with a wide variety of different types of processing and manufacturing facilities and, hence, rich in the broad spectrum of systems problems likely to be countered in industrial applications

(iii) the steel industry represents, at the present time, the most advanced area of technology with respect to the application of an integrated systems approach and also in the application of computers for real time information processing and decision-making.

Besides describing the results of the state-of-the-art survey, the review presents a formalization of the multilevel-multilayer hierarchical control approach oriented to the problem of complex industrial systems. The approach reflects a number of modifications of the hierarchical structuring of the decision-making and control system. These modifications are motivated by some of the experiences gained from the steel industry study.

Following a review of hierarchical control techniques, the objective of this thesis is to interpret and relate the theory of multilevel coordination to the problems of control design for complex processes. The hot-strip mill of the steel industry is used to serve as the vehicle for the attainment of the objectives. The optimal control problem treated is one of minimizing the overall cost involved in heating slabs to a given output temperature from the reheat furnace and reducing the thickness of these slabs to some desired final thickness using a reversing mill. The hot-strip mill process is analyzed from the multilevel viewpoint and the responsibilities of the first three levels of the coordination hierarchy are given relative to the portion of the coordination problem chosen for analysis. The development proceeds in essentially nine steps, viz:

(a) the development of the mathematical models for the reheating furnace and the heating process

(b) the development of the mathematical model for the reversing mill

(c) combining the mathematical models into a form which is suitable for the application of control theory

(d) defining an optimization criterion which incorporates the main objective of minimizing the reheat furnace fuel consumption

(e) defining an optimization criterion which incorporates the main objectives of minimizing the reversing mill energy utilization and the time taken to reduce a slab to its final thickness

(f) choosing the optimization techniques most suitable for the problems

(g) solving the steady-state optimization problem for the reheat furnace

(h) solving the dynamic optimization problem for the reversing mill and also incorporating the odd pass constraint

(i) solving the combined optimization problem using a hierarchical control structure.

In Chapter 2 hierarchical control is reviewed, together with alternative methods of decomposition and coordination. Chapter 3 outlines

a typical steel works and how its major components are decomposed, and the relationship between a reheating furnace and reversing mill is highlighted. Chapter 4 is concerned with the mathematical modelling and optimization of the reheat furnace subproblem, whilst Chapter 5 looks at the reversing mill subproblem with special emphasis placed on meeting an odd multi-pass criterion. In Chapter 6 the coordination and optimization of the combined subsystems are examined and results presented. Chapter 7 looks at the on-line considerations which need to be considered in a large-scale hierarchically-controlled system, and reviews some later developments in the field of hierarchical control.

2.0 HIERARCHICAL CONTROL

A theory (Mesarovic et al, 1970) of hierarchical, multilevel systems has been developed to handle large-scale complex systems consisting of several subsystems, each having its own objectives and operating constraints.

The most natural way to view a large-scale system, which is often too complicated to comprehend in its entirety, is to consider it as a collection of interconnected subsystems. An understanding of the properties of each individual subsystem, together with an understanding of the interconnections between the subsystems, including interconnections with the environment, then defines the properties of the integrated system.

In a large dynamic system, each subsystem has its own state, control and output vectors. In addition, there will be a vector of inputs to each subsystem composed of some of the outputs from other subsystems. This vector will thus define the interconnection between the subsystems. Each subsystem will also contain its own equality and inequality constraints. The integrated system is formed by adjoining the subsystems so that the overall state and control vectors are defined as combinations of all the subsystems' state and control vectors. Such a structure is quite general and can be used to describe many industrial processes.

By exploiting the structure of a large-scale system as an interconnected assembly of subsystems, it is possible to decompose the problem of controlling a complex system into interlinked subproblems of manageable size. Each subproblem can be solved independently of the other subproblems by taking into account the interconnections by some form of coordination procedure. Such an approach leads naturally to decentralized, distributed and hierarchical control methods.

Decentralized control systems are structured in such a manner that the subsystems have available only strict subsets of the overall system information. Centralized control systems, however, are such that all the system information is available centrally and all the system variables are manipulated directly from the centre. A distributed control system is a decentralized control system whereby the individual subsystem control units are distributed among the physical subsystems of the overall process. Microprocessors are playing an important role in distributed industrial control systems. Due to their relatively low

cost and increasing power, microcomputers are now replacing centralized control systems and, hence, permit systems which have the benefits of improved control, reliability, flexibility and reduced cabling costs.

Hierarchical control systems consist of decision-making units arranged in a priority structure where, at each level, a number of units may operate in parallel, thus giving rise to a pyramid structure.

2.1 Basic Types of Hierarchies

In this section, three types of hierarchical systems are introduced which, in a sense, represent a classification of hierarchical systems. These three types of hierarchical structures are

(i) stratified
(ii) multilayer
(iii) multilevel

although it is important to note that this classification does not exclude the possibility of a system belonging to more than one class.

2.1.1 Stratified systems

In a stratified system, the system is defined as a family of models, each of which is concerned with the behaviour of the system as viewed from a different level of abstraction. Mesarovic et al (1970) refer to these levels of abstraction as strata, and for each level there is a set of relevant features, variables, laws and principles in terms of which the system behaviour is described. For such a hierarchical description to be effective, it is necessary that the functioning on any level be as independent of the functioning on other levels as possible.

Consider, for example, an integrated steelworks as shown in Figure 2.1. The total task of running the plant is specified on three strata, i.e. the total system is a stratified system. The complete system has a large number of units and tasks to perform, but only the main functions will be described here.

From the total systems' viewpoint, three main functions to be performed by the system are:

(i) production planning
(ii) scheduling and coordination of operation

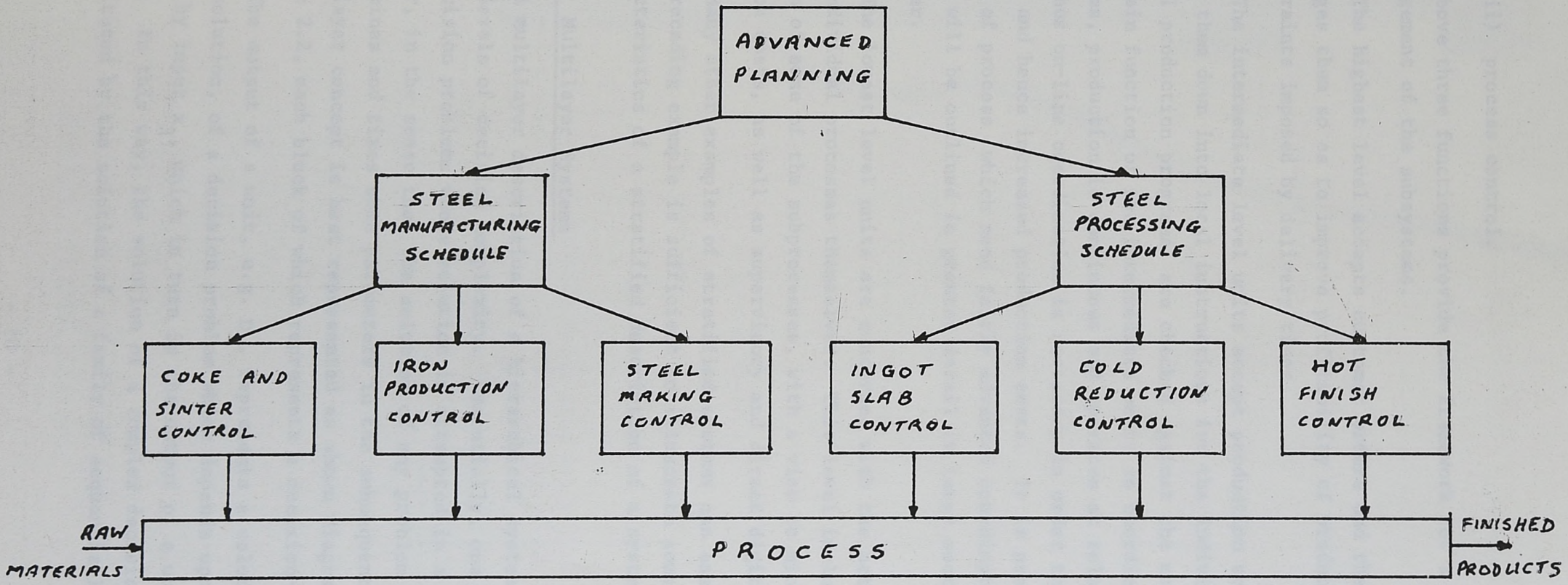

FIG. 2.1 BLOCK DIAGRAM OF A STEEL MAKING INTEGRATION CONTROL SYSTEM

(iii) process control.

The above three functions provide the framework for a hierarchical arrangement of the subsystems.

The highest level accepts customer orders and then groups and arranges them so as to improve profitability of production within the constraints imposed by delivery times.

The intermediate level units accept production schedules and break them down into local instructions for the individual processes. Actual production programs are checked against the master schedule. The main function of the intermediate units is coordination. In some systems, production is continuous and operates at relatively high speeds, and thus on-line coordination is necessary in order to avoid bottlenecks and hence increased production costs. It is precisely these types of process which need fairly advanced coordination methods, which will be outlined in greater detail in later sections of this chapter.

The lowest level units are concerned with the actual control of the individual processes themselves. This level includes the optimization of some of the subprocesses, with a view to minimizing the production costs, as well as supervisory and direct digital control.

Many other examples of stratified systems can easily be given. The preceding example is sufficient to illustrate some of the general characteristics of a stratified description of a system.

2.1.2 Multilayer Systems

A multilayer description of a hierarchical system is concerned with levels of decision complexity. Essentially, one defines a family of decision problems whose solution is attempted in a sequential manner, in the sense that the solution of any problem in the sequence determines and fixes some parameters in the subsequent problem. The multilayer concept is best represented as shown diagrammatically in Figure 2.2, each block of which represents a decision-making unit.

The output of a unit, e.g. D_2, represents a solution, or consequence of a solution, of a decision problem which depends upon a parameter fixed by input x_2, which in turn is the output of a unit on a higher level. In this way, the solution of a complex decision problem is substituted by the solution of a family of sequentially arranged simpler

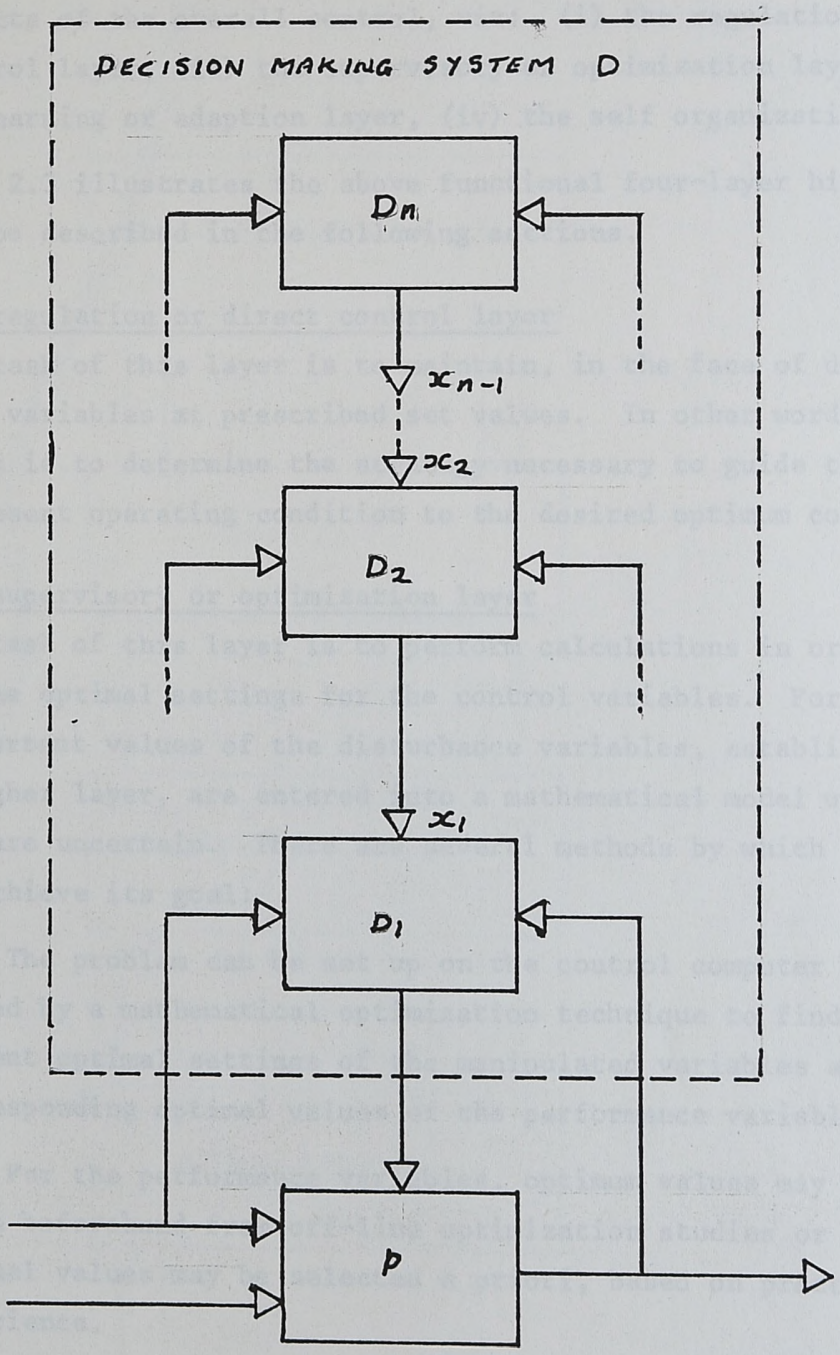

FIG 2.2 MULTILAYER HIERARCHY OF A DECISION MAKING SYSTEM

problems, so that the solution of all subproblems in the family implies the solution of the original problem.

Consider the control of a large-scale system. In this situation, a multilayer hierarchy emerges naturally in reference to four functional aspects of the overall control, viz: (i) the regulation or direct control layer, (ii) the supervisory or optimization layer, (iii) the learning or adaption layer, (iv) the self organization layer.

Figure 2.3 illustrates the above functional four-layer hierarchy. These will be described in the following sections.

(i) The regulation or direct control layer

The task of this layer is to maintain, in the face of disturbances, the process variables at prescribed set values. In other words, the control task is to determine the strategy necessary to guide the process from its present operating condition to the desired optimum condition.

(ii) The supervisory or optimization layer

The task of this layer is to perform calculations in order to determine the optimal settings for the control variables. For this step, the current values of the disturbance variables, established in the next higher layer, are entered into a mathematical model whose parameters are uncertain. There are several methods by which this layer can achieve its goal:

(a) The problem can be set up on the control computer and solved by a mathematical optimization technique to find the current optimal settings of the manipulated variables and the corresponding optimal values of the performance variables.

(b) For the performance variables, optimum values may be known beforehand from off-line optimization studies or sub-optimal values may be selected a priori, based on practical experience.

(c) A table of solutions to the optimization problem is obtained off-line and stored in a look-up table, and the optimal control settings are retrieved after the current disturbance values have been identified.

(iii) The learning or adaption layer

This layer is concerned with specifying the uncertainties used by the optimization layer. The uncertainties are viewed as encompassing

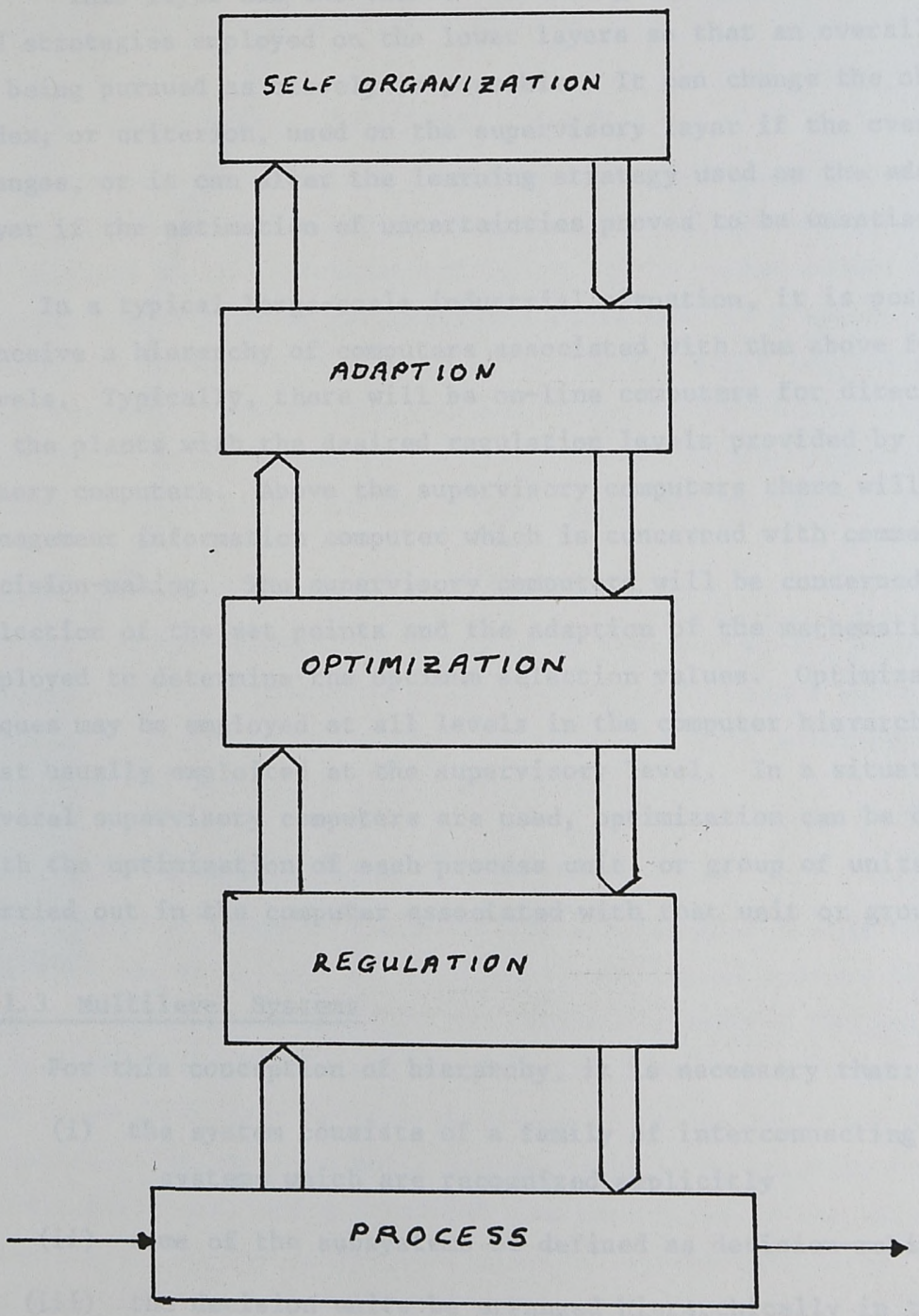

FIG. 2.3 FUNCTIONAL FOUR LAYER HIERARCHY

the ignorance about the behaviour of the system, and are typically model parameters derived from observations and communications with the system. The main aim of this layer is to reduce the uncertainty about the process under control in order to simplify the task of the supervisory or optimization layer.

(iv) The self organization layer

This layer has the task of selecting the structure, functions and strategies employed on the lower layers so that an overall goal is being pursued as closely as possible. It can change the objective index, or criterion, used on the supervisory layer if the overall goal changes, or it can alter the learning strategy used on the adaption layer if the estimation of uncertainties proves to be unsatisfactory.

In a typical large-scale industrial situation, it is possible to conceive a hierarchy of computers associated with the above functional levels. Typically, there will be on-line computers for direct control of the plants with the desired regulation levels provided by the supervisory computers. Above the supervisory computers there will be a management information computer which is concerned with commercial decision-making. The supervisory computers will be concerned with the selection of the set points and the adaption of the mathematical models employed to determine the optimum selection values. Optimization techniques may be employed at all levels in the computer hierarchy but are most usually exploited at the supervisory level. In a situation where several supervisory computers are used, optimization can be decentralized, with the optimization of each process unit, or group of units, being carried out in the computer associated with that unit or group.

2.1.3 Multilevel Systems

For this conception of hierarchy, it is necessary that:

(i) the system consists of a family of interconnecting subsystems which are recognized explicitly

(ii) some of the subsystems be defined as decision-making units

(iii) the decision units be arranged hierarchically in the sense that some units are influenced by other decision units.

In general, the various decision units have conflicting goals, and it is essential that the units are given some freedom of action, where the

higher level units condition, but do not completely control, the goal-seeking activities of the lower level units.

Multilevel systems can be divided into various categories of decision-making systems, viz:

(i) single-level, single-goal systems

(ii) single-level, multi-goal systems

(iii) multilevel, multi-goal systems

2.1.3.1 Single-level, single-goal systems

Figure 2.4 represents a single-level, single-goal system. Here, a goal is defined for the overall system, and all decision variables are selected so as to satisfy this goal. This system treats the optimization problem as an integrated whole and, as previously discussed, the implementation in this form is extremely complex for large-scale systems. However, the conceptual simplicity of the single-level, single-goal system should be noticed, with particular emphasis on the absence of conflict within the boundaries of the system.

2.1.3.2 Single-level, multi-goal systems

This system consists of a family of decision units, each with its own goal, and is represented diagrammatically in Figure 2.5. The goals are not necessarily conflicting, but when they are, solutions to this problem may be attempted using game theory.

2.1.3.3 Multilevel, multi-goal systems

Figure 2.6 represents a multilevel, multi-goal system. One important characteristic of multilevel, multi-goal systems is the fact that the higher level units do not completely control the goal-seeking activities of the lower level units. The lower level decision units have to be given some freedom of action to select their own decision variables. The decision units are arranged in a hierarchy having a pyramid structure, and a principal characteristic is the existence of a supremal, i.e. top level, unit. At an intermediate level, each decision unit receives information from units superior to it in the hierarchy and transmits information to units inferior to it. The decision units have different objectives which may be in conflict, and these conflicts are resolved by higher level units which play the

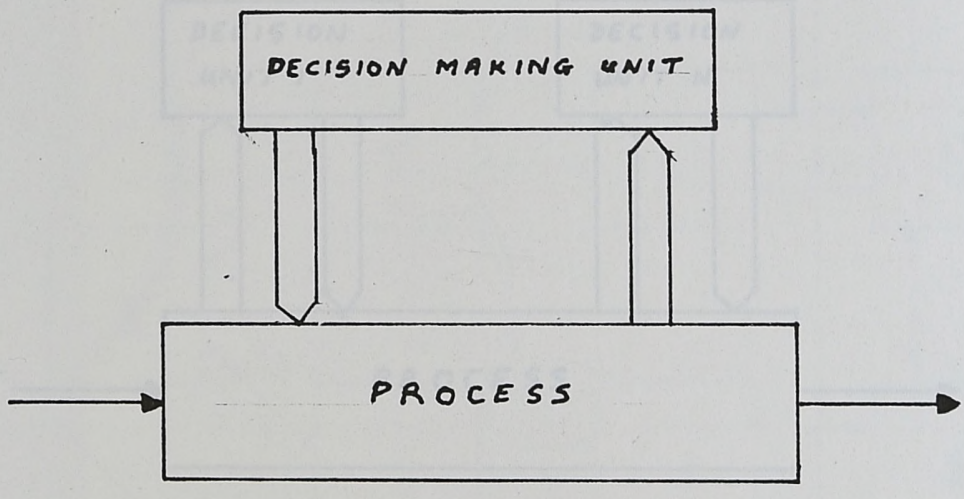

FIG. 2.4 SINGLE-LEVEL SINGLE GOAL SYSTEM

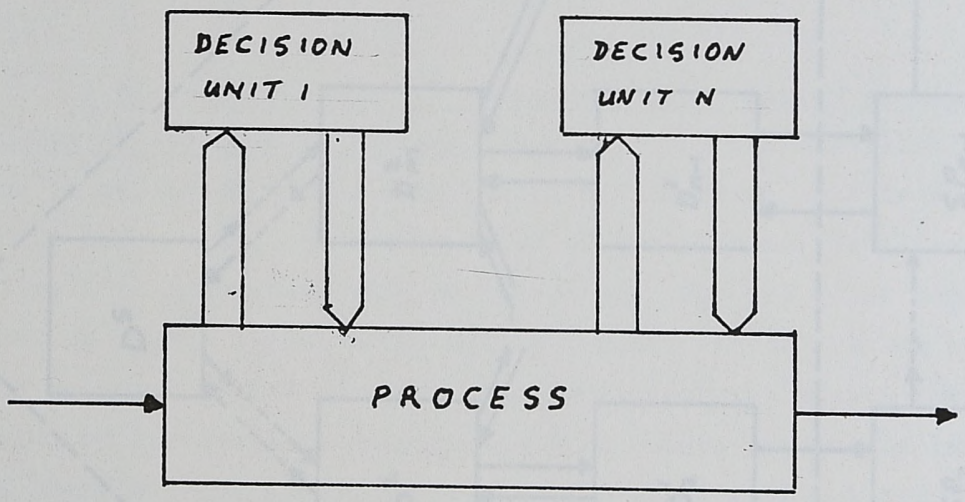

FIG. 2.5 SINGLE-LEVEL MULTI-GOAL SYSTEM

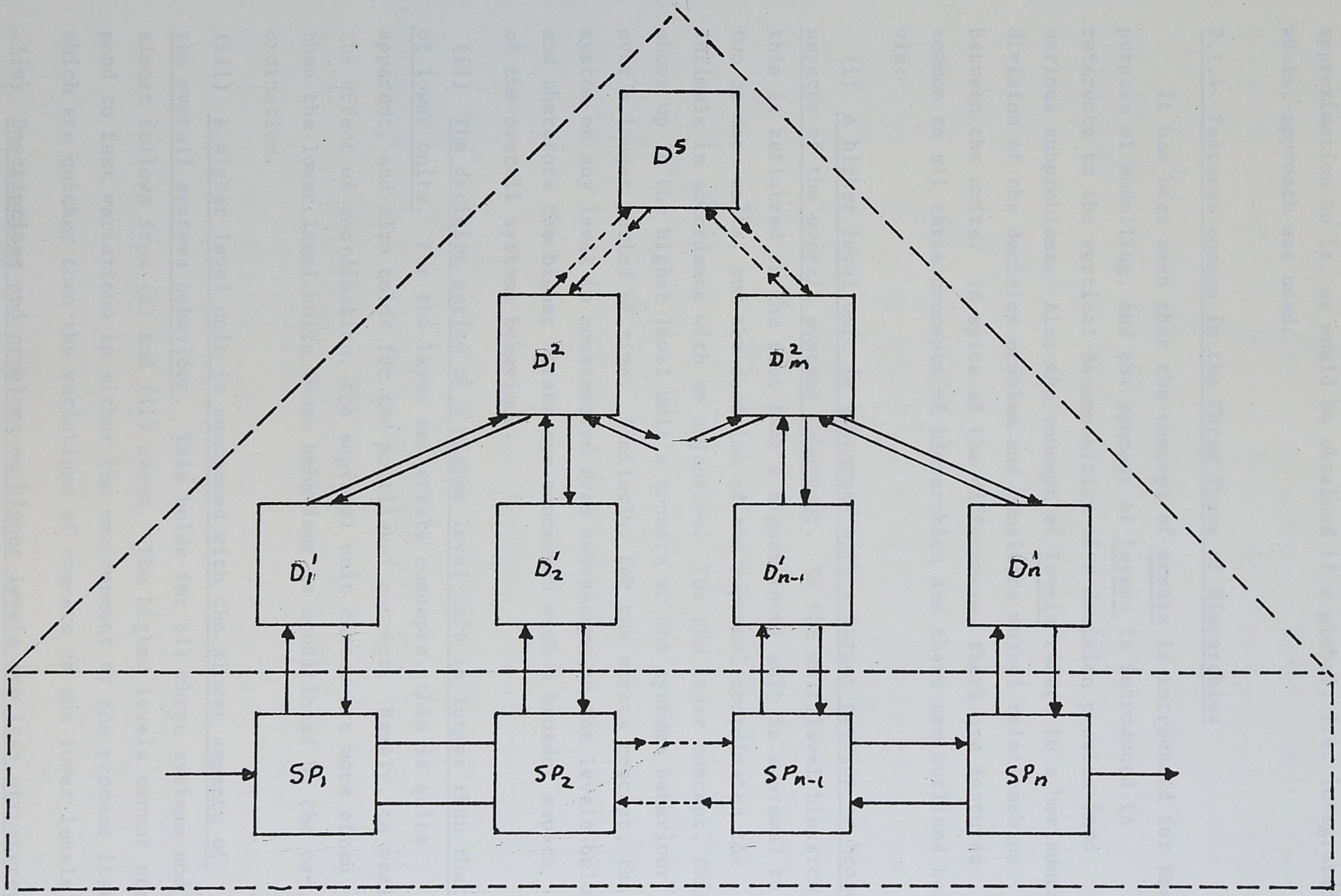

FIG. 2.6 MULTI-LEVEL MULTI-GOAL PYRAMID STRUCTURE

role of coordinators. It is important to note that the higher levels in the hierarchy must act so as to obtain the same solution, or an approximation to it, as would be obtained if a global, i.e. integrated whole, approach was used.

2.1.4 Features common in the Three Types of Hierarchies

It has been seen that the concept of strata is introduced for the purpose of modelling, and the concept of layers is introduced in reference to the vertical decomposition of a decision problem into various subproblems. Also the concept of levels refers to a horizontal division of the decision problem and considers mutual relationships between the units. In spite of the differences, there are features common to all three concepts of hierarchies and these are outlined below, viz:

(i) A higher level unit is concerned with a larger portion or broader aspects of the overall systems behaviour. In the multilevel hierarchy, this is reflected in the fact that a higher level unit is supremal to two or more units, and the decision of the supremal coordinates the infimals in accordance with an objective. For the layer concept, this shows up in the higher level unit's concern of the systems behaviour over a longer period of time. Similarly, for the strata concept, the system on any level is constructed from subsystems on the levels below, and therefore the higher strata are concerned with a broader aspect of the overall systems behaviour.

(ii) The decision period of a higher level unit is longer than that of lower units. For the layer and strata concepts, this is quite apparent, and also holds for the multilevel concept. Namely, to evaluate the effect of coordination, the supremal unit cannot act more often than the lower level units whose behaviour is conditioned by the co-ordination.

(iii) A higher level unit is concerned with the slower aspects of the overall systems behaviour. This holds for all three systems and almost follows from (i) and (ii) above. The higher levels cannot respond to fast variations in either the environment or the process itself, which are quicker than the variations of concern to the lower levels.

(iv) Descriptions and problems on higher levels are less structured, with more uncertainties, and more difficult to formalize quantitively. Decision problems on the higher levels can be considered to be more

complex than those on the lower levels. Usually, an approximation can be used to arrive at the solution of a higher level problem, but accuracy is then reduced and care has to be taken in interpreting the results. In general, for any level, there is a specific set of techniques suitable for the solution of the respective tasks. For example, for each layer in the multilayer hierarchy, there is a different set of methods and techniques. On the selection layer, feedback control and numerical optimization methods are used, whereas on the adaptation layer, statistical or pattern recognition techniques can be used.

In a typical industrial situation (Roberts, 1979), the desired strategy may be concerned with the maximization of profit or the minimization of costs. If the lowest layer achieves stable control, the optimization problem may be regarded as a static optimal control problem of selecting the set points of standard two- or three-term-controllers which regulate the process at the lower layer. The optimization layer then requires a steady-state mathematical model, together with standard finite dimensional numerical optimization procedures for solving the problem. However, if dynamic considerations are important, the optimization layer would involve the solution of a dynamic control problem. Thus, two different views of the behaviour of the system are involved, one for the steady-state behaviour and another for the dynamic behaviour, giving rise to a stratified decomposition occurring at the optimization layer.

When considering the optimization problem at the optimization layer, it is often essential in large-scale situations to decompose the problem into separate optimization problems, one for each of the process units which constitute the overall industrial plant. However, the interconnections between the individual units must be accounted for and this may be achieved by using a higher level unit to coordinate the activities of the individual unit problems. Thus, the optimization layer can be decomposed into two levels, where the lower level consists of local optimization problems and the upper level is designed to coordinate the solutions of the lower level problems. This coordination is such that the overall global objectives and subsystem interconnections are satisfied, thus giving rise to a multilevel decomposition occurring at the optimization layer.

2.2 Coordination

In order to introduce the concepts of coordination, consider the two-level structure shown in Figure 2.7. Here, a single coordinator at the upper level (supremal level) controls two units at the lower level (infimal level). Each infimal decision unit has its own local system model and local objective. In order that the units arrive at solutions coherent with overall system objectives, the supremal unit has the task of coordinating the tasks of the infimal level units by some means or another. Thus, the supremal unit transmits intervention signals, $\underline{c}$, to each infimal decision unit and, in turn, receives information, $\underline{f}$, concerning the performance of the infimal units.

The above system is of special interest for a theory of multi-level systems since (i) it is the simplest type of system that exhibits the most essential characteristic of a multilevel system, and (ii) more complex multilevel systems can be built using the two-level system as a building block.

The relationship between the supremal unit and one of the infimal units is such that the action (success) of one depends upon that of the other. Since both are decision-making units, this means that, in general, the decision problem of the infimal unit depends upon the action of the supremal unit. Conversely, the decision problem of the supremal unit depends upon the action or response of the infimal unit. This gives rise to an apparent deadlock situation, but the dilemma is resolved by the priority of action of the supremal unit. Due to priority of action, the supremal unit has the broad responsibilities of, first, instructing the infimal units on how to proceed, and, second, influencing them to change their actions if needed.

How a given infimal unit will communicate with other infimal units, and which aspects of the infimal decision problem are available for change in order to improve the overall performance, determines a co-ordination mode. The relationship of a unit with others on the same level can be characterized by its action, and the response of the rest of the system, as it influences that unit. This influence is referred to as the interface input. The main question here is, therefore, how the given infimal unit will consider, or take into account, the inter-face input.

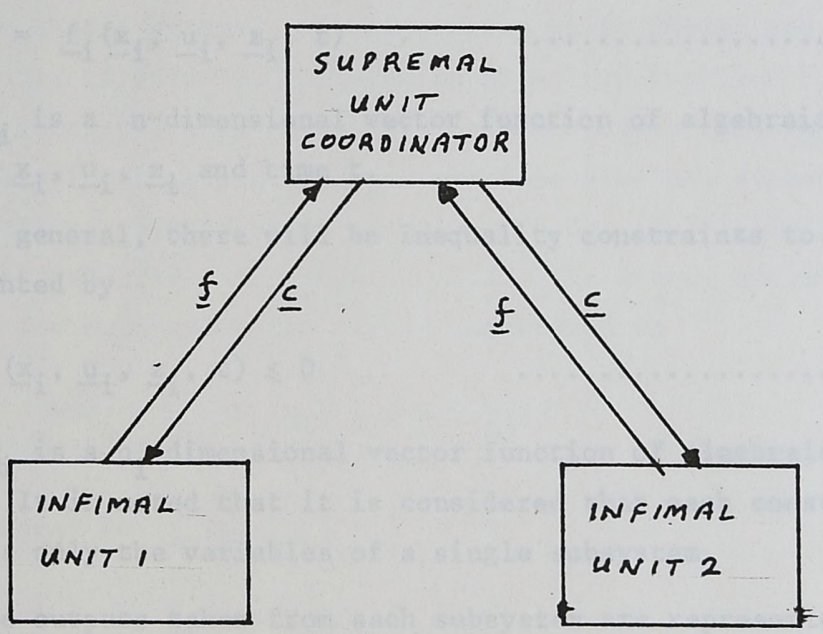

FIG. 2.7 BASIC TWO LEVEL STRUCTURE

2.3 Decomposition of the Subsystems

Consider a dynamic system consisting of N coupled subsystems with its variables defined as follows:

$\underline{u}_i$ = m_i - dimensional vector of manipulated inputs to subsystem i

$\underline{x}_i$ = n_i - dimensional vector of state variables in subsystem i

$\underline{z}_i$ = r_i - dimensional vector of inputs to subsystem i which are composed of outputs from other subsystems

$\underline{y}_i$ = r_i - dimensional vector of outputs from subsystem i.

The state equations describing subsystem i are

$$\dot{\underline{x}} = \underline{f}_i(\underline{x}_i, \underline{u}_i, \underline{z}_i, t) \qquad \ldots\ldots\ldots\ldots\ldots\ldots \quad (2.1)$$

where $\underline{f}_i$ is a n-dimensional vector function of algebraic relationships between $\underline{x}_i$, $\underline{u}_i$, $\underline{z}_i$ and time t.

In general, there will be inequality constraints to be satisfied represented by

$$\underline{g}_i(\underline{x}_i, \underline{u}_i, \underline{z}_i, t) \leq 0 \qquad \ldots\ldots\ldots\ldots\ldots\ldots \quad (2.2)$$

where $\underline{g}_i$ is a p_i-dimensional vector function of algebraic relationships. It is noted that it is considered that each constraint equation involves only the variables of a single subsystem.

The outputs taken from each subsystem are represented by

$$\underline{y}_i = \underline{h}_i(\underline{x}_i, \underline{u}_i, t) \qquad \ldots\ldots\ldots\ldots\ldots\ldots \quad (2.3)$$

where $\underline{h}_i$ is a r_i-dimensional vector function.

The input variables $\underline{z}_i$ are defined by interconnections with other subsystems and are expressed by the interconnection constraints

$$z_i = \sum_{j=1}^{N} [C_{ij}] y_j \qquad \ldots\ldots\ldots\ldots\ldots\ldots \quad (2.4)$$

where $[C_{ij}]$ are constant matrices whose elements are 0 or 1.

The integrated system is formed by adjoining the subsystems in order. Let $\underline{x}$, $\underline{u}$, $\underline{z}$ and $\underline{y}$ be vectors formed by adjoining their components $\underline{x}_i$, $\underline{u}_i$, $\underline{z}_i$ and $\underline{y}_i$ in order. Let n, m, r and p be the sums of n_i, m_i, r_i and p_i. Then, the integrated system is represented by the

equations

$$\dot{\underline{x}} = \underline{f}(\underline{x}, \underline{u}, \underline{z}, t) \quad \ldots\ldots\ldots\ldots\ldots\ldots\ldots \quad (2.5)$$

$$\underline{g}(\underline{x}, \underline{u}, \underline{z}, t) \leqslant 0 \quad \ldots\ldots\ldots\ldots\ldots\ldots\ldots \quad (2.6)$$

$$\underline{y} = \underline{h}(\underline{x}, \underline{u}, t) \quad \ldots\ldots\ldots\ldots\ldots\ldots\ldots \quad (2.7)$$

$$\underline{z} = [C]\underline{y} \quad \ldots\ldots\ldots\ldots\ldots\ldots\ldots \quad (2.8)$$

where $\underline{f}' = (\underline{f}_1', \underline{f}_2', \ldots, \underline{f}_N')$, $\underline{g}' = (\underline{g}_1', \underline{g}_2', \ldots, \underline{g}_N')$, $\underline{h}' = (\underline{h}_1', \underline{h}_2', \ldots, \underline{h}_N')$ and $[C]$ is a r x r permutation matrix whose ijth partitioned block is C_{ij}.

The static optimal control problem is to choose the manipulated inputs, $\underline{u}_i$, in order to minimize an objective function $F_i(\underline{x}_i, \underline{u}_i, \underline{z}_i, \underline{y}_i)$ in each subsystem. In the static optimal control problem, only steady-state relationships are employed and time does not appear explicitly in any equation. Hence, using equations (2.2), (2.3), (2.4), and the steady-state version of equation (2.1), the static optimal control problem for each subsystem may be summarized as

$$\min_{\underline{x}_i, \underline{u}_i, \underline{z}_i, \underline{y}_i} F_i(\underline{x}_i, \underline{u}_i, \underline{z}_i, \underline{y}_i)$$

$$\text{subject to} \quad \underline{f}_i(\underline{x}_i, \underline{u}_i, \underline{z}_i) = 0$$

$$\underline{g}_i(\underline{x}_i, \underline{u}_i, \underline{z}_i) \leqslant 0$$

$$\underline{y}_i = \underline{h}_i(\underline{x}_i, \underline{u}_i)$$

$$\underline{z}_i = \sum_{j=1}^{N} [C_{ij}]\underline{y}_i \quad \ldots\ldots\ldots\ldots\ldots \quad (2.9)$$

The objective function for the integrated system is assumed to be of the additively separable form, viz:

$$F(\underline{x}, \underline{u}, \underline{z}, \underline{y}) = \sum_{j=1}^{N} F_i(\underline{x}_i, \underline{u}_i, \underline{z}_i, \underline{y}_i) \quad \ldots\ldots\ldots\ldots \quad (2.10)$$

and the integrated static optimal control problem is

$$\min_{\underline{x},\,\underline{u},\,\underline{z},\,\underline{y}} \quad F(\underline{x},\,\underline{u},\,\underline{z},\,\underline{y})$$

$$\text{subject to} \quad \underline{f}(\underline{x},\,\underline{u},\,\underline{z}) = 0$$

$$\underline{g}(\underline{x},\,\underline{u},\,\underline{z}) \leq 0$$

$$\underline{y} = \underline{h}(\underline{x},\,\underline{u})$$

$$\underline{z} = [C]\,\underline{y} \qquad \ldots\ldots\ldots\ldots\ldots\ldots \quad (2.11)$$

2.4 Multilevel Optimization of the Static Optimal Control Problem

To give some idea of the decomposition-coordination aspects, a brief description will be given of two fundamental principles. These are (i) the interaction prediction principle, and (ii) the interaction balance principle. These two ideas were first formulated in a precise form by Mesarovic et al (1970).

For the interaction prediction principle, the coordinator at the supremal level attempts to predict the values of the interface or interconnection inputs and outputs of the subsystems. The global optimum is obtained when the real interactions are identical to the predicted interactions, as observed when the optimal solution based on the predicted interactions is applied. At each iteration at the supremal level, the coordinator specifies the interconnection values and the infimal units proceed to solve their local decision problems on the assumption that the interconnections are exactly as predicted by the supremal unit. Based on the solution of the infimal units, which is transmitted back to the supremal unit, the coordinator modifies its predictions until the global optimum is achieved.

The interaction balance principle involves "cutting" the interconnection variables in a mathematical model of the process. The interconnections are then considered as additional constraints to be satisfied, and suitable modifications to the infimal level unit objective functions are chosen in order to take account of the interactions between the subsystems. The supremal unit task is to select the coordination inputs to the infimal units such that when the final overall optimum solution is obtained, all interconnection constraints are satisfied. In other words, they are in balance.

2.4.1 Interaction prediction principle

Alternative names of coordination methods based on this principle, which are all essentially the same approach, are:

(i) model coordination
(ii) primal coordination
(iii) method of projection
(iv) parametric decomposition
(v) direct method.

In this approach, the integrated problem is converted into a two-level problem by fixing the interconnection variables, $\underline{y}_i$ and $\underline{z}_i$, in the infimal level sub-problems. From the output equation, (2.3), this process will also fix some of the state variables, $\underline{x}_i$. Let $\underline{w}_i$ be the component of state vector $\underline{x}_i$ whose elements are not fixed by constraining the interconnection variables. In addition, from the interconnection constraints given by equation (2.4), it is necessary only to consider the variables $\underline{z}_i$.

The i^{th} sub-problem at the infimal level then becomes

$$\begin{aligned} &\min_{\underline{w}_i,\ \underline{u}_i} F_i'(\underline{w}_i, \underline{u}_i, \underline{z}) \\ &\text{subject to } \underline{f}_i'(\underline{w}_i, \underline{u}_i, \underline{z}) = 0 \\ &\qquad\qquad \underline{g}_i'(\underline{w}_i, \underline{u}_i, \underline{z}) \leq 0 \end{aligned} \qquad \ldots\ldots\ldots\ldots\ldots\ldots \quad (2.12)$$

It should be noted that the output equation, (2.3) and the interconnection constraints equation, (2.4) have been employed to eliminate the components of $\underline{x}_i$ and $\underline{y}_i$, which are fixed by constraining the interconnection variables. Also, the $'$ denotes the resulting modified equations.

The task of the supremal unit is to supply the interconnection variables z to the infimal units by solving the integrated minimization problem

$$\min_{\underline{z}} \sum_{i=1}^{N} P_i(z) \qquad \ldots\ldots\ldots\ldots\ldots\ldots\ldots\ldots \quad (2.13)$$

where $P_i(\underline{z}) = \min_{\underline{w}_i,\ \underline{u}_i} F_i'(\underline{w}_i, \underline{u}_i, \underline{z})$ is the solution of the i^{th} sub-problem at the infimal level for a given estimate of the values of $\underline{z}$ supplied by the supremal unit.

From equation (2.13), gradients can be obtained, at the supremal level, from the equation

$$\nabla_{\underline{z}}\left[P(z)\right] = \nabla_{\underline{z}}\left[\sum_{i=1}^{N} F_i'(\underline{w}_i^*, \underline{u}_i^*, \underline{z})\right] \quad \ldots\ldots\ldots\ldots\ldots \quad (2.14)$$

where * denotes evaluation at the minimizing values. Depending upon the form of $F_i'(\underline{w}_i, \underline{u}_i, \underline{z})$, equation (2.14) may give an explicit expression for the gradient vector, in which case an efficient gradient numerical optimization algorithm can be employed at the supremal level. Often, though, this is not possible as w and u are functions of z and cannot be explicitly solved.

In summary, the interaction prediction approach solves the problem

$$\begin{aligned} &\min_{\underline{z}} P(z) \\ &\text{subject to } P(z) = \sum_{i=1}^{N} \min_{\underline{w}_i, \underline{u}_i} F_i'(\underline{w}_i, \underline{u}_i, \underline{z}) \\ &\quad \text{and } \underline{f}_i'(\underline{w}_i, \underline{u}_i, \underline{z}) = 0 \\ &\quad\quad \underline{g}_i'(\underline{w}_i, \underline{u}_i, \underline{z}) \leq 0 \quad \ldots\ldots\ldots\ldots\ldots\ldots \quad (2.15) \end{aligned}$$

Figure 2.8 shows the multilevel scheme obtained in the particular case of two interacting subsystems.

The interaction prediction principle is an example of a feasible coordination strategy in which <u>all</u> intermediate results of the iterative optimization can be applied directly to the real process and, hence, can be directly applied on-line. This occurs because the intervention inputs are the interconnection variables in a model of the real process and, hence, the interconnection constraints are always satisfied. There is, however, a situation whereby the above principle fails. In this case, the number of manipulated inputs is less than the intermediate outputs and therefore gives rise to over-determined subsystem problems at the infimal level. In order to solve such a problem, it is necessary to use some other decomposition technique (e.g. see section 2.7.2), or a global technique. The latter is a real possibility since here the number of controls is smaller than the number of outputs, and therefore all multilevel decomposition methods are less appealing. An alternative is the use of a penalty function method.

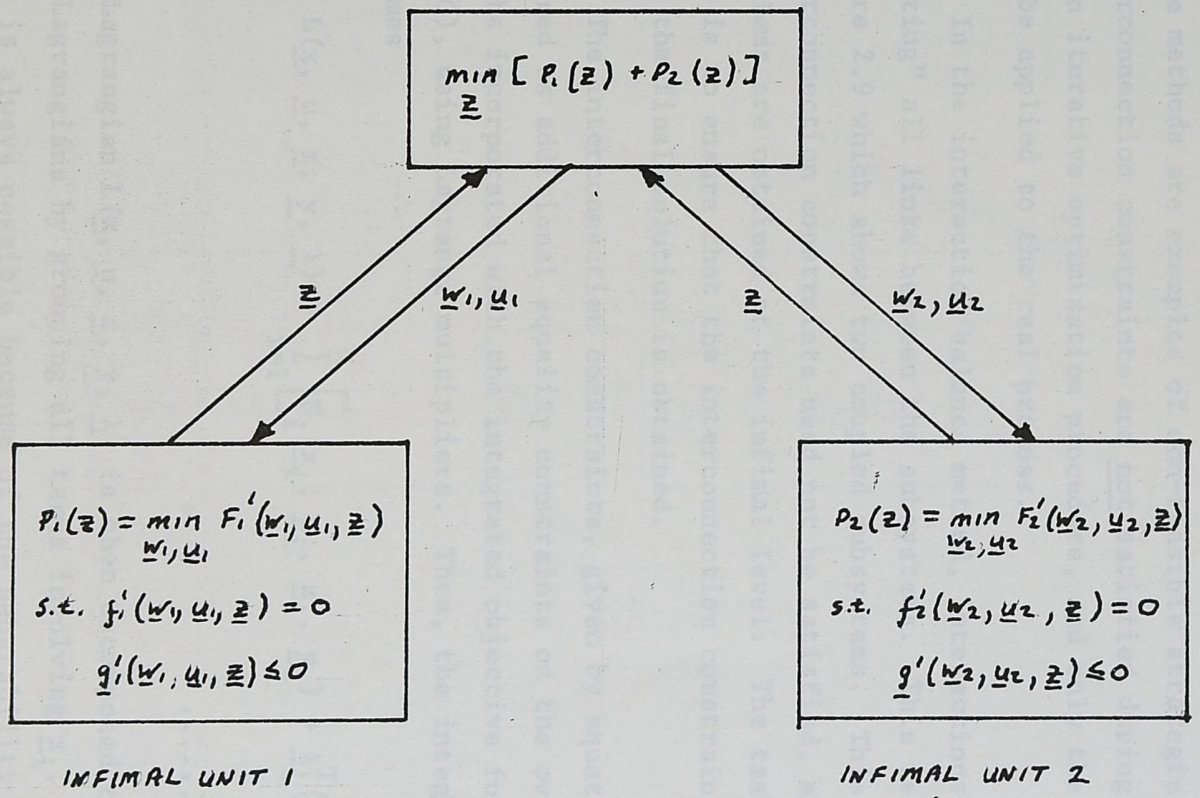

FIG. 2.8 MULTI-LEVEL SOLUTION USING THE INTERACTION PREDICTION PRINCIPLE

2.4.2 Interaction balance principle

This principle is also known by alternative names of coordination methods in this category, viz:

(i) goal coordination
(ii) price coordination
(iii) dual coordination.

These methods are examples of non-feasible strategies in that the interconnection constraints are not satisfied during the initial stages in an iterative optimization procedure, and only the final solution can be applied to the real process.

In the interaction balance method, interactions are removed by "cutting" all links between the subsystems. This is illustrated in Figure 2.9 which shows two coupled subsystems. This means that the interconnection constraints need not be satisfied, and independent subproblems are obtained at the infimal level. The task of the supremal unit is to ensure that the interconnection constraints are satisfied when the final solution is obtained.

The interconnection constraints, given by equation (2.4) are considered as additional equality constraints on the overall problem and may be incorporated with the integrated objective function, equation (2.10), using Lagrange multipliers. Then, the integrated Lagrangian becomes

$$L(\underline{x}, \underline{u}, \underline{z}, \underline{y}, \underline{\lambda}) = \sum_{i=1}^{N} \left[F_i(\underline{x}_i, \underline{u}_i, \underline{z}_i, \underline{y}_i) + \underline{\lambda}_i^T \left(\underline{z}_i - \sum_{j=1}^{N} [C_{ij}] \underline{y}_j \right) \right] \quad \ldots\ldots\ldots\ldots\ldots \quad (2.16)$$

The Lagrangian $L(\underline{x}, \underline{u}, \underline{z}, \underline{y}, \underline{\lambda})$ is then decomposed to form individual sub-Lagrangians by grouping all terms involving $\underline{x}_i$, $\underline{u}_i$, $\underline{z}_i$ and $\underline{y}_i$. This is always possible because of the separability assumptions in equations (2.2) and (2.10). Hence, the i^{th} infimal unit problem is

$$\min_{\underline{x}_i, \underline{u}_i, \underline{z}_i, \underline{y}_i} \left[F_i(\underline{x}_i, \underline{u}_i, \underline{z}_i, \underline{y}_i) + \underline{\lambda}_i^T \underline{z}_i - \sum_{k=1}^{N} \underline{\lambda}_k^T [C_{ki}] \underline{y}_i \right]$$

$$\text{subject to} \quad \underline{f}_i(\underline{x}_i, \underline{u}_i, \underline{z}_i) = 0$$

$$\underline{g}_i(\underline{x}_i, \underline{u}_i, \underline{z}_i) \leq 0$$

$$\underline{y}_i = \underline{h}_i(\underline{x}_i, \underline{u}_i) \quad \ldots\ldots\ldots\ldots\ldots \quad (2.17)$$

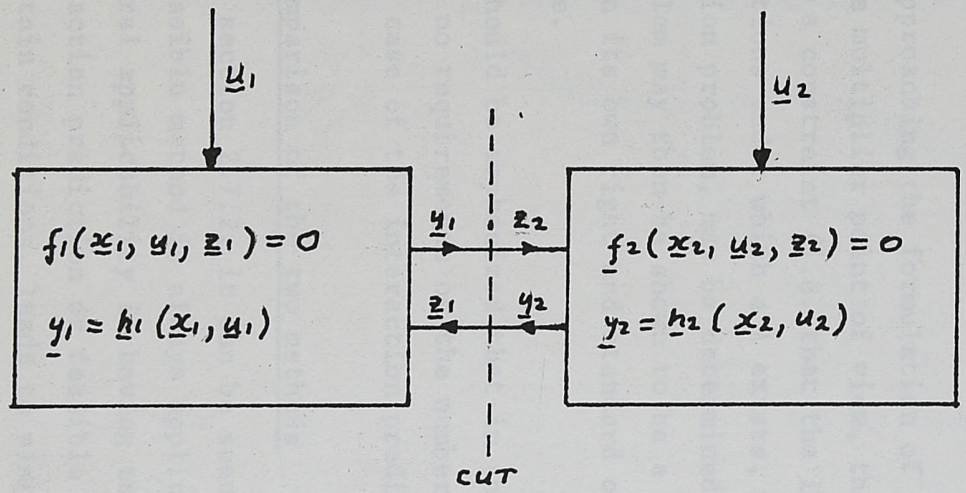

FIG. 2.9 CUTTING THE LINKS BETWEEN SUBSYSTEMS

Note that the goals of the individual subsystems have been modified, in that coordinating variables $\underline{\lambda}$ enter each subsystem objective function. The task of the supremal unit is to choose the coordinating variables to force interaction balance which is achieved when the interconnection constraints

$$\underline{z} = [C]\, y \qquad \ldots\ldots\ldots\ldots\ldots\ldots \quad (2.18)$$

are satisfied. The multilevel scheme for the particular case of the two interacting subsystems, shown in Figure 2.9, is illustrated in Figure 2.10.

By approaching the formulation of the optimization problem from a Lagrange multiplier point of view, the penalty functions may be viewed as a constraint (i.e. that the interactions must balance) and the conditions under which a λ exists, which solves the integrated optimization problem, may be determined. Furthermore, the supremal unit problem may then be shown to be a well-behaved optimization problem in its own right and standard optimization techniques are applicable.

It should be emphasized that in the interaction balance method there are no requirements on the number of components of u_i, z_i and y_i as in the case of the interaction prediction method.

2.4.3 Comparison of the two methods

From section 2.7.2, it can be seen that the interaction balance or non-feasible method is always applicable, but the price to pay for this general applicability is having to solve more complex sub-problems. The interaction prediction or feasible method, which is only applicable under certain conditions, leads to simplifications and an easier implementation.

In both of the two methods, it has been assumed that there already is a division of the system into the various subsystems. However, there does not exist, at the present time, any well-established rule for dividing systems into subsystems, although several researchers (Sage, 1977; Evans et al, 1980) have investigated the use of graph theory methods for the division of systems into subsystems. In view of this it should be noted that the above results could perhaps be used as general guidelines for this purpose. Thus, if a feasible method is to be used, so as to satisfy the interconnection constraints at each

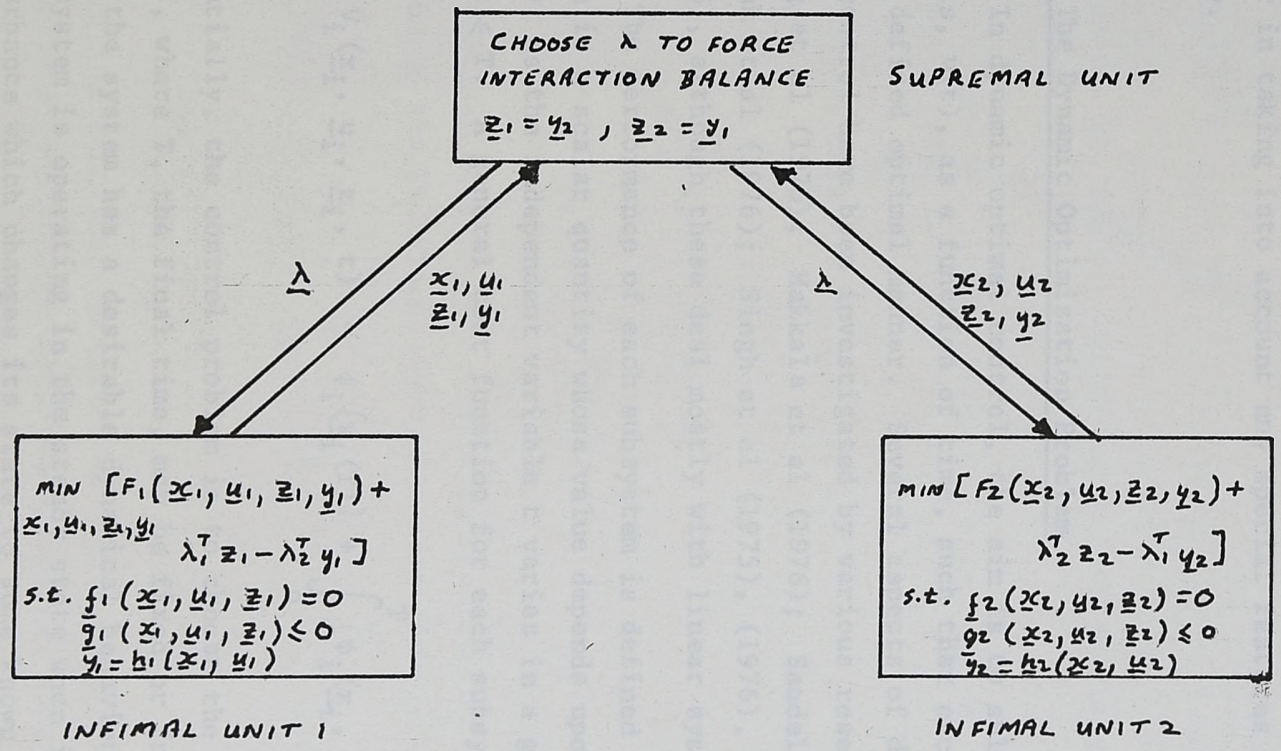

FIG. 2.10 MULTI-LEVEL SOLUTION USING THE INTERACTIVE BALANCE PRINCIPLE

instant, then a decomposition is needed such that the manipulated inputs are greater than or equal to the number of intermediate outputs. On the other hand, the non-feasible method allows a bigger choice for the decomposition and any physical peculiarities of the system could be taken into account. In general, it should be noted that the decomposition of the system and the multilevel optimization should not be done completely independently, but rather they should complement each other in taking into account any special features of the system under study.

2.5 The Dynamic Optimization Problem

In dynamic optimal control, the aim is to select the manipulated inputs, u(t), as a function of time, such that each subsystem behaves in a defined optimal manner. Several aspects of dynamic optimization and control have been investigated by various researchers, namely: Chong et al (1975); Hakkala et al (1976); Sandell et al (1976); Siljak et al (1976); Singh et al (1975), (1976), (1978); Tamura (1975), although these deal mostly with linear systems.

The performance of each subsystem is defined by a functional which is a scalar quantity whose value depends upon $\underline{x}_i(t)$, $\underline{u}_i(t)$ and $\underline{z}_i(t)$, as the independent variable t varies in a given time interval $0 \leq t \leq T$. A general cost function for each subsystem can be given as

$$V_i(\underline{x}_i, \underline{u}_i, \underline{z}_i, t) = \phi_i\left(\underline{x}_i(T)\right) + \int_0^T \psi_i(\underline{x}_i, \underline{u}_i, \underline{z}_i, t)dt \quad (2.19)$$

Essentially, the control problem is to choose the control trajectories, $\underline{u}_i(t)$, where T, the final time, may be fixed or free, so as to ensure that the system has a desirable dynamical behaviour. For example, if the system is operating in the steady state when it receives an unknown disturbance which changes its state to some known or measurable state, then the desirable dynamical behaviour could be represented by the control vector $\underline{u}_i$ which minimizes the cost function in equation (2.19). In this cost function, ϕ_i and ψ_i are, in general, scalar non-linear functions. The term $\phi_i\left(\underline{x}_i(t)\right)$, in the cost function, ensures that at the final time T, the state vector $\underline{x}_i$ will approach some target state. The integral ensures that over the optimizations interval, excessive

control effort is not being expended and also it does not allow significant deviations from any given desired trajectories that the control system is required to follow.

Minimization of V_i should take account of any given inequality constraints, defined by equation (2.2), and any given boundary condition on $\underline{x}_i$. For simplicity, assume that all initial conditions on $\underline{x}_i$ are known, viz:

$$\underline{x}_i(0) = \underline{x}_i 0, \quad i = 1, 2, \ldots, N \qquad \ldots\ldots\ldots\ldots \quad (2.20)$$

Hence, the dynamic optimization problem for each subsystem may be summarized as

$$\min_{\underline{x}_i,\ \underline{u}_i,\ \underline{z}_i,\ \underline{y}_i} \left[\phi_i\left(\underline{x}_i(T)\right) + \int_0^T \psi_i(\underline{x}_i,\ \underline{u}_i,\ \underline{z}_i,\ t)dt \right]$$

$$\text{subject to } \dot{\underline{x}}_i = \underline{f}_i(\underline{x}_i,\ \underline{u}_i,\ \underline{z}_i)$$

$$\underline{g}_i(\underline{x}_i,\ \underline{u}_i,\ \underline{z}_i) \leq 0$$

$$\underline{y}_i = \underline{h}_i(\underline{x}_i,\ \underline{u}_i)$$

$$\underline{z}_i = \sum_{j=1}^{N} [C_{ij}] y_j \qquad \ldots\ldots\ldots\ldots\ldots\ldots \quad (2.21)$$

The cost function for the integrated system is considered to be the sum of the individual subsystem cost functions, giving

$$V(\underline{x},\ \underline{u},\ \underline{z},\ t) = \sum_{i=1}^{N} \left[\phi_i\left(\underline{x}_i(T)\right) + \int_0^T \psi_i(\underline{x}_i,\ \underline{u}_i,\ \underline{z}_i,\ t)dt \right]$$

$$\ldots\ldots\ldots\ldots \quad (2.22)$$

Both the interaction prediction and interaction balance techniques can be employed to decompose the dynamic optimal control problem. The application of multilevel optimization theory will be illustrated here by employing the interaction balance principle.

In a similar manner as employed in the static optimal control situation, the interconnection constraints are incorporated with the integrated performance functional to give

$$J(\underline{x}, \underline{u}, \underline{z}, t) = \sum_{i=1}^{N} \left\{ \phi_i(\underline{x}_i(t)) + \int_o^T \left[\psi_i(\underline{x}_i, \underline{u}_i, \underline{z}_i, t) + \underline{\lambda}_i^T (\underline{z}_i - \sum_{j=1}^{N} [C_{ij}] \underline{y}_j) \right] dt \right\} \quad \ldots\ldots\ldots \quad (2.23)$$

where, in the dynamic case, the Lagrange multipliers $\underline{\lambda}_i$ are functions of time.

The modified integrated performance functional can then be decomposed into modified subsystem performance functionals by grouping together all terms involving $\underline{x}_i$, $\underline{u}_i$, $\underline{z}_i$ and $\underline{y}_i$. This gives the i^{th} infimal unit problem as:

$$\min_{\underline{x}_i, \underline{u}_i, \underline{z}_i, \underline{y}_i} \left\{ \phi(\underline{x}_i(T)) + \int_o^T \left[\psi_i(\underline{x}_i, \underline{u}_i, \underline{z}_i, t) + \underline{\lambda}_i^T \underline{z}_i - \sum_{k=1}^{N} \underline{\lambda}_k^T [C_{ki}] \underline{y}_i \right] dt \right\}$$

$$\text{subject to } \dot{\underline{x}}_i = \underline{f}_i(\underline{x}_i, \underline{u}_i, \underline{z}_i)$$

$$\underline{g}_i(\underline{x}_i, \underline{u}_i, \underline{z}_i) \leq 0$$

$$\underline{y}_i = \underline{h}_i(\underline{x}_i, \underline{u}_i) \quad \ldots\ldots\ldots\ldots \quad (2.24)$$

and Pontryagin's Maximum Principle may be employed to attempt the solution of each infimal unit sub-problem.

Under certain conditions, the solution of equation (2.23) can be given by

$$\max D(\underline{\lambda}(t)) = \min_{\underline{x}, \underline{u}, \underline{z}, \underline{y}} J(\underline{x}, \underline{u}, \underline{z}, \underline{\lambda}, t) \quad \ldots\ldots\ldots \quad (2.25)$$

which is commonly known as dual formulation. At the supremal level, the λ trajectory can be improved in order to maximise $D(\underline{\lambda}(t))$. This can be done by using the steepest descent method, i.e. from iteration k to k + 1

$$\underline{\lambda}(t)^{k+1} = \lambda(t)^k + \alpha^k \underline{d}^k \quad \ldots\ldots\ldots\ldots\ldots\ldots \quad (2.26)$$

where

$$\underline{d} = \nabla D(\underline{\lambda}(t)) = \int_o^T (\underline{z}_i^*(t) - \sum_{k=1}^{N} [C_{ki}] \underline{y}_i^*(t)) dt \quad \ldots\ldots\ldots \quad (2.27)$$

and the * indicates optimal values obtained by solving the infimal level sub-problems for a given $\underline{\lambda}(t)$.

At the optimum, $\underline{d}^k \to 0$ and the appropriate Lagrange multiplier trajectory is the optimum one.

In general, equation (2.25) may not be valid, so that maximizing $D\{\underline{\lambda}(t)\}$, using a hierarchical structure, may not give the optimal control. This situation occurs when the values on the L.H.S. and R.H.S. of equation (2.25) are different and this difference is commonly known as the "duality gap". An excellent study of duality in non-linear systems has been made by Geoffrion (1971). Unfortunately, at the present time, it cannot be said a priori for any given problem if there will be a duality gap. Nevertheless, the method has an intrinsic simplicity which makes it highly attractive. It is worth noting here that the above gradient type of approach can also be applied in the static optimal control case.

3.0 SYSTEM DESCRIPTION

Automatic control of a modern steel plant, whether achieved by a computer-based system or by conventional means, involves an extensive system for the automatic monitoring of a vast number of different variables operating under a wide range of process dynamics. Figure 3.1 shows the major processes concerned with the manufacture of steel. If under computer control, a normal requirement would be for the development of a large number of complex, usually non-linear relationships for the translation of the plant variable values into the required control commands. In addition to the control decisions undertaken by the computer, plant personnel, both operating and management, must be kept aware of the current status of the plant and of each of its processes.

Whether by conventional or a computer-based control system, the operation of a typical steel plant, as shown in Figure 3.1, would involve a number of processes as outlined in Table 3.1.

Table 3.1

Processes associated with a typical steel plant

(i) The blast furnace is used for iron ore reduction. It is quite possible that a computer control system would accommodate varying analyses of blast furnace charging materials.

(ii) The basic oxygen furnace and the electric furnace are used for refining pig iron to steel. Online adaptive control would be necessary for these processes in order to minimize the energy input whilst still maintaining a high quality of steel output.

(iii) Conversion of molten steel to slabs for the rolling mills is carried out by a continuous casting machine and a combination of ingot casting, ingot storage, soaking pit and slabbing mill processes. These are considered to operate both alternately and in parallel as two separate processes.

(iv) Forming and related operations normally consist of the following processes:

(a) Slab conditioning

(b) Reheat furnace

(c) Reversing mill

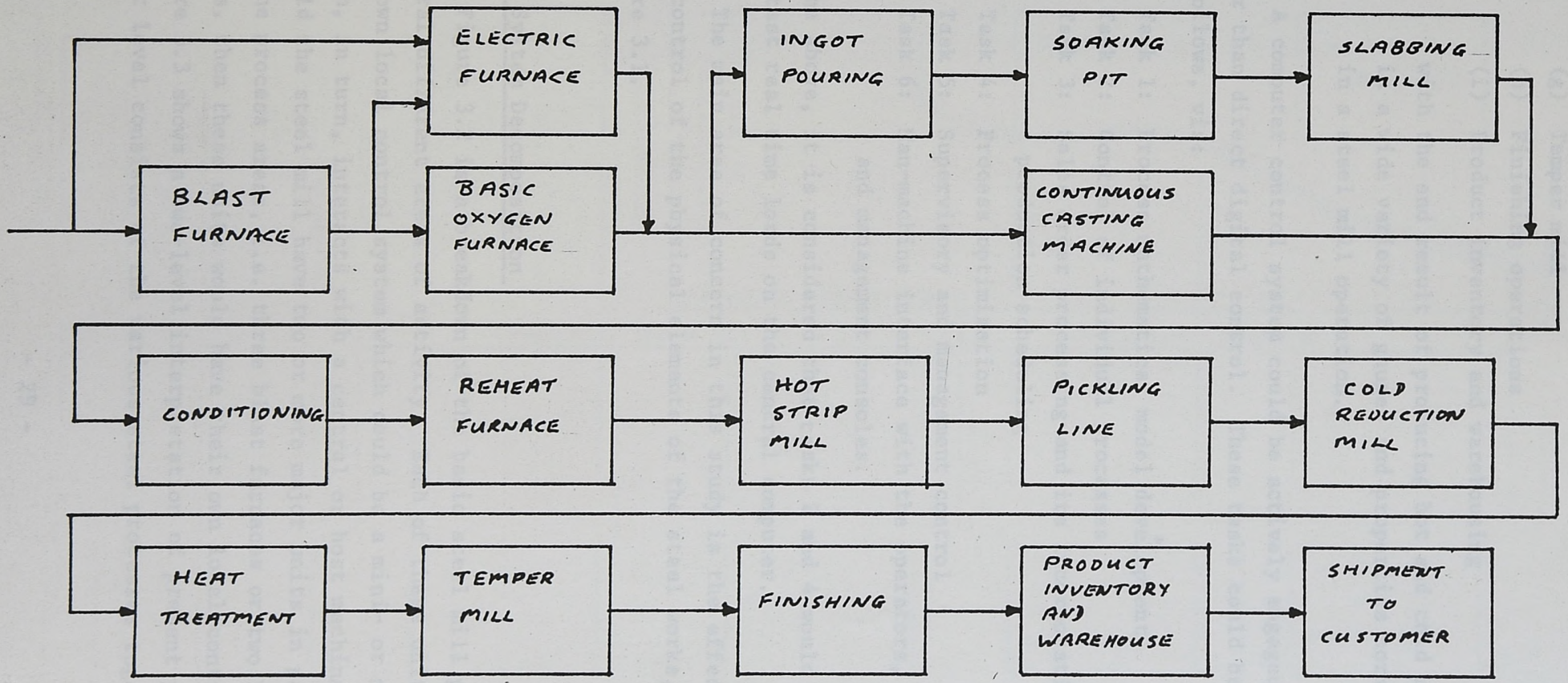

FIG. 3.1. THE MAJOR FLOW OF STEEL IN A BASIC STEEL MILL

(d) Pickling line
(e) Cold reduction mill
(f) Heat treating
(g) Temper mill
(h) Finishing operations
(i) Product inventory and warehousing

with the end result of producing hot and cold rolled steel in a wide variety of gauges and properties normally involved in a steel mill operation.

A computer control system could be actively engaged in tasks other than direct digital control. These tasks could be broken down as follows, viz:

Task 1: Process mathematical model development
Task 2: Control of individual processes
Task 3: Sales order processing and its incorporation into production scheduling
Task 4: Process optimization
Task 5: Supervisory and management control
Task 6: Man-machine interface with the operators, supervisors and management consoles.

Of the above, it is considered that tasks 2 and 4 would represent the greatest real time loads on the central computer.

The main area of concern in this study is the effective decomposition and control of the physical elements of the steel works, as indicated by Figure 3.1.

3.1 System Decomposition

Figure 3.2 is a breakdown of the basic steel mill process into several different areas of activity. Each of these units would have its own local control system which could be a mini- or micro-computer, which, in turn, interacts with a central or host machine. In addition, should the steel mill have two or more major units in parallel in any of the process areas, i.e. three blast furnaces or two hot rolling mills, then these units would have their own local control systems. Figure 3.3 shows a two-level interpretation of present practice. The first level consists of the various steel processes together with their

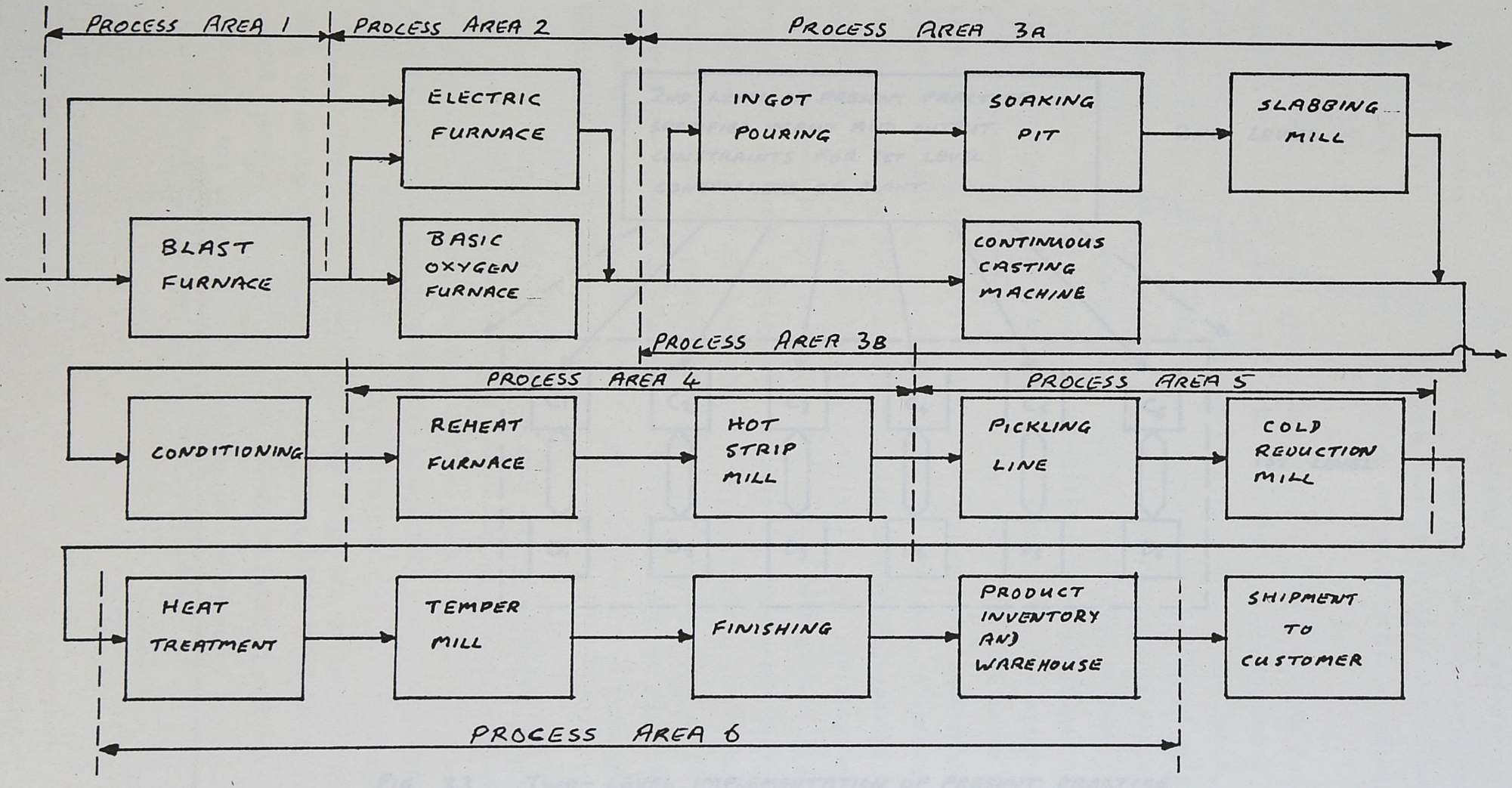

FIG. 3.2. MODIFICATION OF STEEL MILL SKETCH TO SHOW PROCESS CONTROL AREAS

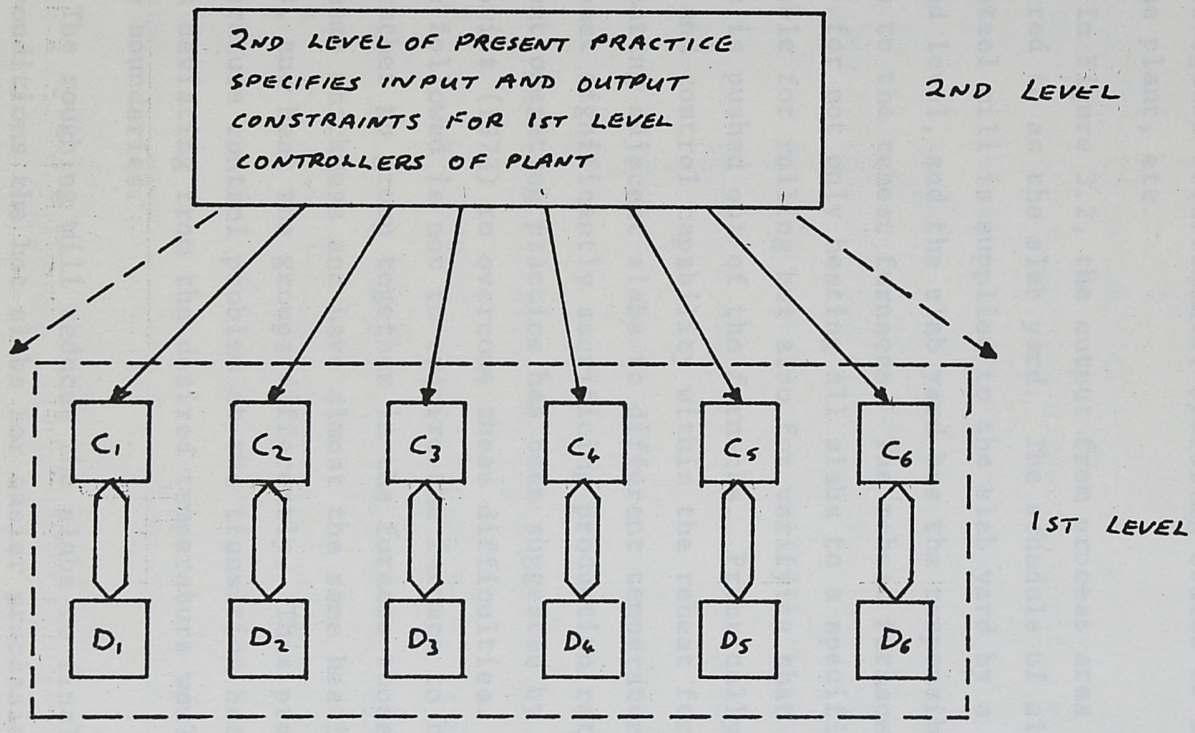

FIG. 3.3 TWO-LEVEL IMPLEMENTATION OF PRESENT PRACTICE

associated controllers. These are represented by D_i and C_i, i = 1, 6, respectively. The second level simply specifies the input and output constraints (production sequence, heating, rolling temperatures, etc.) which are commands to be followed by the plant subprocess controllers. Motivating these decisions are such factors as order specification, metallurgical requirements, operating status of other processing portions of the plant, etc.

In Figure 3.2, the output from process area 3 will in future be referred to as the slab yard. The schedule of slab sequences through the steel mill is supplied to the slab yard by a higher level, i.e. second level, and the slab yard has the responsibility of delivering slabs to the reheat furnaces. The reheat furnaces have the responsibility for not only heating all slabs to a specified uniform temperature suitable for rolling but also for verifying that the proper sequence of slabs is pushed out of the furnaces. Practically, the state of measurement and control capability within the reheat furnaces makes the task of heating adjacent slabs to different temperatures impossible without at least significantly sacrificing production rate. A modification to current operating practice has been suggested by Matuszewski and Lefkowitz (1973) to overcome these difficulties. The strategy suggested to be followed is not to require the furnace to heat each slab differently, but rather to group together in the furnace those slabs that are almost the same thickness and have almost the same heating temperature requirements, and heat the groups differently. This procedure still has the temperature control problem at the transition between groupings, and slabs deviating from the desired temperature would be expected at the group boundaries.

The roughing mill reduces the slabs to final width, and shapes and conditions the hot slabs for easier processing by the finishing mill. A delay table is incorporated after the roughing mill to allow slabs which are too hot for finishing to be cooled, and also to allow unacceptable slabs to be removed. In the finishing mill, the roughened slabs are transformed into ribbons of steel which are cooled by a water spray to a temperature suitable for coiling. When the strips are completely coiled, they are removed from the coiler, weighed, bundled to prevent uncoiling and tagged with identifying characteristics before being put on a conveyor for storage or further processing.

Matuszewski (1970) has made a study of the multilevel model of present practice and has outlined the input and output interactions between sub-processes, together with their constraints. Figure 3.4 is a block diagram showing the interaction constraint specifications. The next stage is to identify the input/output constraints for each sub-process in turn.

3.1.1 Slab yard sub-process - D_1-

The interaction input has two components, viz:

u_{11} = sequence of slabs into steel mill

u_{12} = delivery schedule of slabs to the slab yard.

These are given specified values by the second-level schedulers, viz:

α_{11} = specified sequence of slabs into steel mill

α_{12} = specified delivery schedule of slabs.

The interaction from the slab yard to the reheat furnaces is expressed as two components:

y'_{11} = output sequence of slabs from slab yard

y'_{12} = production rate or pacing of slabs from slab yard

which are also given specified values by the second-level unit

α_{21} = specified output sequence of slabs from slab yard

α_{22} = specified production rate or pacing of slabs from slab yard.

The slab yard cost, G_1, can be broken into three areas, viz:

(i) the cost of handling the slabs upon receipt
(ii) the manipulation and conditioning of slabs
(iii) handling them for output sequencing and pacing.

It is assumed that the slab yard is capable of meeting the specifications (α_{21}, α_{22}) and that there are various ways that slabs can be handled by the control, m_1. The local decision problem is to minimize slab handling costs, subject to the above specifications.

Thus,

$$G_1(m_1, \underline{y}_1, \underline{u}_1) = G_1(m_1, (\underline{\alpha}_2, y''_1), \underline{\alpha}_1)$$

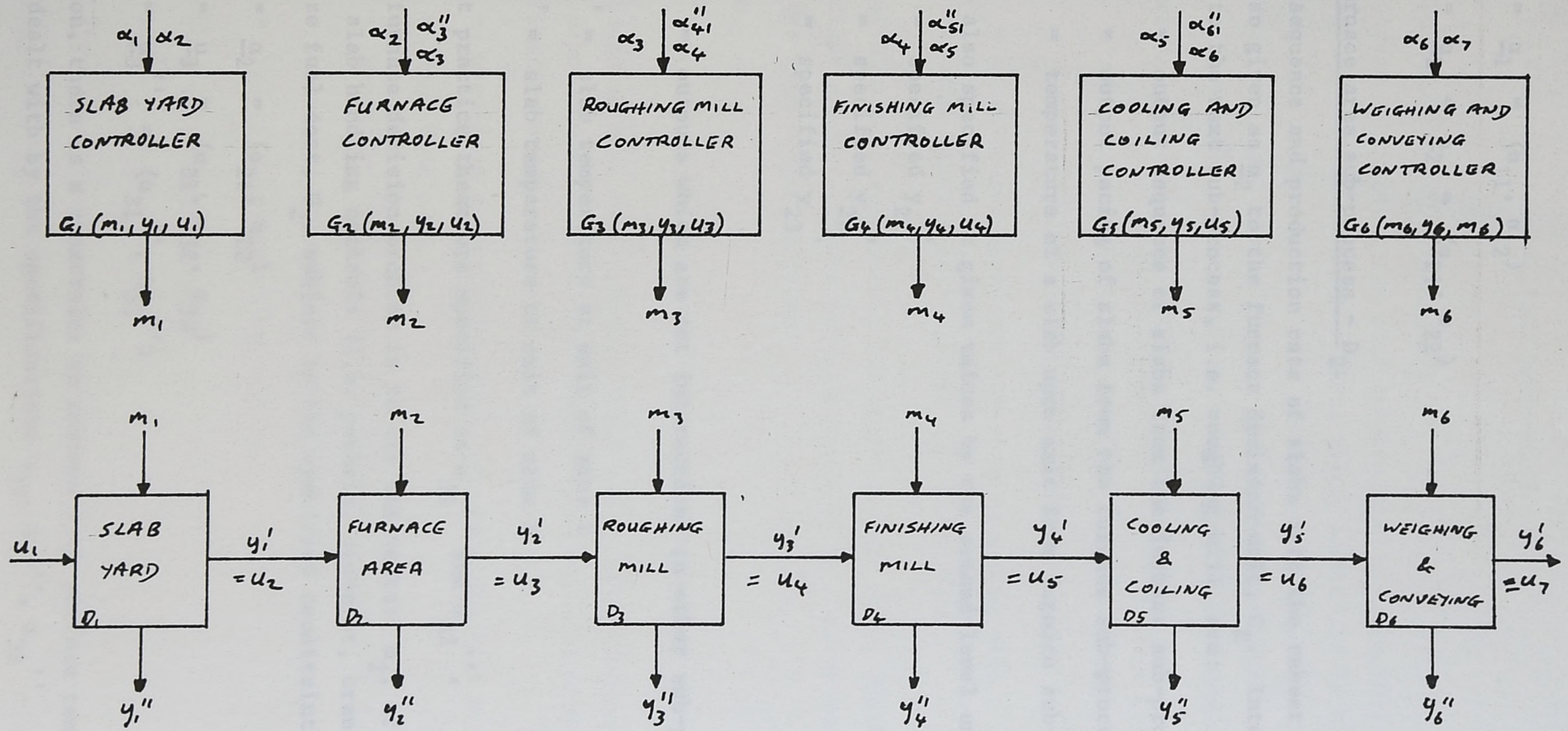

FIG. 3.4 BLOCK DIAGRAM SHOWING INPUT AND OUTPUT INTERACTION CONSTRAINT SPECIFICATIONS

and the constraints are represented by

$$\underline{u}_1 = \underline{\alpha}_1 = (\alpha_{11}, \alpha_{12})$$

$$\underline{y}_1' = \underline{u}_2 = \underline{\alpha}_2 = (\alpha_{21}, \alpha_{22})$$

3.1.2 Furnace area sub-process - D_2-

The sequence and production rate of slabs into the reheat furnace, $\underline{u}_2$, is also given as $\underline{\alpha}_2$ to the furnace decision unit, C_2. Interaction variables to the next sub-process, i.e. roughing mill, are:

y_{21}' = output sequence of slabs from the furnace sub-process

y_{22}' = output pacing of slabs from the furnace sub-process

y_{23}' = temperature of a slab upon exit from furnace sub-process.

These are also specified at given values by the second-level unit as

α_{31} = specified y_{21}'

α_{32} = specified y_{22}'

α_{33} = specified y_{23}'

Now,

$\underline{y}_2''$ = outputs which are not interactions to other sub-processes

where

y_{21}'' = slab temperature at exit of zone 1

y_{22}'' = slab temperature at exit of zone 2.

In current practice these are specified as α_{31}'' and α_{32}''.

The furnace decision problem is to use the vector, m_2, of fuel rates and slab handling controls (i.e. pushers, conveyor, crane, etc.) to minimize fuel cost, G_2, subject to the specified constraints

$$\underline{u}_2 = \underline{\alpha}_2 = (\alpha_{21}, \alpha_{22})$$

$$\underline{y}_2' = \underline{u}_3 = (\alpha_{31}, \alpha_{32}, \alpha_{33})$$

$$\underline{y}_2'' = \underline{\alpha}_3'' = (\alpha_{31}'', \alpha_{32}'')$$

In addition, there is a constraint on maximum slab surface temperature which is dealt with by the specifications α_{33}, α_{31}'', α_{32}''. The

maximum surface temperature is defined by

α_{34} = slab surface melting temperature.

3.1.3 Roughing mill sub-process - D_3.

Input sequence, pacing and slab temperature, u_3, are the inputs to the roughing mill sub-process. These are specified to be α_3 by the second-level unit. The roughing mill decision unit, C_3, has to minimize the power cost, G_3, and manipulate m_3, the vector of reversing mill roll settings for gauge and width reductions and table roller speeds.

Interaction variables to the next sub-process are

y_{31}' = sequence of slabs from roughing mill

y_{32}' = pacing of slabs from roughing mill

y_{33}' = slab temperature upon exit from roughing mill

y_{34}' = slab gauge after roughing mill reduction.

The mill is also responsible for achieving the final width required for the coiled product. These are components of y_3'' which are not interactions with other subsystems.

Hence,

y_{31}'' = width of slab at exit from roughing mill.

The roughing mill roll speed is fixed and is not a degree of freedom. Also, the mill cannot influence the sequence of slabs. Hence, the specification constraints are:

α_{41} = specified sequence of slabs from roughing mill = α_{31}

α_{42} = specified pacing

α_{43} = specified lower limit on slab temperature upon exit

α_{44} = specified gauge to be achieved

α_{41}'' = specified width to be achieved.

The constraint relationships are:

(i) $y_{31}' = \alpha_{41}$

$y_{32}' = \alpha_{42}$

$y_{33}' \geq \alpha_{43}$

$y_{34}' = \alpha_{44}$

(ii) $y_{31}'' = \alpha_{41}''$

3.1.4 Finishing mill sub-process - D_4

The inputs, u_4, to the finishing mill are the incoming slab speed, sequence, temperature and gauge constraints, α_4. The decision unit, C_4, is responsible for affecting m_4, the finishing mill roll opening settings and roll speed, delay table roller speeds and pusher controls.

The interaction variables to the next sub-process are:

y_{41}' = sequence of strips from finishing mill

y_{42}' = pacing of strips to be coiled

y_{43}' = exit temperature from finishing mill

y_{44}' = strip speed as it leaves finishing mill.

The outputs which are not interactions are:

y_{41}'' = gauge of strip after finishing mill reduction.

The specification constraints, as determined by the supremal unit, are:

α_{51} = specified sequence of strip from the mill - the same as α_{41}, α_{31}

α_{52} = specified pacing

α_{53} = specified lower limit on strip exit temperature

α_{54} = specified maximum last roll speed until strip has been coiled

α_{55} = specified upper limit on slab temperature in order for reduction to be performed on that slab

α_{51}'' = specified gauge to be achieved by the finishing mill.

Hence, the constraints are given by

$y_{41}' = \alpha_{51}$

$y_{42}' = \alpha_{52}$

$y_{43}' \geqslant \alpha_{53}$

$y_{43}' \leqslant \alpha_{55}$

$y_{44}' = \alpha_{54}$

$y_{41}'' = \alpha_{51}''$

The decision unit problem is to minimize power cost subject to the indicated constraints.

3.1.5 Cooling and coiling sub-process - D_5

The inputs to this sub-process are the constraints, α_5, acting on the interactive inputs, u_5.

Outputs, y_5', interacting with the next sub-process, are:

y_{51}' = sequence of coils

y_{52}' = pacing of coils.

Non-interacting outputs, y_5'', are:

y_{51}'' = strip temperature immediately prior to coiling, i.e. coiling temperature.

Specified constraints from the supremal unit are:

α_{61} = specified sequence of coils from the sub-process (the same as α_{51}, α_{41}, α_{31})

α_{62} = specified pacing

α_{61}'' = specified coiling temperature.

Hence, the constraints to be satisfied are:

$y_{51}' = \alpha_{61}$

$y_{52}' = \alpha_{62}$

$y_{51}'' = \alpha_{61}''$

The components of control, m_5, include cooling water flow, spray configuration, coiler thread opening and coiler speed. The cost, G_5, includes the power cost and water cost for coiling and cooling. The decision unit problem is to minimize the power and water costs.

3.1.6 Weighing and conveying sub-process - D_6

The interaction outputs $\underline{y}_6'$, from this sub-process are:

y_{61}' = sequence of conditioned coils from hot mill

y_{62}' = pacing of coils from the hot mill.

Specifications, from the second-level scheduler, are:

α_{41} = specified sequence of coils to be produced by the steel mill (the same as α_{61}, α_{51}, α_{41}, $_{31}$)

α_{42} = specified pacing

Hence, constraints are:

$y_6' = \alpha_4$

The decision unit problem is to minimize the cost of handling the coils and the cost of preparing them for exit from the steel mill process.

3.2 Application of Coordination Theory to the Steel Mill Problem

From the work of Matuszewski (1970), interactions and constraints of the steel mill process have been identified. In order to test the feasibility of applying multilevel optimization to a system of this complexity, a starting point is the multilevel control of two of the subsystems. In this study, the reheat furnace and rolling sub-processes have been chosen as they contain important conflicts. The conflict chosen is that between fuel cost of the furnace subsystem and power cost of the roughing mill. For desirable metallurgical properties, the slabs must complete roughing mill reduction at a temperature above what is called the finishing temperature. This places a lower bound on the temperature at which the slabs leave the reheat furnace in order to allow for cooling losses. There is also an upper bound on temperature, above which the steel is too hot for desired reduction as its metallurgical properties could be altered.

Reheat furnace fuel costs increase with increasing required slab exit temperature, whereas for the roughing mill, power costs increase as resistance of slabs to deformation increases, i.e. low roughing mill input temperature.

The supremal unit problem, then, is to specify the exit temperature from the reheat furnace such that the combined cost of both sub-processes is at a minimum.

3.2.1 Slab reheating furnace optimization

Pike (1969) describes the optimization of a reheat furnace in terms of choosing fuel flow rates to minimise fuel costs subject to achieving a desired slab exit temperature. The mathematical model derived relates average slab temperature, as each slab passes through the furnace, to fuel rates and slab velocity. In addition, an expression for the slab surface temperature is given which is used to test against a surface melting constraint. Two manipulated variables are given,viz. the normalized fuel rates for the preheat and heat zones in the furnace. A complete furnace description, outlining the furnace zones, is given in chapter 4. Optimization is a dynamic optimal control problem to choose the two fuel rates as functions of time in order to minimise a time integral which relates normalized fuel rates to the actual heating cost. Minimization is subject to the differential and algebraic equations of the mathematical model of the reheat furnace, a surface melting constraint, the known slab temperature on input to the furnace and the desired slab temperature at the furnace exit.

Considerable computation is needed to solve the above dynamic optimal control problem, as repeated iterations are needed to solve a two-point boundary value problem. However, due to the policy of grouping together slabs of the same thickness and heating requirements and to the fact that these slabs move through the furnace at a constant velocity, the solution of the optimization problem gives constant fuel rates. In this situation the problem is simplified and reduces to a steady-state optimal control problem.

3.2.2 Rolling mill optimization

Lopresti and Patton (1970) have developed an approach to minimum cost steel rolling in a hot strip reversing mill which determines a sequence of screw settings to give a specified plate thickness and temperature after the final pass. This is achieved at a minimum cost without violating physical limits on force and torque. The cost of rolling a slab is defined as a weighted sum of the total slab pass-time through the mill and the total energy required. Lopresti and

Patton (1970) base their analysis on a reversing mill empirical mathematical model developed by Schulz and Smith (1965) which describes a reversing mill on a pass-by-pass basis as a series of difference equations. The state variables are slab thickness and temperature, and the output variables are roll force, roll torque, time per pass and energy per pass. The control variables are the screw settings for each pass. The optimization problem is formulated as the solution of a dynamic programming problem which determines the required sequence of screw settings.

The dynamic programming solution of the problem is investigated in chapter 5 with the further addition, not accounted for by Lopresti and Patton, that there must be an odd total number of passes of each slab through the reversing mill. This ensures that the slabs exit the reversing mill in the correct direction.

3.3 Mathematical Description

In this section brief mathematical descriptions will be given for both the sub-processes in question. For ease of understanding, the notation in this section will be simplified from that of section 3.1, which is a fairly rigorous breakdown of the various sub-processes.

In the mathematical description of the reheat furnace, it is considered that the air temperature spatial distribution along the furnace length is regulated by local zone temperature controllers whose set points can be manipulated for optimization purposes.

The temperatures of the slabs,in the furnace, are given by:

$$\dot{\underline{\theta}}_f = F_f(\underline{\theta}_f, \underline{u}_f, v_f) \qquad \ldots\ldots\ldots\ldots\ldots\ldots\ldots \quad (3.1)$$

where $\underline{\theta}_f$ is a vector of slab temperatures, $\underline{u}_f$ is a vector of controller set points which determines the furnace air temperature, and v_f is the slabs' speed. Equation (3.1) is subject to boundary conditions, θ_{fi}, the slab temperature at the input to the furnace, and θ_{fo}, the desired slab temperature at exit from the furnace. This is the same as the input to the roughing mill, neglecting cooling.

The zone fuel consumptions are described by:

$$w_f = G_f(\underline{\theta}_f, \underline{u}_f) \qquad \ldots\ldots\ldots\ldots\ldots\ldots\ldots \quad (3.2)$$

which relates fuel flow rates, w_f, to the slab temperatures and zone temperatures.

In addition, there are algebraic inequality constraints:

$$h_f(\underline{\theta}_f, \underline{u}_f, \underline{w}_f, v_f, \theta_{fi}, \theta_{fo}) \leq 0 \quad \ldots\ldots\ldots\ldots\ldots\ldots \quad (3.3)$$

describing, for example, maximum allowable slab surface temperatures, maximum and minimum fuel flow rates, maximum slab speeds, maximum possible number of slabs in the furnace, etc.

In the above mathematical description, the state variables are $\underline{\theta}_f$, the control variables are θ_{fi} and v_f, whilst $\underline{u}_f$ and $\underline{w}_f$ are output variables which are not connected to any other process in the overall hot strip mill. θ_{fo} is an output variable which connects to the reversing mill.

A local objective function for optimizing the reheat furnace performance in terms of achieving minimum fuel consumption and maximum throughput can be defined as:

$$\min_{\theta_{fi},\, v_f,\, \underline{u}_f} \left[p_1 \int_{t_o}^{t_f} F_f(\underline{w}_f)dt - p_2\, G_f(v_f) \right] \quad \ldots\ldots\ldots \quad (3.4)$$

where $F_f(\underline{w}_f)$ relates fuel costs to fuel flow rates and $G_f(v_f)$ relates throughput to slab speed assuming the furnace is loaded to capacity at all times. Coefficients p_1 and p_2 weigh the relative importance of fuel consumption and throughput.

The following mathematical description of the reversing mill is based on the empirical model employed by Lopresti and Patton. The slab thickness and temperature are described by the following six equations, viz:

$$\theta_{i+1} = \theta(\theta_i, h_i, r_i) \quad \ldots\ldots\ldots\ldots\ldots\ldots\ldots\ldots \quad (3.5)$$

$$h_{i+1} = h(\theta_i, h_i, r_i) \quad \ldots\ldots\ldots\ldots\ldots\ldots\ldots\ldots \quad (3.6)$$

$$e_i = e(\theta_i, h_i, r_i) \quad \ldots\ldots\ldots\ldots\ldots\ldots\ldots\ldots \quad (3.7)$$

$$\ell_i = \ell(\theta_i, h_i, r_i) \quad \ldots\ldots\ldots\ldots\ldots\ldots\ldots\ldots \quad (3.8)$$

$$f_i = f(\theta_i, h_i, r_i) \quad \ldots\ldots\ldots\ldots\ldots\ldots\ldots\ldots \quad (3.9)$$

$$\tau_i = \tau(\theta_i, h_i, r_i) \quad \ldots\ldots\ldots\ldots\ldots\ldots\ldots\ldots \quad (3.10)$$

where h_i and θ_i are slab thickness and temperatures at the end of pass i, and s_i is

the screw setting during pass i. e_i is the energy input during the i^{th} pass, ℓ_i the i^{th} pass time, f_i the roll force and τ_i the torque experienced during the i^{th} pass.

Since expressions (3.5) - (3.10) cannot generally be obtained explicitly, an iterative scheme must be employed to find the unknowns θ_{i+1} and h_{i+1} as functions of θ_i, h_i and r_i. The other quantities are then obtained by substitution. The essential point to note here is that (θ_i, h_i) is the state of this process and r_i is the current input. The other variables, e_i, ℓ_i, f_i and τ_i, are outputs.

In addition, there are constraints, viz:

$$h_r(h_i, \theta_i, r_i) \leq 0 \qquad \ldots\ldots\ldots\ldots\ldots\ldots\ldots\ldots \quad (3.11)$$

representing, for example, maximum roll force, maximum torque, temperature constraints, etc.

The local optimization problem is to determine a sequence of roll settings, r_i, which will give an admissible final state of plate thickness and temperature at minimum cost. The objective function can be defined as

$$\min_{r_i} \left[\sum_{i=1}^{N} \left(p_3 F_r(e_i) - p_4 G_r(\ell_i) \right) \right] \qquad \ldots\ldots\ldots\ldots\ldots \quad (3.12)$$

where $F_r(e_i)$ relates power consumption to energy and $G_r(\ell_i)$ relates throughput to time per pass. The output variables, from the reversing mill to the rest of the sub-processes, are the final thickness and temperature of the slabs after the N^{th} (final) pass.

The initial conditions of the slabs on entry to the reversing mill are h_o, the slab thickness, and $\theta_o = \theta_{fo}$, the slab temperature. The initial temperature represents an interconnection variable with the output of the reheat furnace.

3.4 Decomposition using the Interaction Balance Principle

Figure 3.5 shows the decomposition of the two sub-processes, where the first consists of the reheat furnace and the second the reversing mill. The interconnection between the two sub-processes is

The slab temperature from the reheat furnace to the reversing mill.

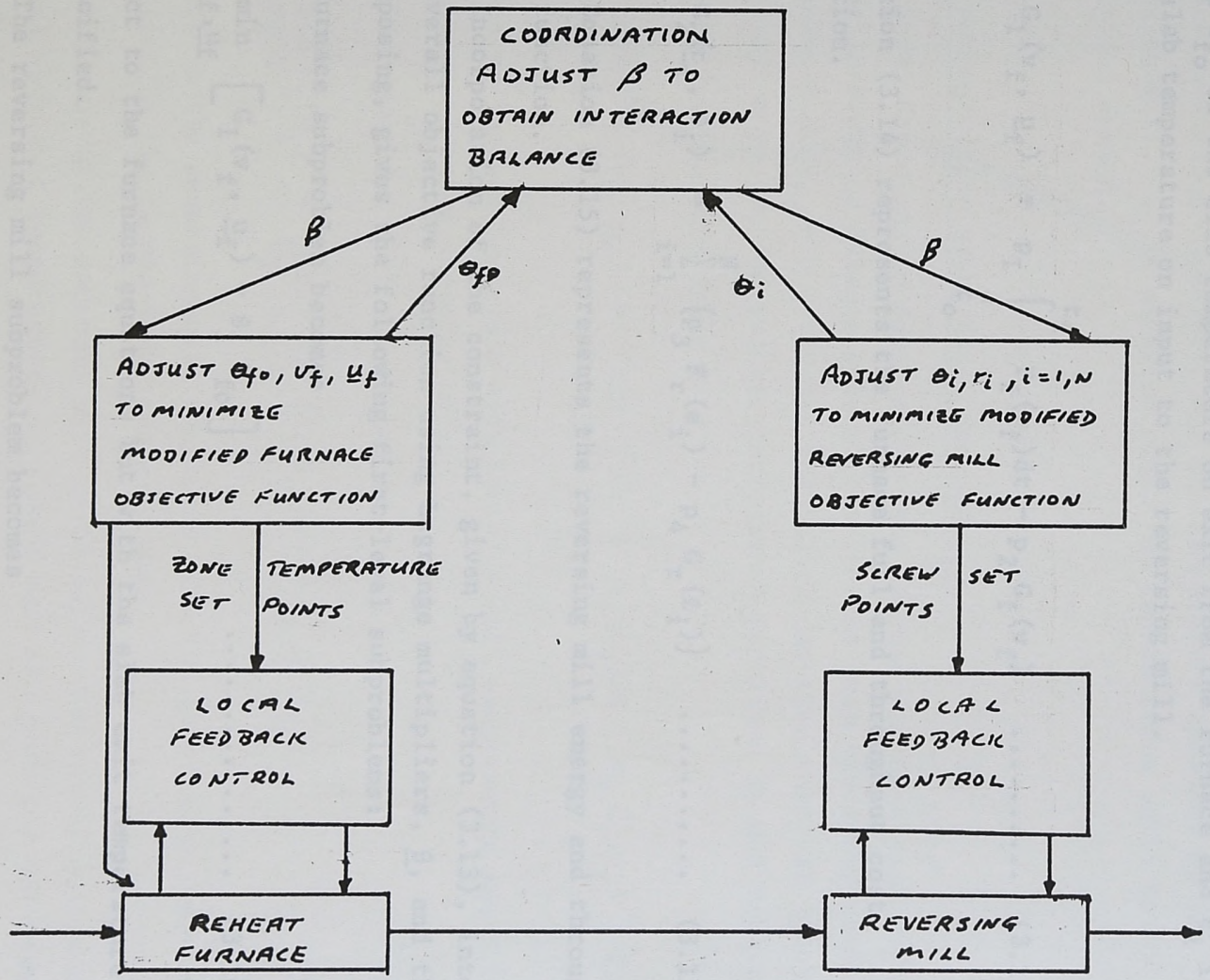

FIG. 3.5 MULTILEVEL SOLUTION USING THE INTERACTION BALANCE PRINCIPLE

In general, the input slab temperature to the furnace from the reversing mill is also an interconnection variable, but in this application the furnace slab input temperature is specified.

Constraints on the system are

$$\theta_{fo} = \theta_i \qquad \ldots\ldots\ldots\ldots\ldots\ldots \quad (3.13)$$

where θ_{fo} is the slab temperature on exit from the furnace and θ_i is the slab temperature on input to the reversing mill.

Let

$$G_1(v_f, \underline{u}_f) = p_1 \int_{t_o}^{t_f} F_f(w_f)dt - p_2\, G_f(v_f) \qquad \ldots\ldots\ldots \quad (3.14)$$

Equation (3.14) represents the furnace fuel and throughput cost function.

Let

$$G_2(\underline{r}_i, \theta_i) = \sum_{i=1}^{N} \left(p_3\, F_r(e_i) - p_4\, G_r(\ell_i)\right) \qquad \ldots\ldots\ldots\ldots \quad (3.15)$$

Equation (3.15) represents the reversing mill energy and throughput cost function.

Incorporation of the constraint, given by equation (3.13), into the overall objective function using Lagrange multipliers, $\underline{\beta}$, and then decomposing, gives the following first-level subproblems:

The furnace subproblem becomes

$$\min_{v_f, \underline{u}_f} \left[G_1(v_f, \underline{u}_f) - \beta_1\, \theta_{fo} \right] \qquad \ldots\ldots\ldots\ldots\ldots \quad (3.16)$$

subject to the furnace equations but with the slab exit temperature unspecified.

The reversing mill subproblem becomes

$$\min_{\underline{r}_i, \theta_i} \left[G_2(\underline{r}_i, \theta_i) + \beta_2\, \theta_i \right] \qquad \ldots\ldots\ldots\ldots\ldots \quad (3.17)$$

subject to the reversing mill equations but with the final slab temperature unspecified.

As the system constraint is $\theta_{fo} = \theta_i$, then $\beta_1 = \beta_2$. The second-level problem is to update the coordination variable, β_1, until the interconnection constraints are satisfied, i.e. when interaction balance is obtained. The first-level decision problems, C_1 and C_2, pick not only the controls $\underline{u}_f$ and $\underline{r}_i$, but, in general, the interaction inputs as well. One method of updating the coordination variable, β_1, is simply by comparing the difference between the slab temperature the furnace is willing to supply, and the temperature demanded by the reversing mill. β_1 is adjusted until the two decision units match supply and demand.

3.5 Decomposition using Model Coordination

Model Coordination employs the same process decomposition as used by the Interaction Balance scheme, but in this case the coordination variable, i.e. $\theta_{fo} = \theta_i$, becomes the interconnection variable itself. Modification to the sub-process performance functions is not required.

The furnace subproblem is

$$\min_{v_f,\, \underline{u}_f} G_1(v_f, \underline{u}_f) = \min_{v_f,\, \underline{u}_f} \left[C_1 \int_{t_o}^{t_f} F_f(w_f)dt - C_2\, G_f(v_f) \right] \quad (3.18)$$

subject to furnace equations with the slab exit temperature specified by the second-level decision unit.

The reversing mill subproblem is

$$\min_{r_i} G_2(s_i) = \min_{r_i} \left[\sum_{i=1}^{N} \left(C_3\, F_r(e_i) - C_4\, G_r(\ell_i) \right) \right] \quad \ldots\ldots \quad (3.19)$$

subject to the reversing mill equations with the input slab temperature specified by the second-level decision unit.

The task of the supremal unit is to adjust the specification of furnace slab exit temperature, θ_{fo}, such that the combined sub-process cost functions are at a minimum, viz:

$$\min_{\theta_{fo}} \left(G_1(v_f, \underline{u}_f) + G_2(r_i) \right) \quad \ldots\ldots\ldots\ldots\ldots\ldots \quad (3.20)$$

Figure 3.6 illustrates the structure for the model coordination scheme. The individual first-level problems are similar to those in the

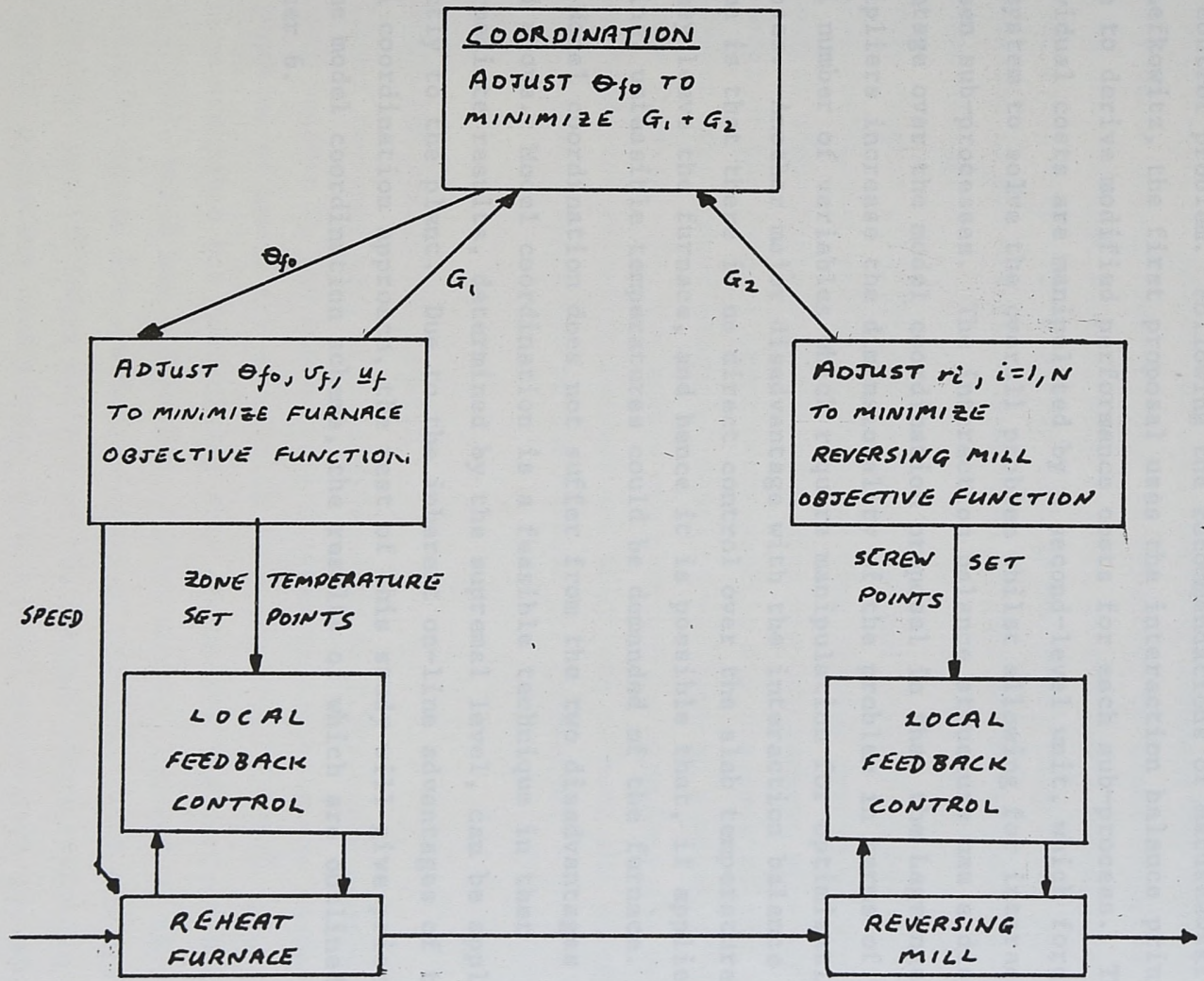

FIG. 3.6 MULTILEVEL SOLUTION USING MODEL COORDINATION

interaction balance scheme and identical considerations of the sub-process optimization solutions are applicable.

3.6 Conclusion

Two proposals have been shown for solving the integrated steel mill control problem. Following the recommendations of Matuszewski and Lefkowitz, the first proposal uses the interaction balance principle to derive modified performance costs for each sub-process. The individual costs are manipulated by a second-level unit, which forces the system to solve the overall problem whilst allowing for interactions between sub-processes. The interaction balance structure has a disadvantage over the model coordination proposal in that the Lagrange multipliers increase the dimensionality of the problem in terms of the total number of variables which require manipulation for optimization purposes. Another major disadvantage with the interaction balance scheme is that there is no direct control over the slab temperatures as they leave the furnace, and hence it is possible that, if applied on-line, unfeasible temperatures could be demanded of the furnace.

Model coordination does not suffer from the two disadvantages outlined above. Model coordination is a feasible technique in that intermediate results, determined by the supremal level, can be applied directly to the plant. Due to the inherent on-line advantages of the model coordination approach, the rest of this study will give priority to the model coordination scheme, the results of which are outlined in chapter 6.

4.0 THE REHEAT FURNACE

The slab reheating furnace forms an integral part of present-day hot strip mill plant. Its function is to heat steel slabs to a temperature sufficient to permit rolling operations without physical damage to the internal structure of the material, at a rate dictated by production requirements, and using minimum power.

Until recently, control of slab reheating furnaces has been almost entirely under manual supervision. As reheating of slabs requires very large amounts of heat energy, when related to the large tonnage rolled in a hot strip mill over a period such as one year, relatively small improvements in the overall consumption of fuel amount to considerable financial savings.

This chapter will attempt to apply optimal control theory to minimize fuel costs, whilst at the same time meeting system constraints. The control study therefore commences with the development of a simplified model of the furnace temperature profile and proceeds to the development of a lumped parameter model of the heating process of a slab in a furnace. The two models are combined to formulate the control problem of a slab reheating furnace and solutions to both the steady-state and dynamic operation of the furnace are presented.

4.1 Modelling the Reheat Furnace

Reheat furnaces have been considered to be distributed parameter in nature because T, the temperature distribution within the furnace, is a function of space ($\bar{x}$) as well as time (t), i.e. $T = T(\bar{x}, t)$. The variables available for controlling this system are the various fuel inputs (U(t)), which are a function of time alone. Therefore, it is reasonable to search for a model in terms of the fuel rates and certain predetermined spatial terms defined by the furnace characteristics under normal operating conditions. Such a model would have the advantage of being lumped parameter in nature.

The modelling of a system may be done before taking data ("a priori") or after ("a posteriori"). The a priori approach has two advantages: it may show the easiest way to collect the relevant data, thus eliminating the irrelevant, and it may also, if used early enough in the design of a system, considerably ease the later control of the system. Modelling a

system prior to design may often mean the difference between an unstable parameter-sensitive system and a stable, less sensitive one. One has only to consider the importance of reliable stable control over fast nuclear reactors and jet aircraft to realise the full significance of this.

The a posteriori approach is often used on existing plant. Sometimes it may consist of simply fitting a three-term controller and adjusting it, if the plant is simple. In more complex plants, such as a five-zone steel reheat furnace, data logging over a year or more may be necessary to obtain sufficient data for a model to be formulated and identified (Pike, 1969).

In his study on the control of a slab reheating furnace, Pike (1969) chose a typical five-zone furnace and made the following assumptions in the derivation of a mathematical model. Figure 4.1 shows a typical five-zone reheat furnace.

(1) Little heating is done in the soak zone, so the problem may be formulated in terms of delivering slabs to this zone at some required average temperature, and model only the first four zones of the furnace.

(2) The upper and lower preheat zones are slaved as are the upper and lower heat zones. In addition, the effect of skids is small enough to be neglected so a symmetric heating process may be considered.

(3) The furnace is loaded with slabs of a uniform length (pushed sideways) so variations across the width of the furnace may be ignored.

In Pike's study, the furnace to be modelled consisted of the preheat and heat zones of the furnace shown in Figure 4.1. The temperature profile is determined, for some given pushing rate and loading, by the fuel input rates for the various zones. Considering this, it is reasonable to seek an expression for $T(\bar{x}, t)$, the temperature distribution in the furnace, of the form

$$T(\bar{x}, t) = T\left(F(x), \bar{U}(t)\right) \qquad \ldots\ldots\ldots\ldots\ldots\ldots \quad (4.1)$$

where $F(x) = \left[f_1(x), \ldots, f_r(x)\right]$ is a set of functions determined by the physical characteristics of the furnace, and $U(t) = \left[u_1(t), \ldots, u_m(t)\right]$

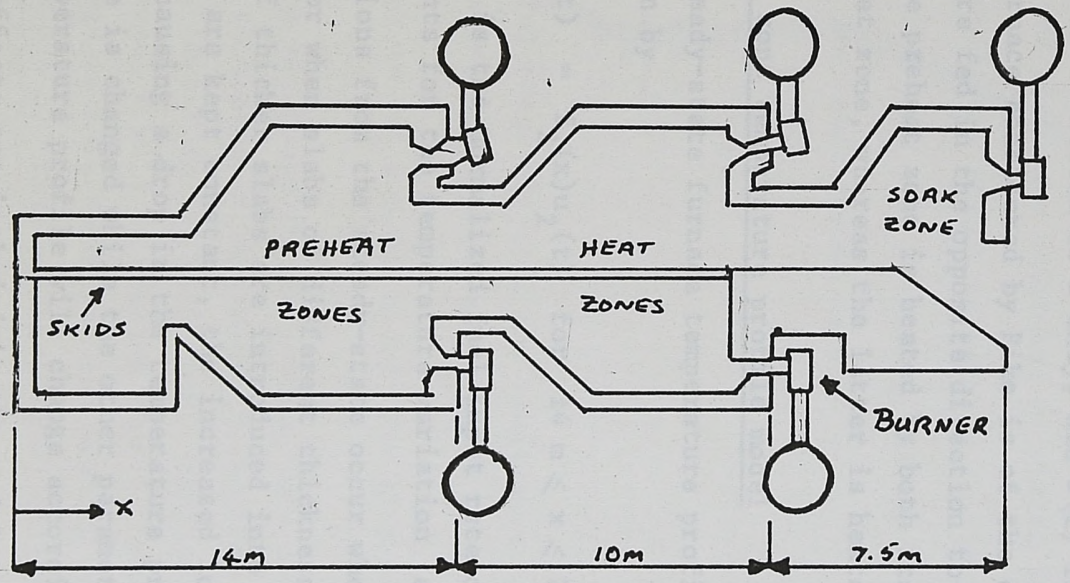

FIG. 4.1 A FIVE-ZONE REHEAT FURNACE

is a lumped parameter control vector. Let x be the position along the length of the furnace and assume that the temperature variation in the other directions is not significant.

Assuming that $T(\bar{x}, t)$ may be represented by the product of a function, then equation (4.1) may be written as

$$T(\bar{x}, t) = f(x)\, U(t) \qquad \ldots\ldots\ldots\ldots\ldots\ldots\ldots \quad (4.2)$$

where $f(x)$ is a function of x only, and $U(t)$ is a function of t only.

The furnace considered by Pike is of the counterflow type, where the slabs are fed in the opposite direction to the flow of gas. Consequently, the preheat zone is heated by both its own burners and by gas from the heat zone, whereas the latter is heated by its own burners.

4.1.1 Heat zone temperature profile model

The steady-state furnace temperature profile in the heat zone may be given by

$$T_H(x, t) = f_2(x)u_2(t) \quad \text{for} \quad 14\ \text{m} \leq x \leq 24\ \text{m} \qquad \ldots\ldots\ldots \quad (4.3)$$

where $u_2(t)$ is the normalized fuel input rate of the heat zone and $f_2(x)$ accounts for the temperature variation along its length.

Deviations from the steady-state occur when either the pushing rate is changed or when slabs of different thicknesses are pushed into the furnace. If thicker slabs are introduced into the furnace while the other slabs are kept constant, the increased load will absorb more heat, thus causing a drop in the temperature profile. Also, if the pushing rate is changed while the other parameters are constant, the furnace temperature profile will change accordingly.

These effects are included in the model equation by letting the load in any zone be directly proportional to the average thickness of the slabs in that zone. Define

w_o = the nominal slab thickness

$\bar{w}_H$ = the average thickness of the slabs in the heat zone

δ_H = the normalized deviation from the nominal load in the heat zone.

δ_H is then given by

$$\delta_H = \frac{\bar{w}_H - w_o}{w_o} \qquad \ldots\ldots\ldots\ldots\ldots\ldots \quad (4.4)$$

Parameter η_H, which will determine the general effect due to loading, is introduced by writing

$$\eta_H = 1 - \beta_H \delta_H \qquad \ldots\ldots\ldots\ldots\ldots\ldots \quad (4.5)$$

where β_H = the heat zone thickness weighting factor.

Introducing the effect of varying v, the push rate, define

β_v = the push rate weighting factor

v_o = the nominal push rate

hence

$$\Phi = 1 - \beta_v \delta_v \qquad \ldots\ldots\ldots\ldots\ldots\ldots \quad (4.6)$$

where

$$\delta_v = \frac{v - v_o}{v_o} \qquad \ldots\ldots\ldots\ldots\ldots\ldots \quad (4.7)$$

Including these effects, the temperature profile in the heat zone, for non-steady-state operation, is given by

$$T_H(x, t) = \eta_H \Phi f_2(x) u_2(t) \quad \text{for } 14 \leqslant x \leqslant 24 \text{ m} \quad \ldots\ldots \quad (4.8)$$

Assuming no change in the pushing rate and the fuel rate, and that the average thickness is increased in the heat zone, then η_H will be less than 1, thus $T_H(x, t)$ will drop. Similarly, if the average thickness is reduced, Φ will be greater than 1, causing $T_H(x, t)$ to rise. With no change in both thickness and pushing rate from their nominal values, $\eta_H = \Phi = 1$. Thus equation (4.8) will be reduced to that of the steady-state case, equation (4.3).

4.1.2 The preheat zone temperature profile

As previously stated, being of the counterflow type, the furnace temperature in the preheat zone is a function of its own fuel input rates, u_1, as well as that from the heat zone, u_2. In the steady-state operation of the furnace, the temperature profile in the preheat zone is given by

$$T_P(x, t) = f_1(x)\, u_1(t) + f_2(x)\, u_2(t) \quad \text{for } 0 \leqslant x \leqslant 14 \text{ m} \qquad (4.9)$$

where $u_1(t)$ is the normalized fuel input rate in the preheat zone and $f_1(x)$ accounts for the temperature variation along the length of the zone. The second term is added to include the effects of the heat zone thermal energy.

By a similar argument to that given in the previous section, define

$$\delta_P = \frac{\bar{w}_P - w_o}{w_o} \qquad \ldots\ldots\ldots\ldots\ldots\ldots\ldots\ldots\ldots\ldots\ldots\ldots \qquad (4.10)$$

where δ_P = the normalized deviation from the nominal load in the preheat zone.

Hence,

$$\eta_P = 1 - \beta_p\, \delta_p \qquad \ldots\ldots\ldots\ldots\ldots\ldots\ldots\ldots\ldots\ldots\ldots \qquad (4.11)$$

where δ_P = the preheat zone thickness weighting factor.

First, consider the effect of varying the loading on the preheat zone temperature-profile. By a similar argument to that given in the formulation of equation (4.8), the preheat zone temperature profile may be written in the form

$$T_P(x, t) = \left(f_1(x)u_1(t) + f_2(x)u_2(t)\eta_H\right)\eta_P \qquad \ldots\ldots\ldots\ldots \qquad (4.12)$$

This allows for the fact that the loading in the preheat zone not only affects this zone but also the temperature profile in the heat zone in the non-steady-state operation of the furnace. Similarly, the effect of varying v, the push rate, can be introduced by modifying equation (4.12) to the form

$$T_P(x, t) = \Phi\left(f_1(x)u_1(t) + f_2(x)u_2(t)\eta_H\right)\eta_P \qquad \ldots\ldots\ldots\ldots \qquad (4.13)$$

$$\text{for } 0 \leqslant x \leqslant 14 \text{ m}$$

Thus, equation (4.13) gives the temperature profile in the preheat zone in the non-steady-state, accounting for changes in thickness and pushing rate.

4.1.3 Description of pilot plant furnace

The furnace on which this study is based is shown, diagrammatically, in Figure 4.2. The furnace is of the travelling load type and has been constructed in the Systems Science Department of The City University (London). It comprises a 2.8 m electrically-heated tunnel and is designed to heat eight blocks of metal, to temperatures of 500°C, at any one time. The heating is achieved using banks of radiators grouped into eight distinct zones situated along the length of the furnace. Such zones can supply a maximum of 6 kW of radiant energy.

The loads are aluminium blocks of dimension 20.32 cm x 20.32 cm x 10.16 cm They are conveyed through the furnace suspended from a conveyor belt which is driven by a D.C. motor. The conveyor belt is formed into a loop to facilitate the recycling of the loads after suitable cooling. The load temperatures are measured using chromel-alumel thermocouples which are inserted inside the individual loads. Measurements from the furnace and control signals to it are carried out under the supervision of an on-line digital computer (Ferranti Argus 500).

The measurement of temperature using thermocouples inserted into the loads is clearly not acceptable in practical situations. At the temperature range envisaged ($\leq 500^{\circ}C$), it is difficult to monitor continuously the temperatures cheaply and accurately ($\pm 2^{\circ}C$) in a radiation furnace, bearing in mind the movement of the loads through the furnace. Detailed specifications of the furnace and the interface with the computer may be found in Caffin (1972).

In order for the furnace to behave like a typical three-zone reheat furnace, it is necessary to couple together some of the individual eight zones so that the overall effect is three independently-controlled regions. This is achieved by applying the same power input to the first three zones, thus simulating a preheat zone. The next three zones are also coupled together, simulating a heat zone, whilst the remaining two simulate a soak zone. The arrangement is illustrated in Figure 4.3. The choice of coupling arrangements is purely arbitrary, but it is felt that the preheat and heat zones should dominate the furnace as, in practice, little heating is done in the soak zone (Pike, 1969).

Unlike the typical reheat furnace, discussed by Pike (1969), there is a fair amount of interaction between adjacent zones in the pilot rig. Heating in the preheat zone affects the temperature profile of the

furnace in the heat zone, and vice-versa. Also, there is a fair amount of interaction between the heat and soak zones.

For the initial investigations in this study it is assumed that the loads are of constant thickness. This being the case, the parameters, η_P and η_H, which determine the effect due to loading, will be set to unity. The same, however, cannot be said about the parameter Φ, which determines the effect of push rate changes. As it is difficult to measure the effect of push rate changes, due to lack of instrumentation for measuring the furnace temperature with the loads moving, it is considered that the effects of push rate changes are negligible, and hence Φ can also be set to unity.

This being the case, equation (4.13), which gives the preheat zone temperature profile, reduces to the form as given by equation (4.9), i.e.

$$T_P(x, t) = f_1(x)\, u_1(t) + f_2(x)\, u_2(t).$$

The heat zone temperature profile, as given by equation (4.8), reduces to the form as in equation (4.3), i.e.

$$T_H(x, t) = f_2(x)\, u_2(t).$$

As previously discussed, this equation is valid for furnaces of the counterflow type where there is very little effect on the heat zone profile from the preheat and soak zones. This, however, is not the case with the modified eight-zone electrically-heated furnace. To take account of the interaction from the preheat and soak zones, equation (4.3) is modified to take account of this interaction. The heat zone temperature profile thus becomes,

$$T_H(x, t) = f_1(x)\, u_1(t) + f_2(x)\, u_2(t) + f_3(x)\, u_3(t) \quad \ldots\ (4.14)$$

$$\text{for } 1.07 \text{ m} \leqslant x \leqslant 2.13 \text{ m}$$

where $f_3(x)\, u_3(t)$ is the interaction effect of the soak zone in the heat zone.

Similarly, the soak zone temperature profile is given by

$$T_S(x, t) = f_2(x)\, u_2(t) + f_3(x)\, u_3(t) \quad \ldots\ (4.15)$$

$$\text{for } 2.13 \text{ m} \leqslant x \leqslant 2.84 \text{ m}$$

Due to the distance between the preheat and soak zones, the effects of these on one another have been neglected, as it will be shown, experimentally, that these effects can be considered negligible. Hence, a basic model structure of the electrically-heated furnace, modified to simulate a typical three-zone furnace, is given as:

Preheat zone temperature profile

$$T_P(x, t) = f_1(x)\, u_1(t) + f_2(x)\, u_2(t) \quad \ldots\ldots\ldots\ldots \quad (4.16)$$

$$\text{for } 0 \leqslant x \leqslant 1.07 \text{ m}$$

Heat zone temperature profile

$$T_H(x, t) = f_1(x)\, u_1(t) + f_2(x)\, u_2(t) + f_3(x)\, u_3(t) \quad \ldots \quad (4.17)$$

$$\text{for } 1.07 \text{ m} \leqslant x \leqslant 2.13 \text{ m}$$

Soak zone temperature profile

$$T_S(x, t) = f_2(x)\, u_2(t) + f_3(x)\, u_3(t) \quad \ldots\ldots\ldots\ldots\ldots \quad (4.18)$$

$$\text{for } 2.13 \text{ m} \leqslant x \leqslant 2.84 \text{ m}$$

The above equations will be used to represent the pilot plant electrically-heated furnace. The values of η_P, η_H, η_S and Φ might be determined by a carefully designed experimental program. Such a program, whilst refining the accuracy of the result, does not affect the validity of this study.

4.2 Parameter Estimation of Pilot Plant Reheat Furnace Model

The problem now is to select the functions $f_1(x)$, $f_2(x)$ and $f_3(x)$, which will yield a realistic model of the furnace in order that its properties may be examined. In order to keep the model as simple as possible, the functions are selected to be of the form

$$f_i(x) = \sum_{j=0}^{N} a_j\, x^j \quad \ldots\ldots\ldots\ldots\ldots\ldots \quad (4.19)$$

the coefficients, a_j, and the order, to be determined by taking temperature profile data and then using Least Squares polynomial fitting techniques. In order to do this, accurate temperature profile data have to be obtained.

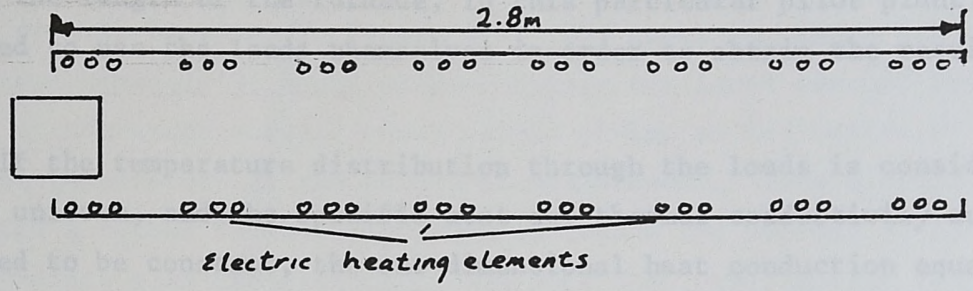

FIG. 4.2 DIAGRAMMATIC REPRESENTATION OF PILOT PLANT FURNACE

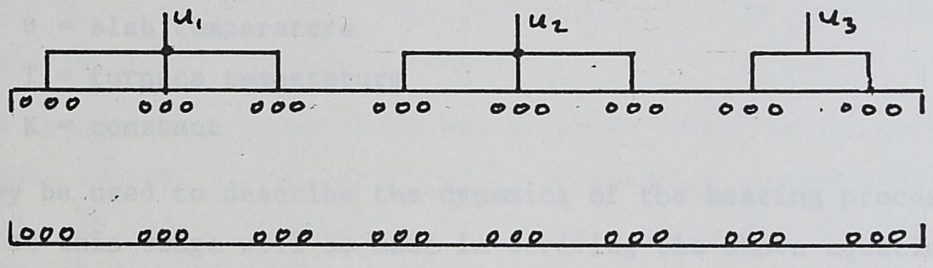

FIG. 4.3 DIAGRAM SHOWING SUB-ZONE COUPLING

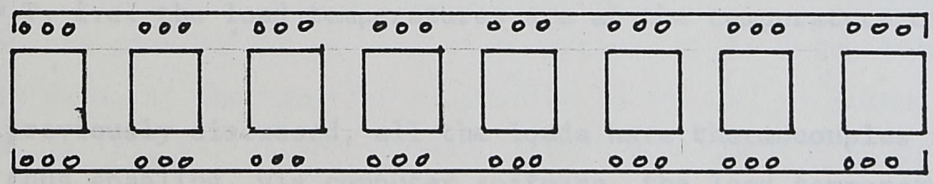

FIG. 4.4. DIAGRAM SHOWING CENTRALLY LOCATED SLABS

4.2.1 Gathering of furnace temperature profile data

As there is no direct way of measuring the furnace temperature along the length of the furnace, in this particular pilot plant it was decided to use the loads themselves in order to obtain the required data.

If the temperature distribution through the loads is considered to be uniform, and the specific heat and thermal conductivity are assumed to be constant, the one dimensional heat conduction equation may be integrated over its spatial variable and combined with the radiation boundary condition to yield

$$\frac{d\theta}{dt} = K(T^4 - \theta^4)$$

where θ = slab temperature

T = furnace temperature

K = constant

which may be used to describe the dynamics of the heating process. (No attempt at this stage will be made in deriving the above equation as this is fully outlined in section 4.3.)

With the slabs at a steady-state temperature, then

$$\frac{d\theta}{dt} = 0$$

thus $\theta = T$, i.e. the load temperatures are at the temperature of the furnace.

As previously discussed, all the loads have thermocouples imbedded in them thus enabling, via computer software, the load temperatures to be measured. It has been determined that the accuracy of the thermocouple temperature measurements is to within $\frac{1}{2}^{o}C$, experimental evidence of this to be found in Caffin (1972). In order to determine the temperature profile of the furnace, for given power input set points, eight loads are placed centrally in each sub-zone, as shown diagrammatically in Figure 4.4. The next step in the process is to determine the effect each of the zones has on the temperature profile along the length of the furnace, for various power input set points.

The effect of the preheat zone on the furnace temperature profile is determined in the following manner. A power input set point of 0.1 (set point of 1.0 = maximum power) is applied to the preheat zone (i.e.

first three sub-zones), via computer software, and the system allowed to settle down. The temperature of all eight loads is measured at ten-minute intervals, and the response of the loads, for a power input set point of 0.1, is shown in Figure 4.5. The plots in Figure 4.5 show that approximately $3\frac{1}{2}$ hours elapsed before the loads reached their final steady-state values, these values giving an indication of the furnace temperature at the points of measurement. This exercise is repeated a number of times in order to obtain the average of the steady-state slab temperatures . In each case, the ambient temperature is recorded and subtracted from the final temperature measurement so as to give the actual steady-state slab temperatures. After the deduction of the ambient temperature, for each run, a high degree of repeatability of the steady-state results is observed to within approximately $\pm$ 5°C, or roughly 10%, thus indicating that the system had not been affected by any undue disturbances.

The preheat zone power input set point is increased in steps of 0.1 and the average of the steady-state temperature measurements is taken for each set point setting. Figure 4.6 shows the average temperature profile along the furnace for the various set point changes in the preheat zone. Figures 4.7 and 4.8 show the furnace temperature profiles for various power input set points applied to the heat and soak zones, respectively.

4.2.2 Determining the form of the temperature profile equations

The next step in the process is to determine the form, from the available data, of the temperature profile equations, as given in equations (4.16), (4.17) and (4.18). Before this is done it is necessary to determine how the temperatures of the eight sub-zones vary with the power applied to each of the three main zones separately. This information is obtained from the same data shown in Figures 4.6, 4.7 and 4.8. Figure 4.9 shows the preheat sub-zone temperatures versus the power input set point, applied to the preheat zone only. As can be seen, the curves are non-linear. Figure 4.10 shows the heat sub-zone temperatures versus the power input set point applied to the preheat zone only. As before, these curves are non-linear. Figures 4.11 - 4.13 provide similar information for sub-zone temperatures versus power input applied to the heat zone only. Figures 4.14 and 4.15 are for power input applied to the soak zone only. Generally, in most cases the sub-zone temperatures

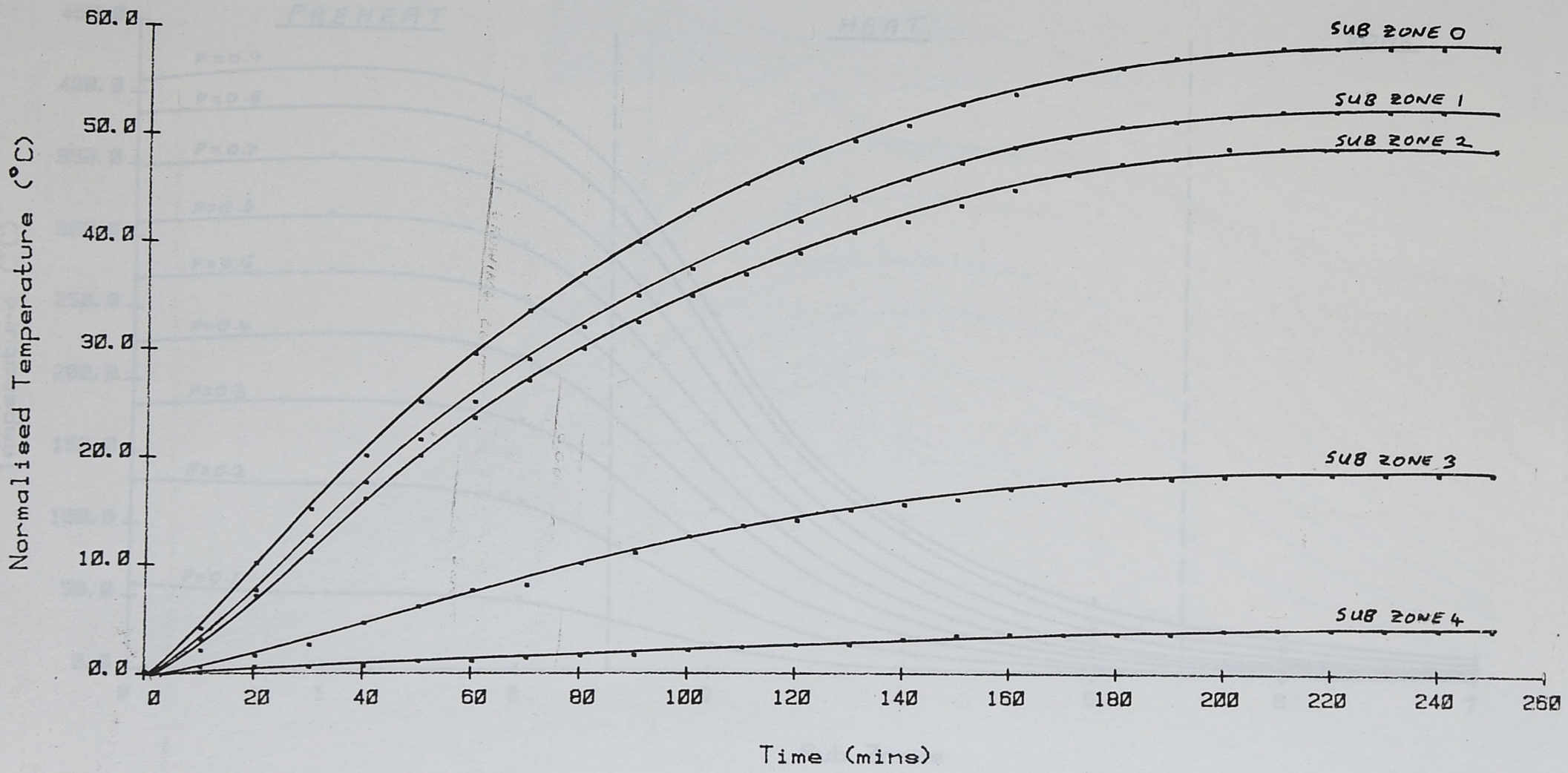

FIG. 4.5 RESPONSE OF FURNACE SUB-ZONES
TO A PREHEAT ZONE POWER INPUT SET POINT OF 0.1

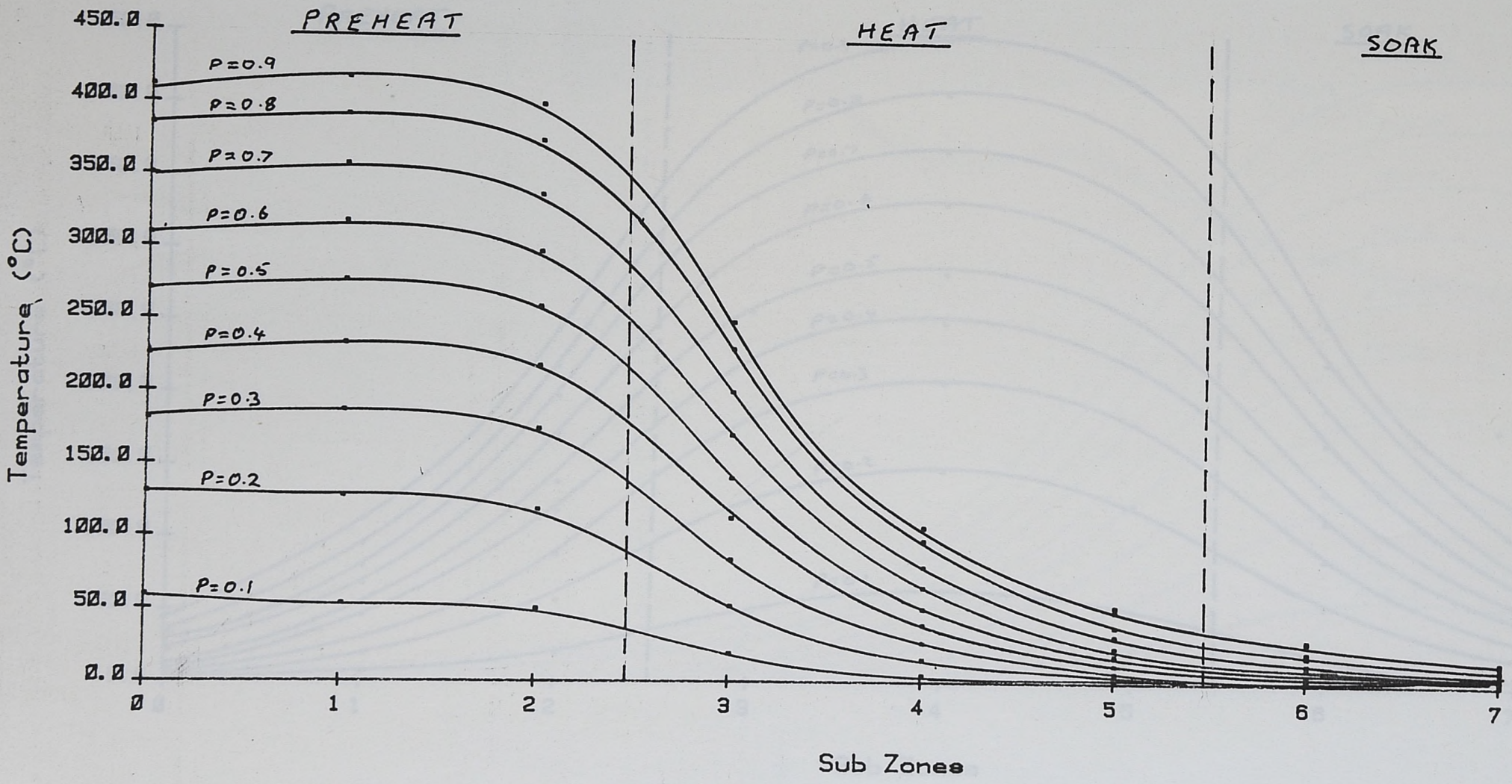

FIG. 4.6 PREHEAT ZONE ON - FURNACE TEMPERATURE PROFILES

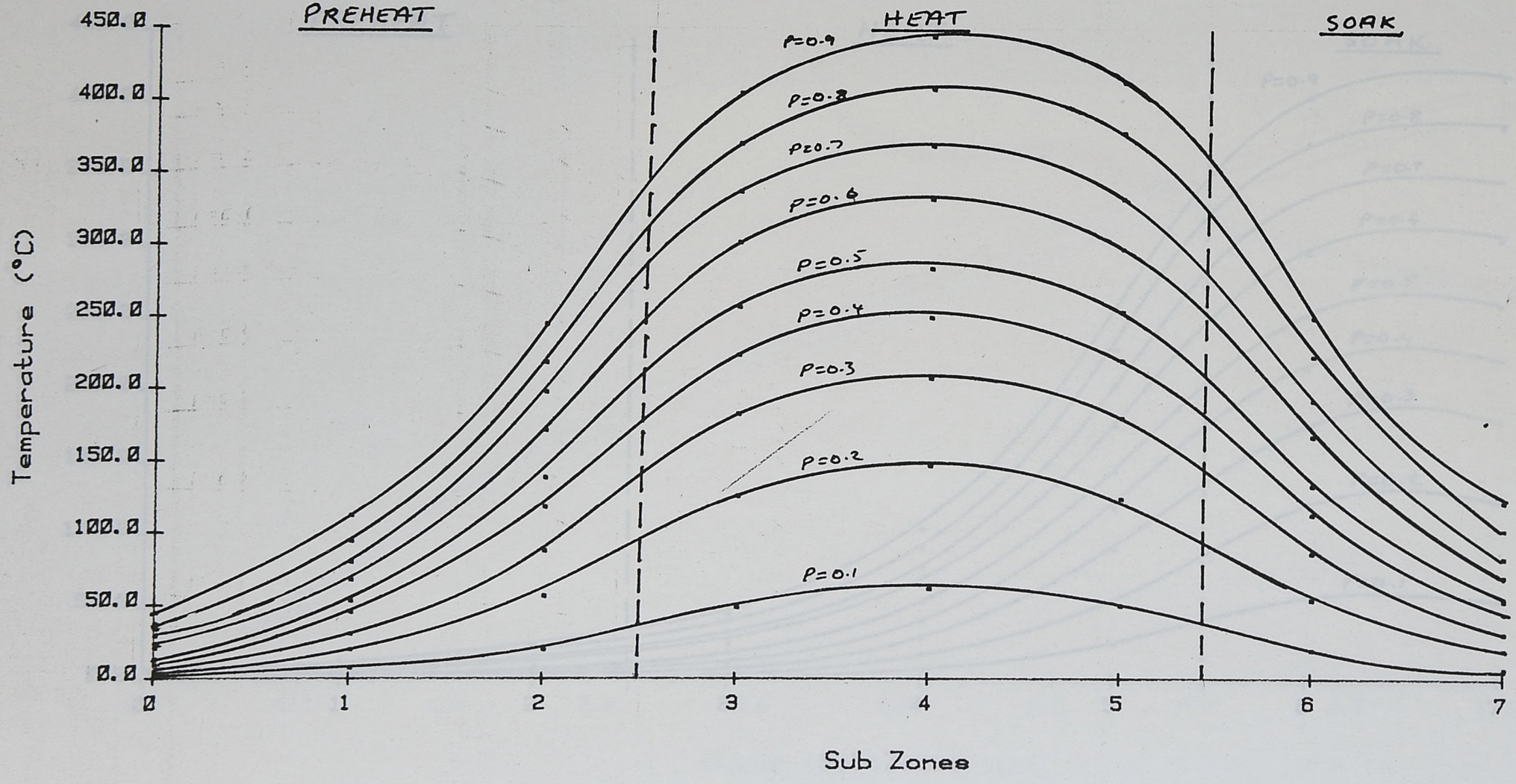

FIG 4.7 HEAT ZONE ON - FURNACE TEMPERATURE PROFILES

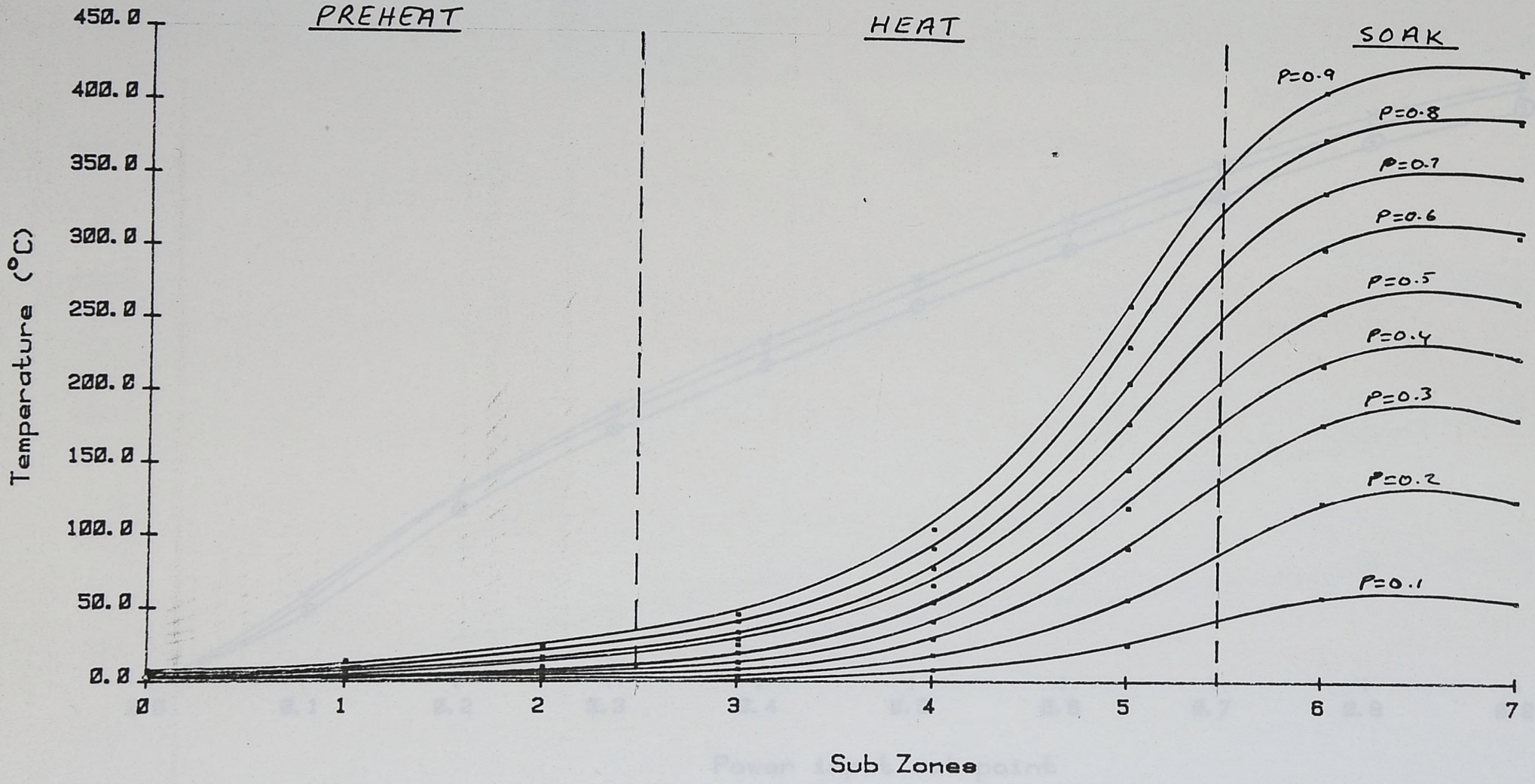

FIG. 4.8 SOAK ZONE ON - FURNACE TEMPERATURE PROFILES

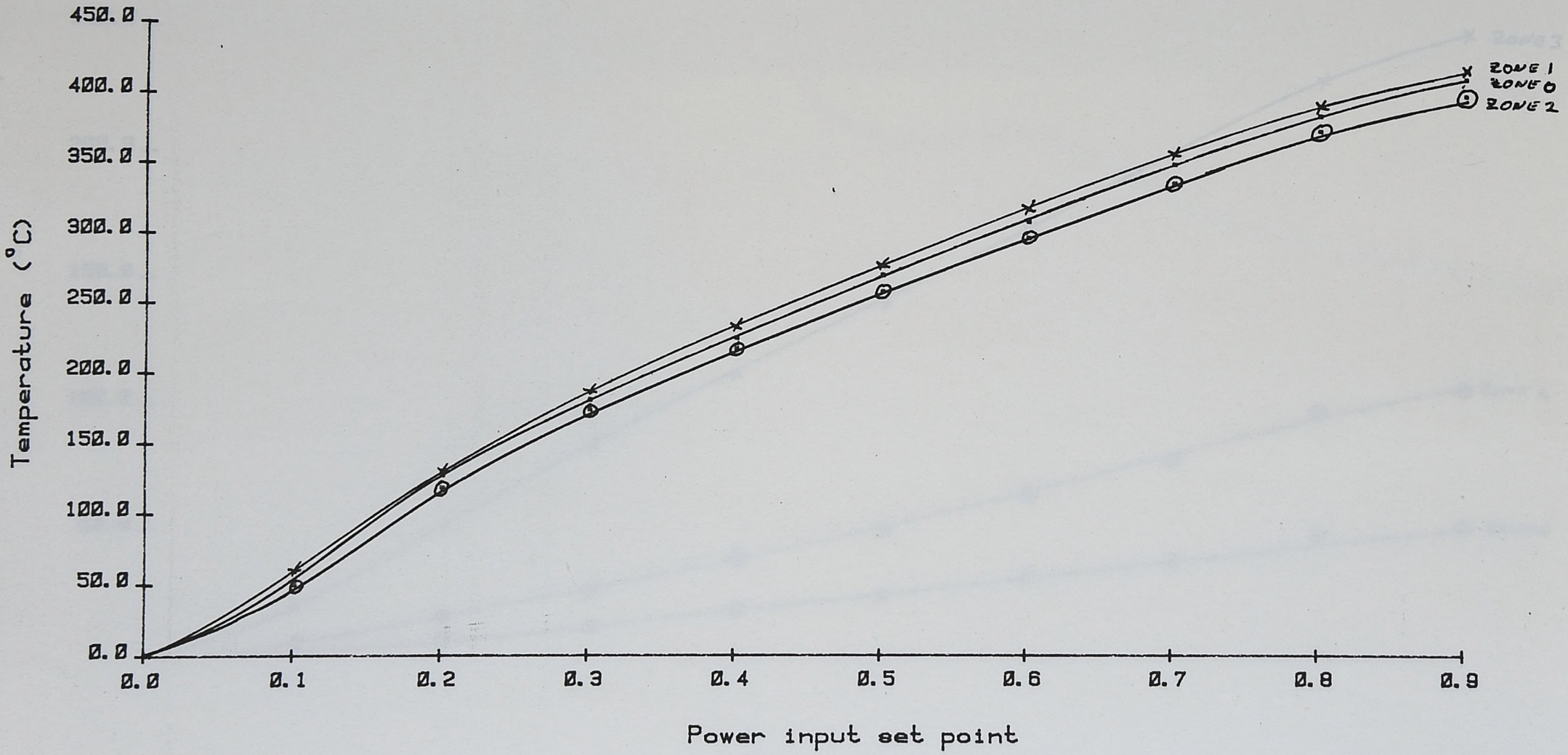

FIG. 4.9 PREHEAT SUB-ZONE TEMPERATURE PROFILES WITH PREHEAT ZONE ON

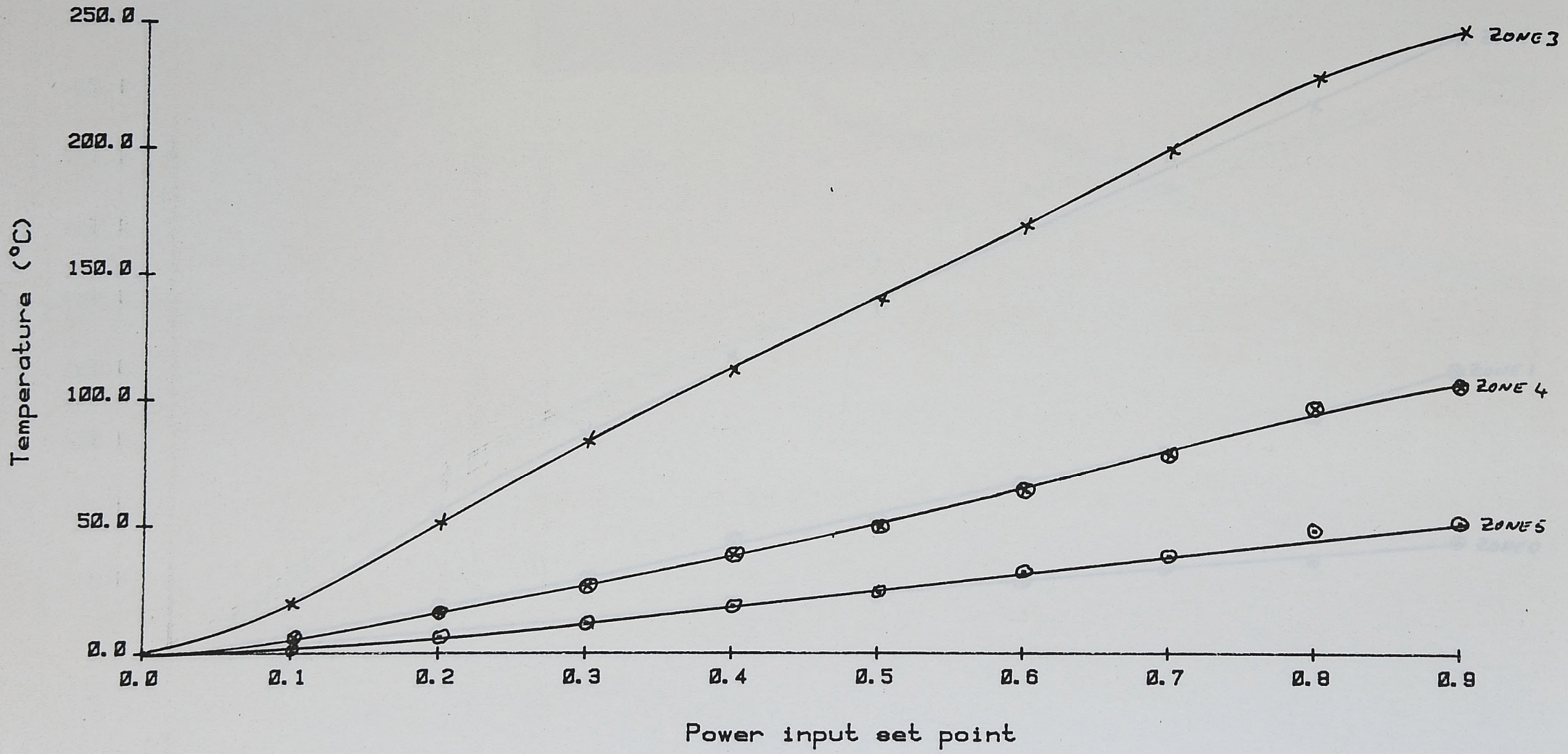

FIG. 4.10 HEAT SUB-ZONE TEMPERATURE PROFILES WITH PREHEAT ZONE ON

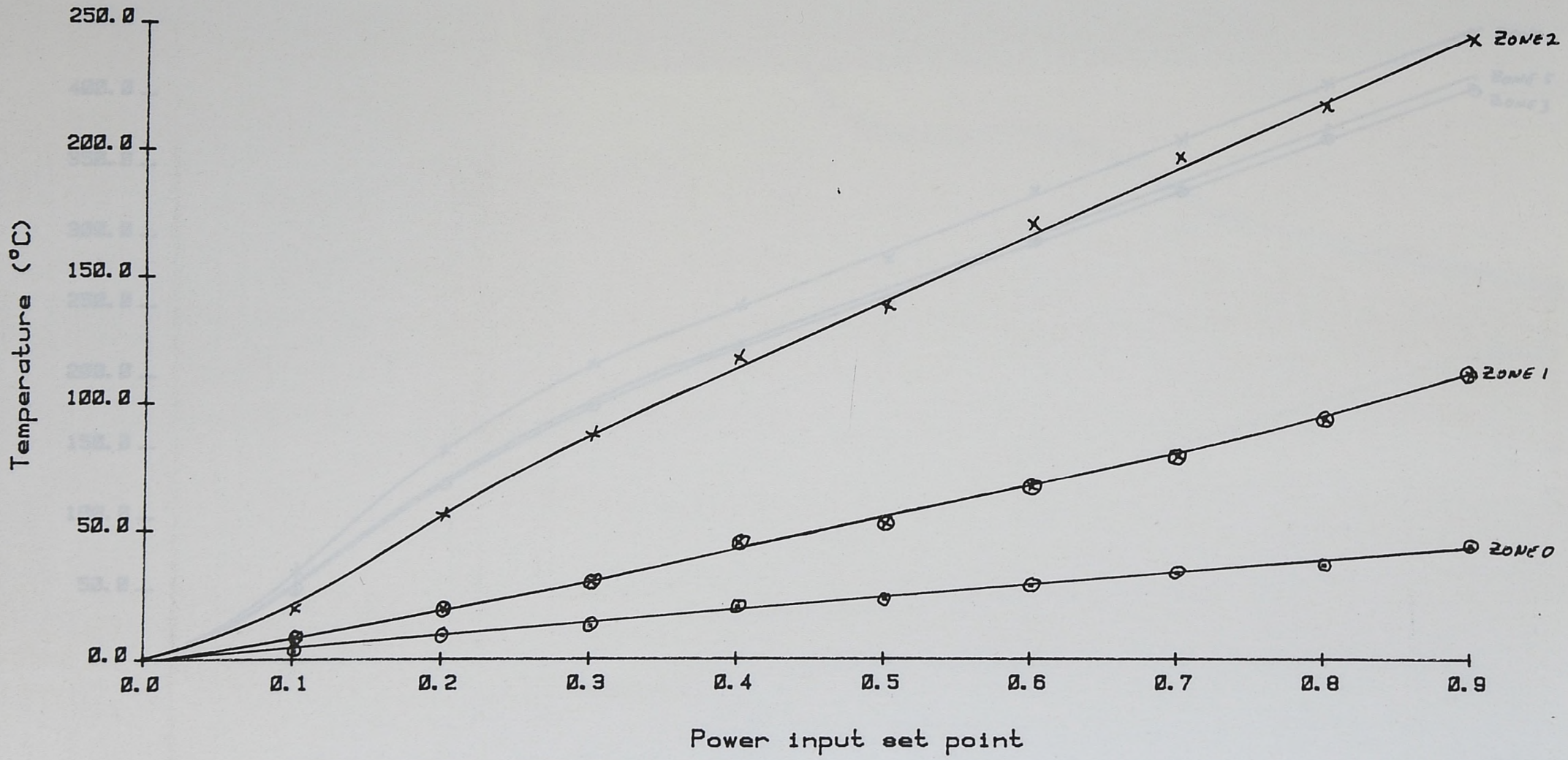

FIG. 4.11 PREHEAT SUB-ZONE TEMPERATURE PROFILES WITH HEAT ZONE ON

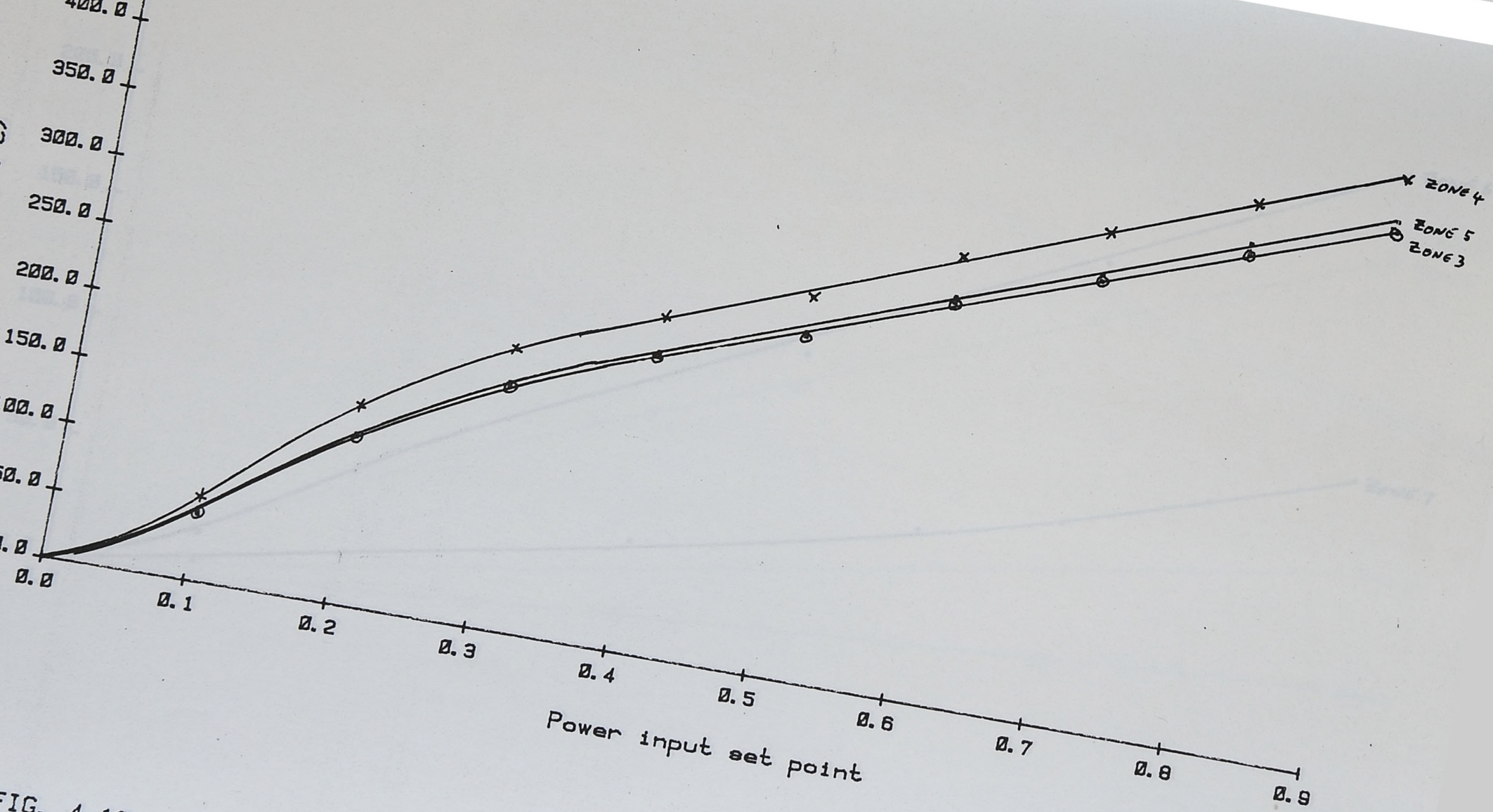

FIG. 4.12 HEAT SUB-ZONE TEMPERATURE PROFILES WITH HEAT ZONE ON

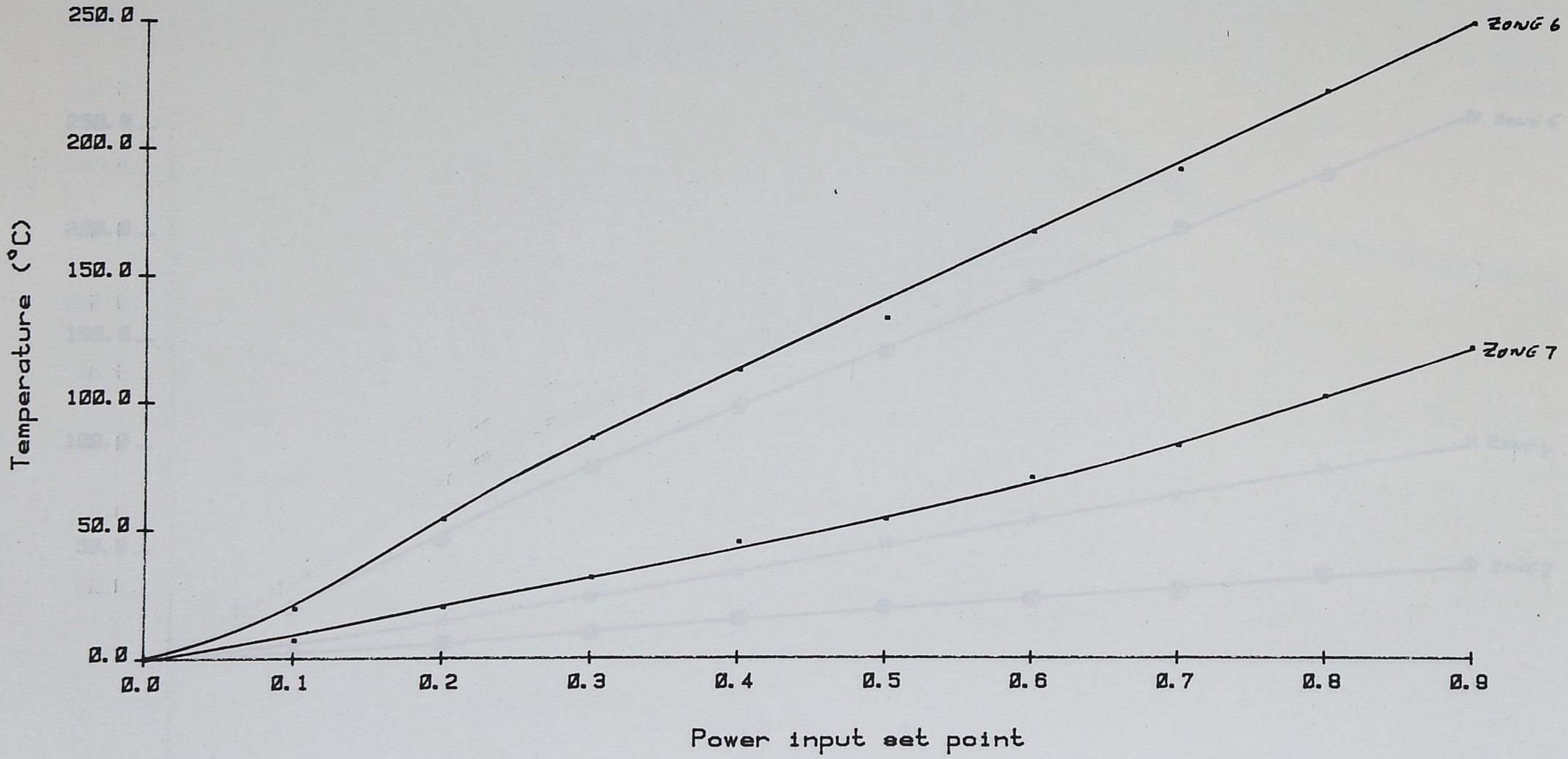

FIG. 4.13 SOAK SUB-ZONE TEMPERATURE PROFILES WITH HEAT ZONE ON

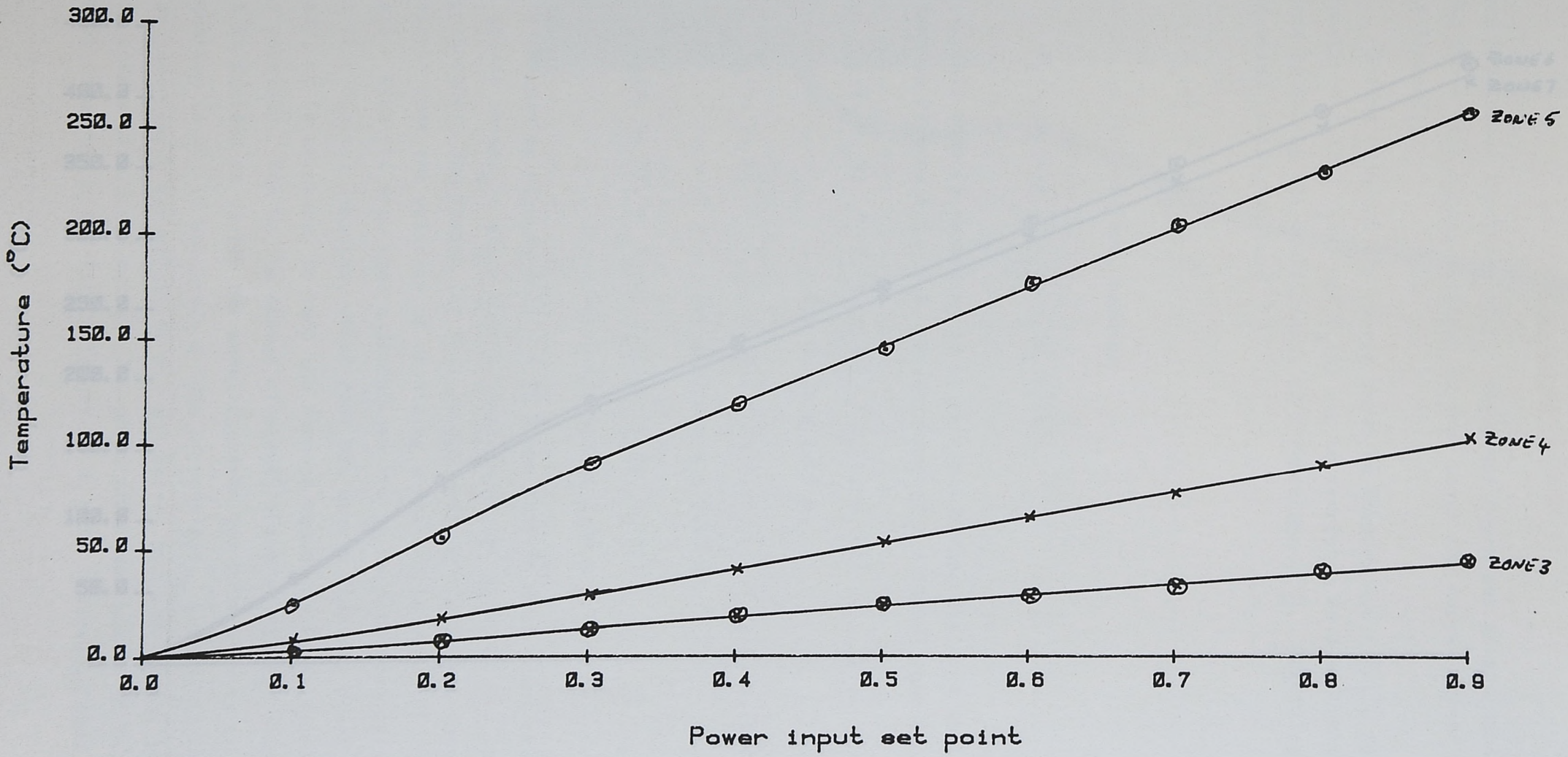

FIG. 4.14 HEAT SUB-ZONE TEMPERATURE PROFILES WITH SOAK ZONE ON

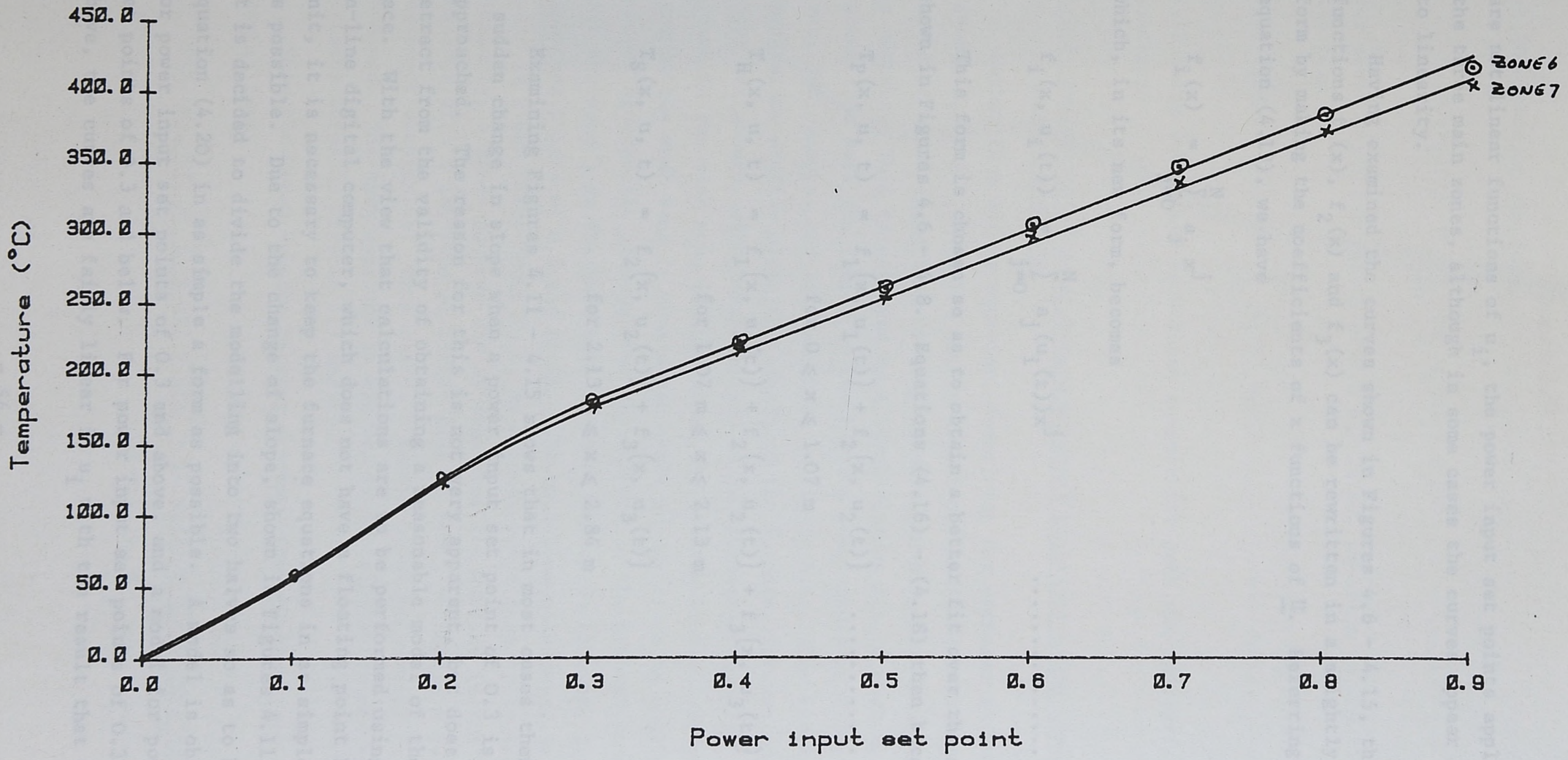

FIG. 4.15 SOAK SUB-ZONE TEMPERATURE PROFILES WITH SOAK ZONE ON

are not linear functions of u_i, the power input set points applied to the three main zones, although in some cases the curves appear close to linearity.

Having examined the curves shown in Figures 4.6 - 4.15, the functions $f_1(x)$, $f_2(x)$ and $f_3(x)$ can be rewritten in a slightly different form by making the coefficients of x functions of $\underline{U}$. Referring back to equation (4.19), we have

$$f_i(x) = \sum_{j=0}^{N} a_j x^j$$

which, in its new form, becomes

$$f_i(x, u_i(t)) = \sum_{j=0}^{N} a_j(u_i(t))x^j \qquad \ldots\ldots\ldots\ldots\ldots \quad (4.20)$$

This form is chosen so as to obtain a better fit over the surfaces shown in Figures 4.6 - 4.8. Equations (4.16) - (4.18) then become

$$T_P(x, u, t) = f_1\left(x, u_1(t)\right) + f_2\left(x, u_2(t)\right) \qquad \ldots\ldots\ldots\ldots \quad (4.21)$$

$$\text{for } 0 \leq x \leq 1.07 \text{ m}$$

$$T_H(x, u, t) = f_1\left(x, u_1(t)\right) + f_2\left(x, u_2(t)\right) + f_3\left(x, u_3(t)\right) \quad (4.22)$$

$$\text{for } 1.07 \text{ m} \leq x \leq 2.13 \text{ m}$$

$$T_S(x, u, t) = f_2\left(x, u_2(t)\right) + f_3\left(x, u_3(t)\right) \quad (4.23)$$

$$\text{for } 2.13 \text{ m} \leq x \leq 2.84 \text{ m}$$

Examining Figures 4.11 - 4.15 shows that in most cases there is a sudden change in slope when a power input set point of 0.3 is approached. The reason for this is not very apparent, but does not detract from the validity of obtaining a reasonable model of the furnace. With the view that calculations are to be performed using an on-line digital computer, which does not have a floating point hardware unit, it is necessary to keep the furnace equations in as simple a form as possible. Due to the change of slope, shown in Figures 4.11 - 4.15, it is decided to divide the modelling into two halves so as to keep equation (4.20) in as simple a form as possible. A model is obtained for power input set points of 0.3 and above, and a model for power input set points of 0.3 and below. For power input set points of 0.3 and above, the curves are fairly linear in u_i with the result that equation

(4.20) takes on the form

$$f_i(x, u_i(t)) = \sum_{j=0}^{N} (\alpha_j u_i(t) + \beta_j)x^j \quad \ldots\ldots\ldots \quad (4.24)$$

For power input set points of 0.3 and below, equation (4.20) takes on the form

$$f_i(x, u_i(t)) = \sum_{j=0}^{N} \alpha_j x^j u_i(t) \quad \ldots\ldots\ldots\ldots\ldots \quad (4.25)$$

α, β being determined by a least squares fit over the appropriate surfaces.

4.2.3 Evaluation of general form of model equations using Least Squares analysis

Rather than fit an equation, describing the surfaces shown in Figures 4.6 - 4.8, over the entire length of the furnace with the result of obtaining a high order polynomial in x, a piecewise approach is adopted. This is achieved by a least squares fit to each zone rather than over the length of the furnace temperature profile surface. Take, for example, the surface shown in Figure 4.6. This indicates the temperature profile along the length of the furnace, for various power input set points, with power applied to the preheat zone only. The effect in the soak zone is ignored as the contribution of the preheat zone in the soak zone is considered small enough as to be negligible. A least squares fit is made over the surface in the preheat zone, together with sub-zone 3 in the heat zone so as to ensure continuity, for power input set points of 0.3 and above. The resulting polynomial is of second order in x and first order in u_1 as already predefined by equation (4.24). Similarly, a least squares fit is made over the surface in the heat zone, together with a sub-zone on either side in order to obtain a reasonable degree of continuity. Once again, a second order polynomial in x is obtained. The same approach is adopted in deriving equations to fit the surfaces shown in Figures 4.7 and 4.8.

From the least squares fitting program, the equations are of the general form

$$T(x, u_i, t) = (A u_i(t) + B)x^2 + (C u_i(t) + D)x + (E u_i(t) + F)$$

$$i = 1, 2, 3 \quad \ldots\ldots\ldots \quad (4.26)$$

where T is the temperature along the furnace

u_i is the power input set point to the appropriate zones

x is the distance along the length of the furnace.

For further details on the coefficients, A - F, the reader is referred to Appendix A.

Figures 4.16 - 4.22 show the curves generated by equation (4.26), together with the actual data points taken from the furnace. The curves are for power input set points of 0.3 and above, and in the majority of cases a good fit is obtained. Due to scaling, it is difficult to plot the 95% tolerance band on the estimated outputs, but the reader is again referred to Appendix A for a statistical analysis of the derived equations. Also shown are the equations derived for power input set points of 0.3 and below.

So far, the temperature at any point in the furnace is estimated due to the action of only one zone being switched on at any one time. In practice, of course, all the zones are operating at the same time and therefore a temperature profile model is needed which includes the effect of power operating in all zones. With all three zones activated at various power settings, steady-state temperature data are gathered. Due to heat losses and other thermal phenomena, there are discrepancies between the combining of the equations and the actual gathered data when all zones are switched on. In order to minimize the differences between the actual and empirical model, weighting factors are introduced into the combined model equations. In order to simplify matters, the weighting factors are derived in a piecewise manner and hence vary when going from one zone to another. The reader is referred to Appendix A for a full description of the weighting factors.

The temperature in any one zone is thus defined by

$$T_P = W_1(T_{PP} + T_{HP}) \quad \text{.....(4.27)}$$

$$0 \leq x \leq 1.07 \text{ m}$$

$$T_H = W_2(T_{PH} + T_{HH} + T_{SH}) \quad \text{..... (4.28)}$$

$$1.07 \text{ m} \leq x \leq 2.13 \text{ m}$$

$$T_S = W_3(T_{HS} + T_{SS}) \quad \text{..... (4.29)}$$

$$2.13 \text{ m} \leq x \leq 2.84 \text{ m}$$

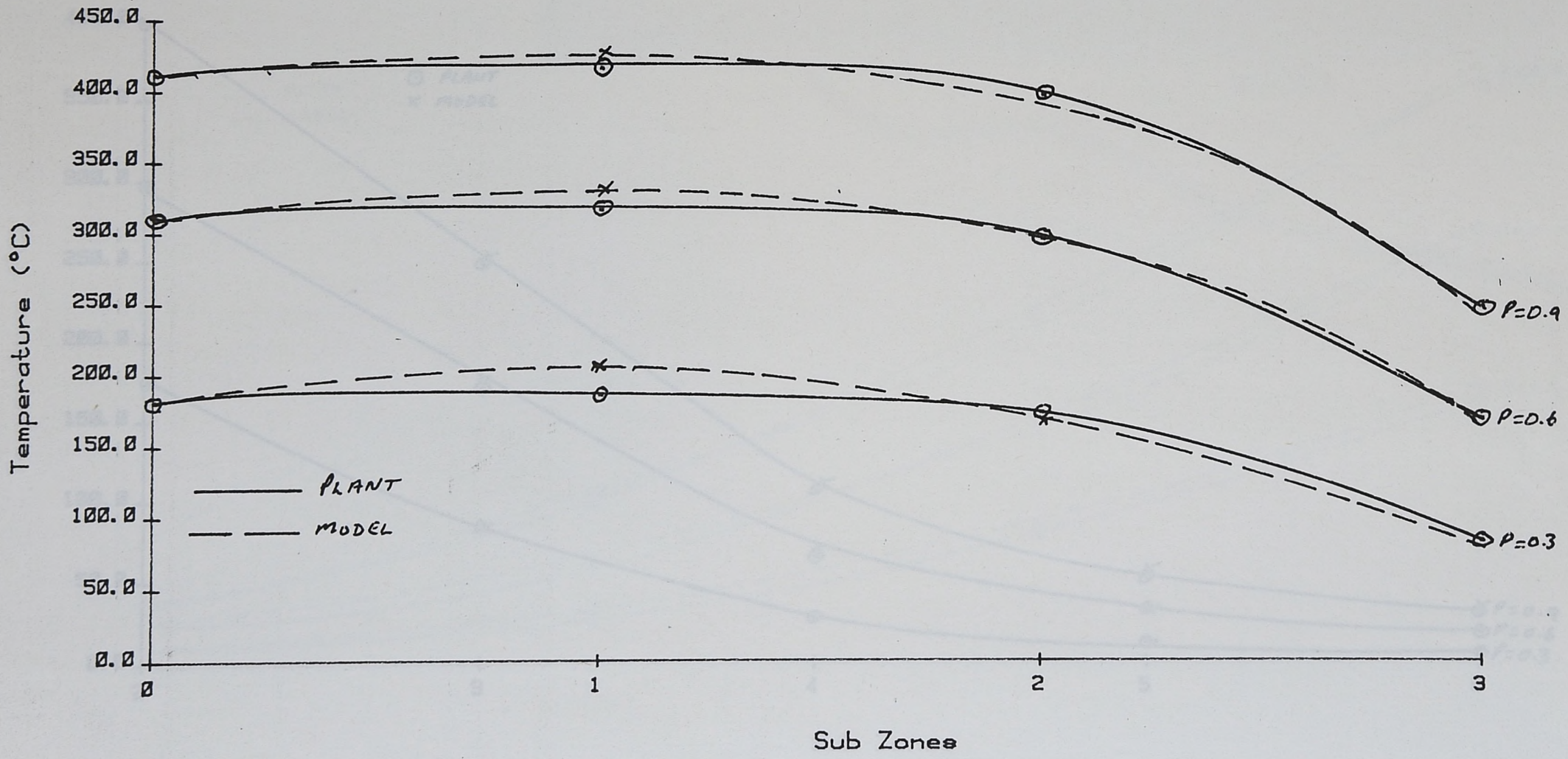

FIG. 4.16 PLANT AND MODEL PREHEAT ZONE TEMPERATURE PROFILES WITH PREHEAT ZONE ON ONLY

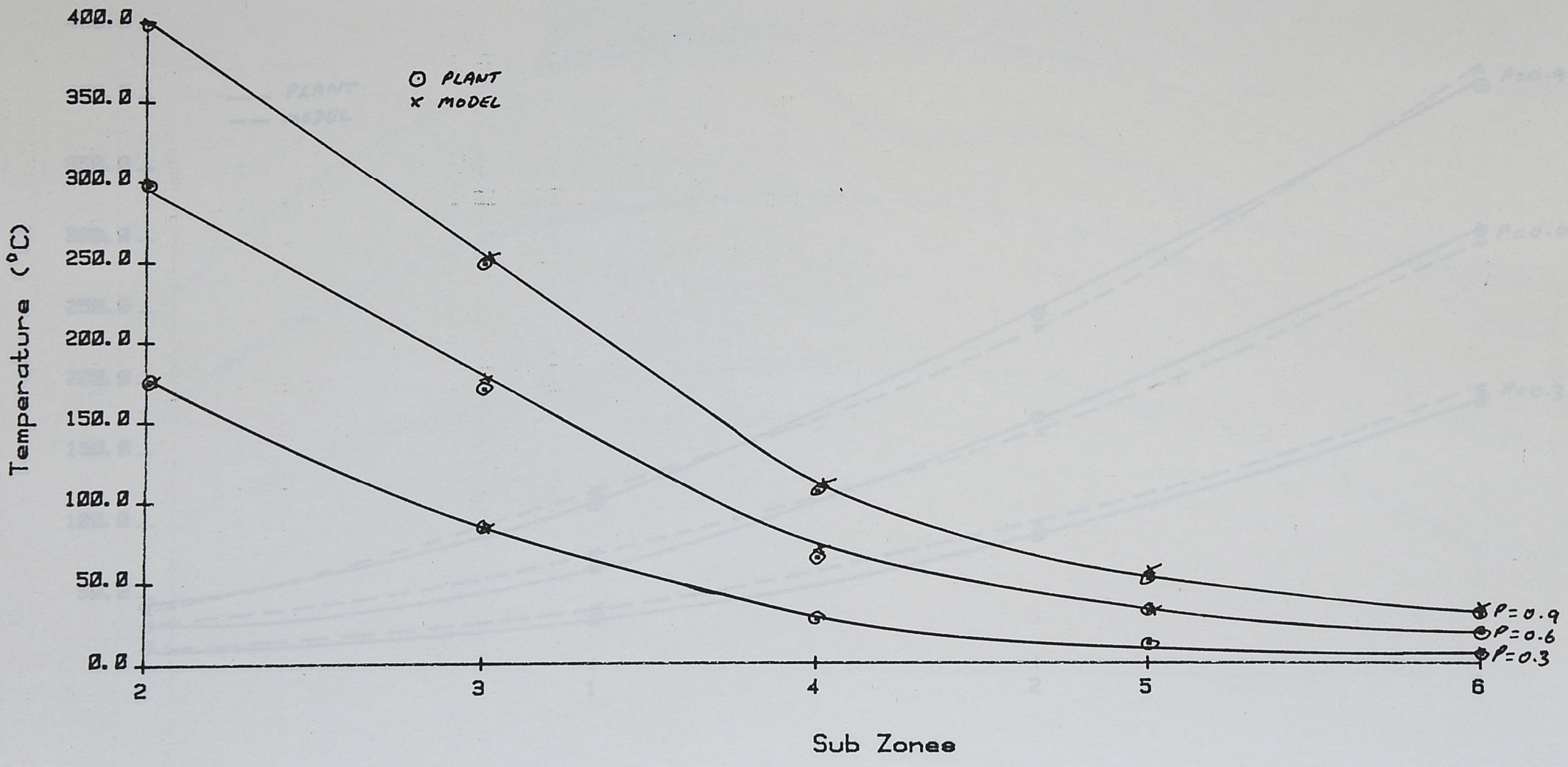

FIG. 4.17 PLANT AND MODEL HEAT ZONE TEMPEREATURE PROFILES WITH PREHEAT ZONE ON ONLY

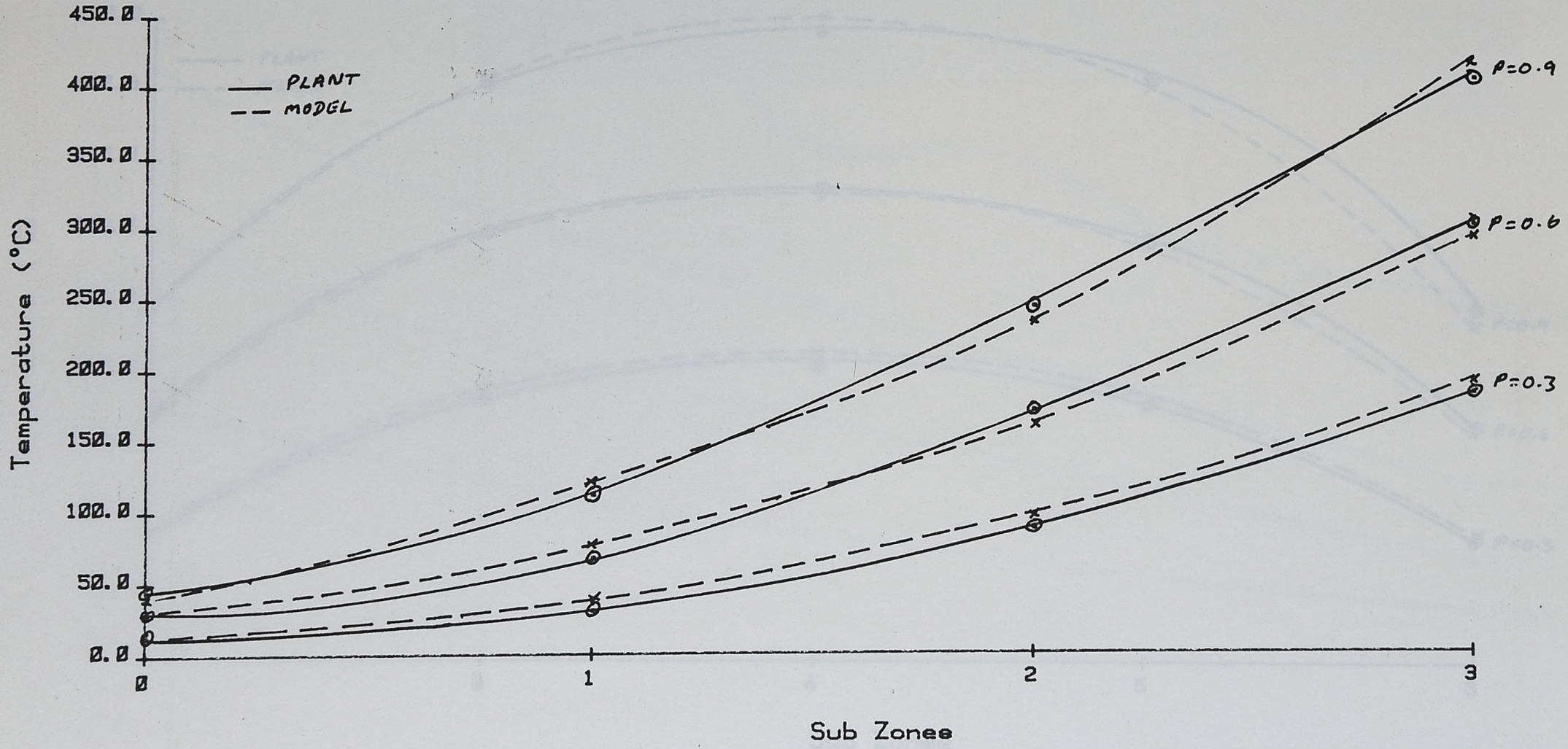

FIG. 4.18 PLANT AND MODEL PREHEAT ZONE TEMPERATURE PROFILES WITH HEAT ZONE ON ONLY

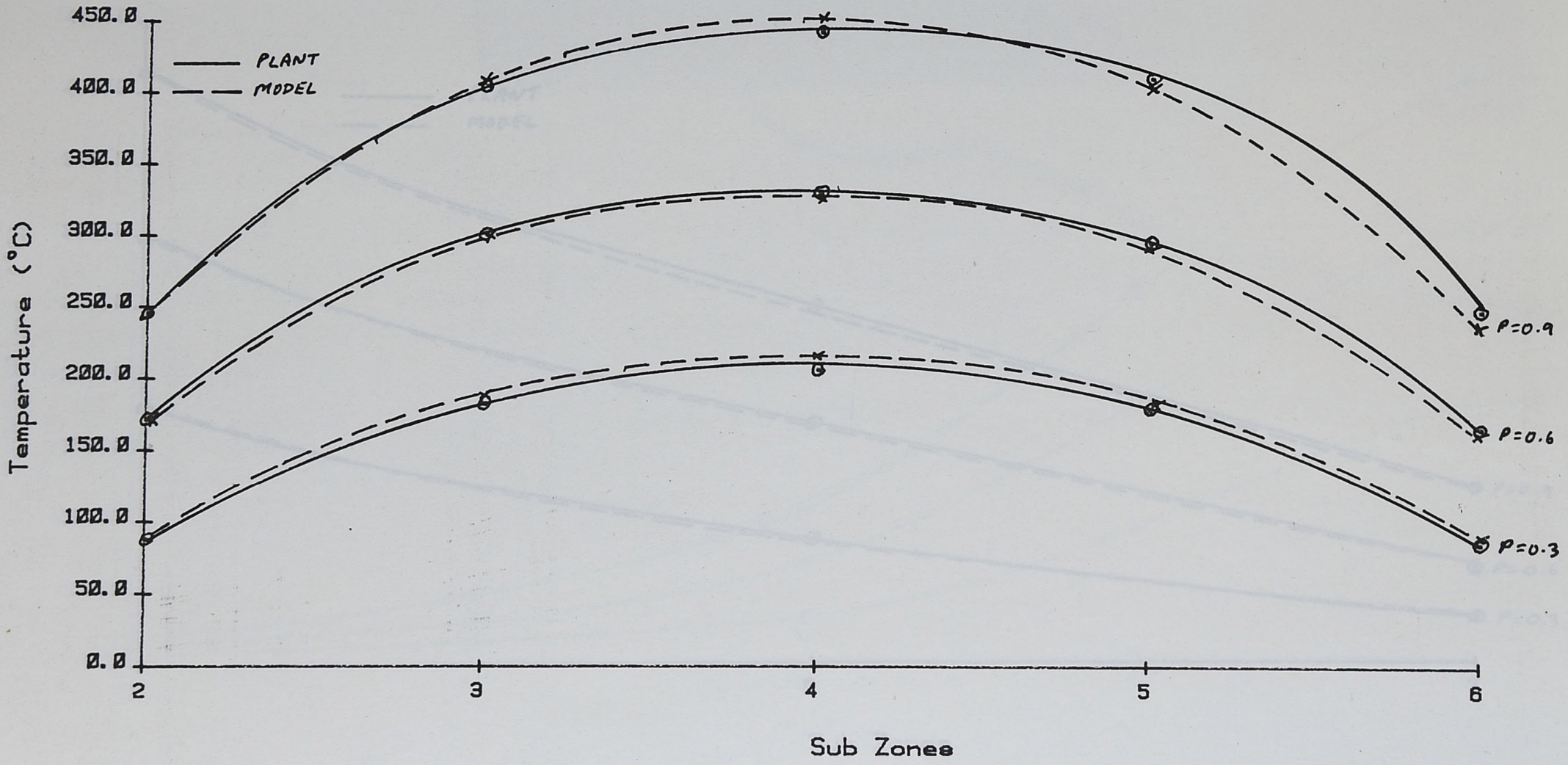

FIG. 4.19 PLANT AND MODEL HEAT ZONE TEMPERATURE PROFILES WITH HEAT ZONE ON ONLY

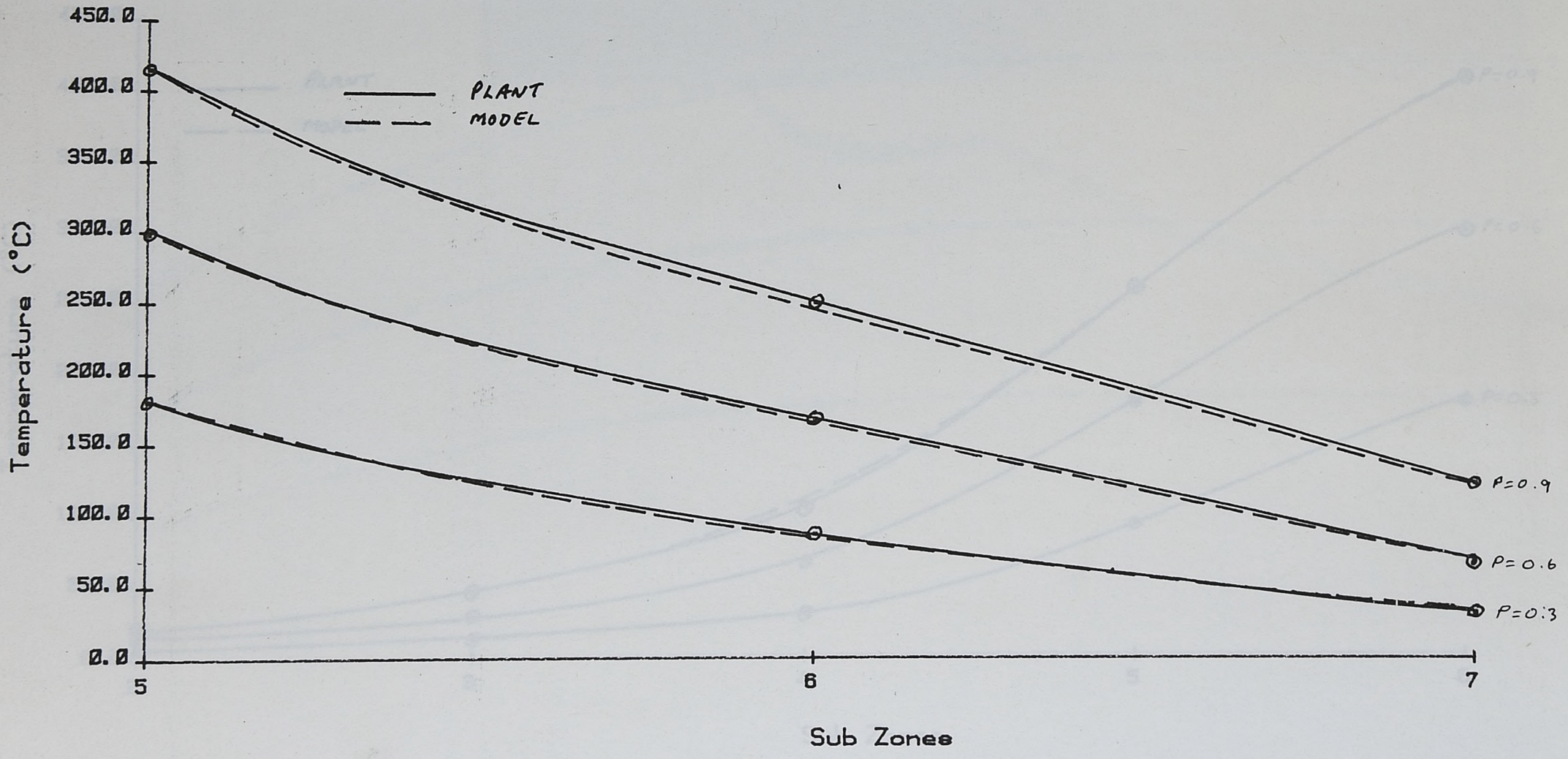

FIG. 4.20 PLANT AND MODEL SOAK ZONE TEMPERATURE PROFILES WITH HEAT ZONE ON ONLY

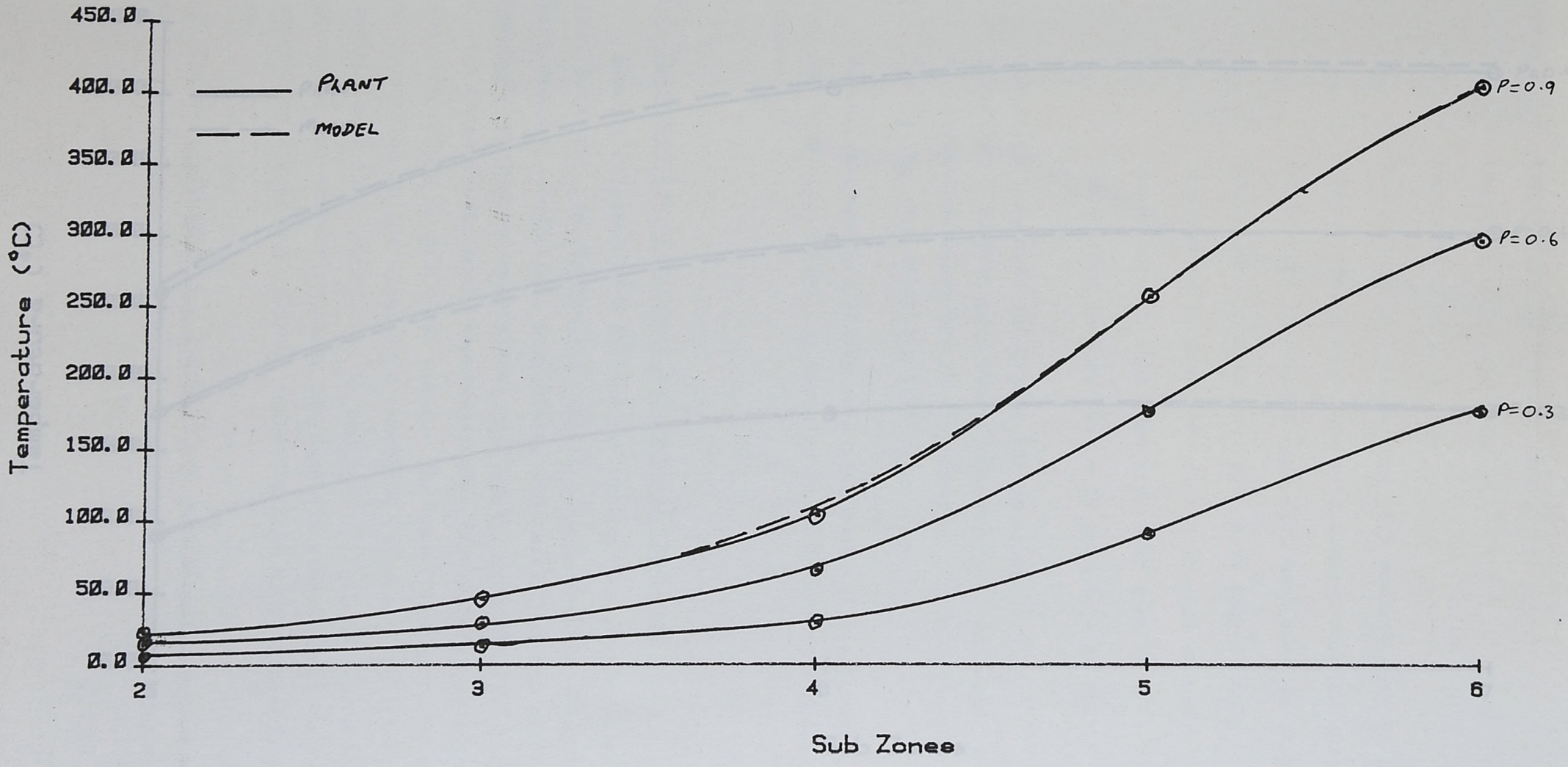

FIG. 4.21 PLANT AND MODEL HEAT ZONE TEMPERATURE PROFILES WITH SOAK ZONE ON ONLY

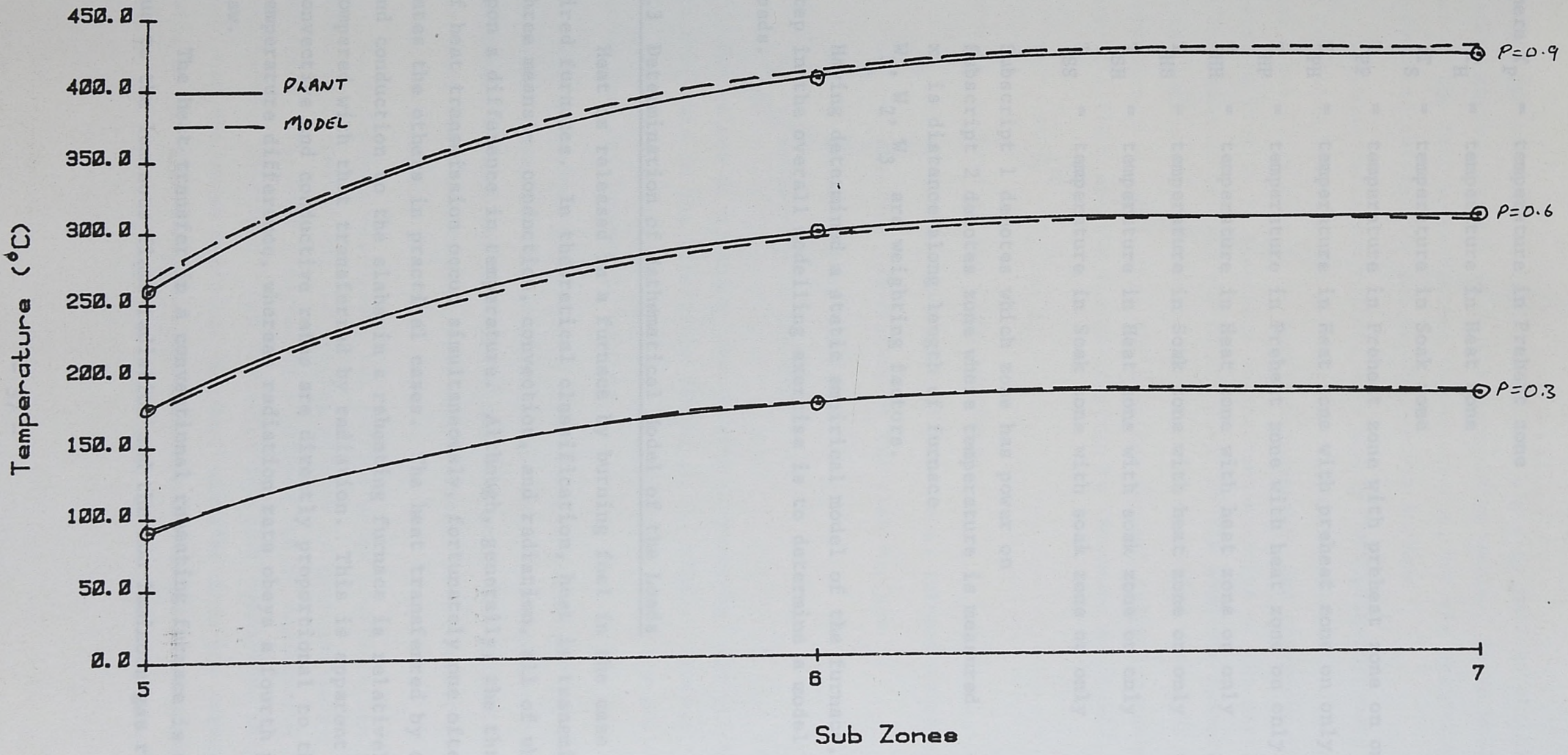

FIG. 4.22 PLANT AND MODEL SOAK ZONE TEMPERATURE PROFILES WITH SOAK ZONE ON ONLY

where T_P = temperature in Preheat zone

T_H = temperature in Heat zone

T_S = temperature in Soak zone

T_{PP} = temperature in Preheat zone with preheat zone on only

T_{PH} = temperature in Heat zone with preheat zone on only

T_{HP} = temperature in Preheat zone with heat zone on only

T_{HH} = temperature in Heat zone with heat zone on only

T_{HS} = temperature in Soak zone with heat zone on only

T_{SH} = temperature in Heat zone with soak zone on only

T_{SS} = temperature in Soak zone with soak zone on only

Subscript 1 denotes which zone has power on

Subscript 2 denotes zone where temperature is measured

x is distance along length of furnace

W_1, W_2, W_3 are weighting factors.

Having determined a static empirical model of the furnace, the next step in the overall modelling exercise is to determine a model for the loads.

4.3 Determination of Mathematical Model of the Loads

Heat is released in a furnace by burning fuel in the case of fuel-fired furnaces. In theoretical classification, heat is transmitted by three means:- conduction, convection, and radiation, all of which depend upon a difference in temperature. Although, generally, the three kinds of heat transmission occur simultaneously, fortunately one often dominates the others in practical cases. The heat transferred by convection and conduction to the slabs in a reheating furnace is relatively small compared with that transferred by radiation. This is apparent because convective and conductive rates are directly proportional to the temperature difference, whereas radiation rate obeys a fourth power law.

The heat transfer in a conventional reheating furnace is mainly due to the luminous flame radiation and the non-luminous gas radiation.

The hot gas passing through the furnace gives up heat to the direct heating surface as well as to the surrounding walls. These walls lose part of the heat by conduction to the outside, but the greater part is re-radiated through the gas to the heating surface.

Luminous radiation follows more nearly the Stefan-Boltzmann law of radiation that applies to solids. A luminous flame is different from a solid, in that it is partly transparent, and therefore the radiation from it is dependent on the concentration of the particles in the flame as well as the fourth power of the absolute temperature. If the luminosity is affected due to solid particles caused by the combustion, i.e. soot, then the equation for net radiation exchange between a flame and the charge is given by (Brown et al, 1958):

$$q = \sigma A(T_f^4 - \theta_s^4)e_f\, e_s \qquad \text{..... (4.30)}$$

where A = area of the flame envelope

T_f = absolute temperature of the flame, furnace temperature

θ_s = absolute temperature of the slab surface

e_f = emissivity of the flame

e_s = emissivity of the slab

The values of e_f and e_s change with temperature, for which graphs are available in the literature (Brown et al, 1958). However, in practice, an overall emissivity factor is employed. This overall emissivity varies from one furnace to another.

Radiation from non-luminous flames and clear gases does not follow the fourth power law, nor does it follow any other exponential law. The reason is that non-luminous flames and gases are selective radiators, i.e. they emit radiation in only certain bands of the spectrum and not at all wavelengths.

As previously discussed, the furnace under consideration is electrically-heated and the heating process is governed solely by radiation. The heat transfer in a furnace can be represented by two simultaneous equations. One describes the heat conduction within the slab, and the other describes the heat transfer from the furnace atmosphere to the slab surface. The latter is the boundary condition for the partial differential equation describing the transient conduction

within the slab. The solution of the two equations gives the temperature of the slab.

4.3.1 Mathematical model assumptions

(a) Slabs are assumed to enter the furnace with uniform temperature distribution.

(b) Slabs are subjected to symmetrical heating from both sides.

(c) In the soaking zone, no heat is exchanged between the slab and the refractory hearth

(d) Heat is transferred to the top and bottom surfaces of the slab by radiation. Other means of heat transfer are neglected.

(e) The furnace temperature over its width is uniform.

(f) Slabs are assumed to be moving with a velocity depending on the pushing rate, although they may be stationary at times, during their passage through the furnace.

4.3.2 The model

The equations for heat transfer within a large flat slab in a reheating furnace, together with initial and boundary conditions, are shown below.

The heat conduction equation is given by:

$$\rho c \frac{\partial \theta}{\partial t}(x_s, t) = \frac{\partial}{\partial x_s}\left\{ k \frac{\partial \theta}{dx_s}(x_s, t) \right\} \quad \ldots\ldots\ldots\ldots \quad (4.31)$$

with the initial condition given by

$$\theta(x_s, 0) = \theta_o(x_s), \quad 0 \leq x_s \leq s \quad \ldots\ldots\ldots\ldots\ldots \quad (4.32)$$

where ρ = density (g/cm^3)

c = specific heat ($cal/g\ ^oC$)

k = thermal conductivity ($cal/cm.sec.\ ^oC$)

θ = slab temperature (^oK)

θ_o = initial temperature (^oK)

s = slab thickness

t = time

x_s = coordinate in the direction of slab thickness (see Figure 4.23)

According to assumptions (b) and (d), the boundary conditions on the surface of the slab in the preheat and heat zones are expressed by

$$- k \frac{\partial \theta}{dx_s} (x_s, t) \Big|_{\substack{x_s = 0 \\ x_s = s}} = e \sigma \left\{ T^4(y, t) - \theta_s^4(t) \right\} \quad \ldots\ldots\ldots \quad (4.33)$$

where e = effective emissivity of the furnace

σ = Stefan-Boltzmann constant (cal/cm^2.sec. $^oK^4$)

T = furnace temperature (^oK)

According to assumption (c), in the soaking zone the boundary condition on the heating surfaces of the slab is expressed mathematically as

$$- k \frac{\partial \theta}{\partial x_s} (x_s, t) \Big|_{x_s = s} = 0 \quad \ldots\ldots\ldots\ldots\ldots \quad (4.34)$$

where $\theta(x_s, t)$ is the slab temperature as a function of its thickness and time. The furnace temperature, $T(y, t)$, varies along its length and also varies with time, but for steady-state operation of the furnace (i.e. slabs of the same thickness pushed at a constant rate), it is only a function of the furnace length.

It is necessary to point out here that the slab surface temperature, θ_s, should not exceed a specified limit, i.e.

$$\theta(0;\ s, t) = \theta_s(t) \leq \theta_{s\ max} \quad \ldots\ldots\ldots\ldots\ldots\ldots \quad (4.35)$$

Table 4.1 gives the properties of the aluminium slabs.

Table 4.1: Aluminium Slab Properties

Melting point = 660^{o}C

Density, ρ = 2707.1265 Kg/m^3

Specific heat, c = 895.975 J/Kg ^{o}C

Thermal conductivity, k = 228.36 Wm/m^2 ^{o}C

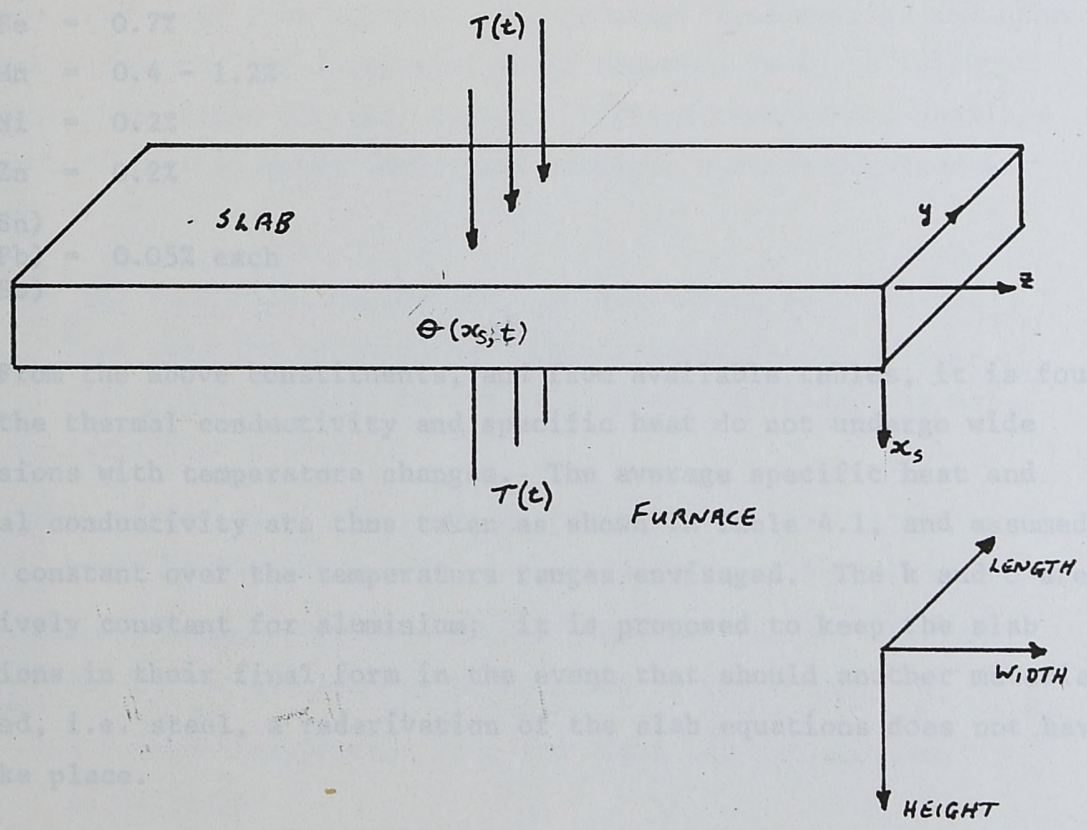

FIG. 4.23 SLAB HEATING IN A FURNACE SHOWING COORDINATES NOTATION

The full derivation of the average temperature is given within Appendix B. By substituting the values given in Table 4.1, the average slab temperature is given by the solution of the differential equation:

$$\frac{d\bar{\theta}}{dt} = \frac{7.95 \times 10^{-8}}{\rho\, c(\theta)} \left(T^4 - \bar{\theta}^4\right) \left(1 - 2.64 \times 10^{-8} \frac{s}{k(\theta)} \bar{\theta}^3\right) \quad .. \quad (4.36)$$

The slab surface temperature is given by

$$\theta_s = \bar{\theta} + \frac{\rho\, c\, s^2}{720\, k(\theta)} \frac{d\bar{\theta}}{dt} \quad ..... \quad (4.37)$$

The constituents of the aluminium extrusions are as follows:

Cu = 3.5 - 5.0%
Mg = 0.4 - 1.2%
Si = 0.7%
Fe = 0.7%
Mn = 0.4 - 1.2%
Ni = 0.2%
Zn = 0.2%
Sn)
Pb) = 0.05% each
Sb)

From the above constituents, and from available tables, it is found that the thermal conductivity and specific heat do not undergo wide excursions with temperature changes. The average specific heat and thermal conductivity are thus taken as shown in Table 4.1, and assumed to be constant over the temperature ranges envisaged. The k and c are relatively constant for aluminium; it is proposed to keep the slab equations in their final form in the event that should another material be used, i.e. steel, a rederivation of the slab equations does not have to take place.

4.4 Furnace/Slab Model Evaluation

Having determined a static empirical model of the furnace and a dynamic model of the slabs, the next step is to evaluate how well the models behave compared to the real existing plant. In order to test the model of the slabs, slab trajectories are required as they pass from one end of the furnace to the other at a constant velocity. The

velocity set point is related to the actual slab velocity by the relationship:

$$v = SP \times 5.588 \times 10^{-3} \text{ m/s} \quad \ldots\ldots\ldots\ldots\ldots\ldots\ldots \quad (4.38)$$

where SP = velocity set point in the range 0.0 - 1.0

v = actual slab velocity in m/s.

This relationship is determined by measuring the actual slab velocities for various set point settings and is found to be linear. Figure 4.24 shows the relationship between velocity and velocity set point.

With a chosen set of power input set points and at a constant velocity, slab temperature readings are taken and compared with those produced by the model for the same input and velocity conditions. Initial conditions such as ambient temperature and initial slab temperature are also taken into account. Due to model inadequacies and other physical phenomena, the integrated model equation is not a faithful representation of the physical system. Various reasons are possible contributors to this model inadequacy problem, and are outlined as follows:

(i) In the slab model derivation, the derivation works on the fact that the equation for heat transfer is for a large flat plate, whereas in the pilot plant the slabs are not large flat plates.

(ii) The emissivity of the slabs is taken as 0.7, but in fact could be higher or lower due to surface finish deterioration.

(iii) Thermal conductivity and specific heat of the actual slabs may not be the same as those given in the model.

(iv) The furnace temperature over its width may not necessarily be uniform.

(v) Heat transfer between adjacent slabs may not be insignificant.

To compensate for the model inadequacy, a weighting factor, W_x, is introduced which modifies the slab model equation so that the model and plant trajectories are as close as possible. W_x is chosen to modify the slab model equation rather than the actual furnace profile equations as, due to lack of instrumentation, it is virtually impossible to measure

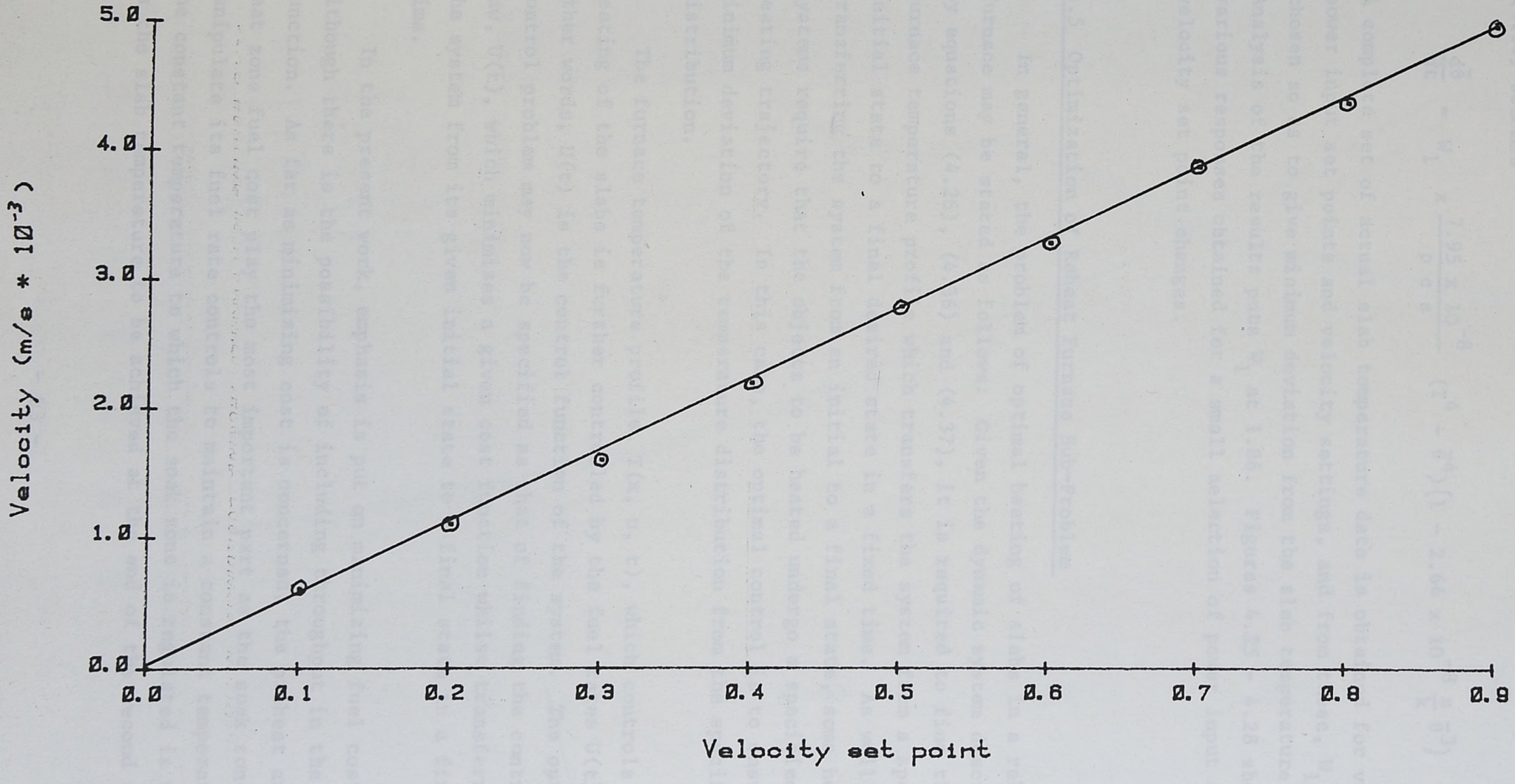

FIG. 4.24 SLAB VELOCITY VERSUS VELOCITY SET POINT

the effects of furnace temperature with moving slabs. Thus, equation (4.36) becomes

$$\frac{d\bar{\theta}}{dt} = W_1 \times \frac{7.95 \times 10^{-8}}{\rho\ c\ s} (T^4 - \bar{\theta}^4)\left(1 - 2.64 \times 10^{-8} \frac{s}{k} \bar{\theta}^3\right) \quad (4.39)$$

A complete set of actual slab temperature data is obtained for various power input set points and velocity settings, and from these, W_1, is chosen so as to give minimum deviation from the slab temperature profiles. Analysis of the results puts W_1 at 1.86. Figures 4.25 - 4.28 show the various responses obtained for a small selection of power input and velocity set point changes.

4.5 Optimization of Reheat Furnace Sub-Problem

In general, the problem of optimal heating of slabs in a reheat furnace may be stated as follows: Given the dynamic system described by equations (4.26), (4.36) and (4.37), it is required to find the furnace temperature profile which transfers the system from a specified initial state to a final desired state in a fixed time. As well as transferring the system from an initial to a final state, some heating systems require that the objects to be heated undergo a specified heating trajectory. In this case, the optimal control is to ensure a minimum deviation of the temperature distribution from the specified distribution.

The furnace temperature profile, T(x, u, t), which controls the heating of the slabs is further controlled by the fuel rates U(t). In other words, U(t) is the control function of the system. The optimal control problem may now be specified as that of finding the control law, U(t), which minimizes a given cost function whilst transferring the system from its given initial state to a final state in a fixed time.

In the present work, emphasis is put on minimizing fuel cost although there is the possibility of including throughput in the cost function. As far as minimizing cost is concerned, the preheat and heat zone fuel cost play the most important part as the soak zone will manipulate its fuel rate controls to maintain a constant temperature. The constant temperature to which the soak zone is regulated is the same as the slab temperature to be achieved at the end of the second zone.

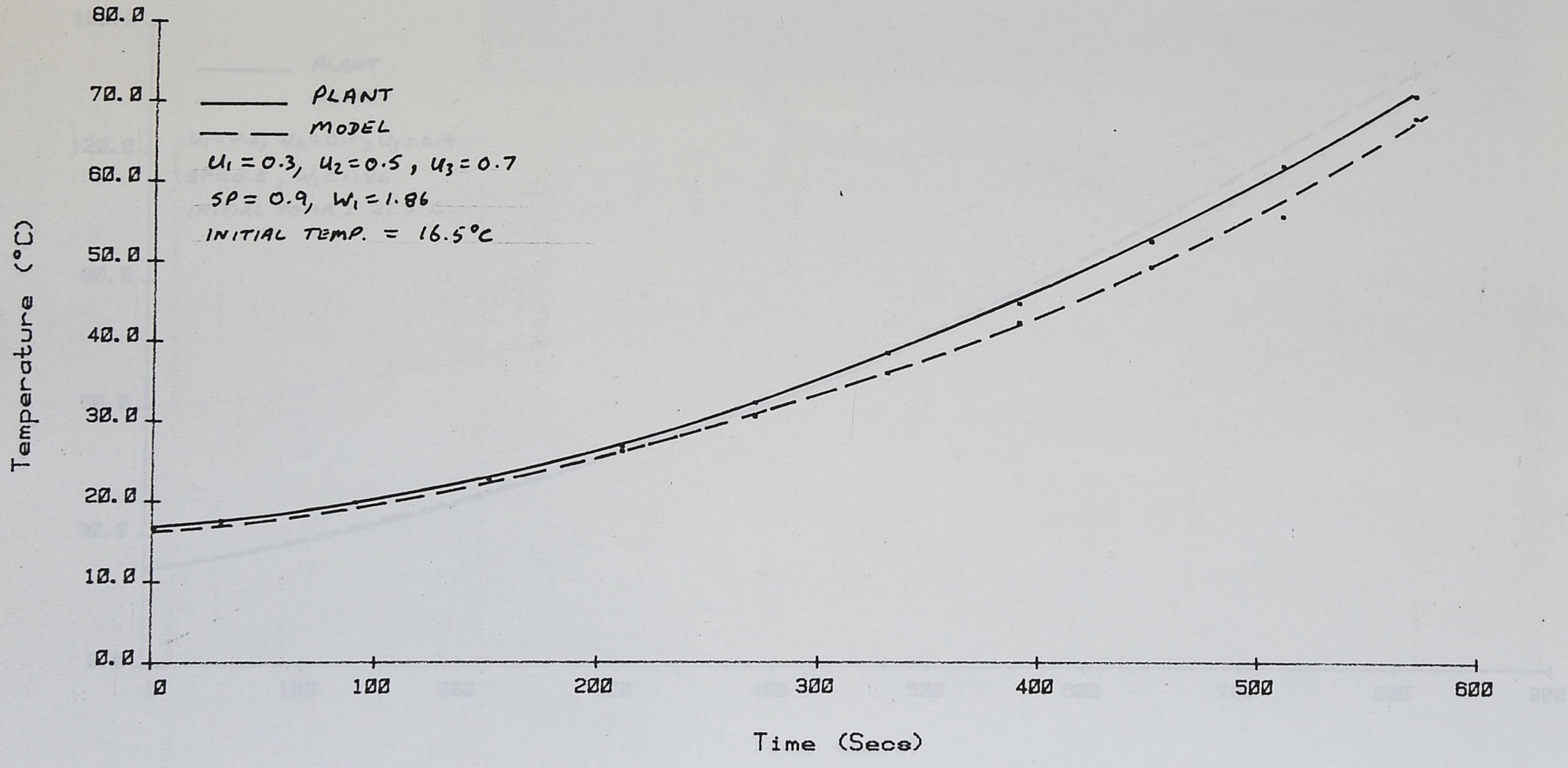

FIG. 4.25 COMPARISON OF SLAB MODEL AND PLANT TEMPERATURES

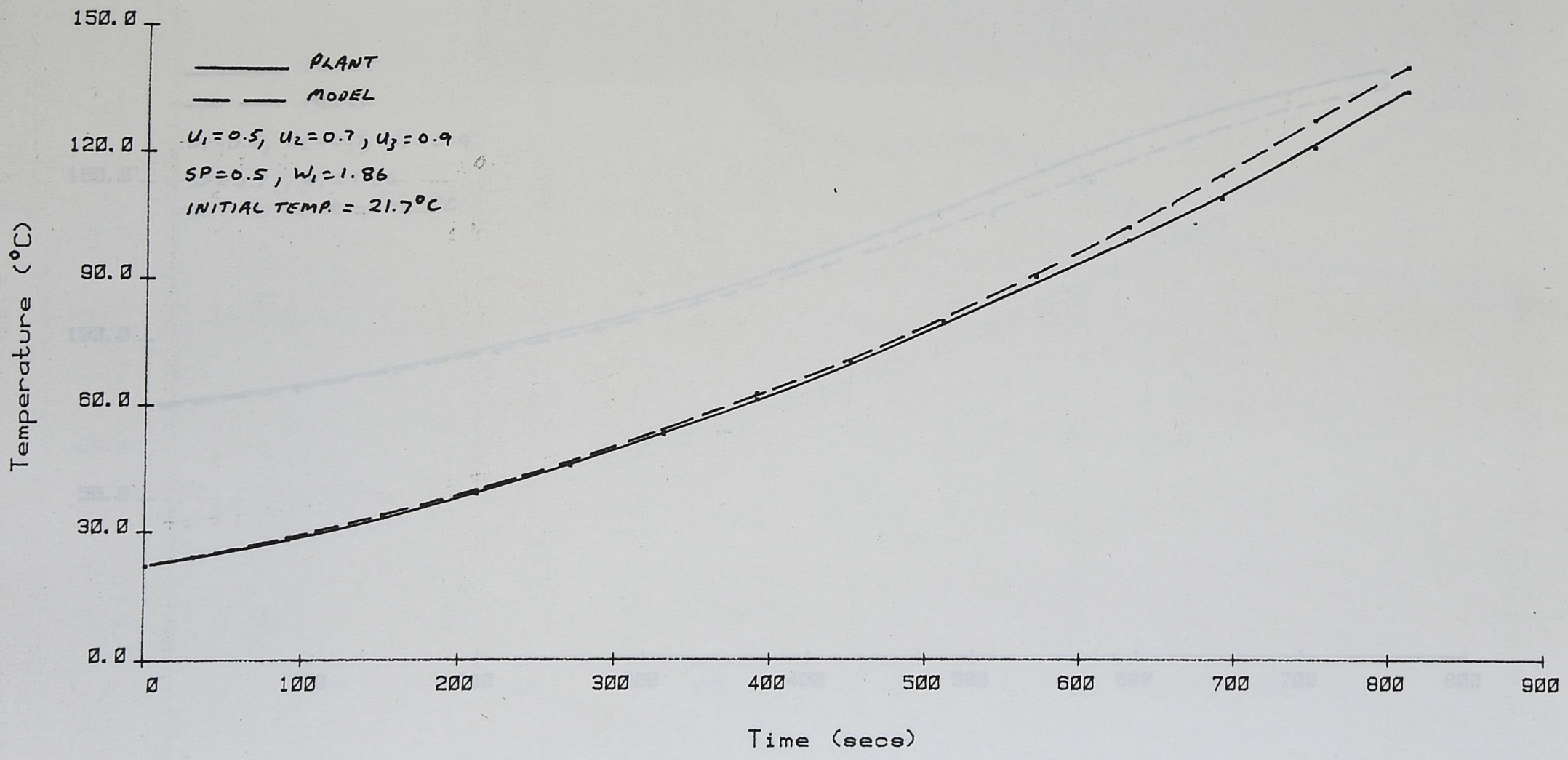

FIG. 4.26 COMPARISON OF SLAB MODEL AND PLANT TEMPERATURES

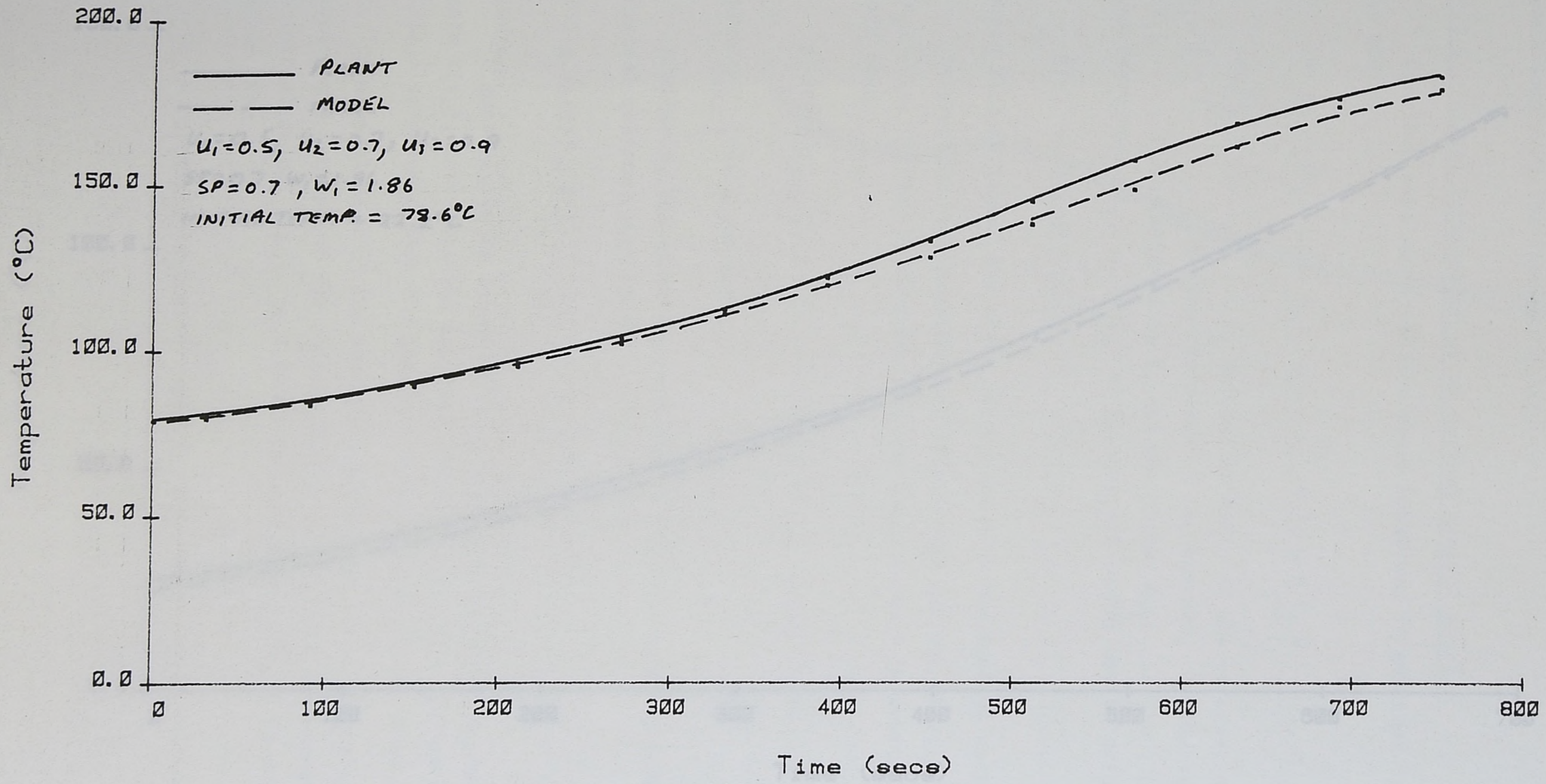

FIG. 4.27 COMPARISON OF SLAB MODEL AND PLANT TEMPERATURES

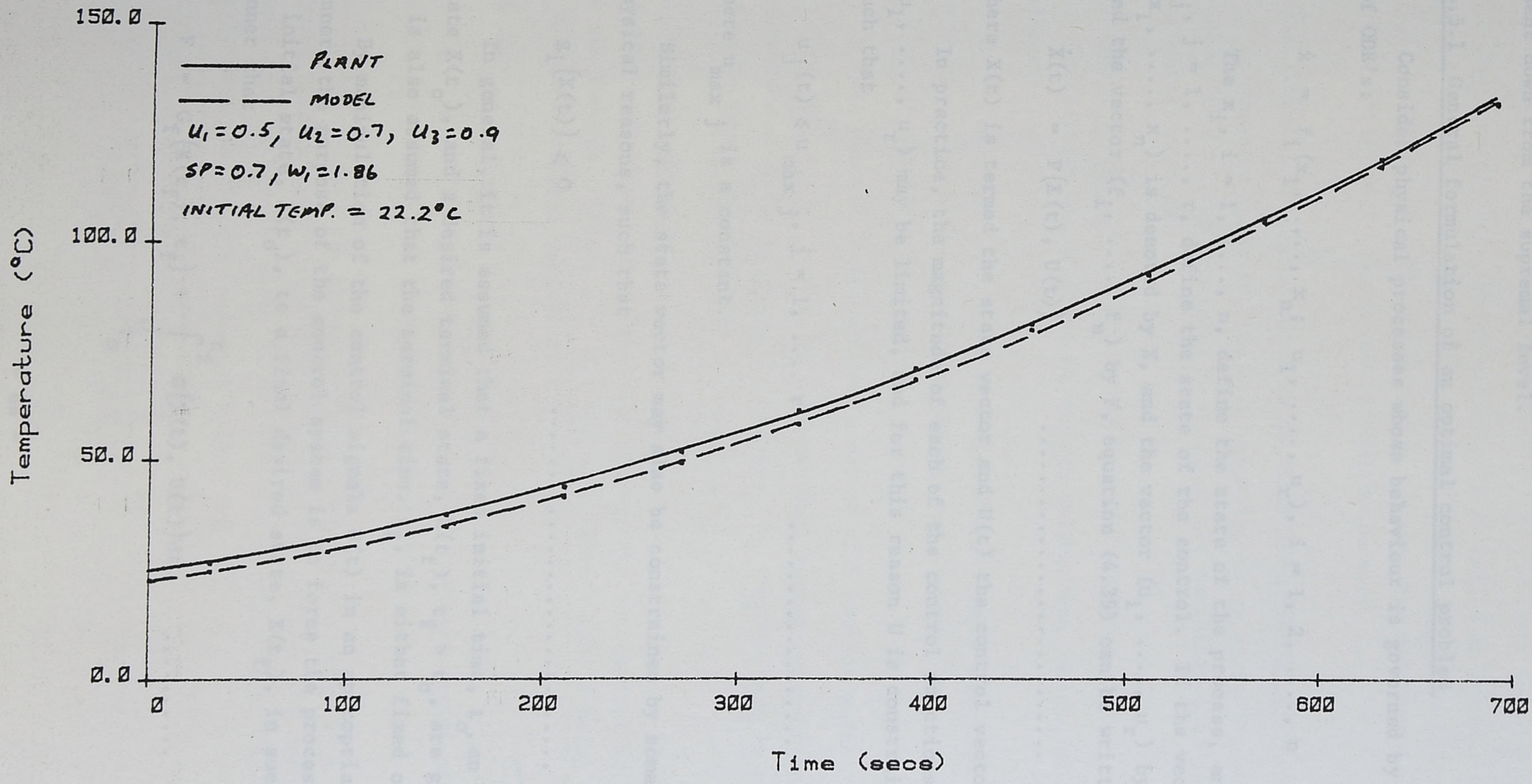

FIG. 4.28 COMPARISON OF SLAB MODEL AND PLANT TEMPERATURES

The temperature to be achieved at the end of the heat zone is that as sent down from the supremal level.

4.5.1 General formulation of an optimal control problem

Consider physical processes whose behaviour is governed by a system of ODE's:

$$\dot{x} = f_i(x_1, \ldots, x_n; u_1, \ldots, u_r), \quad i = 1, 2, \ldots, n \qquad (4.40)$$

The x_i, $i = 1, \ldots, n$, define the state of the process, and the u_j, $j = 1, \ldots, r$, define the state of the control. If the vector $(x_1, \ldots, x_n)$ is denoted by X, and the vector $(u_1, \ldots, u_r)$ by U, and the vector $(f_i, \ldots, f_n)$ by F, equation (4.39) can be written as

$$\dot{X}(t) = F\big(X(t), U(t)\big) \qquad \ldots\ldots\ldots\ldots\ldots\ldots\ldots \qquad (4.41)$$

where X(t) is termed the state vector and U(t) the control vector.

In practice, the magnitude of each of the control functions $(u_1, \ldots, u_r)$ may be limited, and for this reason U is constrained, such that

$$u_j(t) \leqslant u_{\max\, j}, \quad j = 1, \ldots r \qquad \ldots\ldots\ldots\ldots\ldots\ldots \qquad (4.42)$$

where $u_{\max\, j}$ is a constant.

Similarly, the state vector may also be constrained by some physical reasons, such that

$$g_i\big(X(t)\big) \leqslant 0 \qquad \ldots\ldots\ldots\ldots\ldots\ldots\ldots\ldots \qquad (4.43)$$

In general, it is assumed that a fixed initial time, t_o, an initial state $X(t_o)$, and a desired terminal state, $X(t_f)$, $t_f > t_o$, are given. It is also assumed that the terminal time, t_f, is either fixed or free.

By manipulation of the control signals U(t) in an appropriate manner, the purpose of the control system is to force the process from an initial state, $X(t_o)$, to a final desired state, $X(t_f)$, in such a manner that

$$F = G_f\big(X(t_f), t_f\big) + \int_{t_o}^{t_f} G\big(X(t), U(t)\big)dt \qquad \ldots\ldots\ldots \qquad (4.44)$$

is a minimum. F is called the cost function or performance criterion and is a measure of system performance.

The control, U(t), which minimizes F is called an optimal control. The corresponding transition from initial state, $X(t_o)$, to final state, $X(t_f)$, is called an optimal trajectory. Hence, the main problem is in finding the optimal control and optimal trajectory.

4.5.2 Formulation of slab heating as an optimal control problem

In order to formulate the slab reheating as an optimal control problem, it is first necessary to describe the variables that define the overall process.

(1) Input variables

These are a set of slabs of various thicknesses defined as follows:

$S = (s_1, s_2, \ldots, s_n)$, an n-dimensional vector representing the thickness of slabs travelling through the furnace. $s_i \in S$, where S is a set of allowable thicknesses.

$v \in V$, where V is the allowable set of slab pushing rates.

$\theta = (\theta_1, \theta_2, \ldots, \theta_n)$, an n-dimensional vector representing the temperature of slabs entering the furnace. $\theta_i \in Q_i$, where Q_i is a set of allowable input temperatures.

(2) Control variables

The power input set points, u_1, u_2, u_3, are the control variables for the furnace. Hence, $U = (u_1, u_2, u_3)$, where $U \in \mathcal{Z}$, $\mathcal{Z}$ being a set of allowable control variables.

(3) Output variables

$\theta_d \in \Phi_d$, where Φ_d is an allowable set of temperatures of slabs leaving the furnace and is an n-dimensional vector.

Having defined the system variables, consider a group of n slabs passing through the furnace with a pushing rate, v(t). The average temperature of the j^{th} slab, at any time during its passage through the furnace, is given by equation (4.36), i.e.

$$\frac{d\bar{\theta}_j}{dt} = \frac{(T_j^4 - \theta_j^4)}{\beta(\bar{\theta}_j)} \left(1 - \frac{4}{3}\frac{\alpha}{k(\bar{\theta}_j)}\bar{\theta}_j^3\right) \quad \ldots\ldots\ldots\ldots \quad (4.45)$$

where T_j is the furnace temperature which the j^{th} slab sees on its journey through the furnace. T_j is determined by solving equations (4.21) - (4.23). The position of the j^{th} slab at any time t, is given by

$$x_j(t) = x_j(t_o) + \int_{t_o}^{t_f} v(t)dt \qquad \ldots\ldots\ldots\ldots\ldots\ldots \quad (4.46)$$

where $x_j(t_o)$ is the initial position of the slab.

The optimal control problem may now be stated as: given the system described above, it is required to transfer the system from its initial state, $X(t_o)$, to a final desired state, $X(t_f)$, whilst minimizing a cost function of a form given by equation (4.44). As with most physical systems, the system is governed by a set of constraints, namely:

(a) The slab surface temperature (equation (4.37)) should not exceed a specified limit, i.e.

$$\theta_{sj}(t) \leq \theta_{s\ max} \qquad \ldots\ldots\ldots\ldots\ldots\ldots\ldots \quad (4.47)$$

(b) The control variables must lie within their permitted limits, i.e.

$$0 \leq u_j \leq u_{j\ max} \qquad \ldots\ldots\ldots\ldots\ldots\ldots\ldots \quad (4.48)$$

(c) The furnace temperature is limited by

$$T \leq T_{max} \qquad \ldots\ldots\ldots\ldots\ldots\ldots\ldots \quad (4.49)$$

4.5.3 The steady state optimization problem

If slabs of a constant thickness and initial temperature are pushed into the furnace at a constant velocity, and the power input set points are constant, then the furnace is said to be operating under steady-state conditions. As the slabs undergo the same heating process, they will leave the furnace with the same temperature.

In order to make the third zone represent, as nearly as possible, a true soak zone, a feedback scheme incorporating a proportional plus integral controller is employed, as shown in Figure 4.29. The set point given to the soak zone is the desired output temperature, as sent down by the supremal level, and is the same as the desired exit temperature from the second (heat) zone.

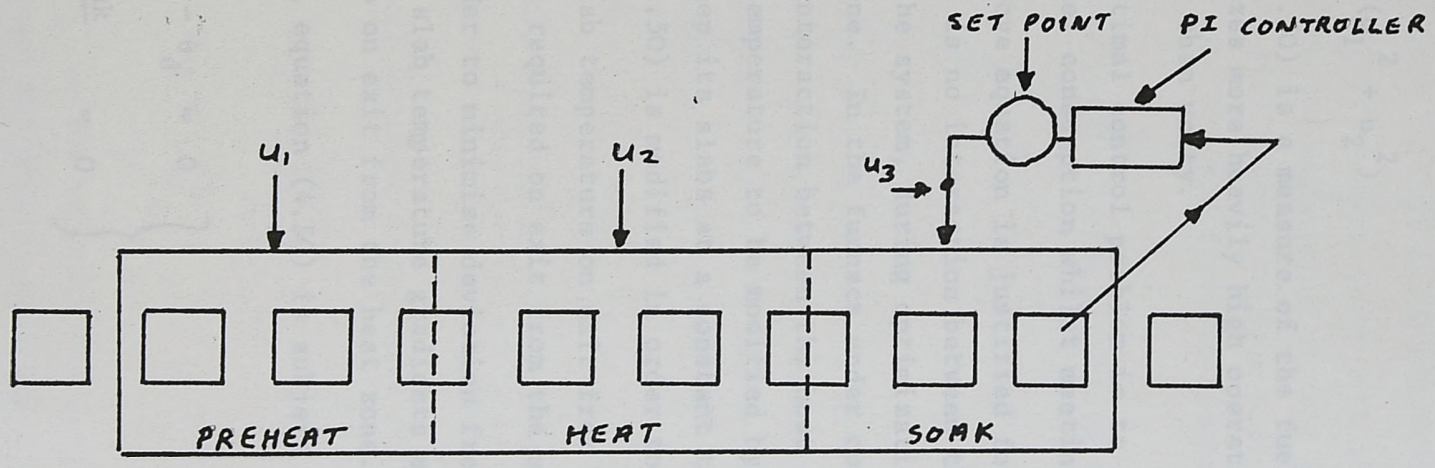

FIG. 4.29 REPRESENTING THE SOAK ZONE BY A PI CONTROLLER

In the steady state, there may exist more than one pair of (u_1, u_2) within the set U that will satisfy the condition $\theta(t_f) = \theta_d$ and equations (4.47) - (4.49), where θ_d is the desired set of output temperatures.

The chosen cost function for the steady-state case is given by

$$F = (u_1^2 + u_2^2) \qquad \ldots\ldots\ldots\ldots\ldots\ldots \quad (4.50)$$

Equation (4.50) is a measure of the fuel consumption and the quadratic form penalizes more heavily high operating fuel rates when u_1 and u_2 are greater than unity.

The optimal control problem is to choose (u_1, u_2) such as to minimize fuel consumption whilst meeting the above constraints.

The above equation is justified for furnaces of the counterflow type where there is no interaction between the heat and soak zones and the output of the system, during optimization, is the exit temperature from the heat zone. In the furnace under consideration, there is a fair degree of interaction between the heat and soak zones which causes the heat zone temperature to be modified by the soak zone as the soak zone tries to keep its slabs at a constant temperature. As a result of this, equation (4.50) is modified in order to meet two requirements:

(1) The slab temperature on exit from the heat zone is the same as that required on exit from the soak zone

(2) In order to minimize deviation from the chosen output temperature, the slab temperature gradients should be as near as possible to zero on exit from the heat zone.

Hence, equation (4.50) is subject to additional equality constraints, namely:

$$\left.\begin{aligned} \theta_{soak} - \theta_d &= 0 \\ \frac{d\theta_{soak}}{dt} &= 0 \end{aligned}\right\} \qquad \ldots\ldots\ldots\ldots\ldots\ldots \quad (4.51)$$

as well as the equality and inequality constraints of the system.

θ_{soak} is the entry temperature into the soak zone

$\frac{d\theta_{soak}}{dt}$ is the slab temperature gradient on entry to the soak zone.

The requirement now is to find a (u_1, u_2) from the allowable set U that minimizes equation (4.50), subject to the equality and inequality constraints.

4.5.4 Including throughput in the static optimization problem

The previous section dealt with the static optimization problem and dealt with the minimizing of fuel input at a constant velocity. This section will proceed to show one possible method of incorporating throughput into the optimization scheme, i.e. minimize fuel and maximize throughput.

Consider the following objective function

$$F(U, v) = c_1(u_1^2 + u_2^2) - c_2 v \qquad \ldots\ldots\ldots\ldots\ldots \quad (4.52)$$

where $v \geq 0$.

It is required here to minimize F with respect to u_1, u_2 and v, subject to the equality and inequality constraints of the system, where c_1 and c_2 are weighting factors. c_1 can be normalized and incorporated with c_2, thus equation (4.52) becomes

$$F(U, v) = u_1^2 + u_2^2 - c\, v \qquad \ldots\ldots\ldots\ldots\ldots\ldots \quad (4.53)$$

In order to minimize the objective function it is required to obtain $\frac{\partial F}{\partial u_1}$, $\frac{\partial F}{\partial u_2}$ for use in a gradient optimization routine. Also needed is $v = f(u_1, u_2)$ in order to evaluate F(U, v).

$$\left.\begin{aligned} \text{Now } \frac{\partial F}{\partial u_1} &= 2u_1 - c\frac{\partial v}{\partial u_1} \\ \frac{\partial F}{\partial u_2} &= 2u_2 - c\frac{\partial v}{\partial u_2} \end{aligned}\right\} \qquad \ldots\ldots\ldots\ldots\ldots\ldots \quad (4.54)$$

$v = f(u_1, u_2)$ is the velocity set point required which, for a given set of power input set points, will bring a load to its final desired output temperature.

For a known $\bar{U}$, $(\bar{U} = u_1, u_2)$, guess $v^{(1)}$ which will bring the load to its desired temperature.

Hence,

$$\theta_f = f(\bar{U}, v^{(1)}) \qquad \ldots\ldots\ldots\ldots\ldots\ldots \quad (4.55)$$

where θ_f = final slab temperature.

If the initial choice of velocity is incorrect, then a new velocity is determined by the relationship

$$v^{(2)} = v^{(1)} + \frac{\varepsilon}{\frac{\partial \theta_f}{\partial v}} (\theta_d - \theta_f), \quad 0 < \varepsilon \leq 1 \qquad \ldots\ldots\ldots \quad (4.56)$$

This gives $v = f(u_1, u_2)$. In order to evaluate equation (4.54), it is required to determine $\frac{\partial v}{\partial u_1}$, $\frac{\partial v}{\partial u_2}$.

Consider the equation

$$\delta\theta_f = \frac{\partial \theta_f}{\partial v} \cdot \delta v + \frac{\partial \theta_f}{\partial u_i} \cdot \delta u_i = 0, \quad i = 1, 2$$

From this is obtained

$$\frac{\partial v}{\partial u_i} = - \frac{\partial \theta_f}{\partial \theta_f} \Big/ \frac{\partial u_i}{\partial v} \qquad \ldots\ldots\ldots\ldots\ldots\ldots\ldots \quad (4.57)$$

An approximate model of the slab equation is given by

$$\frac{\partial \theta}{\partial t} = K\left(T^4(t) - \theta^4(t)\right) \qquad \ldots\ldots\ldots\ldots\ldots\ldots\ldots \quad (4.58)$$

where $T(t)$ is the furnace temperature as "seen" by a slab at any instant in time, $\theta(t)$ is the average slab temperature at any instant in time, K is a constant.

Therefore,

$$\frac{\partial}{\partial t}\left(\frac{\partial \theta}{\partial u_i}\right) = 4K\left[T^3(t)\left(\frac{\partial T}{\partial u_i}\right) - \theta^3(t)\left(\frac{\partial \theta}{\partial u_i}\right)\right] \qquad \ldots\ldots\ldots \quad (4.59)$$

$$i = 1, 2$$

from which $\frac{\partial \theta}{\partial u_i}$ can be evaluated. Similarly,

$$\frac{\partial}{\partial t}\left(\frac{\partial \theta}{\partial v}\right) = 4K\left[T^3(t)\left(\frac{\partial T}{\partial v}\right) - \theta^3(t)\left(\frac{\partial \theta}{\partial v}\right)\right] \qquad \ldots\ldots\ldots\ldots \quad (4.60)$$

from which $\frac{\partial \theta}{\partial v}$ can be evaluated.

A correction term is needed for $\frac{\partial \theta}{\partial v}$, as calculated in equation (4.60), as the value calculated is for fixed time. What is needed is $\left.\frac{\partial \theta}{\partial v}\right|_x$ at a

fixed distance, i.e. furnace length, which is independent of slab velocity.

Correction to $\frac{\partial \theta}{\partial v}$

Consider

$$\theta = \theta(x, u) \qquad \ldots\ldots\ldots\ldots\ldots\ldots\ldots\ldots \quad (4.61)$$

The gradient required $= \left.\frac{\partial \theta}{\partial v}\right|_x$ at $x = X$ where X is the final distance.

Now

$$\delta\theta = \left.\frac{\partial \theta}{\partial x}\right|_v \delta x + \left.\frac{\partial \theta}{\partial v}\right|_x \delta v \qquad \ldots\ldots\ldots\ldots\ldots\ldots\ldots \quad (4.62)$$

hence

$$\left.\frac{\partial \theta}{\partial v}\right|_t = \left.\frac{\partial \theta}{\partial x}\right|_v \left.\frac{\partial x}{\partial v}\right|_t + \left.\frac{\partial \theta}{\partial v}\right|_x = \left.\frac{\partial \theta}{\partial x}\right|_v .t + \left.\frac{\partial \theta}{\partial v}\right|_x \qquad \ldots\ldots\ldots\ldots \quad (4.63)$$

Also

$$v \left.\frac{\partial \theta}{\partial x}\right|_v = \left.\frac{\partial \theta}{\partial t}\right|_v$$

hence

$$\boxed{\left.\frac{\partial \theta}{\partial v}\right|_x = \left.\frac{\partial \theta}{\partial v}\right|_t - \frac{t}{v}\left.\frac{\partial \theta}{\partial t}\right|_v} \qquad \ldots\ldots\ldots\ldots\ldots\ldots\ldots\ldots \quad (4.64)$$

The gradient required, $\frac{\partial \theta}{\partial v}$, in the optimization scheme is reduced by a term $\frac{t}{v}\left.\frac{\partial \theta}{\partial t}\right|_v$ which is clearly positive. At the final time, t is known, t_f, and $\left.\frac{\partial \theta}{\partial t}\right|_v$ is just $\frac{\partial \theta}{\partial t}$ of the model differential equation.

Procedure

(1) Guess an initial value of $\bar{U}$ and v.

(2) Integrate equation (4.58) with the given values of $\bar{U}$ and v, storing values of T(t) and θ(t) at every integration step.

(3) Integrate equations (4.59) and (4.60), substituting in the stored values of T(t) and θ(t), from (2) above, to obtain $\frac{\partial \theta}{\partial u_i}$, i = 1, 2 and $\frac{\partial \theta}{\partial v}f$. Add correction term to $\frac{\partial \theta}{\partial v}f$.

(4) Estimate the next value of v, which will bring the slab to its required final temperature, by using

$$v^{(2)} = v^{(1)} + \frac{\varepsilon}{\frac{\partial \theta}{\partial v}_f} (\theta_d - \theta_f), \quad 0 < \varepsilon \leqslant 1.$$

(5) Repeat steps (2) and (4) until correct value of v is obtained.

(6) Store final values of $\frac{\partial \theta}{\partial u_i}_f$, i = 1, 2 and $\frac{\partial \theta}{\partial v}_f$, from which $\frac{\partial v}{\partial u_i}$, i = 1, 2 can be obtained.

(7) Having obtained $\frac{\partial v}{\partial u_i}$, i = 1, 2, $\frac{\partial F}{\partial u_i}$ can be evaluated.

The above procedure is repeated until the optimal values of u_1, u_2 and v, which minimize the objective function $F(\bar{U}, v)$ are found.

4.5.5 Dynamic optimization

Consider a process whose behaviour is given by

$$\dot{X} = F\big(X(t), U(t)\big) \qquad \ldots\ldots\ldots\ldots\ldots\ldots\ldots \quad (4.65)$$

where X(t) is the state vector and U(t) the control vector.

It is required to force the system from an initial state X(0) to a final desired state, $X(t_f)$, in such a manner that

$$F = G_f\big(x(t_f), t_f\big) + \int_{t_o}^{t_f} G\big[X(t), U(t)\big]\,dt \qquad (4.66)$$

is a minimum, where F is a measure of system performance.

One of the most popular methods of solution of the optimal control problem is the Hamiltonian method, as originated by Pontryagin, and is known as "Pontryagin's Principle" (L. S. Pontryagin et al, 1962). Using Pontryagin's Principle, a scalar function, known as the Hamiltonian, is defined as follows:

$$H\big(X(t), \lambda(t), U(t)\big) = G\big(X(t), U(t)\big) + \lambda(t)F\big(X(t), U(t)\big) \qquad (4.67)$$

The vector $\lambda(t)$ is known as the costate or adjoint of the process defined by equation (4.65). This vector must satisfy the following set of differential equations:

$$\left.\begin{aligned} \dot{\lambda}_i(t) &= -\frac{\partial H}{\partial x_i}\ , \ i = 1, \ldots, n \\ \text{or} \quad \dot{\lambda}(t) &= -\frac{\partial H}{\partial x} \end{aligned}\right\} \qquad (4.68)$$

where the partial derivatives are evaluated along an optimal trajectory. It can be seen from equation (4.66) that

$$\left.\begin{aligned} \dot{x}(t) &= \frac{\partial H}{\partial \lambda_i}\ , \ i = 1, \ldots, n \\ \text{or} \quad \dot{X}(t) &= \frac{\partial H}{\partial \lambda} \end{aligned}\right\} \qquad \ldots\ldots\ldots\ldots\ldots\ldots \quad (4.69)$$

The system of equations (4.68) and (4.69) is called the Hamiltonian system. The main result of Pontryagin's Principle is stated as follows: The optimum control, U(t), which minimizes the performance criterion, equation (4.66), must minimize the Hamiltonian H, given by equation (4.67). This is a necessary condition on the control function U(t).

Therefore, according to Pontryagin's Principle, the control U(t) is optimal if H is minimized. Hence

$$\frac{\partial H}{\partial U} = 0 \qquad \ldots\ldots\ldots\ldots\ldots\ldots\ldots\ldots \quad (4.70)$$

Equation (4.70) is valid only if H is partial differentiable with respect to U(t), and U(t) is unconstrained. It is not valid if the solution lies outside the constraint boundaries. If H is not differentiable with respect to U(t), then U(t) should be chosen which will minimize H. Differentiating equation (4.67), with respect to U, yields

$$\frac{\partial H}{\partial U} = \frac{\partial G}{\partial U} + \frac{\partial F}{\partial U}^{T}(X, U)\lambda(t) = 0 \qquad \ldots\ldots\ldots\ldots\ldots\ldots \quad (4.71)$$

where F^T is the transpose of F.

U(t) may be expressed in the form

$$U(t) = f\big(X(t), \lambda(t)\big) \qquad \ldots\ldots\ldots\ldots\ldots\ldots \quad (4.72)$$

There are cases where U is not an explicit function of X and equation (4.72) may be written in a simplified form as:

$$U(t) = f\big(\lambda(t)\big) \qquad \ldots\ldots\ldots\ldots\ldots\ldots \quad (4.73)$$

Substituting equation (4.72) into equation (4.65) yields

$$\dot{X} = F\big(X(t), \lambda(t)\big) \qquad \ldots\ldots\ldots\ldots\ldots\ldots \quad (4.74)$$

and since H can now be expressed as a function of X(t) and $\lambda(t)$, then from equation (4.69),

$$\dot{\lambda} = L\big(X(t), \lambda(t)\big) \qquad \ldots\ldots\ldots\ldots\ldots\ldots\ldots\ldots \quad (4.75)$$

Equations (4.74) and (4.75) are known as Pontryagin's equations. In this form, U has been eliminated by the minimization of H, subject to any constraints.

Before equation (4.75) can be solved, its boundary conditions must be specified. In general, these boundary conditions are not known, but some terminal conditions can be drawn from the transversality condition. For the Hamiltonian formulation of the problem, the transversality condition can be shown to be (Pontryagin et al, 1962):

$$\Big(H\,dt - \sum_{i=1}^{n} \lambda_i \, dx_i\Big)_{t=t_f} = 0 \qquad \ldots\ldots\ldots\ldots\ldots\ldots \quad (4.76)$$

The two terms in equation (4.75) must be zero independent of one another.

There are a number of things that the transversality condition tells about the boundary conditions and these are depicted below.

(1) Fixed end point

If $X(t_f)$ is known, the transversality condition requires $\lambda(t_f)$ to be completely free. This means that $\lambda(t_f)$ is unknown. If the final time is specified, the value of H is unspecified. Also, if the final time is unspecified, the value of H is zero. H is constant along an optimal path.

(2) Free end point

In this case the final time is fixed and the transversality condition requires that $\lambda(t_f) = 0$.

(3) Partially free end point

The transversality condition shows that the final values of the $\lambda_i(t_f)$ corresponding to the fixed $x_i(t_f)$ are free, whilst the corresponding $\lambda_i(t_f)$, for the free $x_i(t_f)$, will be zero.

The above results can be summarized in the following manner:

For the fixed end point problem,

$$X(t_f) \text{ known, } \lambda(t_f) \text{ unknown,}$$

and for the free end point problem,

$$X(t_f) \text{ free, } \lambda(t_f) = 0.$$

In all cases, the initial conditions of the state variables, X(0), are assumed to be known. The above set of boundary conditions forms a two-point boundary problem and the conditions are mixed due to the fact that, although solved simultaneously, X is specified at the beginning of the interval and λ at the end. In general, the solution of the two point boundary value problem is an extremely difficult task and has attracted many researchers.

4.5.6 Computational procedure - steady state

In the steady state, it is required to minimize a cost function of the form

$$F_{u_1, u_2} = (u_1^2 + u_2^2) \qquad \ldots\ldots\ldots\ldots\ldots\ldots\ldots\ldots \quad (4.77)$$

$$\left.\begin{aligned} \text{s.t. } & \theta_{soak} - \theta_d = 0 \\ & \frac{d\theta_{soak}}{dt} = 0 \\ & \theta_s \leq \theta_{s\,max} \\ & T \leq T_{max} \\ & 0 \leq u_j \leq u_{j\,max}, \; j = 1, 2 \end{aligned}\right\} \qquad \ldots\ldots\ldots\ldots\ldots\ldots \quad (4.78)$$

It is only necessary to consider the behaviour of a single slab, in the steady state, since all the slabs undergo a similar heating process. Recapitulating, the average slab temperature is given by the solution of the differential equation (4.36) and the slab surface temperature given by equation (4.37). The furnace temperature experienced by the slab is given by equations (4.27) - (4.29) where, assuming that

the slab enters the furnace at time t = 0,

$$x = v\,t.$$

In order to minimize the function given in equation (4.77), the computation is initiated by choosing a set of (u_1, u_2) points. The slab model equation is then integrated using a fourth order Runge Kutta routine, although in an on-line situation a modified Euler routine would be more appropriate due to the less computational overheads. The integration is stopped when $t = t_f$, where t_f (= 2.84/V secs) is the duration of the heating process including the time spent in the soak zone. The computations are repeated to find the optimum values of (u_1, u_2), by using a direct search optimization routine, that satisfy the conditions as given by equation (4.78).

In practice, however, there is a trade-off in terms of required accuracy and the amount of computational effort needed to achieve the desired accuracy. In order to keep computation time down to a minimum, it is not necessary to adhere rigidly to the equality constraints given in equation (4.78). Also, in a practical situation it is very unlikely that these constraints would be met exactly and at the same time keep the process cost down to a minimum. In view of this the equality constraints are converted into inequality constraints of the form

$$\left.\begin{aligned} \theta_d - \varepsilon_1 \leq \theta_{soak} \leq \theta_d + \varepsilon_1 \\ -\varepsilon_2 \leq \frac{d\theta_{soak}}{dt} \leq \varepsilon_2 \end{aligned}\right\} \quad \ldots\ldots\ldots\ldots\ldots\ldots\ldots \quad (4.79)$$

where ε_1, ε_2 are some small positive scalar quantities and are a measure of the allowable tolerance in the equality constraints.

For simulation purposes, the following set of data is used, unless otherwise specified. (These data, although a lot lower than those found in typical reheat furnaces, are representative of the pilot plant furnace.)

$\theta(0)$ = 20°C, initial slab temperature
$\theta(t_f)$ = 200°C, final slab temperature
$\theta_{s\,max}$ = 500°C, maximum slab surface temperature
$0 \leq u_1 \leq 1.0$
$0 \leq u_2 \leq 1.0$
slab thickness = 20 cm.

The results of simulation studies, at various velocities, are shown in Table 4.2. The simulation studies showed that the slab surface temperature laid closely to the average slab temperature, due to the high thermal conductivity of aluminium. In view of this fact, only the average slab temperature is observed in order to reduce computation time.

Table 4.2

Velocity Set Point	θ_{soak} (°C)	$d\theta_{soak}/dt$	u_1	u_2	$u_1^2 + u_2^2$
0.2	204.0	0.009	0.6432	0.8341	1.109
0.3	205.0	0.0095	0.7939	0.7394	1.171
0.4	205.0	0.01	0.9722	0.7386	1.49
0.5	203.0	0.02	1.0	0.8827	1.78

As is expected, the increase in throughput results in an increase in the power input and hence in the cost of transferring the slab from an initial condition to a final steady state condition, although this would depend on how the throughput cost is weighted against heating contributions to the cost.

4.5.7 Computational procedure - dynamic optimization

As described in section 4.5.3, the system is said to be operating under steady state conditions when slabs of constant thickness are pushed into the furnace at a constant velocity from the same initial conditions.

In the dynamic state, all these conditions will remain constant except for the fact that the desired output temperature is changed after each n-group of slabs. The changing of desired output temperature is a result of the decision made by the supremal level which seeks to find the global optimal operating point. The performance criterion to be minimized is of the form

$$\min_{u_1,u_2} F = \int_0^T \left(u_1^2(t) + u_2^2(t) + u_3^2(t)\right)dt \quad \ldots\ldots\ldots\ldots \quad (4.80)$$

s.t. constraints given by equation (4.78).

As before, the equality constraints are modified and changed to inequality

constraints, as given by equations (4.79).

With the view that the optimization is to be carried out on-line, it is necessary to keep the amount of computational work down to a minimum. Due to the difficulty in solving the two-point boundary problem, and the amount of time required, Pontryagin's Maximum Principle is not used as a method of solution. Instead, the system is continually simulated whilst u_1 and u_2 are adjusted at the beginning of each simulation period and a check made to determine whether any of the constants are violated and/or met. As this process is basically a steady state simulation applied to a dynamic system, u_1 and u_2 are not time-varying over the simulation period. Hence equation (4.80) takes on the form

$$\min_{u_1,u_2} \quad F = u_1^2 + u_2^2 + \frac{1}{T}\int_0^T u_3^2(t)dt \qquad \ldots\ldots\ldots\ldots \quad (4.81)$$

u_3, however, remains time-varying due to the fact that the slabs must maintain their desired temperature whilst in the soak zone.

Unlike the steady state case, where only one slab is simulated, as all slabs follow the same heating profile, the same cannot be said about the dynamic case. Due to the fact that the desired output temperature is redefined after each group of slabs reaches its steady state temperature, there is a transient effect on entry into the soak zone as the slabs try to readjust to their new steady state operating conditions. In this case, a group of slabs is considered to be eight slabs, as the furnace is full when eight slabs occupy its interior. In view of this, it is necessary to determine how well the system behaves as regards the changing of desired output temperature every N-group. This is carried out in the following manner.

The plant is started up optimally using steady state optimization, as described in section 4.5.6. Having allowed the plant to settle down at its steady state operating conditions, the desired output temperature is incremented to a new value. Optimization is performed over the N-group in order to transfer the N-group of slabs from its previous steady state condition to the new steady state condition. The results of this optimization, i.e. a new u_1 and u_2, are applied to the system and the N-group of slabs allowed to transfer through the furnace, arriving at the soak zone at the new designated final temperature. By updating the new final output temperature, up to a predetermined maximum level, a curve can be built up showing function cost versus final output temperature. A

typical curve is shown in Figure 4.30 for a velocity set point of 0.2. The starting temperature is 250°C, in steps of 20°C, up to 500°C. Figure 4.31 shows the temperatures of eight slabs as they enter the soak zone, the dotted lines indicating the desired entry temperature into the soak zone.

From the plots, it can be seen that there is a fair amount of undershoot and overshoot in the first two slabs, respectively. This can best be explained by referring to the following diagram which shows the position of the slabs in the furnace at the time the final temperature set point is to be updated.

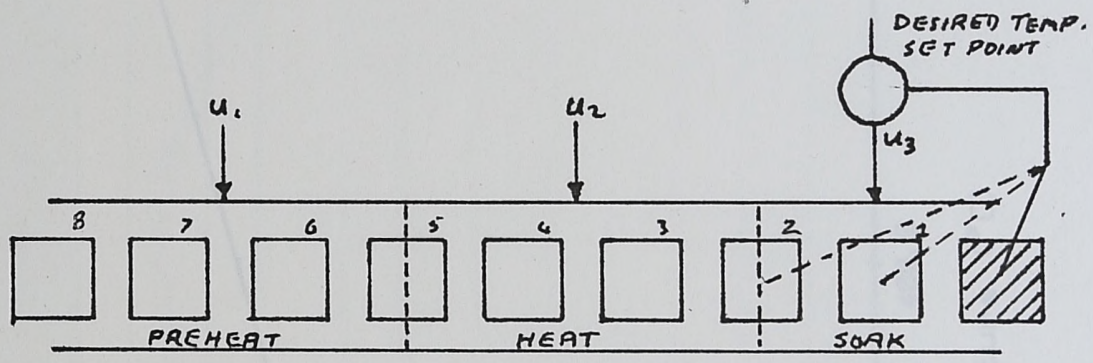

Consider the shaded slab, which is the last of an N-group, which is leaving the furnace at a specified exit temperature, θ_1 out. The slabs shown in the diagram are a new N-group and have to obtain a new desired exit temperature, namely θ_2 out. The power input, u_3, to the soak zone is increased in order to enable slab number 1 to rise to the new desired exit temperature. As slab 1 has only a short distance to travel to the exit of the furnace, it does not reach θ_2 out. Due to the fact that control, at the present time, is centred around slab 1, slab 2 overshoots the desired exit temperature because of the increase in power needed for slab 1 to obtain θ_2 out. As slab 2 is above its desired exit temperature, the power into the soak zone is reduced, when slab 1 leaves the furnace, in order to compensate for the overshoot of slab 2. By continually simulating the process, u_1 and u_2 are selected so as to give the best overall response in transferring the system from θ_1 out to θ_2 out.

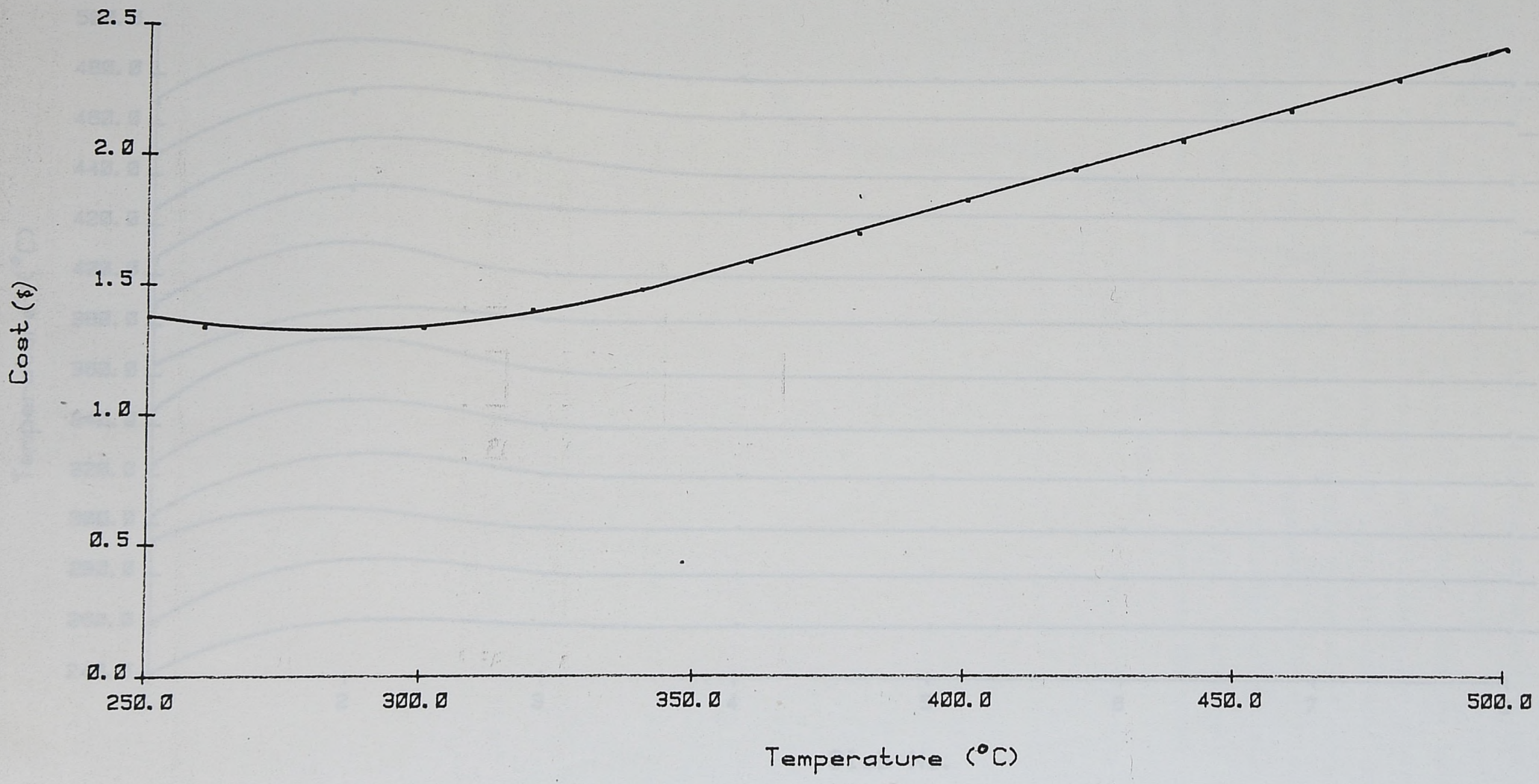

FIG. 4.30 FURNACE COST VERSUS SLAB TEMPERATURE

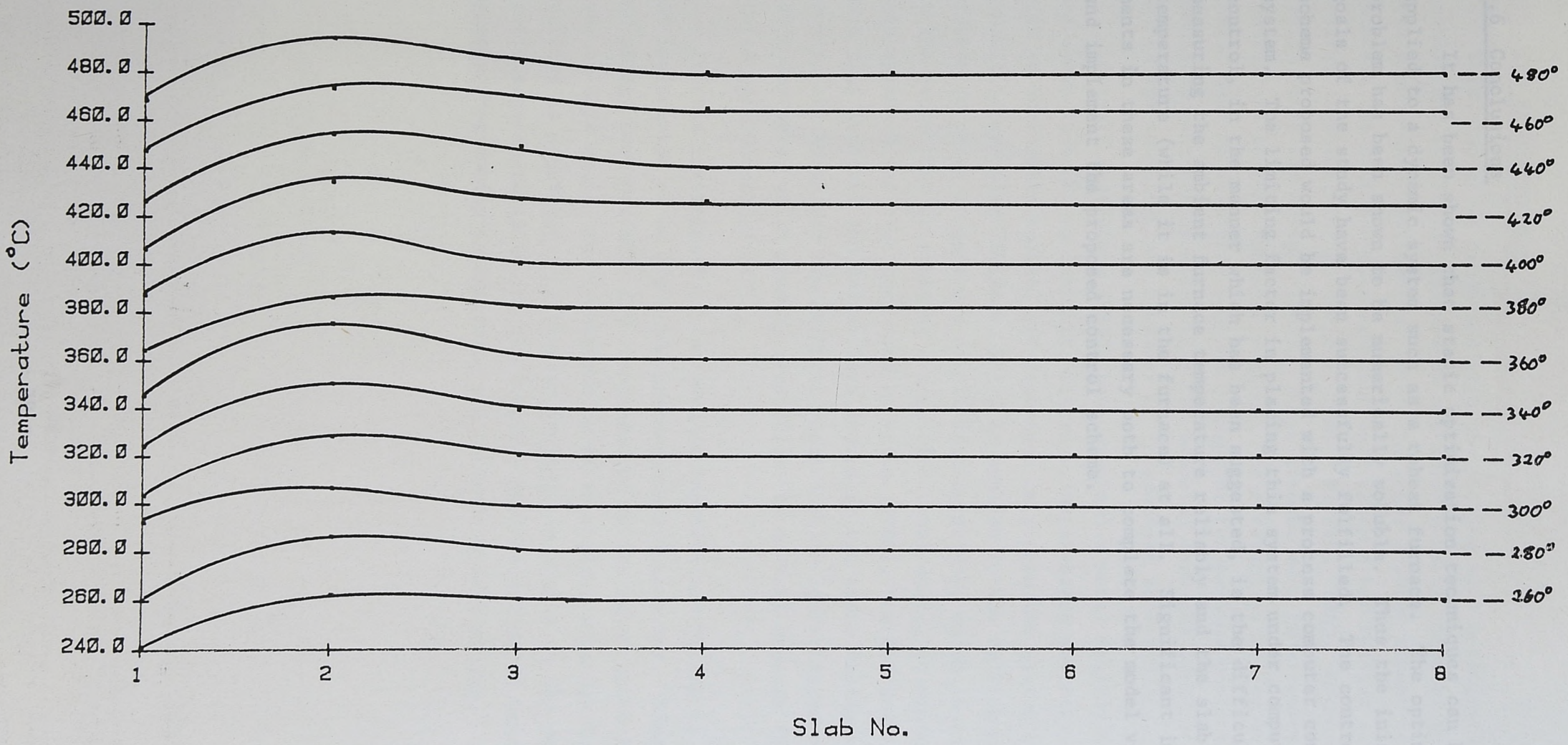

FIG. 4.31 SOAK ZONE SLAB TEMPERATURE TRAJECTORIES

4.6 Conclusions

It has been shown that static optimization techniques can be applied to a dynamic system such as a reheat furnace. The optimization problem has been shown to be numerically soluble. Thus the initial goals of the study have been successfully fulfilled. The control scheme proposed would be implemented with a process computer control system. The limiting factor in placing this system under computer control, in the manner which has been suggested, is the difficulty of measuring the ambient furnace temperature reliably and the slab temperature (while it is in the furnace) at all. Significant improvements in these areas are necessary both to complete the model validation and implement the proposed control scheme.

5.0 THE REVERSING MILL

This chapter is concerned with the rolling mill optimization problem and its implementation on a process control computer for possible on-line application. Over the years a large amount of interest has been shown in computer applications for rolling mill control (Avitzar, 1972; Wallace, 1969; Fapiano, 1963; Krummel, 1961; Smith and Gripp, 1962). These schemes vary from semi-automated controllers to full computer control. More recently, Eaglen et al (1973) have successfully applied a computer for on-line control of a simulated six-stand rolling mill, by breaking down the work carried out by the computer into a number of independent sub-problems.

Lopresti and Patton (1970) have examined a metal rolling mill and shown it to be an implicit, discrete, multi-state control process, with an admissible control set dependent only upon the system state. Dynamic programming (Bellman, 1957) is applied to the rolling mill problem in order to generate a roll setting policy, which is optimal in the sense that it achieves a specified final state, at minimum cost. This approach has also been used by White (1961), the difference being here that Lopresti and Patton have looked at two state variables, namely, thickness and temperature, whereas White concentrates on slab thickness only, which greatly simplifies the overall process (Bellman's "Curse of Dimensionality").

In this investigation, the work of Lopresti and Patton is examined and implemented on an Argus 500 process control computer. Time cost and energy cost per slab are considered to be the major costs involved and, on this basis, the determination of an optimal strategy for roll settings is described. Particular emphasis is placed on the practical problems encountered during the computer implementation of using dynamic programming to determine the optimal control policy.

Parameters of System Model

$p'_1 = 6.757$

$p'_2 = 14.4 \times 10^{-3}$

$p'_3 = 0.52$ (1/m)

$p'_4 = 253 \times 10^{-3}$ ($1/^oK^3.s.m^2$)

$p'_5 = 0.1217$ ($1/^oK^4.s.m^3$)

$p'_6 = 4.32 \times 10^{-10}$ ($^oK/J$)

$p'_7 = 617.76 \times 10^6$ (N/m^2)

$p'_8 = 1.8 \times 10^{-3}$ ($1/^oK$)

$p'_9 = 50 \times 10^{-3}$

$p'_{10} = 92.664 \times 10^6$ (N/m^2)

$p'_{11} = 27.8 \times 10^3$ ($N/m^2.^oK$)

$p'_{12} = 491 \times 10^{-3}$ (m^3) - slab volume

$p'_{13} = 1.27$ (m) - slab width

$p'_{14} = 8.333$ (r/sec) - roll angular velocity

$p'_{15} = 1.27 \times 10^{-10}$ (m/N) - mill deflection constant

$p'_{16} = 4$ (s) - mill reversal time

$p'_{17} = 0.508$ (m) - roll radius

$p'_{18} = 7.473 \times 10^6$ (N) - F_{max}

$p'_{19} = 22.78 \times 10^3$ (Nm) - τ_{max}

$p'_{20} = 0.05$ ($/s)

$p'_{21} = 0.0028$ ($/MJ)

5.1 System Description

The plant to be simulated is a reversing mill which is hot rolling steel plate. The plant is modelled using equations developed by Schulz and Smith (1965) which represent the system on a per pass basis. It is assumed throughout the process that the slab width remains constant, i.e. no turning of the slab during rolling.

5.1.1 Mathematical model

The equations developed by Schulz and Smith are as follows:

Roll force

$$f_i = \left[\left(p'_7 \frac{\Delta h_i}{h_i} \right) 10^{-p'_8 \theta_i + p'_9 p'_{17}/h_i} + (p'_{10} - p'_{11}\theta_i) \right] p'_{13} (p'_{17} \Delta h_i)^{0.5} \quad \ldots\ldots\ldots \quad (5.1)$$

where

f_i = roll force during the i^{th} pass

Δh_i = slab reduction or the i^{th} pass

θ_i = slab temperature before the i^{th} pass

h_i = slab thickness before the i^{th} pass

$p'_7, p'_8, p'_9, p'_{10}, p'_{11}, p'_{13}, p'_{17}$ = empirically determined constants of the simulation model (Lopresti and Patton).

Torque

$$\tau_i = \left[p'_2 + p'_3 (h_i - \Delta h_i) \right] (p'_{17} \Delta h_i)^{0.5} f_i \quad \ldots\ldots\ldots \quad (5.2)$$

where

τ_i = roll torque during the i^{th} pass

Slab thickness

$$h_{i+1} = h_i - \Delta h_i \quad \ldots\ldots\ldots\ldots\ldots\ldots\ldots \quad (5.3)$$

where

h_{i+1} = slab thickness after the i^{th} pass

Time per pass

$$\ell_i = p'_{16} + \frac{p'_{12}}{2\pi\, p'_{13} p'_{14} p'_{17} (h_i - \Delta h_i)} \quad \ldots\ldots\ldots\ldots \quad (5.4)$$

where

ℓ_i = total time required on the i^{th} pass

Energy per pass

$$e_i = p_1' p_{14}' \tau_i (\ell_i - p_{14}) \qquad \ldots\ldots\ldots\ldots\ldots\ldots \quad (5.5)$$

where

e_i = energy required for the i^{th} pass

Slab temperature

$$\theta_{i+1} = \theta_i - p_{12}' \left[p_4' - p_5' \left(\frac{\theta_i}{1000} \right) (h_i - \Delta h_i) \right] \left(\frac{\theta_i}{1000} \right)^4 \left(\frac{\ell_i}{h_i - \Delta h_i} \right) + p_6' e_i$$

$$\ldots\ldots\ldots\ldots\ldots\ldots \quad (5.6)$$

where

θ_{i+1} = slab temperature after the i^{th} pass.

Equation (5.1) indicates that the roll separating force is dependent upon the following process variables: temperature, reduction, entry thickness, width and chemical composition. This equation gives the actual force of deformation needed to transfer the slab from one thickness to another, although there is also an equal and opposite force acting on the mill housing. As a result of this, the actual roll setting used is dependent upon the ability to position the screws to the setting that will compensate for the stretch in the mill housing and for the deflection of the rolls. The reaction force on the mill housing can be presented by

$$f_i = (h_i - \Delta h_i - r_i)/p_{15}' \qquad \ldots\ldots\ldots\ldots\ldots\ldots \quad (5.7)$$

where

r_i = roll setting

p_{15}' = empirically derived constant, i.e. mill deflection constant.

Equation (5.6) represents the temperature change per pass and has been derived from the equation developed by Schulz and Smith (1965). Schulz and Smith decided that since radiation heat transfer is the most dominant mode, then a semi-empirical relationship, based on the radiation law, should be developed to describe the temperature decay. As can be seen, the temperature drop is heavily dependent upon the pass time, ℓ_i, and the emissivity and surface area vary during an actual reduction in thickness. Another effect that has to be considered is the temperature rise caused by the energy added whilst the slab is being reduced by the

rollers. This accounts for the extra term added on in equation (5.6).

5.1.2 Computer simulation

Since equations (5.1) - (5.6) cannot be solved explicitly, an iterative scheme may be used to find the unknowns θ_{i+1} and h_{i+1} as functions of θ_i, h_i and s_i. Before progress can be made, it is necessary to compute Δh_i in order to solve equations (5.1) - (5.6). Δh_i is calculated by equating equations (5.1) and (5.7) and solving for Δh_i. Thus, equating (5.1) and (5.7) results in an equation of the form

$$A\Delta h_i^{3/2} + B\Delta h_i + C\Delta h_i^{1/2} + D = 0 \qquad \ldots\ldots\ldots\ldots \quad (5.8)$$

which is a cubic in $(\Delta h_i)^{1/2}$

where

$$A = \frac{71 \times 10^{-3}}{h_i} \times 10^{\left(-1.8 \times 10^{-3}\ \theta_i + 25.4 \times 10^{-3}\ h_i^{-1}\right)}$$

$$B = 1$$

$$C = 1.15 \times 10^{-10}\ (92.664 \times 10^{6} - 27.8 \times 10^{3}\ \theta_i)$$

$$D = r_i - h_i$$

after substituting the values of the constant, p_n'.

Using Newton's method to solve equation (5.8), convergence to the required solution is obtained within three iterations. Once found, Δh_i may then be substituted into equation (5.1) to determine the force needed for deformation. Substituting the force into equation (5.2) calculates the corresponding torque needed during a pass. Similarly, by substitution, the other equations may be solved, thus resulting in the thickness and temperature of the slab after the i^{th} pass.

The constraints on the system are summarised as:

$$f_i \leq F_{max} \qquad \ldots\ldots\ldots\ldots\ldots\ldots \quad (5.9)$$

$$\tau_i \leq \tau_{max} \qquad \ldots\ldots\ldots\ldots\ldots\ldots \quad (5.10)$$

where F_{max} and τ_{max} are the maximum allowable force and torque, respectively, and are constraints due to the system structure.

The constraints on the states of the slab are as follows

$$\theta_{min} \leq \theta_i \leq \theta_{max} \qquad \ldots\ldots\ldots\ldots\ldots\ldots \quad (5.11)$$

where θ_{min} and θ_{max} are the minimum and maximum allowable slab temperatures. The terminal condition requires that

$$h_{N+1} = h_{min} \qquad \ldots\ldots\ldots\ldots\ldots\ldots \quad (5.12)$$

$$\theta_{min} \leq \theta_{N+1} \leq \theta_{max} \qquad \ldots\ldots\ldots\ldots\ldots\ldots \quad (5.13)$$

Equation (5.12) requires that the slab thickness after its final pass, i.e. pass N+1, where N is the number of passes, be equal to h_{min} (h_{min} being the minimum slab thickness). Equation (5.13) states that the slab temperature after its final pass, i.e. θ_{N+1}, must lie within the region between θ_{max} and θ_{min}, and is a metallurgical constraint rather than a system constraint.

5.2 System Optimization

The problem concerned is: for a given initial state, find the sequence of roll settings $r_1, \ldots, r_N$, which will give an admissible output state, after the N^{th} pass, at the minimum possible cost without violating the system constraints on force and torque.

Being a non-linear discrete system, Lopresti and Patton chose Dynamic Programming as the method for achieving final output at minimum cost. The object of most current control strategies is to minimize the number of passes while at the same time maintaining gauge accuracy. The approach taken by Lopresti and Patton, in achieving an optimal policy, is to take directly into account the major costs subject to control. Time costs per slab and energy costs per slab are considered to be the major costs involved.

5.2.1 Dynamic Programming formulation

The cost of rolling a slab to final thickness in N passes is

$$J_N(h_1, \theta_1, r_1, \ldots, r_N) = \sum_{i=1}^{N} \left(p'_{20}\ell_i + p'_{21}e_1\right) \qquad (5.14)$$

where p'_{20} and p'_{21} are the per unit costs of time and energy in dollars per second and dollars per Mega Joule, respectively.

If the minimum cost function is defined as

$$I_N(h_1, \theta_1) = \min_{r_1} \ldots \min_{r_N} J_N(h_1, \theta_1, r_1, \ldots, r_N) \quad \ldots \quad (5.15)$$

then, from the "Principle of Optimality" (Bellman, 1957),

$$I_N(h_1, \theta_1) = \min_{r_i} \{(p'_{20}\ell_1 + p'_{21}e_1) + I_{N-1}(h_2, \theta_2) \quad (5.16)$$

r_i being chosen from a set of roll settings which do not violate any of the system constraints.

The two state variables, thickness and temperature, are quantized into (P + 1) and (M + 1) points, respectively, by constraining the h and θ values to the sets

$$H = h|h = h_{min} + K\frac{(h_{max} - h_{min})}{P}, \quad K = 0, 1, \ldots, P \quad (5.17)$$

and

$$T = \theta|\theta = \theta_{min} + \ell\frac{(\theta_{max} - \theta_{min})}{M}, \quad \ell = 0, 1, \ldots, M \quad (5.18)$$

This discrete set of points is called Ω. The state of the slab after its final pass must be in Ω_o, where Ω_o is the final state defined by the inequality

$$|h_{N+1} - h_{min}| \leqslant \frac{h_{max} - h_{min}}{2P} \quad \ldots\ldots\ldots\ldots\ldots \quad (5.19)$$

together with equation (5.13).

By evaluating the system equations for each value of (θ, h) in Ω, and testing against constraints, the set of points in Ω which may be transferred to Ω_o in one pass (referred to as Ω_1) may be evaluated. Rather than use one discrete set of allowable roll settings, Lopresti and Patton evaluate an allowable set of roll settings which is dependent upon the slab thickness. The allowable roll settings are those in the discrete set

$$R = r|r = h - j\frac{h}{Q}; \quad h \varepsilon H; \quad j = 0, 1, \ldots, Q \quad \ldots\ldots \quad (5.20)$$

The members of this set which force the state into Ω_o are stored in memory together with the minimum cost, associated with the final pass, for each (θ, h). The set of admissible (θ_N, h_N), Ω_1, is

$$\Omega_1 = (\theta, h) \mid (\theta_{N+1}, h_{N+1}) \in \Omega_o,\ r_N \in R;\ f_N \leq F_{max},\ \tau_N \leq \tau_{max} \quad \ldots\ldots\ldots\ldots\ (5.21)$$

By working backwards in time, until the initial input state is reached, this technique is repeated, each time using partitions of Ω and R to obtain the set

$$\Omega_{i+1} = (\theta, h) \mid (\theta_{N+1-i};\ h_{N+1-i}) \in \Omega_i;\ r_{N-1} \in R \quad \ldots\ldots\ (5.22)$$

together with the minimum costs associated with taking each point in Ω_{i+1} into Ω_o.

The approach to be presented differs from that of Lopresti and Patton in a number of ways. First, as with current practice, there can only be an odd number of rolls during slab reduction due to the fact that rolled slabs must continue in the direction with which they entered the rolling mill. This is, in fact, an obvious requirement, in order to avoid finished slabs piling up with those yet to be rolled. Lopresti and Patton appear to ignore this fact and arrive at results which give an even number of rolls. Secondly, it is assumed that as slabs leave the oven, their actual thickness and temperature are known and appropriate action can be taken in setting the rollers for the first pass. Lopresti and Patton assume that no initial state measurement is available for selecting the first roll setting, and hence the first pass, and possibly the second, results in a non-reduction in slab thickness. This is due to the fact that the initial roll setting is, on occasions, greater than the actual slab thickness. This explains why the results obtained by Lopresti and Patton differ from those to be presented in a later section.

5.2.2 Computer implementation

The first step in the Dynamic Programming formulation is to evaluate the set of points in Ω which may be transferred to Ω_o in one pass, without violating the system constraints. This process is illustrated in Figure 5.1.

The procedure is as follows. Sets H and T are formed, using equations (5.17) and (5.18), respectively. Let the elements of the set H

be h_o, h_1, ..., h_p and those of set T be θ_o, θ_1, ..., θ_m, there being P + 1 and M + 1 elements in each array, respectively, where $h_o = h_{min}$, $h_p = h_{max}$, $\theta_o = \theta_{min}$, $\theta_m = \theta_{max}$. The resulting number of states is (P + 1) x (M + 1) although the actual number of practical states is P x M. This is due to the fact that using an input thickness of h_o, i.e. h_{min}, results in a non-reduction in slab thickness as the slab is already at its required final thickness. In any case, it is unlikely that any slab already at its required final thickness would ever be passed through the oven. Similarly, θ_o, i.e. θ_{min}, cannot be used, as any work done on the slab would result in θ_{N+1} dropping below θ_{min}. For each (θ, h) in Ω, the allowable roll settings, in the discrete set R, were formed as outlined by equation (5.19). Let the elements in this set be r_o, r_1, ..., r_Q. The model was tested for each value of r, each time testing the force and torque against their constraints. The member of the set R which enabled the current state to be transferred to Ω_o, without violating constraints, is stored in memory together with the corresponding cost. By taking each (θ, h) is Ω, in turn, an array is formed of those values of (θ, h), together with roll setting and cost, which could be transferred to Ω_o in one pass.

The next stage in this process is to evaluate the members of the set S, which transfers the set of points in Ω to the next quantization state in H in one pass, together with the associated costs.

By repeating the process N times for each h, in the set H, a complete array of costs and roll settings is formed, together with the (θ, h) in Ω which can be transferred to another state in one pass. It should be noted that the costs associated with each s in S which transfers the (θ, h) in Ω to Ω_o in one pass, are the absolute minimum costs for the relevant states in Ω. Although the actual output states from the model could take on any value within a given tolerance, the values stored by the computer are those members of the sets H and T which are close to the actual state after rolling.

5.2.2.1 Minimum cost strategy

Having formed an array of 1-stage roll costs and roll settings, the next stage in the process is to evaluate the members of the set Ω, which could be transferred to Ω_o in two passes, ignoring those which transferred in one pass as these are already at their absolute minimum

cost. This procedure is illustrated in Figure 5.2 where, for simplicity, a two-dimensional diagram is shown. The corresponding set, T, is assumed to be going into the page.

It can be seen from Figure 5.2 that, for each (θ, h) in Ω, at stage N, there is more than one value, from the set R, that can transfer the state to Ω_1. An example of this is indicated by the thick set lines. The two-stage dynamic programming policy is to find a minimum cost path, from a given initial state, to Ω_o. In the example shown in Figure 5.2 there are three paths from a (θ, h) in Ω which lie on Ω_1. The minimum cost path for a given (θ, h) in Ω, which could be transferred to Ω_o in two passes, is evaluated by summing the cost for each s in Ω_2, together with the costs for the corresponding roll settings in Ω_1. The resulting minimum cost is then stored in memory together with the two corresponding roll settings. This procedure is repeated for each (θ, h) in Ω_2, until a complete array of minimum cost roll settings, which could transfer the elements of Ω_2 to Ω_o in two passes, is formed. By repeating the process, another array of three-stage, minimum cost roll settings is formed, for those values of (θ, h) in Ω which could not be transferred to Ω_o in less than three passes.

5.2.2.2 Even pass conversion

At this point it can be seen that an array of 1-, 2- and 3-stage minimum cost roll settings has been formed, for those values of (θ, h) in Ω which can be transferred to Ω_o. As previously stated, in practice, a 2-stage roll policy is not allowable due to the fact that the slabs end up on the wrong side of the reversing mill. To counteract this problem, an extra pass is necessary for those values of (θ, h) in Ω which transferred Ω_o in two passes. Due to the fact that the slab width is considered to remain constant during the roll period, then the cost of passing a slab through the rollers, with no reduction, is cheaper at its initial thickness, than at its final thickness. The reason for this is that, for a constant volume, the slab must increase in length at lower thickness than at higher thickness and roll cost is a function of pass time which is a function of slab length. Also, energy cost required per pass is cheaper at higher temperatures. As a result of this, a dummy pass is added to the two-stage roll policy before any actual reduction in slab thickness takes place. The procedure is as follows.

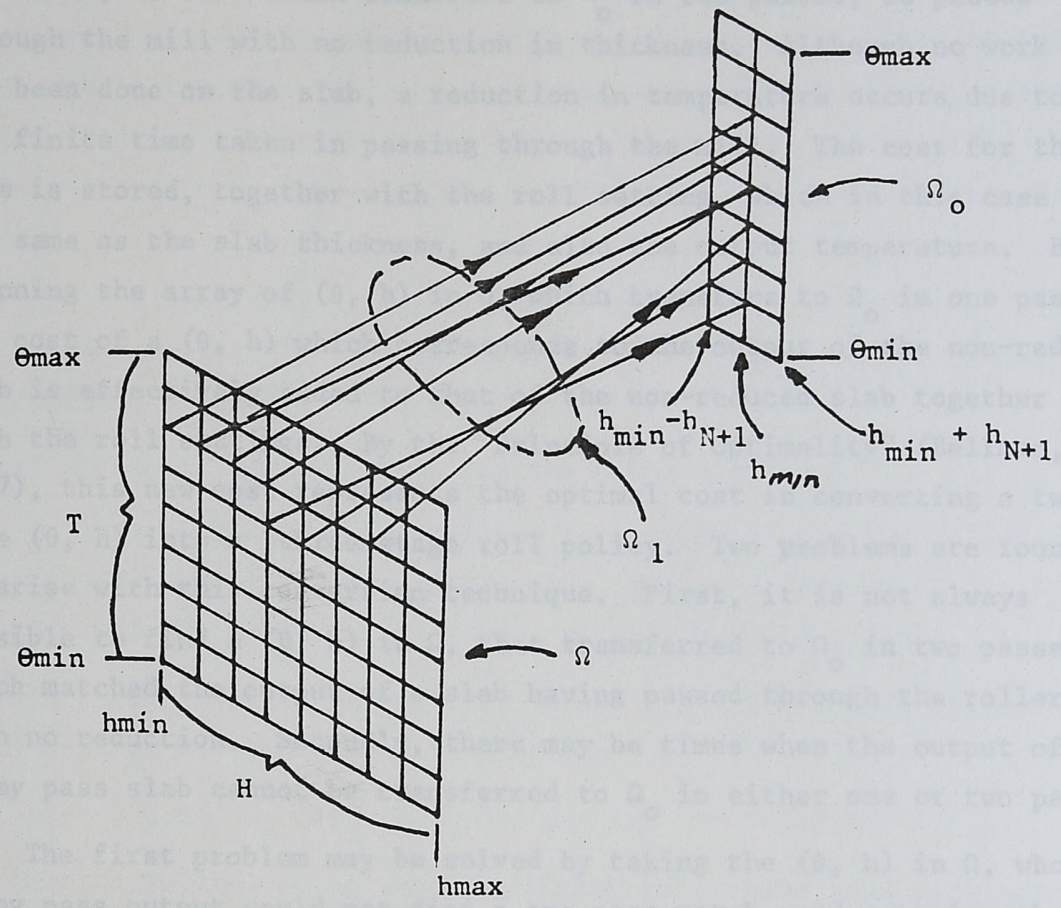

FIG. 5.1 Set of points, Ω_1 in Ω, which may be transferred to Ω_o in one pass, without violating system constraints

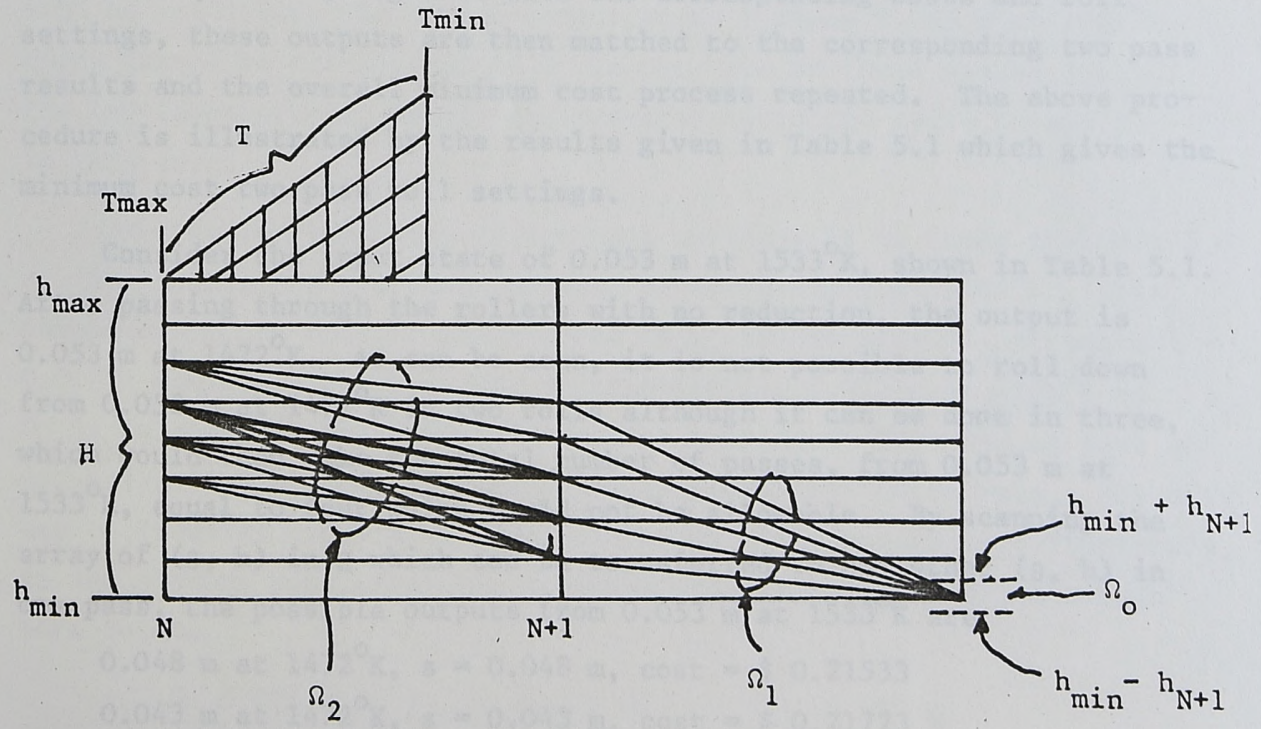

FIG. 5.2 Set of points, Ω_2, which may be transferred to Ω_1 in one pass

A (θ, h) in Ω which transfers to Ω_o in two passes, is passed through the mill with no reduction in thickness. Although no work has been done on the slab, a reduction in temperature occurs due to the finite time taken in passing through the mill. The cost for this pass is stored, together with the roll setting, which in this case is the same as the slab thickness, and also the output temperature. By scanning the array of (θ, h) in Ω, which transfers to Ω_o in one pass, the cost of a (θ, h) which corresponds to the output of the non-reduced slab is effectively added to that of the non-reduced slab together with the roll settings. By the "Principle of Optimality" (Bellman, 1957), this new cost represents the optimal cost in converting a two-stage (θ, h) into a three-stage roll policy. Two problems are found to arise with this conversion technique. First, it is not always possible to find a (θ, h) in Ω, that transferred to Ω_o in two passes, which matched the output of a slab having passed through the rollers with no reduction. Secondly, there may be times when the output of a dummy pass slab cannot be transferred to Ω_o in either one or two passes.

The first problem may be solved by taking the (θ, h) in Ω, whose dummy pass output could not find a two pass match, and scanning the array of all the (θ, h) in Ω, which cannot be transferred to any other state in one pass. Having found all the possible output states for the (θ, h) in question, together with the corresponding costs and roll settings, these outputs are then matched to the corresponding two pass results and the overall minimum cost process repeated. The above procedure is illustrated by the results given in Table 5.1 which gives the minimum cost two pass roll settings.

Consider the input state of 0.053 m at 1533°K, shown in Table 5.1. After passing through the rollers with no reduction, the output is 0.053 m at 1472°K. As can be seen, it is not possible to roll down from 0.053 m at 1472°K in two rolls although it can be done in three, which would then make the total number of passes, from 0.053 m at 1533°K, equal to four which would not be allowable. By scanning the array of (θ, h) in Ω which can be transferred to any other (θ, h) in one pass, the possible outputs from 0.053 m at 1533°K are:

0.048 m at 1472°K, s = 0.048 m, cost = \$ 0.21533

0.043 m at 1472°K, s = 0.043 m, cost = \$ 0.21723

0.038 m at 1472°K, s = 0.038 m, cost = \$ 0.21985

0.033 m at 1472°K, s = 0.033 m, cost = \$ 0.22323

Each of these outputs can be transferred to Ω_o, as shown in the table of two pass roll settings, with the exception of 0.033 at 1472°K which can be transferred in one pass and hence is not picked up as it is not included in the two pass table. The cost of transferring the above outputs to Ω_o in two passes, except 0.033 m at 1472°K, is as follows:

0.048 m at 1472°K = \$ 0.48473
0.043 m at 1472°K = \$ 0.48431
0.038 m at 1472°K = \$ 0.48386

Hence, the total costs of transferring 0.053 m at 1533°K

0.21533 + 0.48473 via 0.048 m at 1472°K = \$ 0.70006
0.21723 + 0.48431 via 0.043 m at 1472°K = \$ 0.70154
0.21985 + 0.48386 via 0.038 m at 1472°K = \$ 0.70375

Therefore the cheapest path is via 0.048 m at 1472°K which gives a total cost of 0.70006 with roll settings

r_1 = 0.048 m, r_2 = 0.033 m, r_3 = 0.012 m.

The second problem, being when the output of a dummy pass slab cannot be transferred to Ω_o in any number of passes, is also best explained by the use of a similar example using the same table. Consider the input state 0.023 m at 1105°K. By passing this through the rollers with no reduction, the actual output state becomes 0.023 m at 1044°K which cannot be transferred to Ω_o in one, two or three passes due to the low temperature. Hence, the previous technique fails to apply in this case.

By scanning the array of one-pass settings it is found that 0.023 m at 1105°K only has one other output, namely 0.018 m at 1044°K. This output state can only be transferred to Ω_o in one pass (Ω_o throughout = 0.0127) and hence the only way of transferring 0.023 m at 1105°K to Ω_o is as shown in the table of two-pass settings. This is not just an optimal policy - it is the only path for this particular case. The only way to transfer 0.023 m at 1105°K to Ω_o in three passes is, effectively, to add a dummy pass after the two-pass reduction. The roll settings then become

r_1 = 0.018 m, r_2 = 0.012 m, r_3 = 0.012 m,

the final output temperature being 983°K, which is within the limits on temperature.

It should be emphasized that this two-roll conversion policy can only be carried out after the optimal three-stage policy has been calculated, as the two-stage policy is needed during the implementation. By working backwards, using previously calculated results, an N-stage rolling policy was computed, each time converting an even roll strategy into an odd roll strategy, as previously outlined.

Table 5.1: Minimum cost two-pass roll settings

Hin (m)	Tin (^{o}K)	r_1 (m)	r_2 (m)	Total Cost ($)
0.053	1533	0.0325	0.0122	0.48129
0.048	1533	0.0328	0.0122	0.48080
0.048	1472	0.0275	0.0123	0.48473
0.048	1411	0.0275	0.0123	0.48466
0.043	1533	0.0328	0.0122	0.48054
0.043	1472	0.0276	0.0123	0.48431
0.043	1411	0.0276	0.0123	0.48423
0.0381	1533	0.0331	0.0122	0.48007
0.0381	1472	0.278	0.0122	0.48386
0.0381	1411	0.0275	0.0123	0.48377
0.0381	1350	0.0225	0.0123	0.48960
0.381	1289	0.0225	0.0123	0.48946
0.033	1411	0.0281	0.0123	0.48329
0.033	1350	0.0228	0.0123	0.48889
0.033	1289	0.0228	0.0123	0.48879
0.0281	1289	0.0229	0.0123	0.48834
0.028	1228	0.0176	0.0124	0.49708
0.028	1166	0.0173	0.0124	0.49745
0.028	1105	0.0173	0.0123	0.49782
0.023	1166	0.0178	0.0124	0.49619
0.023	1105	0.0176	0.0123	0.49706

r_1 = first roll setting

r_2 = second roll setting

A simplified program flow diagram for implementing the Dynamic Programming procedure is shown in Figure 5.3, with a more detailed flow chart shown in Appendix C.

5.3 Discussion of Results

The results obtained by the Argus computer show that a maximum of five passes is necessary to take the allowable (θ, h) in Ω into Ω_o. This differs from the results of Lopresti and Patton where eight passes were necessary for a particular (θ, h) in Ω to be transferred to Ω_o. As mentioned in section 5.2.1, Lopresti and Patton have assumed that no state measurements are available after the slabs leave the oven, and also that initial roll settings are unavoidably, on occasion, greater than the incoming slabs.

Lopresti and Patton chose the final thickness tolerance as

$$|h_{NH} - h_{min}| \leq (h_{max} - h_{min})/2P = 0.0006 \text{ m} \quad \ldots\ldots\ldots \quad (5.23)$$

For the parameters used in this study (see Table 5.2) this would have resulted in 40 quantized states in the set H, which may be considered too large to have been of any practical use on a process control computer. Apart from the storage capabilities of the computer, the computation time was found to be excessive. However, 0.0006 m was still considered to be a reasonable tolerance on final thickness, although using the parameters shown in Table 5.2, in conjunction with equation (5.23), would have resulted in a final thickness tolerance of $\pm$ 0.0025 m, which is considered too large. A table of the optimal roll settings, together with the minimum cost, for taking the allowable (θ, h) in Ω into Ω_o, is shown in Table 5.3. The time taken to compute the array in this table was of the order of 1 min 17 secs. All computation was undertaken on an Argus 500 process control computer, which had a store capability of 24K together with a core cycle time of 2μS. Complete program length, not including data array, was 3.8K (Decimal). All programming was performed in the assembler language, ASTRAL.

Table 5.2: Specification of parameters which specify final and intermediate states

h_{max} = 0.0635 m

h_{min} = 0.0127 m

θ_{max} = 1533°K

θ_{min} = 922°K

P = M = 10 (thickness and temperature quantizing levels, respectively)

Q = 100 (reciprocal of minimum roll setting)

h_{N+1} = $h_{min} \pm$ 0.0006 m (final thickness tolerance)

Table 5.3: Complete table of allowable (θ, h) in Ω which can be transferred to Ω_o in an odd number of passes

Hin (m)	Tin (^oK)	r_1 (m)	r_2 (m)	r_3 (m)	Cost ($)
0.018	1533	0.0128			0.25555
0.018	1472	0.0128			0.25547
0.018	1411	0.0128			0.25537
0.018	1350	0.0126			0.25599
0.018	1289	0.0126			0.25586
0.018	1228	0.0126			0.25570
0.018	1166	0.0124			0.25623
0.018	1105	0.0124			0.25600
0.018	1044	0.0123			0.25641
0.023	1533	0.0126			0.25637
0.023	1472	0.0126			0.25629
0.023	1411	0.0126			0.25620
0.023	1350	0.0126			0.25609
0.023	1289	0.0123			0.25692
0.023	1228	0.0123			0.25676
0.028	1533	0.0123			0.25764
0.028	1472	0.0123			0.25756
0.028	1411	0.0123			0.25748
0.028	1350	0.0123			0.25737
0.033	1533	0.0122			0.25812
0.033	1472	0.0122			0.25805
0.053	1533	0.0480	0.0275	0.0123	0.70006
0.048	1533	0.0483	0.0275	0.0123	0.69979
0.048	1472	0.0483	0.0275	0.0123	0.69972
0.048	1411	0.0376	0.0225	0.0123	0.70933
0.043	1533	0.0432	0.0276	0.0123	0.70115
0.043	1472	0.0432	0.0276	0.0123	0.70107
0.043	1411	0.0380	0.0225	0.0123	0.70887
0.038	1533	0.0381	0.0278	0.0123	0.70294
0.038	1472	0.0381	0.0278	0.0123	0.70285
0.038	1411	0.0381	0.0225	0.0123	0.70868
0.038	1350	0.0381	0.0225	0.0123	0.70853

(Table cont...)

Table 5.3 (continued)

Hin (m)	Tin (^{o}K)	r_1 (m)	r_2 (m)	r_3 (m)	r_4 (m)	r_5 (m)	Cost ($)
0.038	1289	0.0278	0.0176	0.0124			0.72349
0.033	1411	0.0330	0.0228	0.0123			0.71090
0.033	1350	0.0330	0.0228	0.0123			0.71075
0.033	1289	0.0281	0.0176	0.0124			0.72299
0.028	1289	0.0279	0.0176	0.0124			0.72308
0.028	1228	0.0279	0.0173	0.0124			0.72346
0.028	1166	0.0279	0.0173	0.0123			0.72383
0.028	1105	0.0279	0.0173	0.0123			0.72382
0.023	1166	0.0229	0.0176	0.0123			0.72884
0.023	1105	0.0176	0.0123	0.0123			0.75620
0.063	1533	0.0476	0.0275	0.0123			0.70070
0.063	1472	0.0476	0.0275	0.0123			0.70066
0.058	1533	0.0479	0.0275	0.0123			0.70034
0.058	1472	0.0479	0.0275	0.0123			0.70029
0.053	1472	0.0480	0.0275	0.0123			0.69999
0.053	1411	0.0379	0.0225	0.0123			0.70949
0.053	1350	0.0379	0.0225	0.0123			0.70937
0.048	1350	0.0376	0.0225	0.0123			0.70921
0.043	1350	0.0380	0.0225	0.0123			0.70874
0.043	1289	0.0276	0.0176	0.0124			0.72397
0.043	1228	0.0276	0.0173	0.0124			0.72437
0.043	1166	0.0276	0.0173	0.0123			0.72476
0.038	1228	0.0278	0.0173	0.0124			0.72387
0.038	1166	0.0278	0.0173	0.0123			0.72425
0.038	1105	0.0274	0.0173	0.0123			0.72464
0.033	1228	0.0281	0.0173	0.0124			0.72336
0.033	1166	0.0281	0.0173	0.0123			0.72373
0.033	1105	0.0277	0.0173	0.0123			0.72404
0.063	1411	0.0584	0.0426	0.0276	0.0176	0.0124	1.15443
0.058	1411	0.0584	0.0426	0.0276	0.0176	0.0124	1.15424
0.058	1350	0.0584	0.0426	0.0276	0.0176	0.0124	1.15424
0.058	1289	0.0584	0.0426	0.0276	0.0173	0.0124	1.15465
0.058	1228	0.0584	0.0426	0.0276	0.0173	0.0124	1.15468
0.058	1166	0.0584	0.0426	0.0276	0.0173	0.0123	1.15511
0.053	1289	0.0533	0.0427	0.0276	0.0173	0.0124	1.15552

(Table cont...)

Table 5.3 (continued)

Hin (m)	Tin (^{o}K)	r_1 (m)	r_2 (m)	r_3 (m)	r_4 (m)	r_5 (m)	Cost ($)
0.053	1228	0.0533	0.0427	0.0276	0.0173	0.0124	1.15553
0.053	1166	0.0533	0.0427	0.0276	0.0173	0.0123	1.15594
0.053	1105	0.0533	0.0373	0.0274	0.0173	0.0123	1.15862
0.048	1289	0.0483	0.0430	0.0276	0.0173	0.0124	1.15654
0.048	1228	0.0483	0.0430	0.0276	0.0173	0.0124	1.15656
0.048	1166	0.0483	0.0430	0.0276	0.0173	0.0123	1.15695
0.048	1105	0.0483	0.0376	0.0274	0.0173	0.0123	1.15952
0.043	1105	0.0432	0.0380	0.0274	0.0173	0.0123	1.16077
0.063	1350	0.0584	0.0426	0.0276	0.0176	0.0124	1.15443
0.063	1289	0.0584	0.0426	0.0276	0.0173	0.0124	1.15486
0.063	1228	0.0584	0.0426	0.0276	0.0173	0.0124	1.15489
0.063	1166	0.0584	0.0426	0.0276	0.0173	0.0123	1.15533
0.063	1105	0.0527	0.0373	0.0274	0.0173	0.0123	1.15935
0.058	1105	0.0532	0.0373	0.0274	0.0173	0.0123	1.15889

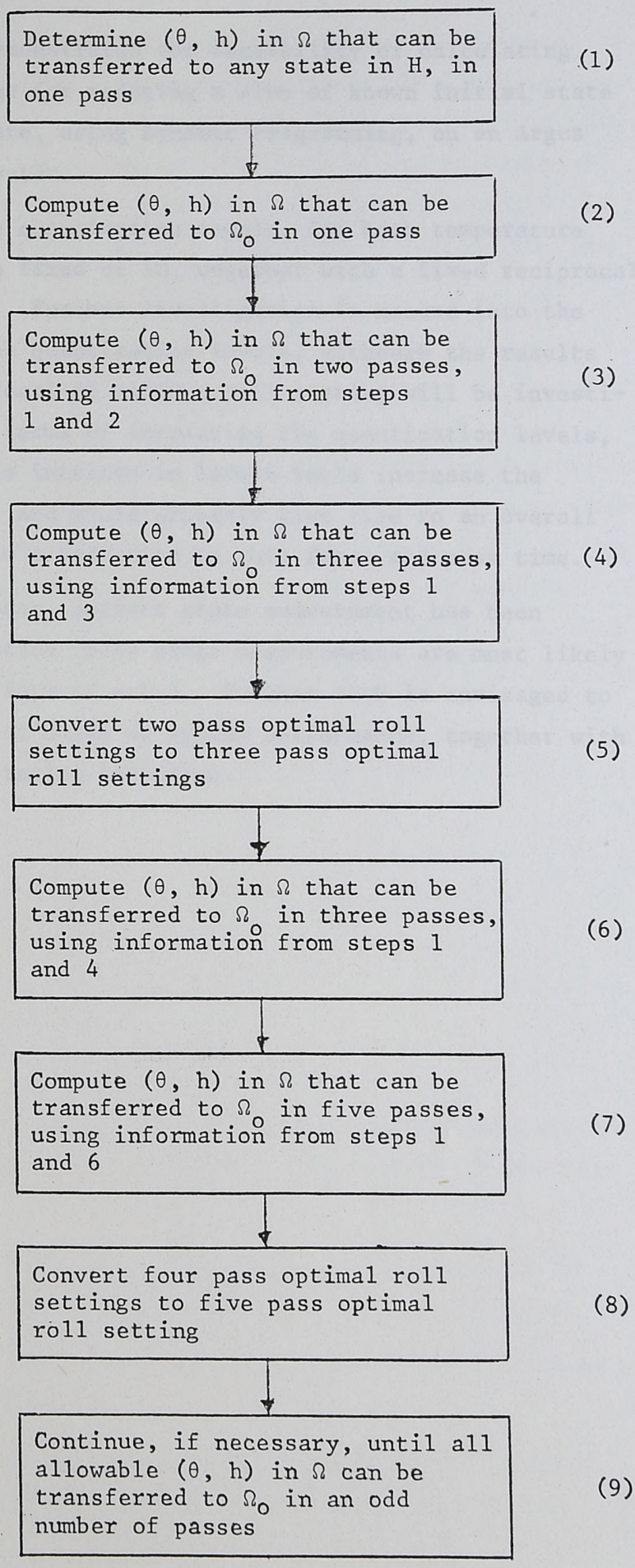

Figure 5.3:
Simplified flow chart of operation performed by the computer

5.4 Conclusions

This chapter has demonstrated the feasibility of calculating the optimal roll settings for reducing a slab of known initial state to some final output state, using Dynamic Programming, on an Argus 500 process control computer.

In the analysis the quantization levels, for both temperature and thickness, have been fixed at 10, together with a fixed reciprocal of minimum roll setting. Further investigation is needed into the effects of increasing the quantization levels, although the results of increasing the reciprocal of minimum roll setting will be investigated in Chapter 6. In terms of increasing the quantization levels, it is considered that the increase in levels would increase the accuracy of the results, and would probably give rise to an overall decrease in costs, due to a reduction in roll force and pass time.

Throughout the chapter, perfect state measurement has been assumed, whereas in practice these state measurements are most likely to be corrupted by some form of noise. Further work is envisaged to investigate the effects of noise on system performance, together with some form of digital filtering technique.

6.0 APPLICATION OF MODEL COORDINATION TO THE COMBINED SUB-SYSTEMS

The previous two chapters have dealt with the local optimization problems of the two independent sub-systems, namely the minimization of energy and passtime costs in the rolling mill and power input costs for the reheat furnace. This chapter will look at the problems of combining these two sub-systems, using Model Coordination theory, in the hope of finding the overall optimal operating conditions for the combined sub-systems.

6.1 System Optimization

In order to study the practical feasibility of the model coordination proposal, discussed in chapter 3, initial investigations are conducted on the simplified sub-systems, as shown in Figure 6.1. In the diagram, everything within the dotted line is, in fact, a process control computer which, in effect, simulates the rolling mill as well as doing the local optimizations for both the rolling mill and furnace sub-systems.

Recapitulating, the reheat furnace optimization problem is:

$$\min_{u_1,u_2} \quad F_f = \int_{t_o}^{t_f} (u_1^2 + u_2^2 + u_3^2)dt \qquad \ldots\ldots\ldots\ldots\ldots \quad (6.1)$$

where

u_1 = power input to the preheat zone

u_2 = power input to the heat zone

u_3 = power input to the soak zone.

The furnace optimization problem is solved subject to the dynamic and algebraic equations of the model, and also takes account of the following requirements:

(i) that the slab temperature on exit from the heat zone be the same as that required on exit from the soak zone;

(ii) that the slab temperature gradients on exit from the heat zone should be zero.

The above are satisfied by incorporating appropriate penalty functions with the performance index given in equation (6.1) and solving using standard optimization techniques.

The rolling mill performance index is given by

$$F_m = c_1\lambda + c_2 e \qquad \ldots\ldots\ldots\ldots\ldots\ldots \quad (6.2)$$

where λ is the total pass time, e is the total energy input, c_1 is the pass time cost weighting, and c_2 the energy cost weighting.

The model coordination approach to the solution of the combined optimization problem uses the temperature of the slabs leaving the furnace as an interconnection variable. The supremal level problem is:

$$\min_{T_{fn}} \{F_f(T_{fn})^* + F_m(T_{fn})^*\} \qquad \ldots\ldots\ldots\ldots\ldots\ldots \quad (6.3)$$

where T_{fn} is the slab exit temperature from the furnace and the inlet slab temperature to the rolling mill, $F_f(T_{fn})^*$ is the optimal value of the furnace performance index, F_f, at a given value of T_{fn} sent down from the supremal unit to the soak zone feedback controller, and $F_m(T_{fn})^*$ is the optimal value of the rolling mill performance index, F_m, at the same value of T_{fn}.

Due to the complexity of the combined system coordination and optimization and the amount of low-level language code needed to carry out the scheme as shown in Figure 6.1, off-line simulations are performed using a large powerful mainframe computer - in this case a CDC 7600 which is situated at the University of London's Computer Centre. For ease of programming, Fortran is used as the main programming language.

Before proceeding with the coordination and optimization of the combined sub-systems, it is worthwhile, at this stage, to examine some of the properties of both the furnace and rolling mill in order to check whether there is a chance of finding a minimum at all for the combined sub-systems.

6.1.1 Furnace sub-system

Figure 4.30 shows how the typical optimal values of the furnace performance index vary with the temperature of the load leaving the furnace, as specified by the set point of the soak zone controller. In order to match those temperatures as required by the reversing mill,

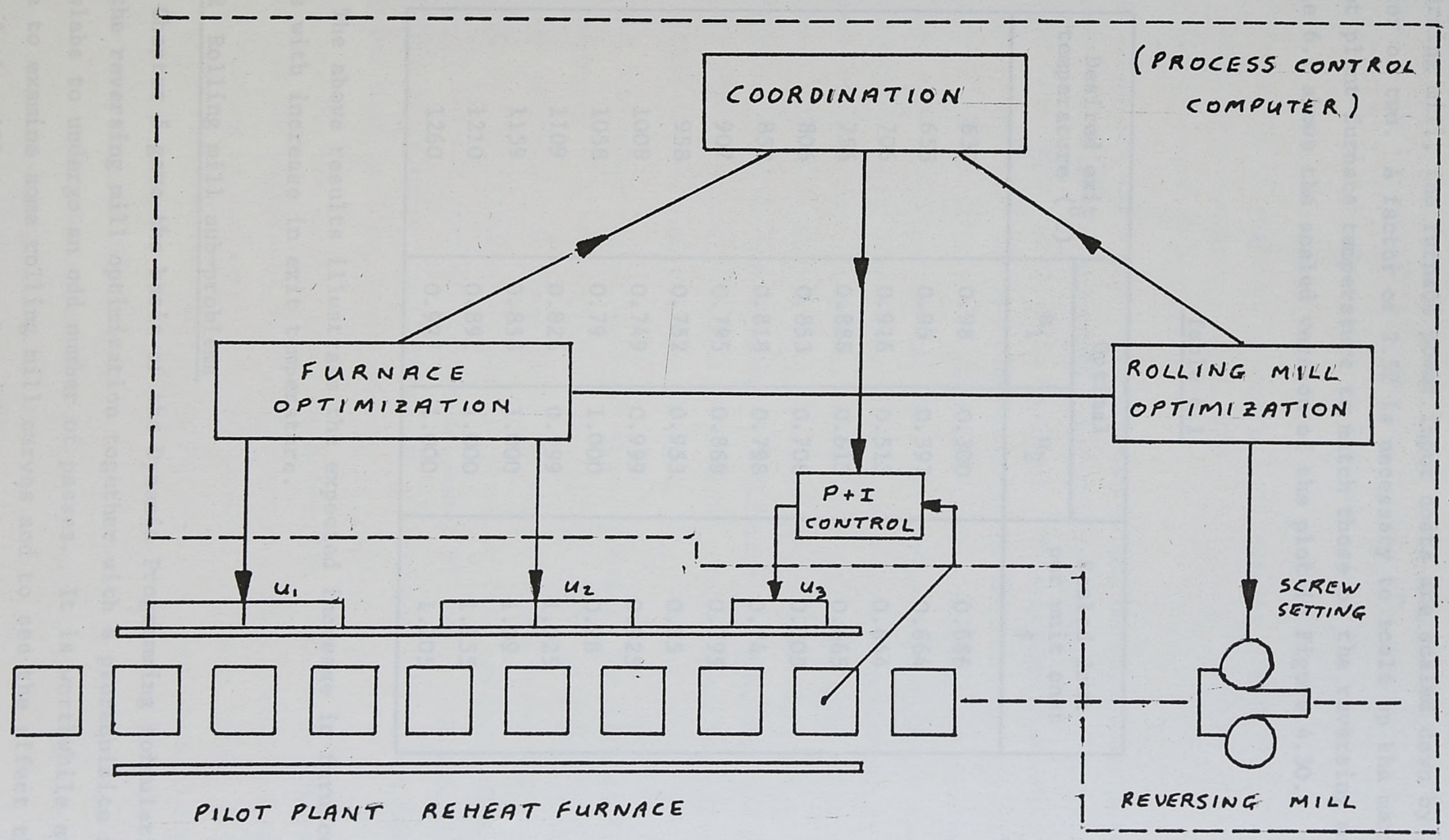

FIG. 6.1 THE SIMULATED FURNACE AND ROLLING MILL SYSTEM

it is necessary to scale up the measured load temperatures produced by the furnace simulation. Also, to match the per unit costs of the reversing mill, the furnace power input costs are scaled down by a factor of two. A factor of 2.52 is necessary to scale up the maximum pilot plant furnace temperature to match those of the reversing mill. Table 6.1 shows the scaled version of the plot in Figure 4.30.

Table 6.1

Desired exit temperature (^{o}C)	Optimal		Scaled down per unit cost $
	u_1	u_2	
630	0.98	0.300	0.686
655	0.95	0.397	0.664
706	0.916	0.513	0.644
756	0.888	0.613	0.665
806	0.853	0.706	0.705
857	0.818	0.798	0.74
907	0.795	0.869	0.795
958	0.752	0.953	0.85
1008	0.749	0.999	0.925
1058	0.79	1.000	0.98
1109	0.826	0.999	1.025
1159	0.858	1.000	1.09
1210	0.891	1.000	1.155
1260	0.927	1.000	1.205

The above results illustrate the expected increase in furnace costs with increase in exit temperature.

6.1.2 Rolling mill sub-problems

Chapter 5 gave the basis of the Dynamic Programming formulation for the reversing mill optimization together with a prerequisite for the slabs to undergo an odd number of passes. It is worthwhile at this stage to examine some rolling mill curves and to see the effect that some of the mill parameters have on the final result.

The graph in Figure 6.2 is a plot of roll mill cost versus slab input temperature for a slab of height 0.018 m. This plot is taken from the figures presented in Table 5.3 using the energy and pass time costs as given by Lopresti and Patton (1970). The parameters used for the graph in Figure 6.2 are as follows:

Input thickness = 0.018 m
Reciprocal of smallest allowable roll setting = 100
Energy cost per pass = \$0.01/MJ
Pass time cost = \$0.05/sec.

If one takes the top three temperatures, it can be seen that there is a decrease in cost for a decrease in input temperature, which is contrary to what might normally be expected. This is explained from the fact that because of the minimum decrement in the roll settings (i.e. reciprocal = 100), then for a particular group of input temperatures, the final roll settings are the same. As a result of this, as the input temperature is decreased, there is a greater reaction force on the mill housing (see chapter 5, equation (5.7)), but because of the coarseness of the allowable roll settings, the rollers are not allowed to "squeeze" together any further to compensate for the increase in reaction force. Apart from this, the slabs still leave the rolling mill within their final thickness bounds.

Figure 6.3 is another plot with the same parameters but with an initial slab thickness of 0.063 m (2.5"). Unlike the slabs of Figure 6.2, which can be reduced to their final thickness in one pass, the slabs in Figure 6.3 are required to undergo three or five passes. This is because of the odd pass constraint and hence the curve exhibits a discontinuity in changing from a three- to a five-pass roll. For details of the odd pass constraint see chapter 5, section 5.1.

Figure 6.4 has exactly the same parameters as those in Figure 6.2, except that the reciprocal of the smallest allowable fractional decrement in roll setting is increased from 100 to 500. In other words, the set of allowable roll settings for any given pass has been more finely quantized. As a result of this, the curve in Figure 6.4 is a lot smoother than that of Figure 6.2, as the wider range of roll settings can compensate for the increase in the mill housing reaction force for decrease in temperature.

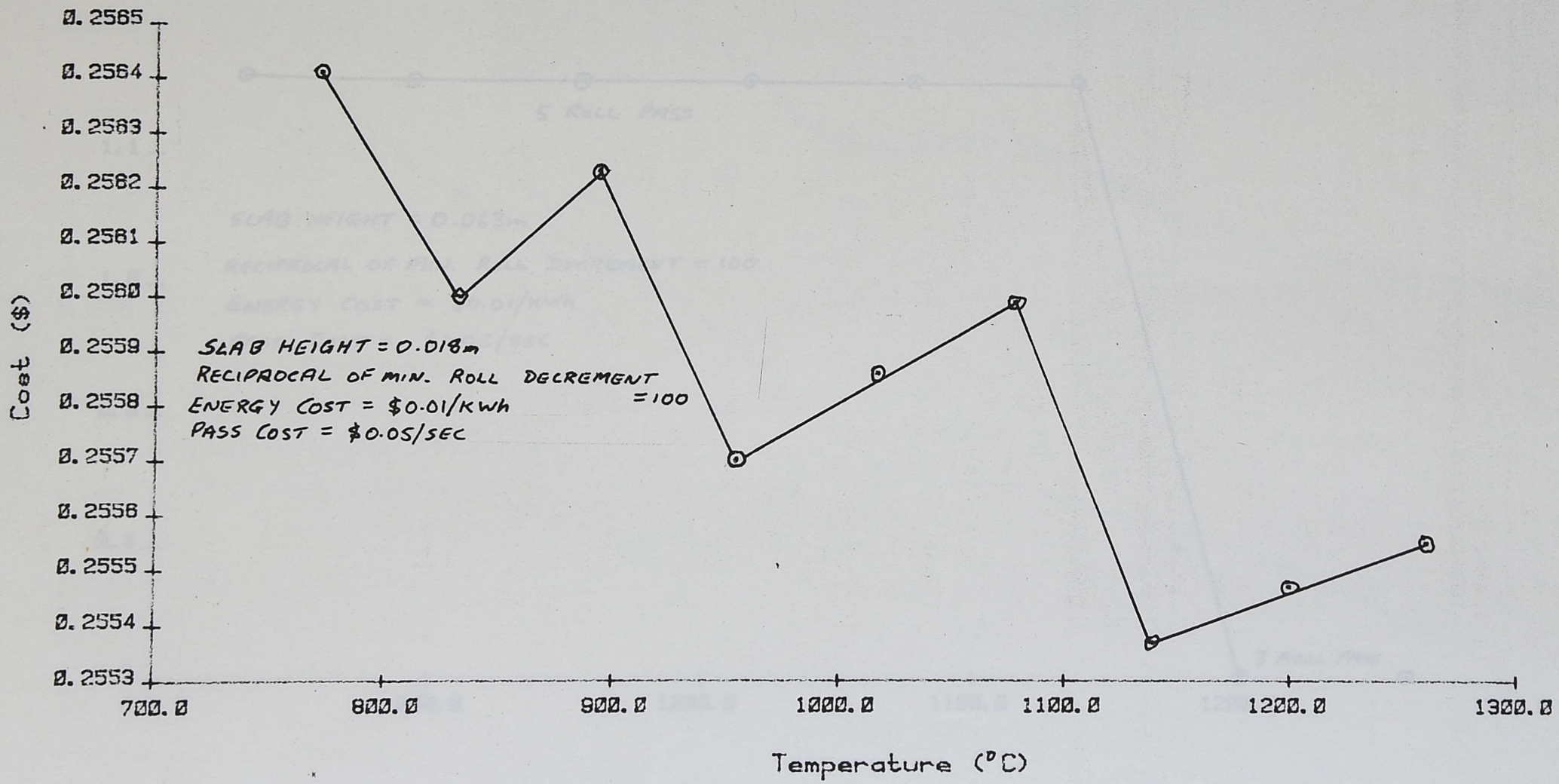

FIG. 6.2 REVERSING MILL COST VERSUS SLAB INPUT TEMPEATURE

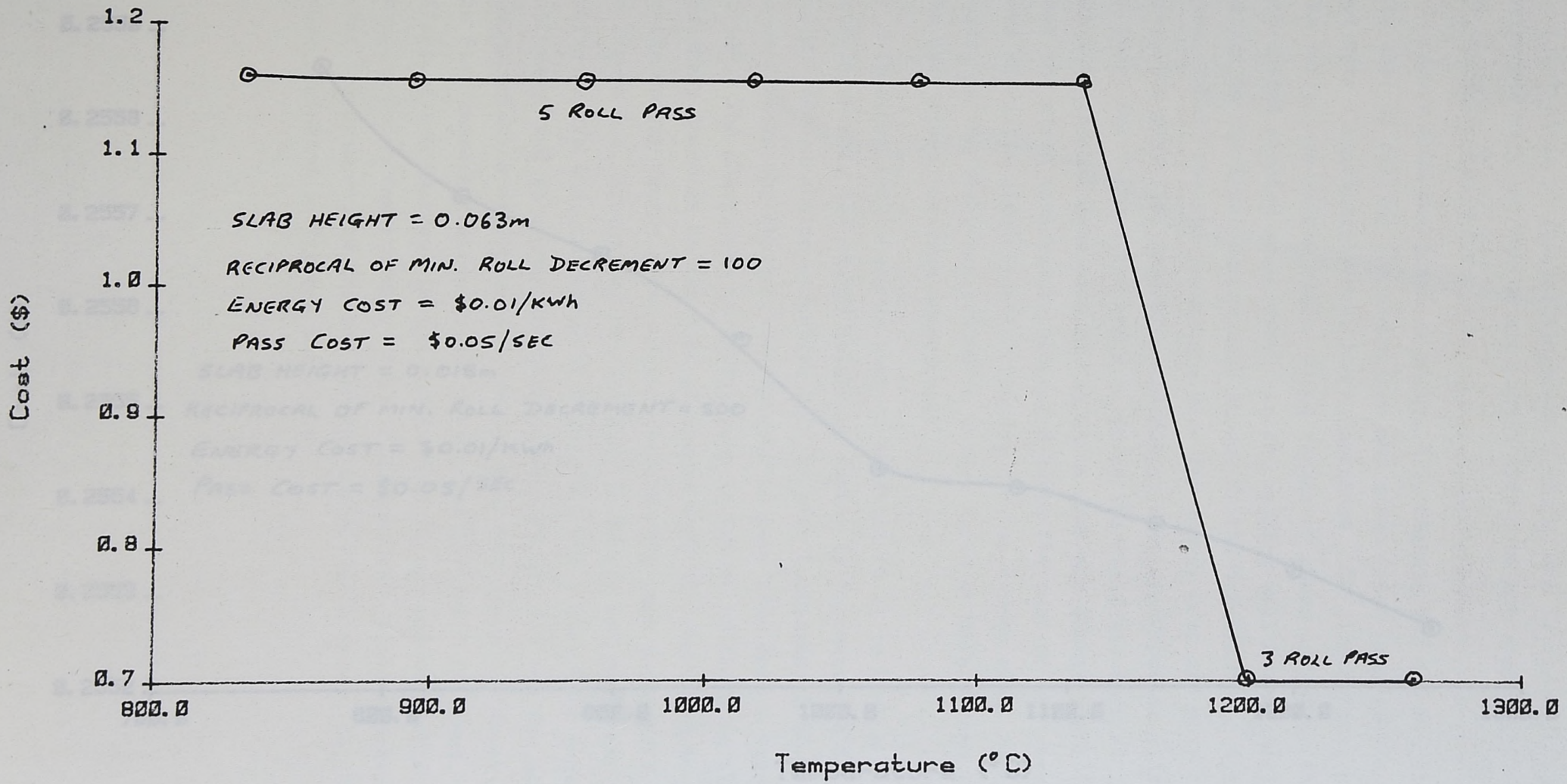

FIG. 6.3 REVERSING MILL COST VERSUS SLAB INPUT TEMPERATURE

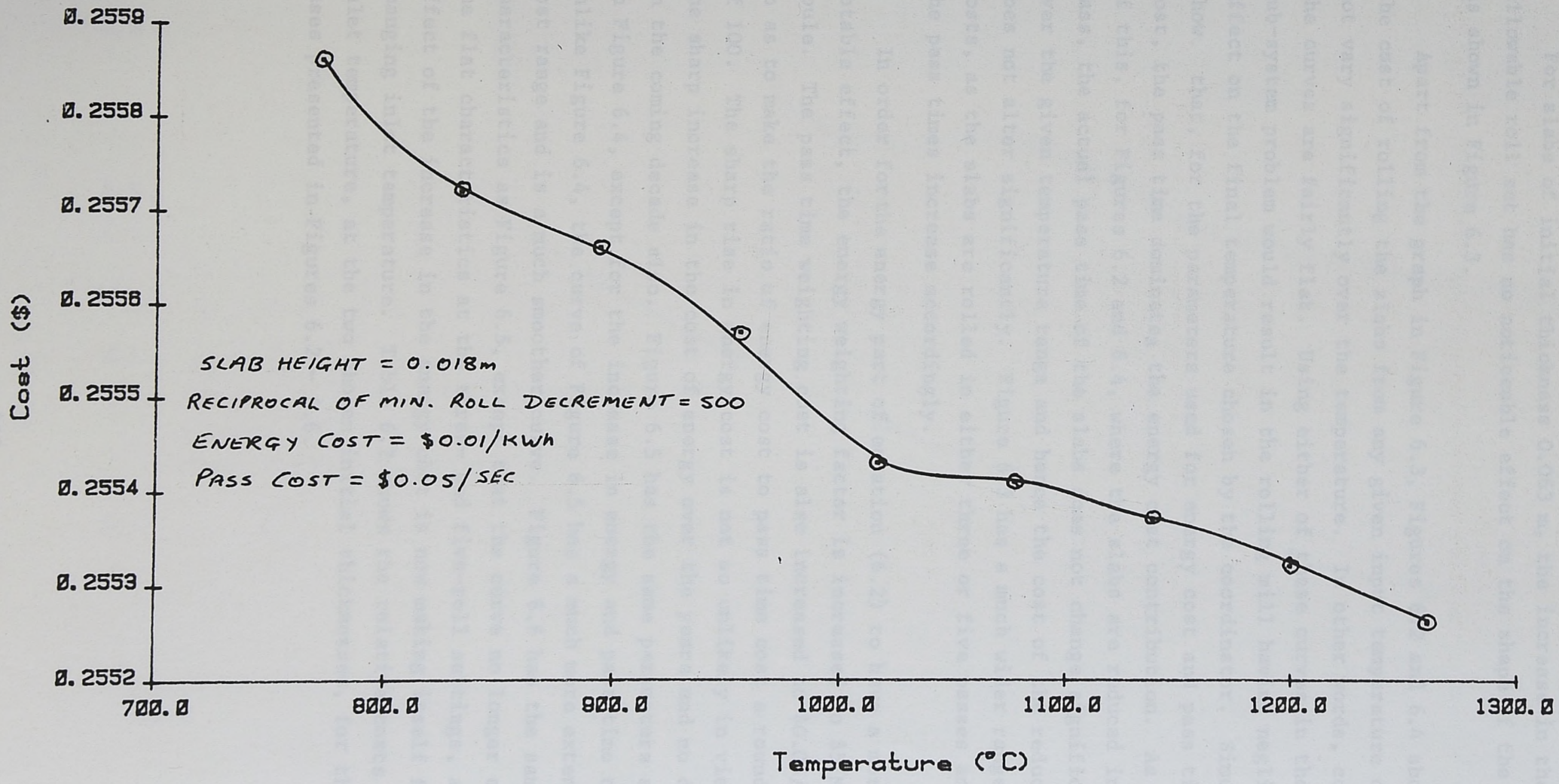

FIG. 6.4 REVERSING MILL COST VERSUS SLAB INPUT TEMPERATURE

For slabs of initial thickness 0.063 m, the increase in the allowable roll set has no noticeable effect on the shape of the curve, as shown in Figure 6.3.

Apart from the graph in Figure 6.3, Figures 6.2 and 6.4 show that the cost of rolling the slabs from any given input temperature does not vary significantly over the temperature. In other words, cost-wise the curves are fairly flat. Using either of these curves in the combined sub-system problem would result in the rolling mill having negligible effect on the final temperature chosen by the coordinator. Simulations show that, for the parameters used for energy cost and pass time cost, the pass time dominates the energy cost contribution. As a result of this, for Figures 6.2 and 6.4, where the slabs are reduced in one pass, the actual pass time of the slabs does not change significantly over the given temperature range and hence the cost of the reduction does not alter significantly. Figure 6.3 has a much wider range in costs, as the slabs are rolled in either three or five passes and hence the pass times increase accordingly.

In order for the energy part of equation (6.2) to have a more notable effect, the energy weighting factor is increased to \$5/Mega Joule. The pass time weighting cost is also increased to \$0.05/sec so as to make the ratio of energy cost to pass time cost a round factor of 100. The sharp rise in energy cost is not so unlikely in view of the sharp increase in the cost of energy over the years and no doubt in the coming decade also. Figure 6.5 has the same parameters as those in Figure 6.4, except for the increase in energy and pass time cost. Unlike Figure 6.4, the curve of Figure 6.5 has a much more extended cost range and is a much smoother curve. Figure 6.6 has the same characteristics as Figure 6.5, except that the curve no longer exhibits the flat characteristics at the three- and five-roll settings, as the effect of the increase in the energy cost is now making itself felt with changing inlet temperature. Table 6.2 shows the relative costs versus inlet temperature, at the two chosen initial thicknesses, for the five cases presented in Figures 6.2 - 6.6.

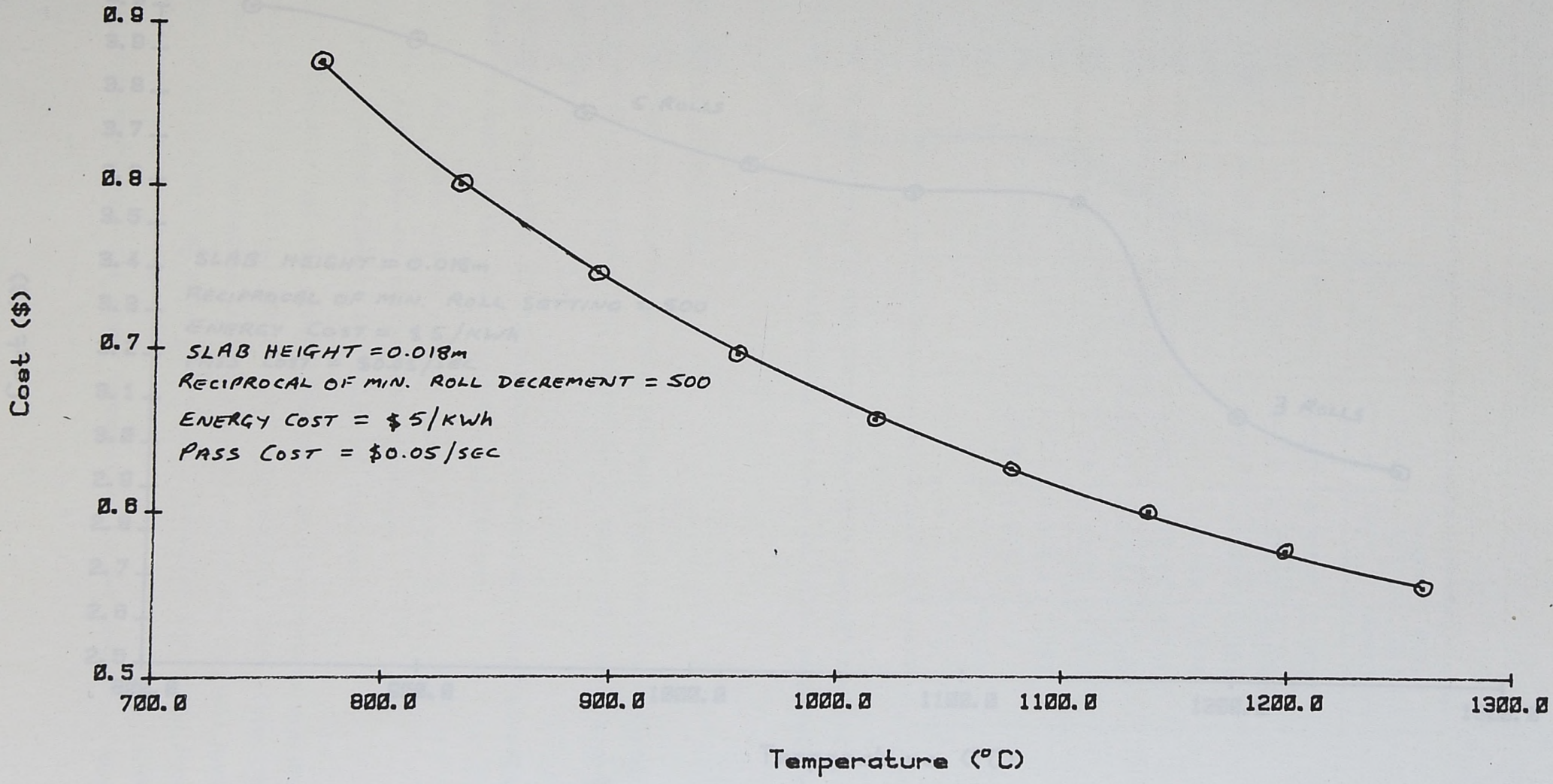

FIG. 6.5 REVERSING MILL COST VERSUS SLAB INPUT TEMPERATURE

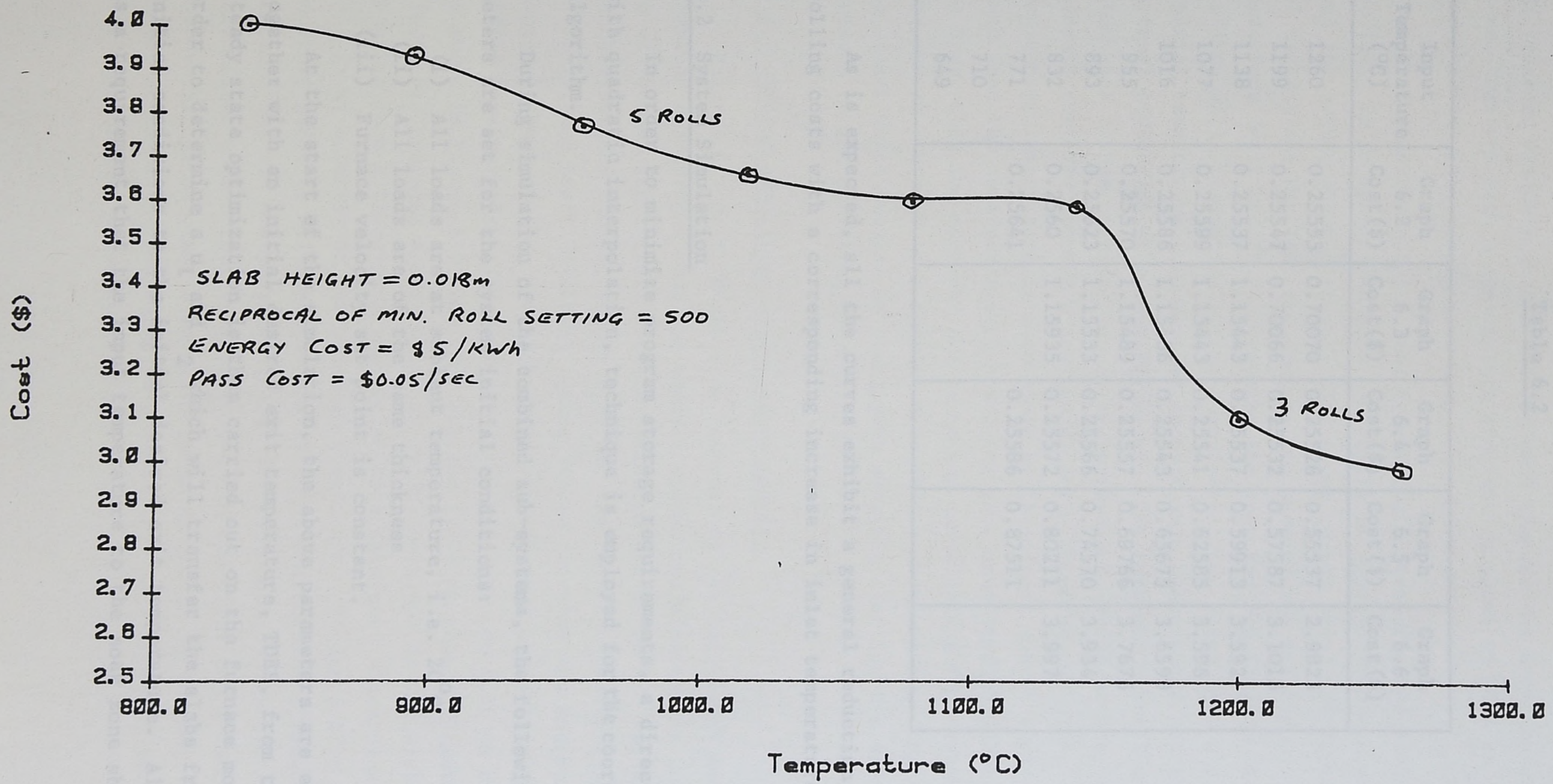

FIG. 6.6 REVERSING MILL COST VERSUS SLAB INPUT TEMPERATURE

Table 6.2

Input Temperature (°C)	Graph 6.2 Cost($)	Graph 6.3 Cost($)	Graph 6.4 Cost($)	Graph 6.5 Cost($)	Graph 6.6 Cost($)
1260	0.25555	0.70070	0.25526	0.55537	2.9823
1199	0.25547	0.70066	0.25532	0.57587	3.1015
1138	0.25537	1.15443	0.25537	0.59913	3.592
1077	0.25599	1.15443	0.25541	0.62585	3.596
1016	0.25586	1.15486	0.25543	0.65675	3.6599
955	0.25570	1.15489	0.25557	0.69766	3.7675
893	0.25623	1.15533	0.25566	0.74570	3.934
832	0.2560	1.15935	0.25572	0.80211	3.997
771	0.25641		0.25586	0.87511	
710					
649					

As is expected, all the curves exhibit a general reduction in rolling costs with a corresponding increase in inlet temperature.

6.2 System Simulation

In order to minimize program storage requirements, a direct search, with quadratic interpolation, technique is employed for the coordination algorithm.

During simulation of the combined sub-systems, the following parameters are set for the system initial conditions:

(i) All loads are at ambient temperature, i.e. 20°C
(ii) All loads are of the same thickness
(iii) Furnace velocity set point is constant.

At the start of the simulation, the above parameters are entered together with an initial desired exit temperature, TDES, from the furnace. Steady state optimization is then carried out on the furnace model in order to determine a u_1 and u_2 which will transfer the slabs from their initial conditions to the initial desired exit temperature. Also, it is a requirement that the input temperature to the soak zone should be

as close as possible to the desired exit temperature from the soak zone, together with a temperature gradient as close to zero as possible on entry to the soak zone.

Having determined a u_1 and u_2 which will transfer the slabs to TDES, in an optimal manner, the result is applied to the plant and the system allowed to run. The plant is run until the first group of eight slabs has left the furnace and entered the rolling mill. Equations (6.1) and (6.2) determine the cost for the furnace and rolling mill, respectively, for transferring the slabs from a given initial temperature to a desired furnace exit temperature and then to a final predetermined output thickness. The combined overall cost is then sent to the supremal level, or coordinator, which stores this overall cost and chooses a new coordinating temperature. This co-ordinating temperature is determined by the direct search algorithm such that the combined system cost, for each coordinating temperature, is lower than the cost for the preceding coordinating temperature. The system iterates in a fashion such that a coordinating temperature is chosen which results in the lowest possible cost for the system subject to its operating constraints.

6.2.1 System simulation optimization results

Figures 6.7 to 6.12 show the response of the individual and combined sub-systems when the overall system optimization is implemented. In all cases, the initial slab temperatures are at 20°C. Two slab thicknesses are chosen, namely 6.35 cm, the upper thickness limit, and 1.778 cm, the lower thickness limit. These two slab thicknesses are chosen because of the fact that their rolling mill characteristics differ considerably. The mill characteristic for the 6.35 cm slab is shown in Figure 6.3, and that for the 1.778 cm slab in Figure 6.5. Figure 6.3 contains a discontinuity in its cost due to the slabs changing from a three-pass conversion to a five-pass conversion. This is as a result of the odd-pass constraint. Figure 6.5 is a smoother curve as all slabs at the 1.778 cm thickness are reduced in one roll and the odd-pass constraint does not enter. The two slab thicknesses used differ from those used in the pilot plant furnace as the overall pilot plant simulation is to be scaled up to meet the requirements of the reversing mill since this is a more representative model of existing reversing mills.

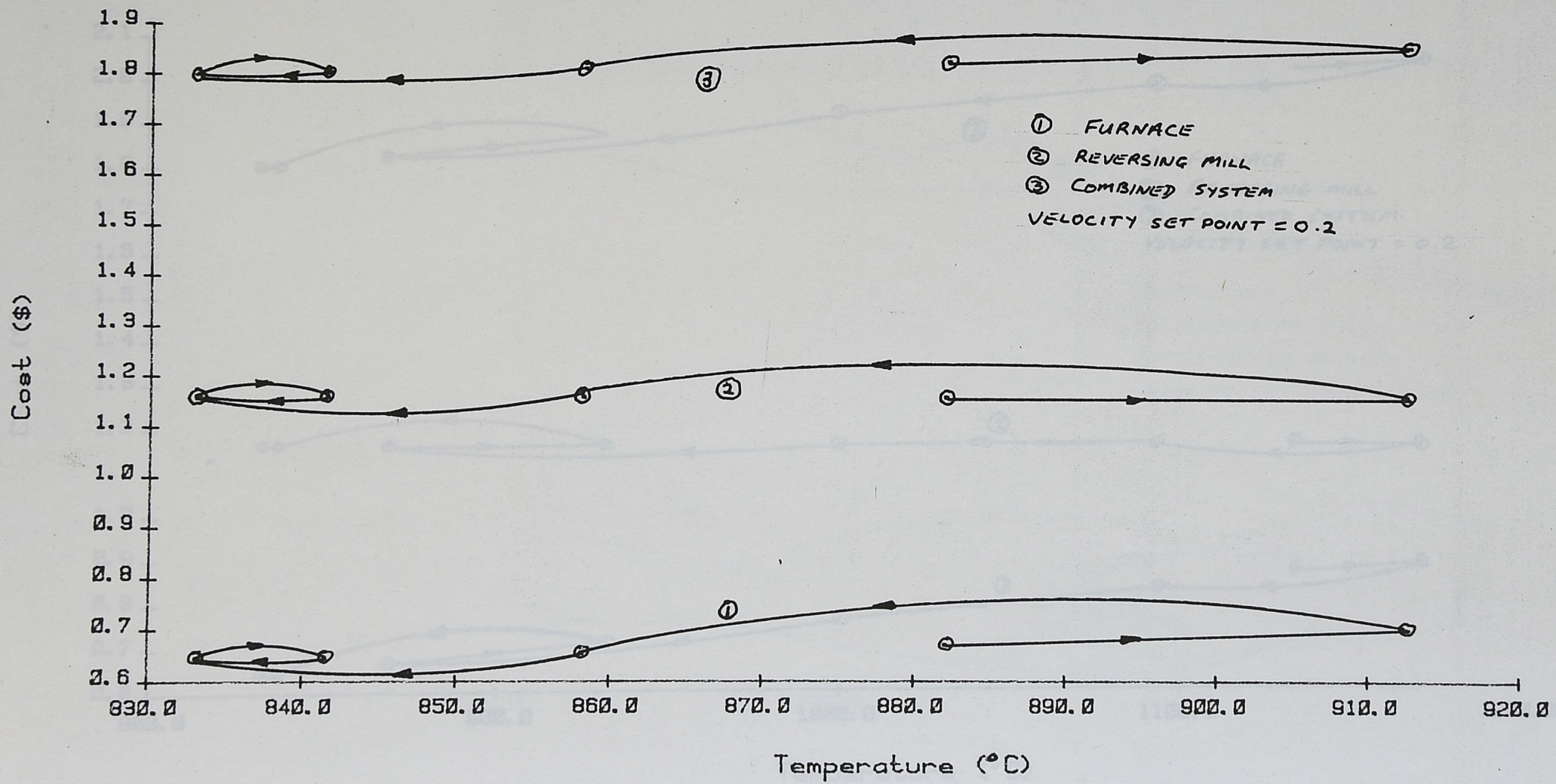

FIG. 6.7 COMBINED SYSTEM OPTIMIZATION-0.063m SLABS
INITIAL TEMPERATURE OF 882°C AND VELOCITY SET POINT OF 0.2

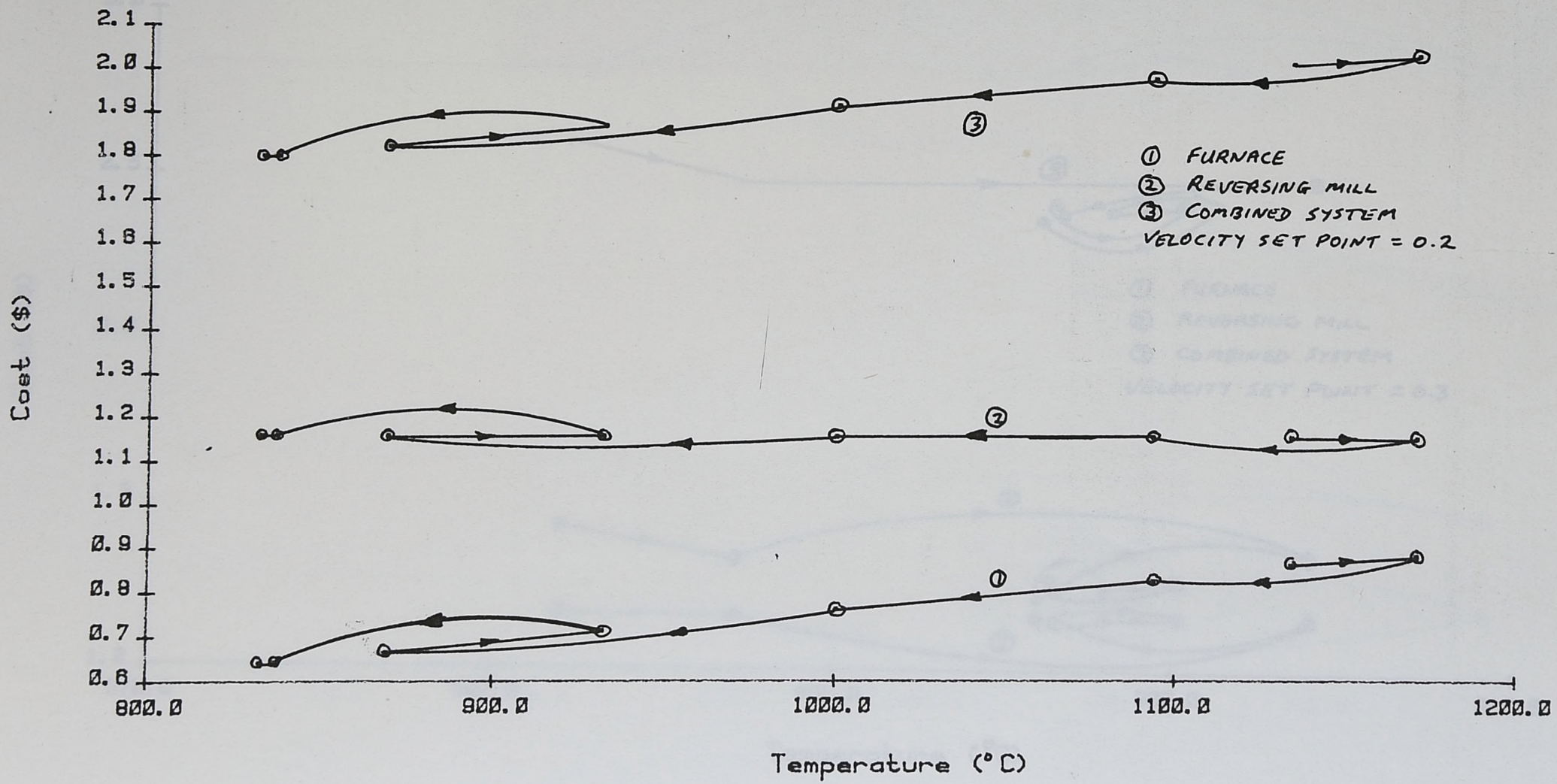

FIG. 6.8 COMBINED SYSTEM OPTIMIZATION-0.063m SLABS
INITIAL TEMPERATURE OF 1134°C AND VELOCITY SET POINT OF 0.2

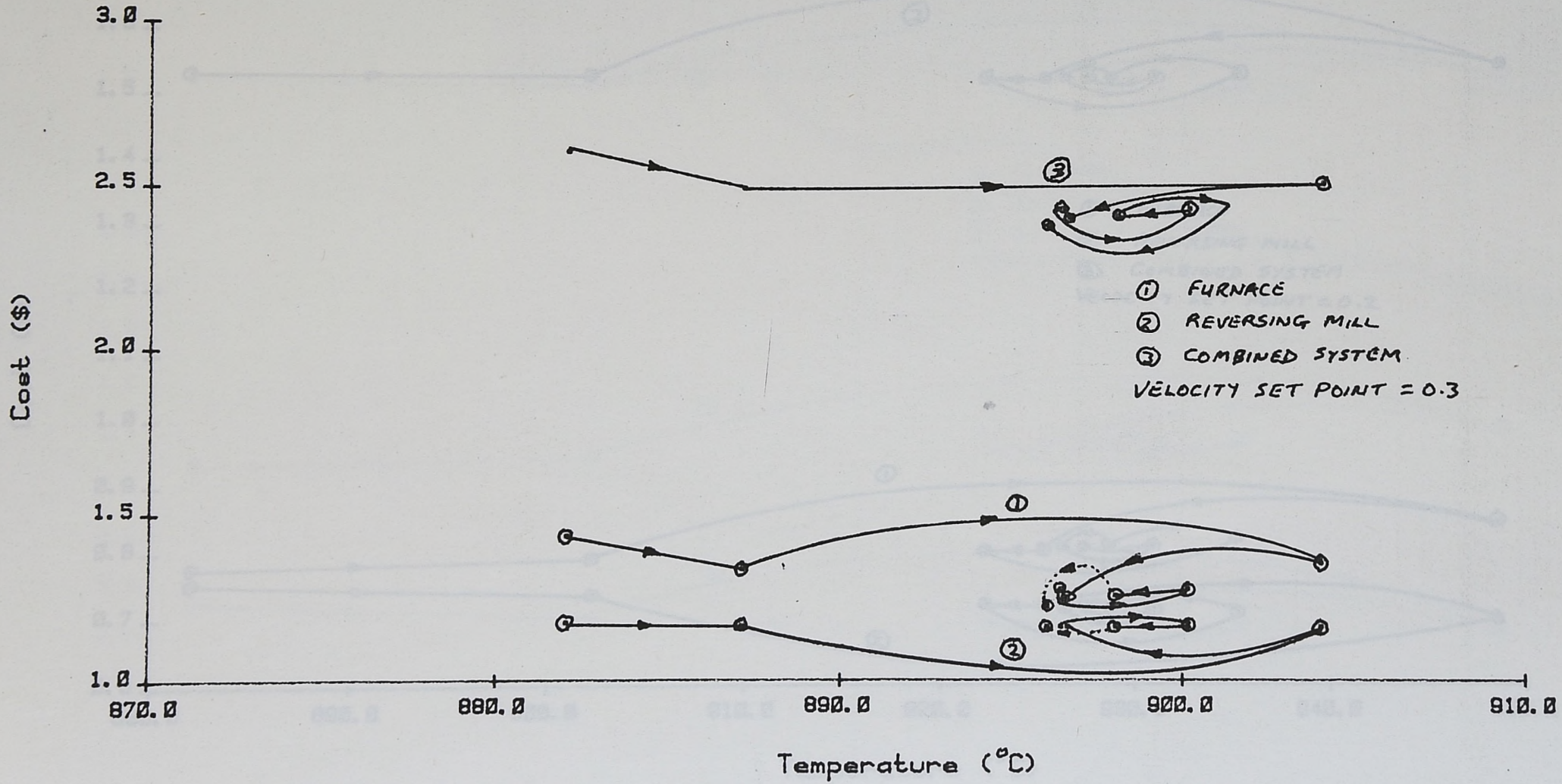

FIG. 6.9 COMBINED SYSTEM OPTIMIZATION-0.063m SLABS
INITIAL TEMPERATURE OF 882°C AND VELOCITY SET POINT OF 0.3

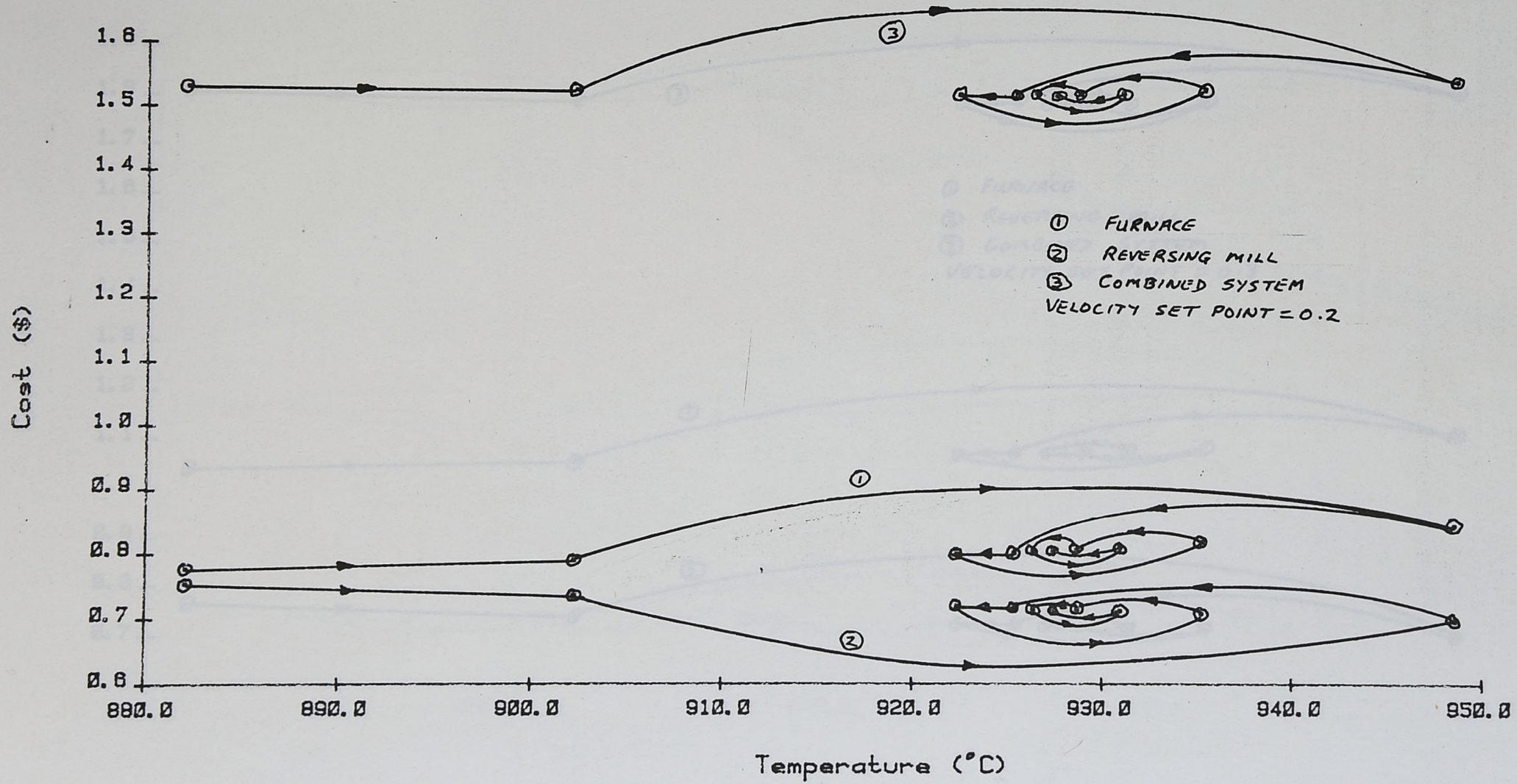

FIG. 6.10 COMBINED SYSTEM OPTIMIZATION-0.018m SLABS
INITIAL TEMPERATURE OF 882°C AND VELOCITY SET POINT OF 0.2

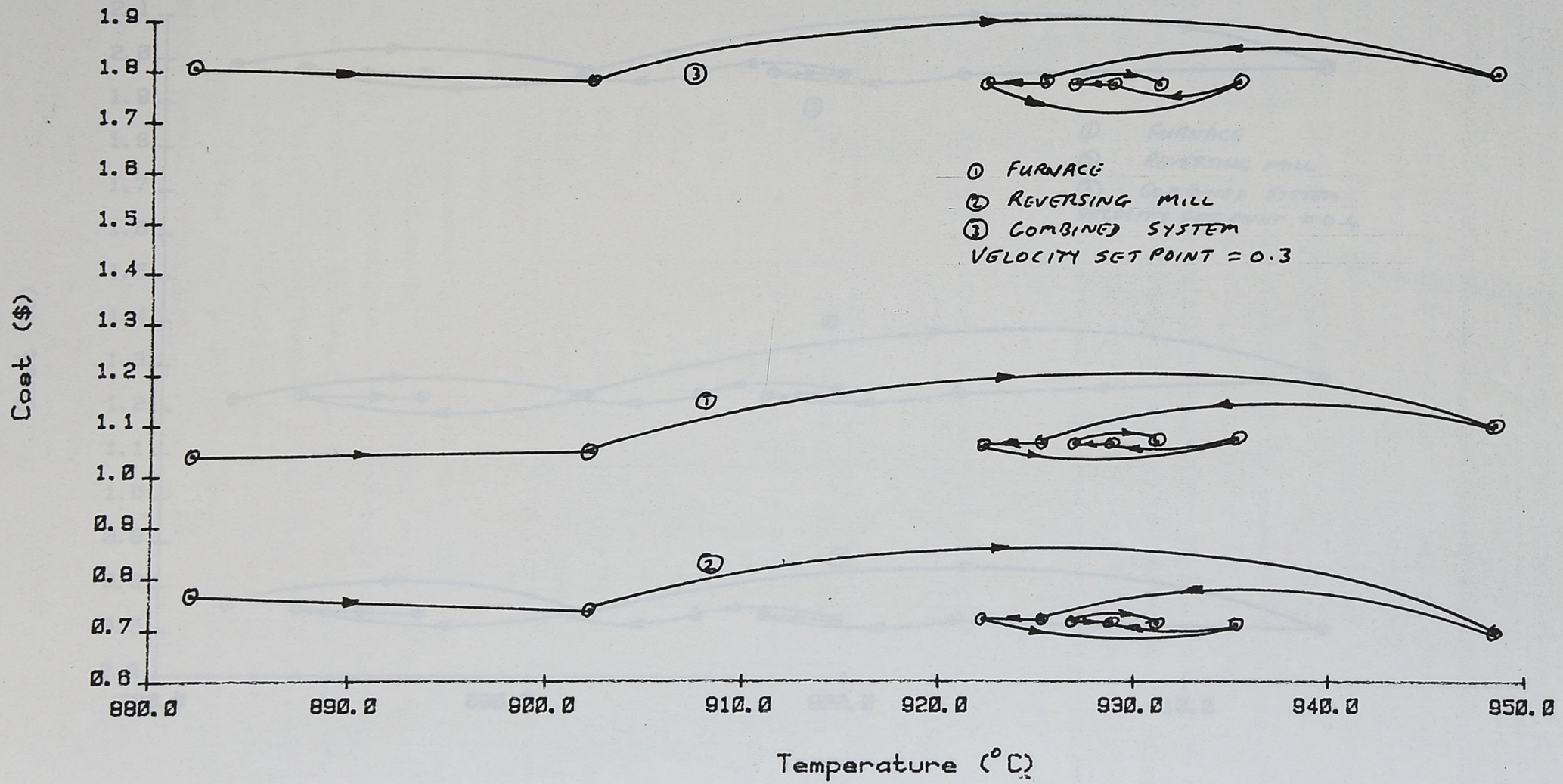

FIG 6.11 COMBINED SYSTEM OPTIMIZATION-0.018m SLABS
INITIAL TEMPERATURE OF 882°C AND VELOCITY SET POINT OF 0.3

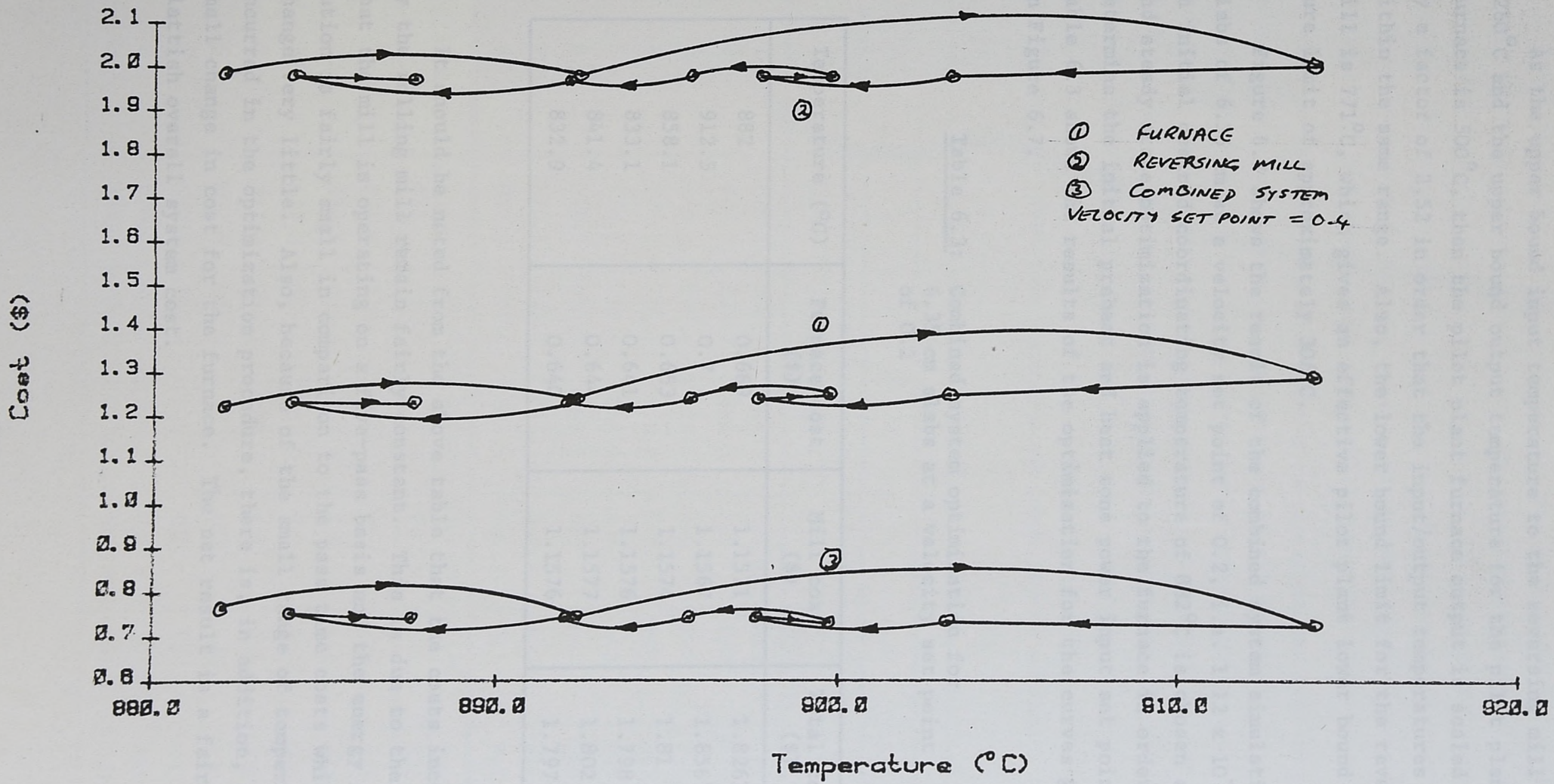

FIG 6.12 COMBINED SYSTEM OPTIMIZATION-0.018m SLABS
INITIAL TEMPERATURE OF 882°C AND VELOCITY SET POINT OF 0.4

As the upper bound input temperature to the reversing mill is 1260°C and the upper bound output temperature for the pilot plant furnace is 500°C, then the pilot plant furnace output is scaled up by a factor of 2.52 in order that the input/output temperatures lie within the same range. Also, the lower bound limit for the reversing mill is 771°C, which gives an effective pilot plant lower bound temperature limit of approximately 306°C.

Figure 6.7 shows the result of the combined system simulation for slabs of 6.35 cm at a velocity set point of 0.2, i.e. 1.12×10^{-3} m/s. An initial desired coordinating temperature of 882°C is chosen arbitrarily and steady state optimization is applied to the furnace in order to determine the initial preheat and heat zone power input set points. Table 6.3 shows the results of the optimization for the curves given in Figure 6.7.

Table 6.3: Combined system optimization for 6.35 cm slabs at a velocity set point of 0.2

Temperature (°C)	Furnace cost ($)	Mill cost ($)	Total cost ($)
882	0.669	1.1571	1.8261
912.5	0.7	1.1567	1.8567
858.1	0.653	1.1574	1.81
833.1	0.641	1.1576	1.798
841.4	0.644	1.1577	1.802
832.9	0.640	1.1576	1.797

It should be noted from the above table that the costs incurred by the rolling mill remain fairly constant. This is due to the fact that the mill is operating on a five-pass basis and the energy contribution is fairly small in comparison to the pass time costs which change very little. Also, because of the small range of temperatures incurred in the optimization procedure, there is, in addition, a fairly small change in cost for the furnace. The net result is a fairly flattish overall system cost.

From Table 6.2, it can be seen that the mill lower bound temperature limit, for 6.35 cm slabs, is 832°C. As the mill characteristics are fairly flat and the furnace characteristics are a curve (see chapter 4, Figure 4.29), with a positive gradient in increasing temperature, then it is to be expected that the results of the optimization procedure should lie at the lower bound of the mill input characteristics.

Due to the fact that the desired coordination temperature is re-defined after each iteration, and because of the dynamics of the heating process, the slabs do not always meet their entry requirements into the soak zone. This is explained in chapter 4, section 4.5.7. Table 6.4 shows the input and output soak zone slab temperatures for the case shown by Table 6.3.

Table 6.4: Soak zone input/output temperatures of slabs

Slab No.	Iteration No.					
	1	2	3	4	5	6
	Desired input temperature (°C)					
	882	912.5	858.1	833.1	841.4	832.9
1	878.1	896.4	924.8	871.9	844.4	850.2
2	878.1	931.1	863.3	829	852	848.4
3	878.1	925.6	865.1	844	856.8	847.3
4	878.1	925.8	878.9	848.2	848.2	847.5
5	878.1	930.4	864.6	839.2	858.3	847.1
6	878.1	930.8	869.6	847	847.2	845.3
7	878.1	930.1	871.7	840.1	853.3	844.7
8	878.1	927.6	868.4	846.5	855	842.4
Slab No.	Desired output temperature (°C)					
	882	912.5	858.1	833.1	841.4	832.9
1	878.9	910	861.3	825	838.2	835.1
2	880.2	905.4	852.8	829.8	835.9	832.4
3	877,3	906.4	853.0	827.1	834.4	832.6
4	877.2	906.3	849.7	826	836.4	832.5
5	877.4	905.2	853	828.3	834	832.5
6	877.5	907.2	852	826.6	836.6	832.7
7	878.1	905.2	851.7	828.3	835.6	832.4
8	878.4	906.2	852.3	826.8	835.1	832.4

Table 6.5 shows the results of the optimization for the curves given in Figure 6.8. These are based on the same system set up as in Figure 6.7, i. e. velocity set point = 0.2, initial ambient temperature = 1134.0°C.

Table 6.5: Combined system optimization for 6.35 cm slabs at a velocity set point of 0.2

Temperature (°C)	Furnace cost ($)	Mill cost ($)	Total cost ($)
1134.0	0.8605	1.154	2.0145
1171.0	0.8818	1.153	2.0348
1093.4	0.8243	1.1542	1.9785
1000.0	0.761	1.1553	1.9163
868.9	0.6635	1.157	1.8205
931.6	0.7123	1.1564	1.8687
836.6	0.6413	1.1576	1.7989
832.1	0.6398	1.1578	1.7976

The minimum cost for the system is about the same as that given in Table 6.3. This is to be expected as the only difference between the two runs is the initial desired coordinating temperature. As, in both cases, the rolling mill trajectories remain fairly flat, it is only to be expected that the final result is determined by the shape of the furnace cost trajectory. Table 6.6 shows the input and output soak zone slab temperatures for the case shown by Table 6.5.

Table 6.6: Soak zone input/output temperatures of slabs

Slab No.	Iteration No.							
	1	2	3	4	5	6	7	8
	Desired input temperature (^{o}C)							
	1134	1171	1093.4	1000	868.9	931.6	836.6	832.1
1	1130.3	1159.4	1192.7	1113.3	1024.4	879.7	945	849.5
2	1132.5	1202.8	1091	1009.7	932.5	957.6	876.2	842.7
3	1133.1	1196.2	1113.8	1022.4	853.0	940.1	821.2	841.7
4	1133.2	1189.4	1123.6	1035.7	883.5	943.9	856.7	849.5
5	1134.6	1199.0	1112.3	1023	888.3	954.5	849.2	840.2
6	1135.0	1189.2	1116.6	1027.4	873.4	937.0	841.7	844.4
7	1135.2	1198.2	1112.1	1024.9	884.8	952.5	852.8	844.4
8	1135.1	1200.3	1117.6	1026.4	879.2	944.0	842.0	843.7
Slab No.	Desired output temperature (^{o}C)							
	1134	1171	1093.4	1000	868.9	931.6	836.6	832.1
1	1129.6	1167.0	1089.4	1019.6	945.5	929.8	880.2	827.8
2	1128.5	1164.0	1088.6	1003.9	870.9	922.6	829.1	827.8
3	1125.2	1164.5	1086.8	1002.7	867.4	926.1	835.9	827.1
4	1128.7	1165.7	1086.1	1000.4	862.6	925.6	828.8	824.3
5	1125.9	1163.9	1087.1	1002.5	860.3	922.6	830.3	827.1
6	1127.0	1165.8	1087.1	1002.7	864.4	926.9	832.1	826.1
7	1127.7	1164.7	1087.6	1002.4	862.1	923.6	829.6	826.1
8	1126.9	1163.7	1086.4	1001.7	863.3	925.3	832.4	826.3

Table 6.7 is a table of the individual and combined sub-systems for 6.35 cm slabs at a velocity set point of 0.3. The initial desired coordinating temperature is at 882°C. This table is plotted in Figure 6.9.

Table 6.7: Combined system optimization for 6.35 cm slabs at a velocity set point of 0.3

Temperature (°C)	Furnace cost ($)	Mill cost ($)	Total cost ($)
882	1.43	1.17	2.60
887.1	1.33	1.16	2.49
904.0	1.348	1.157	2.505
896.6	1.24	1.157	2.397
896.4	1.27	1.157	2.427
900.1	1.27	1.157	2.427
898.0	1.25	1.157	2.407
896.0	1.22	1.157	2.377

Table 6.8: Soak zone input/output temperatures of slabs

Slab No.	Iteration No.							
	1	2	3	4	5	6	7	8
	Desired input temperature (°C)							
	882	887.1	904	896.6	896.4	900.1	898	896
1	878.1	890.82	895.3	910.7	906.2	904.4	908.9	908.4
2	878.1	909.5	924.8	914.5	913.2	920.3	916.7	916.0
3	878.1	899.1	912.7	902.4	900.4	905.6	902.4	899.4
4	878.1	894.85	912.2	912.5	910.2	912.9	913.2	912.7
5	878.1	908.9	923.8	907.7	907.9	917.1	909.5	907.2
6	878.1	893.1	907.2	902.6	901.9	903.4	903.7	901.66
7	878.1	901.9	919.8	911.9	912.5	917.5	913.7	912.5
8	878.1	902.1	915.5	903.4	902.9	908.4	903.7	901.9
Slab No.	Desired output temperature (°C)							
	882	887.1	904	896.6	896.4	900.1	898	896
1	883	888.5	902.4	898.1	897. 4	900.3	899.4	897.6
2	873.2	880.7	895.6	887.5	887.3	891.6	889.3	887.8
3	877.2	880.7	896.6	889.8	890.1	893.6	891.8	890.1
4	877.5	882.7	897.8	888.1	888.5	892.8	890.3	888.1
5	876.2	882	896.6	887.8	887.7	891.8	889.8	887.5
6	876.5	882.3	897.8	890.1	889.8	893.8	892.1	890.1
7	876.4	881.7	896.4	888.3	888.1	892.3	889.8	888.1
8	876.4	880.5	895.8	889.3	889.1	892.3	891.6	889.3

Table 6.9 is a table of the individual sub-system iterations for the curves given in Figure 6.10. Table 6.10 gives the slab temperatures, for every optimization iteration, as they enter and exit the soak zone.

Table 6.9: Combined system optimization for 0.018 m slabs at a velocity set point of 0.2

Temperature (^{o}C)	Furnace cost ($)	Mill cost ($)	Total cost ($)
882	0.776	0.753	1.529
902.16	0.7895	0.735	1.5249
948.5	0.845	0.697	1.542
925.3	0.801	0.717	1.518
922.32	0.8	0.719	1.519
935.17	0.819	0.708	1.527
928.62	0.806	0.714	1.520
926.3	0.8057	0.7157	1.5214
930.88	0.81	0.712	1.522
927.36	0.8042	0.713	1.5172

Table 6.10: Soak zone input/output temperatures of slabs

Slab No.	Iteration No.									
	1	2	3	4	5	6	7	8	9	10
	Desired input temperature (°C)									
	882.0	902.16	948.5	923.3	922.32	935.17	928.62	926.3	930.88	927.36
1	878.1	896.4	915.3	962.1	939.2	934.2	948.3	941.9	939.9	944.2
2	878.1	920.1	974.7	933.6	935.7	956.1	944.0	942.7	949.5	945.7
3	878.1	915.7	961.1	939.7	938.9	950.8	944.2	943.2	946.7	945.7
4	878.1	917.8	961.1	945.3	936.9	950.0	946.0	944.2	946.7	946.1
5	878.1	920.3	955.0	938.0	940.4	957.5	946.3	946.5	952.3	948.7
6	878.1	912.5	956.7	941.5	934.7	944.2	942.5	938.9	941.1	947.1
7	878.1	919.5	969.4	940.2	938.4	954.3	946.8	945.0	950.5	947.0
8	878.1	916.3	965.4	942.2	940.5	952.8	946.3	944.5	948.5	946.7
Slab No.	Desired output temperature (°C)									
	882.0	902.16	948.5	923.3	922.32	935.17	928.62	926.3	930.88	927.36
1	879.2	900.4	946.3	918.3	917.2	931.6	923.3	921.3	926.4	923.8
2	880.2	896.1	940.0	919.5	915.8	927.4	921.8	919.3	923.1	921.8
3	876.9	896.9	942.5	918.8	915.3	928.4	921.8	919.3	923.8	921.8
4	874.4	896.6	942.5	917.5	915.8	928.6	921.6	919.3	924.1	921.8
5	873,7	895.9	939.7	919.0	914.8	926.6	921.3	918.2	922.1	920.8
6	875.2	897.6	943.5	918.5	916.3	929.6	922.3	920.3	925.1	922.8
7	876.4	896.1	940.7	918.8	916.0	927.8	921.6	919.0	923.3	921.8
8	878.2	896.9	941.2	918.0	915.2	927.9	921.3	918.8	923.4	921.3

Table 6.11: Combined system optimization for 0.018 m slabs at a velocity set point of 0.3

Temperature (^{o}C)	Furnace cost ($)	Mill cost ($)	Total cost ($)
882.0	1.040	0.765	1.805
902.2	1.048	0.736	1.784
948.5	1.104	0.698	1.802
925.3	1.066	0.717	1.783
922.3	1.061	0.720	1.781
935.2	1.076	0.709	1.785
928.8	1.067	0.714	1.781
926.9	1.066	0.716	1.782
931.1	1.069	0.711	1.780

Tables 6.11 and 6.13 are the tables of the individual sub-system iterations for the curves given in Figures 6.11 and 6.12, respectively.

Tables 6.12 and 6.14 are the slab temperatures, as they enter and exit the soak zone, for each of the iterations shown in Tables 6.11 and 6.13, respectively.

Table 6.12: Soak zone input/output temperatures of slabs

Slab No.	Iteration No.								
	1	2	3	4	5	6	7	8	9
	Desired input temperature (°C)								
	882.0	902.2	948.5	925.3	922.3	935.2	928.8	926.9	931.1
1	881.3	890.8	904.7	948.0	938.2	933.9	942.2	939.7	938.2
2	881.2	925.3	974.0	938.2	938.2	955.3	947.0	944.5	949.5
3	880.9	914.3	957.3	928.9	927.4	941.5	929.9	930.1	936.4
4	880.7	904.4	949.3	945.8	939.5	946.3	947.8	944.8	944.7
5	880.7	924.3	968.7	933.4	931.9	950.5	937.9	935.9	945.3
6	880.5	906.4	945.5	934.2	931.1	937.7	935.7	934.2	934.9
7	880.6	917.3	963.4	944.0	940.0	957.0	947.5	945.5	947.3
8	880.1	919.3	959.6	929.9	928.1	943.2	931.9	930.1	939.2
Slab No.	Desired output temperature (°C)								
	882.0	902.2	948.5	925.3	922.3	935.2	928.8	926.9	931.1
1	877.0	899.6	942.2	928.1	924.3	934.2	930.4	928.4	931.6
2	877.1	894.6	939.5	916.3	912.7	925.8	919.3	917.0	921.6
3	877.2	894.3	940.2	919.8	916.0	928.4	923.3	921.1	924.3
4	878.2	897.9	943.7	917.3	913.5	928.1	920.1	918.0	923.3
5	876.3	895.9	939.7	917.0	914.0	926.4	920.3	918.8	922.1
6	875.2	896.4	943.5	918.5	915.3	929.4	922.3	921.3	924.8
7	877.2	895.3	941.2	917.0	913.8	927.1	920.3	918.5	922.6
8	878.3	894.6	940.5	918.5	915.3	927.9	922.3	920.3	923.6

Table 6.13: Combined system optimization for 0.018 m slabs at a velocity set point of 0.4

Temperature (^{o}C)	Furnace cost ($)	Mill cost ($)	Total cost ($)
882.0	1.22	0.76	1.98
892.3	1.24	0.74	1.98
914.0	1.29	0.72	2.01
903.2	1.25	0.73	1.98
897.6	1.24	0.74	1.98
899.7	1.25	0.73	1.98
895.6	1.24	0.74	1.98
892.0	1.23	0.74	1.97
884,0	1.23	0.75	1.98
887,8	1.23	0.74	1.97

Table 6.14: Soak zone input/output temperatures of slabs

Slab No.	Iteration No.									
	1	2	3	4	5	6	7	8	9	10
	Desired input temperature (°C)									
	882.0	892.3	914.0	903.2	897.6	899.7	895.6	892.0	884.0	887.8
1	854.1	856.8	864.6	880.2	872.9	868.9	870.4	867.6	864.6	859.1
2	853.2	868.6	886.8	865.9	867.6	870.9	866.1	862.8	855.3	861.1
3	853.7	871.9	889.3	874.4	871.7	874.9	870.7	867.9	861.1	866.9
4	854.8	865.9	880.7	875.2	871.2	872.2	869.7	867.1	861.8	864.1
5	856.1	865.4	882.3	875.2	870.7	871.9	868.9	865.9	860.1	862.3
6	856.1	866.4	882.3	874.7	870.7	871.9	868.9	865.9	860.1	862.6
7	856.0	867.9	883.8	874.4	870.7	872.7	869.4	866.6	860.6	864.1
8	855.9	868.1	884.8	876.2	871.9	873.7	870.4	867.4	861.3	864.6
Slab No.	Desired output temperature (°C)									
	882.0	892.3	914.0	903.2	897.6	899.7	895.6	892.0	884.0	887.8
1	882.5	884.5	904.4	898.4	892.3	893.3	890.1	886.3	879.2	881.2
2	883.1	893.8	913.0	899.9	895.6	898.4	894.1	890.6	883.0	887.8
3	882.4	895.9	914.8	902.9	898.4	900.9	896.9	893.6	886.5	891.3
4	881.5	892.6	911.2	902.4	897.9	899.4	896.1	892.6	886.3	889.3
5	881.7	892.1	910.7	901.9	897.1	898.6	895.4	891.8	885.3	888.3
6	882.3	892.8	911.2	902.2	897.6	899.1	895.9	892.3	885.8	889.1
7	882.3	893.3	912.2	902.2	897.6	899.4	895.9	892.3	885.5	889.1
8	882.5	893.1	911.7	902.2	897.6	899.4	895.9	892.6	886.0	889.3

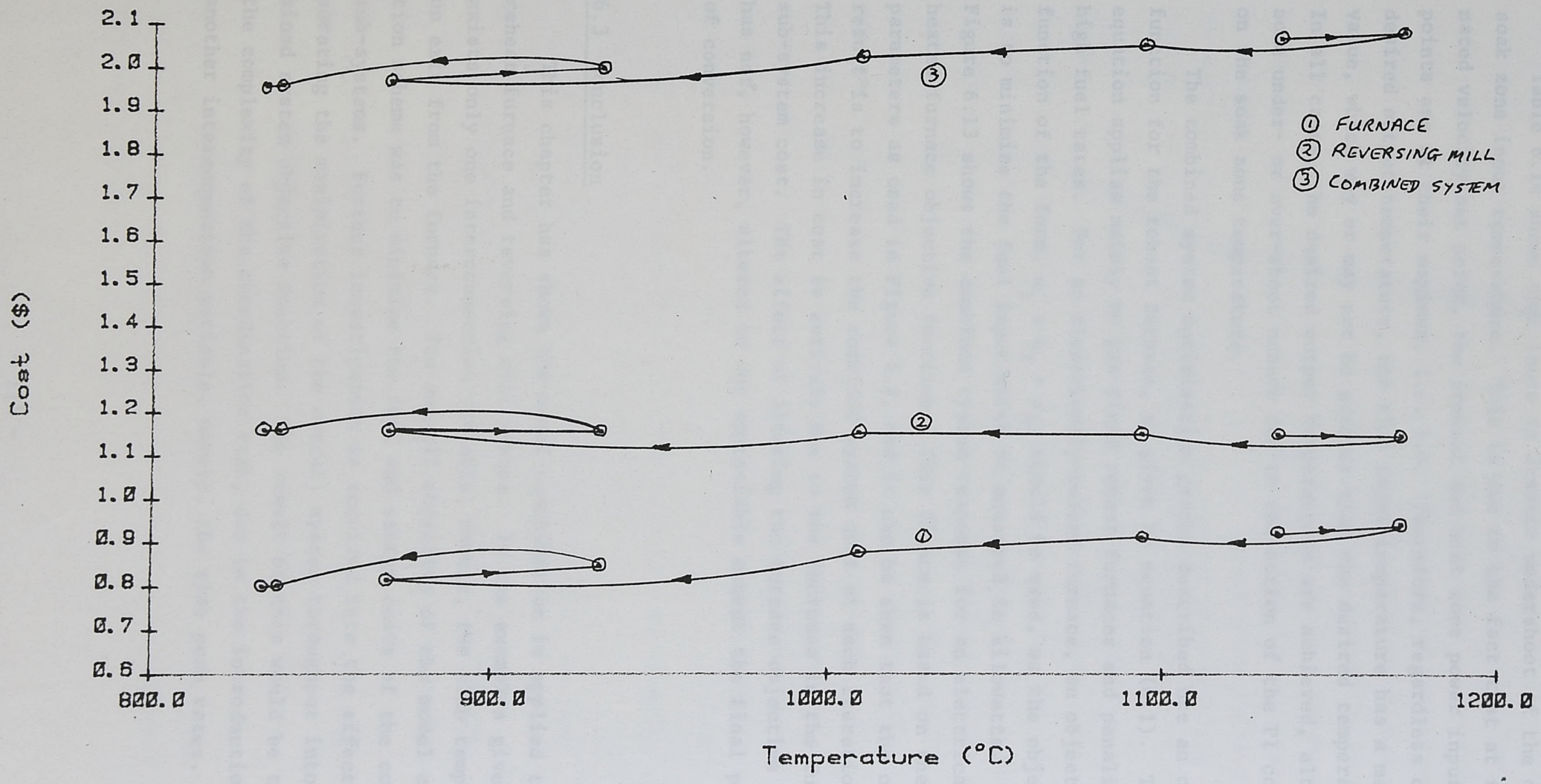

FIG. 6.13 COMBINED SYSTEM OPTIMIZATION-0.063m SLABS
INITIAL TEMPERATURE OF 1134°C AND VELOCITY SET POINT OF 0.2

Table 6.14 shows that there is drastic undershoot of the desired soak zone input temperature. This is due to the fact that at the designated velocity set point, the preheat and heat zone power input set points are at their maximum, i.e. 1.0. Therefore, regardless of the desired output temperature, the slab input temperature has a maximum value, which may or may not be greater than the desired temperature. In all cases, the desired output temperatures are achieved, although some under- or over-shoot occurs due to the action of the PI controller on the soak zone temperature.

The combined system optimization graphs described use an objective function for the reheat furnace, as given by equation (6.1). This equation applies mainly to gas-fired reheat furnaces and penalizes high fuel rates. For an electrically-heated furnace, an objective function of the form, $u_1 + u_2 + u_3$, should be used, as the objective is to minimize the fuel input which is measured in kilowatts. Figure 6.13 shows the combined system response for an electrically-heated furnace objective function. This figure is based on the same parameters as used in Figure 6.8, and it can be seen that the overall result is to increase the combined system cost at each iteration. This increase in cost is entirely due to the increase in the furnace sub-system cost. The effect of altering the furnace objective function has not, however, altered to any appreciable extent the final point of conversion.

6.3 Conclusion

This chapter has shown how model coordination is applied to a reheat furnace and reversing mill system. In the examples given there exists only one interconnection variable, namely, the slab temperatures on exit from the furnace. The overall objective of the model coordination scheme was to minimize the fuel and energy costs of the combined sub-systems. Further investigation is required into the effect of incorporating the maximization of the overall system throughput into the combined system objective function. The result of this would be to increase the complexity of the coordination task, due to the introduction of another interconnection variable, namely, the slab push rates.

7.0 CONCLUSIONS

Initial simulation investigations, based on a semi-pilot scale plant, have demonstrated a satisfactory performance of the model co-ordination method. The model coordination technique implemented has some apparent on-line advantages over the interaction balance scheme, in that less computational effort is required to solve the combined sub-systems problem, and also the intermediate results obtained can be readily applied on-line whilst still producing feasible results. In addition, the temperature of the slabs entering the rolling mill is under the direct control of the coordinator, thus enabling important metallurgical constraints to be readily satisfied.

The coordination scheme outlined is open-loop, in that model inadequacies and real plant feedback are not taken into account. Open-loop implementation of the coordination methods, viz. interaction prediction or interaction balance, relies on the availability of accurate mathematical models of the steady state behaviour of the plant subprocesses. As often occurs in practice, there are usually model reality differences, and the inclusion of feedback measurements from the real process may often be used with advantage. Findeisen et al (1978, 1980) have carried out extensive research in the field of closed-loop hierarchical control and two principal methods in which feedback information from the real process has been identified. These two methods are:

(i) global feedback, in which the process measurements are sent direct to the coordinator;

(ii) local feedback, in which the measurements are sent direct to the local decision units.

The classification produces the following four schemes:

(i) interaction prediction (or model coordination) method with global feedback;

(ii) interaction prediction method with local feedback;

(iii) interaction balance method with global feedback;

(iv) interaction balance method with local feedback.

Findeisen et al (1978, 1980) have shown that the methods give near optimal solutions of real process performance and are better than the open-loop methods.

It is felt that better system performance would be obtained if, as well as using the techniques described above, some form of parameter estimation were included. In general, a mathematical model contains some unknown parameters whose values require to be estimated. The parameter estimation problem can be defined as the evaluation and adjustment of the unknown parameters in order that the response of the model is in agreement, as closely as possible, with the response of the system. This problem of tuning the model is evident in the reheat furnace model evaluation which is outlined in chapter 4. Weighting factors had to be introduced in order to force the furnace model to match the real system. This is adequate in the situation where the proposed model is used as part of a computer simulation, but becomes quite inadequate for accurate on-line model-based control, particularly when the plant parameters are time-varying.

In general, the mathematical model of a system will not be a true or faithful representation of the real system; hence, optimal points derived from the model may no longer be optimal as far as the real system is concerned. In this situation, the parameters whose values are to be identified may be dependent upon the control inputs. These properties cause interaction between the two problems of optimization and parameter estimation. Roberts (1979) has extended the work of Haimes and Wismer (1972) by applying hierarchical systems theory to decouple the interaction between the optimization and parameter estimation problems.

Apart from the two aspects previously described, viz. feedback within a hierarchically-controlled system, and the optimization and parameter estimation problem, it is felt that more work is needed in the field of applying microcomputers in the control of industrial processes. Deshmukh et al (1979) have investigated the use of a hierarchically-structured multi-microprocessor system and its application on an industrial system. The industrial system used is a reheat furnace of the type described in chapter 4. The reheat furnace is divided up into three separate zones, each one of which is controlled by a microprocessor. The microprocessors are linked together via common memory and the control parameters supplied to the microprocessors are determined by a master controller which would either be another microprocessor or a minicomputer. Due to the fact that, at present,

microprocessors, in general, are not as powerful as modern mini-computers, although there are a few fast microprocessors now on the market which will find application in the industrial environment, viz. Intel's 8086 and the iAPX 432, it is felt that more research is needed into producing control algorithms which are suitable for micro-processors.

This thesis has observed that a multi-level hierarchy provides a good tool for the analysis of complex systems as applied to existing practice. A hot strip mill was described by a two-level coordination scheme. While theoretical coordination results apply readily to most complex industrial systems, it is felt, particularly in the case of the hot strip mill, that the interaction prediction or model coordination scheme is more suitable for on-line use because of its ability to use, on-line, intermediate results.

Finally, it is felt that the development of a more rational and analytically-based methodology for systems design would lead to more complete and more efficient integration, for example, the solutions to questions concerning:

(a) criteria for decomposition;

(b) means for coordination applicable to systems operating in real time;

(c) criteria for model simplification which are appropriate to its level in the hierarchy.

8.0 REFERENCES

Avitzur, B.

"Pass reduction schedule for optimum production of a hot strip mill"
Iron and Steel Eng., vol. 39, No. 12, pp. 104-114, December, 1972

Bellman, R.

"Dynamic Programming"
Princeton University Press, 1957

Brown, A. I., Mario, S. M.

"Introduction to Heat Transfer"
McGraw-Hill, 1958

Caffin, R.

"The design and modelling of an experimental travelling load furnace for computer control"
Ph.D. Thesis, The City University (London), 1972

Carlslaw, H. S., Jaeger, J. C.

"Conduction of Heat in Solids"
Clarendon Press, Oxford, 1959

Chong, C. Y., Athans, M.

"On the periodic coordination of linear stochastic systems"
In the Proceedings of the IFAC Sixth World Congress, part 3, session 19, 1975

Deshmukh, H. A., Scott, R. G. F., Roberts, P. D.

"A hierarchically structured multi-microprocessor system"
Presented at EUROMICRO 1979, Götenburg, Sweden, pp. 317-327, August, 1979

Eaglen, C. T., Singh, M. G., Coates, J. F.

"A hierarchical strategy for the temperature control of a hot strip mill roughing process"
Automatica, Vol. 9, No. 2, pp. 209-221, March, 1973

Evans, F. J., Schizas, C.
"Graph theoretical concepts in modern control theory"
Third IMA Conference, Sheffield, September, 1980

Fapiano, D. J.
"An evaluation of automatic control performance in hot rolling"
Iron and Steel Eng., Vol. 40, No. 1, pp. 125-133, January, 1963

Findeisen, W., Pulaczewski, J., Manitus, A.
"Multilevel optimization and dynamic coordination of mass flows in a beet sugar plant"
Automatica, Vol. 6, pp. 581-589, 1970

Findeisen, W., Brdys, M., Malinowski, K., Taljewski, P., Woźniak, A.
"On-line hierarchical control for steady state systems"
IEEE Trans. on Aut. Control, AC-23, No. 2, pp. 189-209, 1978

Findeisen, W. (Ed.)
"Second workshop on hierarchical control"
Inst. of Aut. Control, Technical University of Warsaw, Warsaw, 1979

Findeisen, W., Brdys, M., Bailey, F. N., Malinowski, K., Tatjewski, P., Woźniak, A.
"Control and Coordination in Hierarchical Systems"
Wiley, London, 1980

Geoffrion, A. M.
"Duality in non-linear programming: A simplified applications-oriented development"
SIAM Review, Vol. 13, No. 1, January, 1971

Guran, M., Filip, F. G., Donciulescu, A. D., Orasanu, L., Petrescu, C.
"Computer design of data transmission networks for a large real time computer system"
Problems in Autom. Control, Vol. 10, pp. 221-235, 1978

Haimes, Y. Y., Wismer, D. A.
"A computational approach to the combined problem of optimization and parameter estimation"
Automatica, Vol. 8, pp. 337-347, May, 1972

Hakkala, L., Blomberg, H.
"On-line coordination under uncertainty of weak interacting dynamical systems"
Automatica, Vol. 12, pp. 185-193, 1976

Krummel, W. M.
"Integrated automation for steel plants"
Iron and Steel Eng., Vol. 387, pp. 157-161, October, 1961

Lefkowitz, I.
"Multilevel approach to control system design"
Trans. ASME SER. D., Vol. 88, pp. 392-398, 1966

Lefkowitz, I., Cheliustkin, A., Kelley, D. H.
"State-of-the-art review of integrated industrial control systems"
Integrated Systems Control in the Steel Industry - State-of-the-Art Review and Proceedings of the Conference, December, 1976

Lopresti, P. V., Patton, T. N.
"An approach to minimum cost steel rolling"
Proc. IEEE, Vol. 58, pp. 23-30, January, 1970

Matuszewski, J. P.
"A study of coordination applied to control in steel processing"
Ph.D. Thesis, Case Western Reserve University, 1970

Matuszewski, J. P., Lefkowitz, I.
"Coordination for control in steel processing"
IEEE Trans. on Systems, Man and Cybernetics, T-SMC, pp. 182-184, March, 1973

Mesarovic, M. D., Macko, D., Takahara, Y.
"Theory of Hierarchical Multilevel Systems"
Academic Press, 1970

Mesarovic, M. D.
"Multilevel systems and concepts in process control"
Proc. of the IEEE, pp. 111-125, 1970

Oshima, M., Hirai, N.
"On-line production scheduling and process control in integrated steelworks"
In Proc. of the IFAC Fifth World Congress, Part 1, paper 4.4, Paris, 1972

Pike, M. E.
"Case study on the control of a slab reheating furnace"
1969 Case Studies in Control, IEEE, pp. 63-88, University of Colorado, August, 1969

Pontryagin, L. S.
"The Mathematical Theory of Optimal Processes"
Wiley, N.Y., 1962

Roberts, P. D.
"Parameter estimation in non-linear dynamic mathematical models"
Department of Systems Science, The City University (London), Report No. DSS/PDR/127, February, 1977

Roberts, P. D.
"Introduction to large-scale control systems"
IEE Computing and Control Division Specialist Seminar on "Optimal Control of Large-Scale Systems", pp. 1/1-1/11, September, 1979a

Roberts, P. D.
"An algorithm for steady state system optimization and parameter estimation"
Int. J. Systems Science, Vol. 10, No. 7, pp. 719-734, 1979b

Sage, A. P.
"Methodology for Large-Scale Systems"
McGraw-Hill, 1977

Sandell, N. R., Varaiya, P., Athana, M.
"A survey of decentralized control methods for large-scale systems"
Proc. IFAC Symposium of Large-Scale Systems Theory and Applications, Udine, Italy, 1976

Schulz, R. G., Smith, A. W.
"Determination of a mathematical model for rolling mill control"
Iron and Steel Eng., Vol. 42, pp. 127-133, March, 1965

Siljak, D. D., Sundareshan, M. K.
"A multilevel optimization of large-scale dynamic systems"
IEEE Trans. on Automatic Control, February, 1976

Singh, M. G., Drew, S. A., Coales, J. F.
"Comparison of practical hierarchical control methods for interconnected dynamical systems"
Automatica, Vol. 11, pp. 331-350, 1975

Singh, M. G., Hassan, M. F., Titli, A.
"Multilevel feedback control for interconnected dynamical systems using the Prediction Principle"
IEEE Trans. on Systems, Man and Cybernetics, Vol. SMC-6, pp. 223-239, 1976

Singh, M. G., Titli, A.
"Practical optimization and control algorithms"
A link between science and applications of automatic control.
Preprints of the Seventh Triennial World Congress of IFAC
Pergamon Press, Oxford, pp. 1341-1357, 1978a

Singh, M. G., Titli, A.
"Systems - Decomposition, Optimization and Control"
Pergamon Press, 1978b

Smith, A. W., Gripp, L. P.
"On-line computer control of a reversing plate mill"
Iron and Steel Eng., Vol. 39, pp. 77-82, 1962

Tamura, H.
"Decentralized optimization for distributed-lag models of discrete systems"
Automatica, Vol. 11, pp. 593-602, 1975

Tazaki, E., Shindo, A., Umeda, T.
"Decentralized optimization of a chemical process by a feasible method"
Automatica, Vol. 8, pp. 543-554, 1972

Wallace, J. W.
"Integrated process control rolls steel more efficiently"
Blast Furnace and Steel Plant, pp. 124-130, February, 1969

White, D. J.
"Studies in dynamic programming"
Ph.D. Thesis, University of Birmingham, 1961

APPENDIX A

A.1 Parameter Estimation in Non-Linear Dynamic Mathematical Models

When developing a mathematical model of a system, the analyst is often faced with the problem of determining numerical values of parameters in a model whose structure is non-linear. If responses from the real system are available, it is possible to obtain parameter values by simulating the system and adjusting the parameters until the response from the model agrees with the response from the real system. This process is commonly automated within a digital computer which has been programmed to simulate the system and to adjust the parameters via a numerical optimization procedure. This model-fitting technique is often formulated as a weighted least-squares method in which the optimization algorithm manipulates the model parameters to minimize the sum of squares of weighted errors between the responses of the model and those of the real system.

Optimization algorithms have been developed specifically to take advantage of the sum-of-squares form. A software package (Roberts, 1977) has been developed for estimating values of parameters in mathematical models whose structure is non-linear and dynamic.

The results of the optimization algorithm used for model-fitting yield numerical values of parameters, which correspond to the minimum of the sum of the squares of the weighted errors between the dynamic response of the model and that of the real system. However, these results should not be considered as the end of the model-fitting exercise and it is important to perform sensitivity tests in order to determine the significance of the parameter estimates, the structure of the mathematical model and the data employed as the real system response. For this reason, the software package contains a separate subroutine which performs the required sensitivity tests and determines confidence tolerance levels on the parameter estimates and on the final dynamic response of the model.

Having determined the model parameters which minimize the weighted sum of squares of the residual errors between the output of the model and the real system, the sensitivity of the optimal weighted residuals to changes in the parameter estimates is determined. From this, the Jacobian matrix, J, which contains first derivatives, is computed.

That is

$$J_{ij}(\underline{p}) = \left[\frac{\partial e_i}{\partial p_j}\right]_{\underline{p}} \qquad \ldots\ldots\ldots\ldots\ldots\ldots\ldots\ldots \quad (A.1)$$

where $\underline{p}$ = vector of optimal parameters, $\underline{e}$ = vector of weighted residuals, and the suffix i or j indicates an element in the associated vector or matrix. Using the Jacobian matrix, the gradients of the weighted sum of square residuals with respect to the parameters are computed using the expression

$$\underline{g} = 2J^T\underline{e} \qquad \ldots\ldots\ldots\ldots\ldots\ldots\ldots\ldots\ldots\ldots\ldots\ldots \quad (A.2)$$

where g is the gradient vector.

The sensitivity of the final parameters to small changes in any of the residuals $\underline{e}$ is performed by computing the sensitivity matrix

$$S_m = \left[J^T J\right]^{-1} J^T \qquad \ldots\ldots\ldots\ldots\ldots\ldots\ldots\ldots\ldots\ldots \quad (A.3)$$

The sensitivity matrix, S_m, is then employed to compute the approximate errors, $\underline{\delta}$, in the optimal parameters using the expression

$$\underline{\delta} = - S_m \underline{e} \qquad \ldots\ldots\ldots\ldots\ldots\ldots\ldots\ldots\ldots\ldots\ldots\ldots \quad (A.4)$$

The covariance matrix, C_{ov}, of the optimal parameters is then computed using

$$C_{ov} = \frac{S}{N_s - N_p} \cdot \frac{1}{2} \cdot \left[J^T J\right]^{-1} \qquad \ldots\ldots\ldots\ldots\ldots\ldots \quad (A.5)$$

where S is the weighted sum of squares of the residual errors, N_s is the number of samples, and N_p is the number of estimated model parameters.

From this, the 95% confidence levels on the estimated parameters are determined, assuming that the errors are approximately gaussian.

Finally, the variances of the residuals and 95% confidence intervals on the outputs of the model corresponding to the given estimates of the model parameters are computed. The variance, V_k on the k^{th} weighted residual is computed using the expression

$$V_k = \sum_{i=1}^{N_p} \sum_{j=1}^{N_p} \left(\frac{\partial e_k}{\partial p_i}\right)\left(\frac{\partial e_k}{\partial p_j}\right) C_{ij} \qquad \ldots\ldots\ldots\ldots\ldots\ldots \quad (A.6)$$

where the required partial derivatives are obtained from the Jacobian

matrix, J, and the 95% confidence level on the k^{th} output is obtained from

$$\phi_k = \sqrt{V_k}$$

The above confidence levels imply that there is a 95% confidence that the true parameter lies in the range $p_i \pm \Delta_i$, and that the true output lies in the range $y_k \pm \phi_k$.

A.2 Furnace Model Parameters

For power input set points ≥ 0.3

$$T_{PP} = (A\,u_1 + B)x^2 + (C\,u_1 + D)x + (E\,u_1 + F)$$

$$0 \leq x \leq 1.07 \text{ m}$$

where A = - 212.97 (± 36.1), B = - 134.5 (± 20.8), C = 201.26 (± 52.7),
D = 132.26 (± 30.4), E = 376.2 (± 15.7), F = 40.27 (± 9.0)

$$T_{PH} = (A\,u_1 + B)x^2 + (C\,u_1 + D)x + (E\,u_1 + F)$$

$$1.07 \leq x \leq 2.13 \text{ m}$$

where A = 305.66 (± 17.1), B = 91.45 (± 10.2), C = - 1277 (± 51.9),
D = - 305.9 (± 33.1), E = 1399.0 (± 40.6), F = 238.8 (± 25.7)

$$T_{HP} = (A\,u_2 + B)x^2 + (C\,u_2 + D)x + (E\,u_2 + f)$$

$$0 \leq x \leq 1.07 \text{ m}$$

where A = 55.49 (± 13.0), B = 142.6 (± 8.2), C = 230.31 (± 18.9),
D = - 138.86 (± 11.8), E = 3.51 (± 2.7), F = 18.1 (± 3.6)

$$T_{HH} = (A\,u_2 + B)x^2 + (C\,u_2 + D)x + (E\,u_2 + F)$$

$$1.07 \leq x \leq 2.13 \text{ m}$$

where A = - 275.9 (± 7.75), B = - 155.0 (± 4.65), C = 896.4 (± 25.2)
D = 513.78 (± 15.7), E = - 317.7 (± 18.8), F = - 315.7 (± 11.9)

$$T_{HS} = (A\,u_2 + B)x^2 + (C\,u_2 + D)x + (E\,u_2 + F)$$

$$2.13 \leq x \leq 2.84 \text{ m}$$

where A = - 42.63 (± 21.7), B = 170.5 (± 13.7), C = - 145.28 (± 25.6),
D = - 896.45 (± 63.4), E = 840.0 (± 94.1), F = 1164.0 (± 72.5)

$$T_{SH} = (A\,u_3 + B)x^2 + (C\,u_3 + D)x + (E\,u_3 + F)$$

$$1.07 \leq x \leq 2.13 \text{ m}$$

where A = 338.37 ($\pm$ 7.39), B = 86.77 ($\pm$ 4.65), C = - 762.6 ($\pm$ 23.6),
D = - 264.3 ($\pm$ 15.0), E = 478.3 ($\pm$ 18.4), F = 191.0 ($\pm$ 11.7)

$$T_{SS} = (A\,u_3 + B)x^2 + (C\,u_3 + D)x + (E\,u_3 + F)$$

$$2.13 \leq x \leq 2.84 \text{ m}$$

where A = - 313.72 ($\pm$ 28.7), B = - 245.68 ($\pm$ 18.6), C = 1606.7 ($\pm$ 132.9),
D = 122.17 ($\pm$ 84.1), E = - 1649.0 ($\pm$ 151.7), F = - 1449.0 ($\pm$ 95.9)

For power input set points $\leq$ 0.3

$$T_{PP} = A\,u_1\,x^2 + B\,u_1\,x + C\,u_1$$

$$0 \leq x \leq 1.07 \text{ m}$$

where A = 26.35 ($\pm$ 9.5), B = - 156.69 ($\pm$ 14.7), C = 612.7 ($\pm$ 40.9)

$$T_{PH} = A\,u_1\,x^2 + B\,u_1\,x + C\,u_1$$

$$1.07 \leq x \leq 2.13 \text{ m}$$

where A = 406.7 ($\pm$ 87.1), B = - 1681.5 ($\pm$ 303.1), C = 1740 ($\pm$ 226.6)

$$T_{HP} = A\,u_2\,x^2 + B\,u_2\,x + C\,u_2$$

$$0 \leq x \leq 1.07 \text{ m}$$

where A = 533.5 ($\pm$ 17.05), B = - 231.4 ($\pm$ 25.6), C = 65.53 ($\pm$ 7.69)

$$T_{HH} = A\,u_2\,x^2 + B\,u_2\,x + C\,u_2$$

$$1.07 \leq x \leq 2.13 \text{ m}$$

where A = - 993.5 ($\pm$ 26.3), B = 3174.0 ($\pm$ 85.4), C = - 1766.0 ($\pm$ 64.1)

$$T_{HS} = A\,u_2\,x^2 + B\,u_2 + C\,u_2$$

$$2.13 \leq x \leq 2.84 \text{ m}$$

where A = 588.1 ($\pm$ 45.8), B = - 3419.6 ($\pm$ 212.5), C = 5037.1 ($\pm$ 242.5)

$$T_{SH} = A\,u_3\,x^2 + B\,u_3 + C\,u_3$$

$$1.07 \leq x \leq 2.13 \text{ m}$$

where A = 402.8 ($\pm$ 6.9), B = - 894.8 ($\pm$ 22.4), C = 504.4 ($\pm$ 16.9)

$$T_{SS} = A\,u_3\,x^2 + B\,u_3\,x + C\,u_3$$

$$2.13 \leq x \leq 2.84 \text{ m}$$

where A = - 1163.5 ($\pm$ 307.5), B = 5818.9 ($\pm$ 146.8), C = - 6643.5 ($\pm$ 167.7)

T_{PP} = temperature in preheat zone with preheat zone on only
T_{PH} = temperature in heat zone with preheat zone on only
T_{HP} = temperature in preheat zone with heat zone on only
T_{HH} = temperature in heat zone with heat zone on only
T_{HS} = temperature in soak zone with heat zone on only
T_{SH} = temperature in heat zone with soak zone on only
T_{SS} = temperature in soak zone with soak zone on only

Figures in brackets denote the 95% confidence tolerance on the parameters.

Weighting polynomials

$$W_1 = 0.522\,x^3 - 1.14\,x^2 + 0.889\,x + 0.907$$

$$0 \leq x \leq 1.07$$

$$W_2 = 0.629\,x^2 - 1.96\,x + 2.728$$

$$1.07 \leq x \leq 2.13$$

$$W_3 = - 0.454\,x^2 + 1.95\,x - 0.8477$$

$$2.13 \leq x \leq 2.84$$

APPENDIX B

Slab Model Derivation

The equation for heat transfer within a large flat slab in a reheating furnace, together with initial and boundary conditions, are shown below.

The heat conduction equation is given by:

$$\rho c \frac{\partial \theta}{\partial t}(x, t) = \frac{\partial}{\partial x}\left\{k \frac{\partial \theta(x, t)}{\partial x}\right\} \quad \ldots\ldots\ldots\ldots\ldots\ldots \quad (B.1)$$

with the initial condition given by

$$\theta(x, 0) = \theta_o(x), \quad 0 \leqslant x \leqslant s \quad \ldots\ldots\ldots\ldots\ldots\ldots \quad (B.2)$$

where ρ = density (g/cm^3)

c = specific heat ($cal/g\ ^oC$)

k = thermal conductivity ($cal/cm\ sec\ ^oC$)

θ = slab temperature (^oK)

θ_o = initial condition (^oK)

s = slab thickness

t = time

x = coordinate in the direction of the slab thickness (see Figure 4.23).

The boundary conditions on the surface of the slab in the preheat and heat zones are expressed by:

$$-k \frac{\partial \theta}{\partial x}(x, t)\Big|_{\substack{x=0 \\ x=s}} = e\,\sigma\{T^4(y, t) - \theta_s^4(t)\} \quad \ldots\ldots\ldots \quad (B.3)$$

where e = effective emissivity of the furnace

σ = Stefan-Boltzmann constant ($cal/cm^2\ sec\ ^oK^4$)

T = furnace temperature (^oK)

In the soaking zone the boundary condition on the heating surfaces of the slab is expressed mathematically as:

$$-k \frac{\partial \theta}{\partial x}(x, t)\Big|_{x=s} = 0 \quad \ldots\ldots\ldots\ldots\ldots\ldots\ldots \quad (B.4)$$

where $\theta(x, t)$ is the slab temperature as a function of its thickness and time. The furnace temperature, $T(y, t)$, varies along its length and also varies with time, but for steady state operation of the furnace (i.e. slabs of the same thickness pushed at a constant rate) it is only a function of the furnace length.

It is necessary to point out here that the slab surface temperature, θ_s, should not exceed a specified limit, i.e.

$$\theta(0;\ s,\ t) = \theta_s(t) \leq \theta_{s\ max} \qquad \text{..... (B.5)}$$

To simplify the derivation of the model, dimensionless variables are introduced, as shown in Table B.1. Using these variables, equations (B.1) to (B.5) can be re-written as

$$\alpha\rho^*c^* \frac{\partial\theta^*}{\partial t^*} = \frac{\partial}{\partial x^*}\left(k^* \frac{\partial\theta^*}{\partial x^*}\right) \qquad \text{..... (B.6)}$$

$$-\ k^* \left.\frac{\partial\theta^*}{\partial x^*}\right|_{\substack{x^*=0 \\ x^*=2}} = \alpha(T^{*4} - \theta_s^{*4}) \qquad \text{..... (B.7)}$$

$$\theta^*(x^*,\ 0) = \theta_o^*(x^*) \text{ for } 0 \leq x^* \leq 2 \qquad \text{..... (B.8)}$$

$$\theta^*(0;\ 2,\ t) \leq \theta^*_{s\ max} \qquad \text{..... (B.9)}$$

Table B.1

Variables and Constants introduced for Normalization

Variables	Relations	Meaning
θ^*	$\theta = \theta^* T_r$	Dimensionless slab temperature
T^*	$T = T^* T_r$	Dimensionless furnace temperature
ρ^*	$\rho = \rho^* \rho_r$	Dimensionless density
c^*	$c = c^* c_r$	Dimensionless specific heat
k^*	$k = k^* k_r$	Dimensionless thermal conductivity
x^*	$x = x^*\ s/2$	Dimensionless coordinate
t^*	$t = \frac{\rho_r\ c_r\ s t^*}{2\ T_r^3\ e\ \sigma}$	Dimensionless time
α^*	$\alpha = \frac{s\ \sigma\ e\ T_r^3}{2\ k_r}$	Dimensionless constant

The last two equations in Table B.1 are deduced by substituting the other variables and derivatives in equations (B.1) and (B.2).

Since the situation is symmetric in respect of the initial distribution and the boundary conditions, the history of one half of the slab duplicates that of the other and, hence, only one half need be considered. There is no heat transfer across the centre plane, and so the gradient there is zero. The boundary conditions now become:

$$- k^* \left.\frac{\partial \theta^*}{\partial x^*}\right|_{x^*=0} = \alpha(T^{*4} - \theta_s^{*4}) \qquad \text{..... (B.10a)}$$

$$- k^* \left.\frac{\partial \theta^*}{\partial x^*}\right|_{x^*=1} = 0 \qquad \text{..... (B.10b)}$$

where x = 0 represents the top surface of the slab.

From hereon the * will be dropped, but the variables will retain their dimensionless form unless otherwise stated.

Since it is the average value of the slab temperature which is of interest, this can be represented as

$$\bar{\theta}(t) = \int_0^1 \theta(x, t)dx \qquad \text{..... (B.11)}$$

An ODE for the slab heating process (equations (B.6) to (B.8)) will now be derived. If c and k are assumed to be constant over the temperature range, and the temperature distribution through the slab is uniform, such an equation can readily be found (Carlslaw and Jaeger, 1959):

$$\rho c \frac{d\bar{\theta}}{dt} = (T^4 - \theta^4) \qquad \text{..... (B.12)}$$

In the case of reheating slabs of steel from cold to rolling temperature, where large temperature variations are involved, the thermal properties of steel suffer considerable changes, and therefore c and k cannot be assumed to be constant. This causes equation (B.1) to be insoluble analytically. Therefore no treatment of heat transfer in steel which does not endeavour to take account of these variations, at least approximately, can be regarded as satisfactory for this particular application.

Taking this into account, it is again possible to find an equation of the following form which describes the slab heating process

$$\frac{d\bar{\theta}}{dt} = f(\theta, T) \quad \ldots\ldots\ldots\ldots\ldots\ldots\ldots\ldots\ldots\ldots \quad (B.13)$$

An equation for the surface temperature can also be found to be

$$\theta(0, t) = g(\bar{\theta}, T) \quad \ldots\ldots\ldots\ldots\ldots\ldots\ldots\ldots\ldots\ldots \quad (B.14)$$

Integrating equation (B.6) over the spatial coordinate, x, gives

$$\int_0^1 \alpha\rho c \frac{\partial\theta}{\partial x}\, dx = \int_0^1 \frac{\partial}{\partial x}\, k\left(\frac{\partial\theta}{\partial x}\right) dx$$

$$= \left[k \frac{\partial\theta}{\partial x} \right]_0^1$$

$$= - k \left.\frac{\partial\theta}{\partial x}\right|_{x=1} , \; - k \left.\frac{\partial\theta}{\partial x}\right|_{x=0} \quad \ldots\ldots\ldots\ldots \quad (B.15)$$

substituting equations (B.10a) and (B.10b) into equation (B.15)

$$\int_0^1 \alpha\rho c \frac{\partial\theta}{\partial t}\, dx = (T^4 - \theta_s^4) \quad \ldots\ldots\ldots\ldots\ldots\ldots\ldots\ldots \quad (B.16)$$

Expanding $\theta(x, t)$ about its average value, $\bar{\theta}(t)$, which is, say, at $x = \bar{x}$, then

$$\theta(x, t) = \bar{\theta}(t) + (x - \bar{x})\theta_x(\bar{x}, t) + \frac{1}{2}(x - \bar{x})^2\theta_{xx}(\bar{x}, t) + \text{h.o.t.} \ldots\ldots$$

$$\ldots\ldots\ldots \quad (B.17a)$$

where $\theta_x = \left(\frac{\partial\theta}{\partial x}\right)_{\bar{x}}$, $\theta_{xx} = \left(\frac{\partial^2\theta}{\partial x^2}\right)_{\bar{x}}$

Evaluating $\int_{\bar{x}}^1 \alpha\rho c \frac{\partial\theta}{\partial t}\, dx$ gives

$$\int_{\bar{x}}^1 \alpha\rho c \frac{\partial\theta}{\partial t}\, dx = \int_{\bar{x}}^1 \frac{\partial}{\partial x}\left(k(\theta) \frac{\partial\theta}{\partial x}\right) dx$$

$$= \left[k(\theta) \frac{\partial\theta}{\partial x} \right]_{\bar{x}}^1$$

$$= \left[- k(\theta) \frac{\partial \theta}{\partial x} \right]_{\bar{x}}$$

hence

$$\left(\frac{\partial \theta}{\partial x}\right)_{\bar{x}} = - \frac{\alpha}{k(\theta)} \int_{\bar{x}}^{1} \rho c \frac{\partial \theta}{\partial t} \, dx$$

$$= \alpha F_1(\theta, t) \qquad \ldots\ldots\ldots\ldots\ldots\ldots\ldots \quad (B.17b)$$

An equation for $\theta_{xx}(\bar{x}, t)$ can be derived in the following manner:

$$\alpha \rho c \frac{\partial \theta}{\partial t} = \frac{\partial}{\partial x} \left(k(\theta) \frac{\partial \theta}{\partial x} \right)$$

$$= k(\theta) \frac{\partial^2 \theta}{\partial x^2} + \frac{dk(\theta)}{d\theta} \left(\frac{\partial \theta}{\partial x}\right)^2$$

$$\alpha \rho c \left(\frac{\partial \theta}{\partial x}\right)_{\bar{x}} = k(\bar{\theta}) \left(\frac{\partial^2 \theta}{\partial x^2}\right)_{\bar{x}} + \frac{dk(\theta)}{\partial \theta} \left(\frac{\partial \theta}{\partial x}\right)^2_{\bar{x}}$$

therefore

$$\left(\frac{\partial^2 \theta}{\partial x^2}\right)_{\bar{x}} = \frac{1}{k(\bar{\theta})} \left[\alpha \rho c \left(\frac{\partial \theta}{\partial t}\right)_{\bar{x}} - \left(\frac{dk(\theta)}{d\theta}\right)_{\bar{x}} \alpha^2 F_1^{\,2}(\theta, t) \right]$$

$$= \alpha F_2(\theta, t) + \alpha^2 F_3(\theta, t) \qquad \ldots\ldots\ldots\ldots\ldots\ldots \quad (B.17c)$$

Substituting equations (B.17b) and (B.17c) into (B.17a) gives

$$\theta(x, t) = \bar{\theta}(t) + (x - \bar{x}) \alpha F_1(\theta, t) + \frac{1}{2}(x - \bar{x})^2 \left[\alpha F_2(\theta, t) + \alpha^2 F_3(\theta, t) \right] + \text{h.o.t.}$$

Hence,

$$\theta(x, t) = \bar{\theta}(t) + \alpha f_1(x, t) + f_2(x, t) + \text{h.o.t.} \qquad \ldots\ldots\ldots \quad (B.17d)$$

Let $\beta(\theta) = \rho c(\theta)$ (B.18)

Expanding both β and k about their average values,

$$\beta(\theta) = \beta(\bar{\theta}) + (\theta - \bar{\theta}) \frac{d\beta}{d\theta} + (\theta - \bar{\theta})^2 \frac{d^2 \beta}{d\bar{\theta}^2} + \text{h.o.t.}$$

$$k(\theta) = k(\bar{\theta}) + (\theta - \bar{\theta}) \frac{dk}{d\theta} + (\theta - \bar{\theta})^2 \frac{d^2 k}{d\theta^2} + \text{h.o.t.}$$

Substituting $(\theta - \bar{\theta})$ from equation (B.17d) into the last two equations and keeping only those terms with α of second order or less, the following results:

$$\beta(\theta) = \beta(\bar{\theta}) + \alpha f_1 \frac{d\beta}{d\bar{\theta}} + \alpha^2 \left(f_2 \frac{d\beta}{d\bar{\theta}} + \frac{1}{2} f_1^2 \frac{d^2\beta}{d\bar{\theta}^2} \right) \quad \ldots\ldots \quad (B.19)$$

$$k(\theta) = k(\bar{\theta}) + \alpha f_1 \frac{dk}{d\bar{\theta}} + \alpha^2 \left(f_2 \frac{dk}{d\bar{\theta}} + \frac{1}{2} f_1^2 \frac{d^2k}{d\bar{\theta}^2} \right) \quad \ldots\ldots \quad (B.20)$$

Differentiating equation (B.17d) with respect to t, and then with respect to x, results in

$$\frac{d\theta}{dt} = \frac{d\bar{\theta}}{dt} + \alpha \frac{\partial f_1}{\partial t} + \alpha^2 \frac{\partial f_2}{\partial t} \quad \ldots\ldots\ldots\ldots\ldots\ldots \quad (B.21)$$

$$\frac{d\theta}{dx} = \alpha \frac{\partial f_1}{\partial x} + \frac{\partial f_2}{\partial x} \alpha^2 \quad \ldots\ldots\ldots\ldots\ldots\ldots\ldots \quad (B.22)$$

Substituting equations (B.21) and (B.22) into equation (B.6) gives

$$\alpha\beta(\theta) \left\{ \frac{d\bar{\theta}}{dt} + \frac{\partial f_1}{\partial t} + \alpha^2 \frac{\partial f_2}{\partial t} \right\} = \frac{\partial}{\partial x} \left[k \left(\alpha \frac{\partial f_1}{\partial x} + \alpha^2 \frac{\partial f_2}{\partial x} \right) \right] \quad (B.23)$$

Substituting for β and k (i.e. equations (B.19) and (B.20) in the last equation results in:

$$\alpha \left[\beta(\bar{\theta}) + \alpha f_1 \frac{d\beta}{d\bar{\theta}} + \alpha^2 \left(f_2 \frac{d\beta}{d\bar{\theta}} + \frac{1}{2} f_1^2 \frac{d^2\beta}{d\bar{\theta}^2} \right) \right] \left[\frac{d\bar{\theta}}{dt} + \alpha \frac{\partial f_1}{\partial t} + \alpha^2 \frac{\partial f_2}{\partial t} \right]$$

$$= \frac{\partial}{\partial x} \left\{ \left[k(\bar{\theta}) + \alpha f_1 \frac{dk}{d\bar{\theta}} + \alpha^2 \left(f_2 \frac{dk}{d\bar{\theta}} + \frac{1}{2} f_1^2 \frac{d^2k}{d\bar{\theta}^2} \right) \right] \left[\alpha \frac{\partial f_1}{\partial x} + \alpha^2 \frac{\partial f_2}{\partial x} \right] \right\}$$

$$\ldots\ldots\ldots \quad (B.24)$$

Evaluating equation (B.24) by neglecting high order terms of α and by collecting terms of α and α^2, results in

$$\alpha \left[\beta \frac{d\bar{\theta}}{dt} - k \frac{\partial^2 f_1}{\partial x^2} \right] + \alpha^2 \left[\beta \frac{\partial f_1}{\partial t} + f_1 \frac{d\beta}{d\bar{\theta}} \frac{d\theta}{dt} - k \frac{\partial^2 f_2}{\partial x^2} - f_1 \frac{dk}{d\bar{\theta}} \frac{\partial^2 f_1}{\partial x^2} - \frac{dk}{d\theta} \left(\frac{\partial f_1}{\partial x} \right)^2 \right] = 0 \quad \ldots\ldots \quad (B.25)$$

It can be seen from the definition of α (Table B.1) that it may vary independently from the other terms in equation (B.25), since α is a

function of slab thickness, and when considering one particular slab, this thickness is constant. Therefore, the coefficients of each power of α must be zero.

$$k \frac{\partial^2 f_1}{\partial x^2} = \beta \frac{d\bar{\theta}}{dt} \quad \ldots\ldots\ldots\ldots\ldots\ldots\ldots\ldots \quad (B.26)$$

$$k \frac{\partial^2 f_2}{\partial x^2} = \beta \frac{\partial f_1}{\partial t} + f_1 \frac{d\beta}{d\bar{\theta}} \frac{d\theta}{dt} - f_1 \frac{dk}{d\bar{\theta}} \frac{\partial^2 f_1}{\partial x^2} - \frac{dk}{d\bar{\theta}} \left(\frac{\partial f_1}{\partial x} \right)^2 \quad \ldots \quad (B.27)$$

To find solutions for $f_1(x, t)$ and $f_2(x, t)$

Assume the solution for equation (B.26) to be

$$f_1(x, t) = F_1(x) G_1(t) \quad \ldots\ldots\ldots\ldots\ldots\ldots\ldots \quad (B.28)$$

Differentiating equation (B.28) twice with respect to x gives

$$\frac{\partial^2 f_1}{\partial x^2} = \frac{\partial^2 F_1}{\partial x^2} G_1(t) \quad \ldots\ldots\ldots\ldots\ldots\ldots\ldots\ldots \quad (B.29)$$

Comparing this equation with equation (B.26) yields

$$\frac{\partial^2 F_1}{\partial x^2} = 1 \quad \ldots\ldots\ldots\ldots\ldots\ldots\ldots\ldots \quad (B.30)$$

$$G_1 = \frac{\beta(\bar{\theta})}{k(\bar{\theta})} \frac{d\theta}{dt} \quad \ldots\ldots\ldots\ldots\ldots\ldots\ldots\ldots \quad (B.31)$$

Solution of equation (B.30) is given by

$$F_1(x) = \frac{1}{2} x^2 + C_1 x + C_2 \quad \ldots\ldots\ldots\ldots\ldots\ldots \quad (B.32)$$

where C_1 and C_2 are constants. To find C_1 and C_2, the initial and boundary conditions of equation (B.30) must be specified. Integrating equation (B.17d) over the spatial coordinate x gives

$$\int_0^1 \theta(x, t) dx = \int_0^1 \bar{\theta}(t) dx + \alpha \int_0^1 f_1(x, t) dx + \alpha^2 \int_0^1 f_2(x, t) dx$$

$$\ldots\ldots\ldots \quad (B.33)$$

But, by definition (equation (B.11)), the left-hand side of equation (B.33) becomes $\bar{\theta}(t)$. The first term on the right-hand side is easily integrated to yield

$$\bar{\theta}(t) = \bar{\theta}(t) + \alpha \int_0^1 f_1(x, t)dx + \alpha^2 \int_0^1 f_2(x, t)dx,$$

hence,

$$\int_0^1 f_1(x, t)dx = 0 \qquad \text{..... (B.34)}$$

$$\int_0^1 f_2(x, t)dx = 0 \qquad \text{..... (B.35)}$$

Substituting equation (B.28) into equation (B.34),

$$\int_0^1 F_1(x)G_1(t)dx = 0,$$

$$\text{i.e.} \int_0^1 F_1(x)dx = 0 \qquad \text{..... (B.36)}$$

Equation (B.36) states the initial conditions for equation (B.30). The boundary conditions are deduced as follows:

$$- k \left.\frac{\partial \theta}{dx}\right|_{x=1} = 0$$

because of the symmetry situation at the centre plane of the slab.

Substituting equation (B.22) into the above equation gives

$$- k \left(\alpha \frac{\partial f_1}{\partial x} + \alpha^2 \frac{\partial f_2}{\partial x} \right) \Bigg|_{x=1} = 0 \qquad \text{..... (B.37)}$$

As before, since α can vary independently from the other variables in equation (B.37), then

$$\left.\frac{\partial f_1}{\partial x}\right|_{x=1} = 0 \qquad \text{..... (B.38)}$$

$$\left.\frac{\partial f_2}{\partial x}\right|_{x=1} = 0 \qquad \text{..... (B.39)}$$

Substitution of equation (B.28) into equation (B.38) yields

$$\frac{\partial F_1}{\partial x} = 0 \qquad \ldots\ldots\ldots\ldots\ldots\ldots\ldots\ldots\ldots\ldots \quad (B.40)$$

which is the boundary condition for equation (B.30). Substitution of the assumed solution for F(x) (i.e. equation (B.32)) into equation (B.36) and equation (B.40) gives two simultaneous equations in terms of C_1 and C_2 which are solved to give:

$$C_1 = -1$$

$$C_2 = \frac{2}{3}$$

Thus,

$$F_1(x) = \frac{1}{2}x^2 - x + \frac{2}{3} \qquad \ldots\ldots\ldots\ldots\ldots\ldots\ldots \quad (B.41)$$

Returning to equation (B.27) and substituting equation (B.28) into it gives:

$$\frac{\partial^2 f_2}{\partial x^2} = \frac{1}{k}\left\{\beta F_1 \frac{dG_1}{dt} + F_1 G_1 \frac{d\beta}{d\bar{\theta}}\frac{d\bar{\theta}}{dt} - F_1 G_1^2 \frac{dk}{d\bar{\theta}} - G_1^2 \frac{dk}{d\bar{\theta}}\left(\frac{dF_1}{dx}\right)^2\right\}$$

$\ldots\ldots\ldots$ (B.42)

Equation (B.30) is also used in deriving equation (B.42). Re-arranging the terms of equation (B.42) so that those functions of time and those of x only are grouped together, gives

$$\frac{\partial^2 f_1}{\partial x^2} = \left\{F_1\left(\frac{\beta}{k}\frac{dG_1}{dt} + \frac{G_1}{k}\frac{d\beta}{d\bar{\theta}}\frac{d\bar{\theta}}{dt}\right) - \left(F_1 + \left(\frac{dF_1}{dx}\right)^2\right)\left(\frac{G_1^2}{k}\frac{dk}{d\bar{\theta}}\right)\right\}$$

$\ldots\ldots\ldots$ (B.43)

A solution for $f_2(x, t)$ can also be assumed as

$$f_2(x, t) = F_2(x)G_2(t) + F_3(x)G_3(t) \qquad \ldots\ldots\ldots\ldots \quad (B.44)$$

where

$$\frac{d^2F_2(x)}{dx^2} = F_1(x) \qquad \ldots\ldots\ldots\ldots\ldots\ldots\ldots\ldots \quad (B.45)$$

$$G_2(t) = \frac{\beta}{k}\frac{dG_1}{dt} + \frac{G_1}{k}\frac{d\beta}{d\bar{\theta}}\frac{d\bar{\theta}}{dt} \qquad \ldots\ldots\ldots\ldots\ldots\ldots \quad (B.46)$$

$$\frac{d^2F_3}{dx^2} = F_1(x) + \left(\frac{dF_1(x)}{dx}\right)^2 \quad \text{..... (B.47)}$$

$$G_3(t) = F_1(x) + \left(\frac{dF_1(x)}{dx}\right)^2 \quad \text{..... (B.48)}$$

To solve equations (B.45) and (B.47) the initial and boundary conditions must be specified. These are deduced in the same manner previously outlined for the solution of $F_1(x)$. Hence,

$$\left.\begin{aligned} &\int_0^1 F_2(x)\,dx = 0 \\ &\int_0^1 F_3(x)\,dx = 0 \\ &\left.\frac{dF_2}{dx}\right|_{x=1} = 0 \\ &\left.\frac{dF_3}{dx}\right|_{x=1} = 0 \end{aligned}\right\} \quad \text{..... (B.49)}$$

Hence,

$$F_2(x) = \frac{x^4}{24} - \frac{x^3}{6} + \frac{x^2}{6} - \frac{1}{45} \quad \text{..... (B.50)}$$

$$F_3(x) = \frac{x^4}{8} - \frac{x^3}{2} + \frac{2x^2}{3} - \frac{x}{3} + \frac{2}{45} \quad \text{..... (B.51)}$$

To evaluate the left-hand side of equation (B.16), equations (B.19) and (B.21) are substituted into it. High order terms of α are then neglected from the resulting integral equation. The solution of $f_1(x, t)$ and $f_2(x, t)$ are substituted to yield

$$\int_0^1 \beta(\bar{\theta})\,\frac{\partial\theta}{\partial t}\,dx = \beta(\bar{\theta})\,\frac{d\bar{\theta}}{dt} + \alpha^2\left(G_1\,\frac{d\beta}{d\bar{\theta}}\,\frac{dG_1}{dt} + \frac{1}{2}\,G_1^{\,2}\,\frac{d^2\beta}{d\bar{\theta}^2}\,\frac{d\bar{\theta}}{dt}\right)\int_0^1 F_1(x)^2\,dx$$

$$= \beta(\bar{\theta})\,\frac{d\theta}{dt} + \frac{1}{45}\,\alpha^2\gamma \quad \text{..... (B.52)}$$

where

$$\gamma = G_1 \frac{d\beta}{d\bar{\theta}} \frac{dG_1}{dt} + \frac{1}{2} G_1^2 \frac{d^2\beta}{d\bar{\theta}^2} \frac{d\bar{\theta}}{dt} \qquad \text{..... (B.53)}$$

In view of equation (B.52), equation (B.16) can be rewritten as follows:

$$\boxed{\beta(\bar{\theta}) \frac{d\theta}{dt} + \frac{1}{45} \alpha^2 \gamma = (T^4 - \theta_s^4)} \qquad \text{..... (B.54)}$$

since $\int_0^1 F_1(x)^2 dx = \frac{1}{45}$.

In order to find an equation for θ_s, the surface temperature of the slab, x = 0 is put into equation (B.17d):

$$\theta(x, t) = \bar{\theta}(t) + \alpha f_1(x, t) + \alpha^2 f_2(x, t)$$

$$= \bar{\theta}(t) + \alpha F_1(x) G_1(t) + \alpha^2 \left(F_2(x) G_2(t) + F_3(x) G_3(t)\right)$$

Hence,

$$\theta(0, t) = \theta_s(t) = \bar{\theta}(t) + \frac{1}{3} \alpha G_1(t) + \alpha^2 \left(-\frac{1}{45} G_2(t) + \frac{2}{45} G_3(t)\right)$$

..... (B.55)

Since

$$F_1(0) = \frac{1}{3}$$

$$F_2(0) = -\frac{1}{45}$$

$$F_3(0) = \frac{2}{45}$$

Let $\varepsilon = -\frac{1}{45} G_2(t) + \frac{2}{45} G_3(t)$ ..... (B.56)

Hence

$$\boxed{\theta_s(t) = \bar{\theta}(t) + \frac{1}{3} \alpha G_1(t) + \alpha^2 \varepsilon} \qquad \text{..... (B.57)}$$

Using equations (B.46) and (B.48), ε may be written as

$$\varepsilon = -\frac{1}{45}\left[\frac{2G_1^2}{k}\frac{dk}{d\bar{\theta}} + \frac{\beta}{k}\frac{dG_1}{dt} + \frac{G_1}{k}\frac{d\beta}{d\bar{\theta}}\frac{d\bar{\theta}}{dt}\right] \quad \ldots\ldots\ldots\ldots \quad (B.58)$$

Substituting for $G_1(t)$ in equation (B.57), it becomes

$$\theta_s(t) = \bar{\theta}(t) + \frac{1}{3}\alpha\frac{\beta}{k}\frac{d\bar{\theta}}{dt} + \alpha^2\varepsilon \quad \ldots\ldots\ldots\ldots\ldots\ldots \quad (B.59)$$

Equation (B.54) may now be written as

$$\boxed{\beta(\bar{\theta})\frac{d\bar{\theta}}{dt} + \frac{1}{45}\alpha^2\gamma = T^4 - \left(\bar{\theta}(t) + \frac{1}{3}\alpha\frac{\beta(\bar{\theta})}{k(\bar{\theta})}\frac{d\bar{\theta}}{dt} + \alpha^2\varepsilon\right)^4} \quad (B.60)$$

Neglecting terms in α^2, equations (B.59) and (B.60) can be written as

$$\bar{\theta}_s(t) = \bar{\theta}(t) + \frac{\alpha\beta(\bar{\theta})}{3k(\bar{\theta})}\frac{d\bar{\theta}}{dt} \quad \ldots\ldots\ldots\ldots\ldots\ldots \quad (B.61)$$

$$\beta(\bar{\theta})\frac{d\bar{\theta}}{dt} = T^4 - \left(\bar{\theta}(t) + \alpha\frac{\beta(\bar{\theta})}{k(\bar{\theta})}\frac{d\bar{\theta}}{dt}\right)^4 \quad \ldots\ldots\ldots\ldots\ldots \quad (B.62)$$

Expanding the right-hand side of equation (B.62) results in

$$\beta(\bar{\theta})\frac{d\bar{\theta}}{dt} = T^4 - \left[\bar{\theta}^4(t) + \frac{4\alpha\beta(\bar{\theta})}{3k(\bar{\theta})}\bar{\theta}^3\frac{d\bar{\theta}}{dt} + \frac{2}{3}\left(\frac{\alpha\beta\bar{\theta}}{k}\frac{d\bar{\theta}}{dt}\right)^2 + \ldots\right]$$

$\ldots\ldots\ldots\ldots$ (B.63)

Collecting those terms in $\frac{d\bar{\theta}}{dt}$ and dividing by $\left(1 + \frac{4\alpha\bar{\theta}^3}{3k}\right)$, which is approximated by $\left(1 - \frac{4\alpha\bar{\theta}^3}{3k}\right)$, and neglecting high order terms in α, the following equation is obtained for the average slab temperature:

$$\beta(\bar{\theta})\frac{d\bar{\theta}}{dt} = \left[T^4 - \bar{\theta}^4(t)\right]\left(1 - \frac{4\alpha\bar{\theta}^3}{3k(\bar{\theta})}\right) \quad \ldots\ldots\ldots\ldots \quad (B.64)$$

Equations (B.61) and (B.64) define the proposed model for the temperature distribution within a slab. It is more convenient to express the model equations in dimensional form by substituting for the dimensionless quantities as given in Table B.1. Before proceeding any further it is necessary to relate the model equations to the actual aluminium extrusions used in the model reheat furnace. To

do this, the slab properties must be known and these are given below in Table B.2. Table B.3 shows the reference values.

Table B.2: Aluminium slab properties

Melting point = $660^{o}C$

Density, ρ = $2707.1265\ Kg/m^3$

Specific heat, c = $895.975\ J/Kg^{o}C$

Thermal conductivity, k = $228.36\ Wm/m^2\ ^{o}C$

Table B.3: Reference values

$T_r = 933^{o}K$

$c_r = 896\ J/Kg\ ^{o}K$

$k_r = 230\ Wm/m^2\ ^{o}K$

$\sigma_r = 5.67 \times 10^{-8}\ W/m^2\ ^{o}K^4$

$e = 0.7$

$\rho_r = 2700\ Kg/m^3$

Thus, substituting in the reference values gives

$$\frac{d\bar{\theta}}{dt} = \frac{7.95 \times 10^{-8}}{\rho c(\theta) s}\left(T^4 - \bar{\theta}^4\right)\left(1 - 2.64 \times 10^{-8}\ \frac{s}{k(\theta)}\ \bar{\theta}^3\right) \quad \ldots\ldots \quad (B.65)$$

The average temperature is given by the solution of the above ordinary differential equation.

The surface temperature is given by

$$\theta_s = \bar{\theta} + \frac{\rho c s^2}{720\ k(\theta)} \frac{d\bar{\theta}}{dt} \quad \ldots\ldots\ldots\ldots\ldots\ldots\ldots\ldots \quad (B.66)$$

Computer programs (Appendix C) removed for copyright reasons